REINFORCED CONCRETE COLUMNS OF VARIABLE CROSS SECTION

BY

N.F.A. BRANT, B.Sc.,M.Sc.,MASCE

A thesis submitted in partial fulfilment of the
requirements for the award of the Degree of
Doctor of Philosophy in Civil Engineering (Structures)

DEPARTMENT OF CIVIL ENGINEERING
THE CITY UNIVERSITY
LONDON

September, 1984

To my wife, Suzana, to whom I am deeply indebted for her moral support in times of stress, providing always the uplift needed and for her enormous patience and devotion during the course of this work.

CONTENTS

LIST OF FIGURES

LIST OF TABLES

ACKNOWLEDGEMENTS

The investigation reported in this thesis was carried out under the supervision and constant guidance of Dr. K.S. VIRDI, to whom the author is deeply grateful for his encouragement and valuable advice throughout the duration of the work.

The author is deeply grateful to MR. J. ROSE who was most helpful during the experimental investigation which was carried out at The City University. Thanks are also due to the technical staff members of the Civil Engineering Laboratory for their help in carrying out the tests and the construction of the Loading Rig.

The author is indebted to the Department of Transport, and Transport and Road Research Laboratory for their financial support and sponsorship of the investigation. In particular, thanks are due to DR. G.P. TILLY and MR. I.E.W. BROWN for their interest in the project.

Thanks are due to DR. C. D'MELLO, a colleague who helped with valuable discussions during the course of this work and to MISS C.M. THEW for her typing.

ABSTRACT

The results of a series of 19 full scale tests carried out on pin-ended reinforced concrete columns are reported. The columns tested had either tapered rectangular sections along the length or octagonal cross sections. All columns, except the last 6, were subjected to uniaxial eccentricities at one of the ends (the stronger end), and a nominally concentric load at the other end. For the case of the last six columns the loading applied at the stronger end was biaxially eccentric. For each of these tests, a complete set of measurements, covering the entire range of loading, are reported.

The test results are compared with the analytical results produced by the program VARCOLS, and the design strengths predicted by the Limit State Code for Bridges BS5400: Part 4 [8]

The thesis also includes a survey of published literature on reinforced concrete columns, covering mainly the period from 1955 to 1981. The available information has been reviewed under three headings : predominantly theoretical research, methods of design, and tests on reinforced concrete columns. Most of the test data available on slender reinforced concrete columns, have been used to verify a computer program VARCOLS, which was originally written for composite columns, and had been verified for that type of application, but is also suitable for slender reinforced concrete columns. The comparisons show that the program predicts the ultimate strength safely in almost all cases.

A new method of design for slender reinforced concrete columns with uniform and tapered cross sections is developed and design charts and worked example are presented. The method is shown to be simple and easy to be used and when compared with test results a good agreement was obtained.

NOTATION

A_c = area of concrete

A_s = area of steel reinforcement

a_i, a_j = Coordinates of Gauss Points

A'_{s1} = Area of compression reinforcement in the more highly compressed face

A_{s2} = Area of reinforcement in other face

b = width of cross section

d = Distance of Gauss point from the neutral axis

d_c = Depth of concrete in compression

D = depth of octagonal cross section

e_{1x}, e_{1y} = eccentricities of the load at one end of the column about the weak and the strong axes, respectively

e_{2x}, e_{2y} = eccentricities of the load at the other end of the column about the weak and the strong axis, respectively

f_{cu} = characteristic cube strength

f_y = characteristic yield strength

H_i, H_j = Weighting coefficients in Gauss Quadrature

h = depth of rectangular cross section

h_t = depth at mid-length for tapered columns

J = Jacobean Matrix

L = Length of the column

L/h_t = slenderness ratio

N_u = Ultimate load calculated from the proposed method of design

$N_{u\ calc}$ = ultimate load from theory (program VARCOLS) based on initial imperfection of 0.001L

$N_{u\ c1}$ = ultimate load from BS5400:Part 4 using safety factor values 1.0 and observed strengths of concrete and steel

$N_{u\ c2}$ = ultimate load from BS5400:Part 4 using safety factor values of the code and design stregths of concrete and steel

$N_{u\ test}$ = ultimate load from test

N_{uv1} = ultimate load from theory (program VARCOLS) based on initial imperfection of 0.001L

N_{uv2} = ultimate load from theory (program VARCOLS) based on zero initial imperfection

u_i, v_i = Deflections along x and y axes respectively

w = General term for displacement

x,y = Coordinates axes across the column section

ρ = ratio A_s/A_c

ε = Strain at a point

ξ,η = Special coordinates

θ = inclination of neutral axis

σ = Stress at a given strain

ϕ = Biaxial components of curvature

EXPLANATION OF THE COLUMN SYMBOLS

FIRST CHARACTER: Column Length

S = 3m

M = 6m

L = 9m

SECOND CHARACTER: Column Shape

C = Uniform

T = Taper in one plane

D = Taper in two planes

G = Octagonal

THIRD AND FOURTH CHARACTERS: End Loading

One character for each end

O = Nominally concentric loading

U = Uniaxially eccentric loading

B = Biaxially eccentric loading

FIFTH AND SIXTH CHARACTERS: A two digit sequence number

e.g. LDBO - 16

COLUMN LENGTH = 9m

TAPER IN TWO PLANES

Biaxially eccentric loading at the stronger end

Nominally concentric loading at the weaker end

Column number 16

CHAPTER 1

INTRODUCTION

1.1. GENERAL

Possibly the first ever national code to include limit state design principles was CP110 [15], published by the British Standards Institution in 1972. This code was preceded by the very extensive work by Cranston, published in the form of a C&CA Research Report [16], and which formed the principal basis for the column clauses in CP110 [15]. This code, in turn, formed the basis of BS5400:Part 4 [8], the British standard relating to the design of concrete bridges. Many of the clauses in BS5400:Part 4 dealing with the design of columns are direct excerpts from CP110.

It is recognised that while the majority of the common clauses in the two codes may be regarded as satisfactory for the design of columns in both buildings and bridges, there are some specific types of columns, encountered in bridge structures but rarely in buildings, for which there was no sufficient guidance available in BS5400:Part 4. These include columns with tapering sections, as well as columns with sections other than rectangular and circular in shape, for example octagonal columns. The work described in this thesis was initiated at The City University objective of filling this void.

An extensive literature review from around 1955 is given later in this chapter. The review has been set out under three headings: predominantly theoretical research, methods of design, and test results reported. Data on all the currently available tests on reinforced concrete columns was collated and used later.

Chapter 2 deals with the presentation and validation of the computer program VARCOLS written to obtain the ultimate loads of reinforced concrete

columns, of arbitrary cross section and varying along the length, including the effects of material and geometrical nonlinearities. The comparisons between the collated test results and those calculated by the program VARCOLS are given in this chapter.

Chapter 3 introduces the experimental program describing the manufacture of specimens, the instrumentation, the loading rig and the test procedure adopted.

Chapters 4, 5 and 6 present the test results for series A and B, C and D, respectively. The 7 columns in series A and B had a medium length of 6.0 m and were tested under uniaxially eccentric loading. Series C and D had 6 specimens each, all with a length of 9.0 metres. Columns in Series C were subjected to uniaxially eccentric loading while columns in Series D had biaxially eccentric loading. The test results were used to make comparisons with the analytical results produced by the program VARCOLS as well as the design strengths predicted by the Limit State Code for Bridges BS5400: Part 4[8]. The test results were also used to check the applicability of the method of design developed in Chapter 7.

Chapter 7 presents a new method of design for slender reinforced concrete columns with uniform or tapered section along the length. The design charts were developed from the ultimate strength data generated from the program VARCOLS.

The conclusions drawn from the theoretical and experimental studies described in the thesis have been grouped together in the final chapter.

An amendment to the expression of the additional eccentricity for slender reinforced concrete columns proposed originally by Cranston [16] and adopted by BS5400: Part 4 [8] is given in Appendix A.

1.2. LITERATURE REVIEW

1.2.1 INTRODUCTION

This Section covers a review of technical and research papers on reinforced concrete columns. Most of the published work included here dates from around 1955, about the time of the start of work on a European (later renamed International) recommendations for the analysis and design of concrete structures. The CEB-FIP recommendations [11] were eventually published in 1970, but contained no specific proposals for the design of concrete columns. A separate manual on the stability analysis of reinforced concrete columns appeared in 1978 [12]. This manual included a rigorous method of analysis of columns upto collapse. Tables and charts were included to make this analysis somewhat simpler to use.

Other codes which have included limit state design principles for the design of concrete structures, including concrete columns, apart from the two British codes mentioned, are the American code ACI 318-77 [2] and the Australian code AS 1480:1974 [4]. The Australian code is very similar to the ACI code in its approach.

At the present moment, considerable effort is being made towards the drafting of a Eurocode on reinforced concrete structures with the wider aim of having a code that may be acceptable in a number of European countries. This code, as the others mentioned so far, is also based on the limit state approach.

With so many national and international codes drafted in the last 20-25 years, it is not surprising that a very large number of research projects have been undertaken involving ultimate load behaviour of concrete structures. A

significant number of these have been concerned with reinforced concrete columns. In what follows a majority of the research papers and reports published in recent years and dealing with reinforced concrete columns are reviewed. The review includes mainly the work on isolated columns and only a few of the papers dealing with columns as part of a frame have been included.

The review has been set out under three headings : predominantly theoretical research, methods of design, and tests. Inevitably, there is some overlap among the sections.

The data collected on tests has been used to validate a computer program VARCOLS, written and verified originally for composite columns in biaxial bending, but also applicable to reinforced concrete columns. A brief description of the program has been included in Chapter 2 which also contains the comparison between the theoretical results obtained by the program VARCOLS and the experimental results collected from the published literature

1.2.2. PREDOMINANTLY THEORETICAL RESEARCH

Initial research on ultimate load behaviour of concrete structures naturally was concerned with the problem of the distribution of concrete stress in the cross section. This is intrinsically related to the stress-strain characteristic of concrete in compression. The first studies in this regard were made by Hognestad [26], Jensen [27], and Whitney [50]. Hognestad's stress strain curve for concrete has since been adopted in much of the research on reinforced concrete columns, among other concrete structures. Whitney's rectangular stress block for use in the ultimate analysis of concrete structures made feasible the derivation of simple, yet sufficiently accurate, formulae for the ultimate strength of concrete structures. The lasting contribution made by the above three authors was noted early by the joint ASCE-ACI committee report [52].

The earliest rational analysis for the ultimate strength of reinforced concrete columns appears to be that of Ernst, Hromadik, and Riveland [19], published in 1953. For steel, an elastic plastic stress-strain relation was used, and for concrete, Hognestad's stress strain relation [26] was used, together with a cosine wave assumption for the column deflected shape. The method was, therefore, applicable only to columns with symmetrical bending about the column midpoint.

In 1958, Broms and Viest [7] extended the method due to Ernst, Hromadik, and Riveland, to cover slender columns with end rotational restraints as well as unequal end eccentricities of the applied load.

In the same year, Chu and Pabarcius [14] developed a failure criterion based on cracking of the member and its inability to support additional loading. The method could be applied to sections of arbitrary shape subjected to biaxial

bending. A trapezoidal stress distribution for both steel and concrete was assumed.

In 1962, Gere and Carter [25] published formulae and graphs for the determination of elastic critical buckling loads for uniformly tapered columns loaded axially. Various end conditions were considered :

1. Columns with pinned ends
2. Columns with one end fixed and the other free
3. Columns with one end fixed and the other pinned
4. Columns with fixed ends

The paper by Gere and Carter is of interest only in so far as it deals with tapered columns. It is of little significance in the context of reinforced concrete columns in view of the inelastic behaviour of concrete and steel.

In the same year, Fogel and Ketter [22] published formulae for calculating elastic strength of pin ended tapered columns with axial loading and uniaxially applied end moments. The strength criterion was first yield of an extreme fibre, an approach more suitable for steel columns than for reinforced concrete columns.

Furlong [23] described an approach to calculate the ultimate strength of square reinforced concrete columns with biaxially eccentric loading. Use was made of Whitney's rectangular stress block in calculating the section capacity. No slenderness effects were considered, and hence the findings should be applicable only to short columns. It was noted that the maximum capacity was obtained for bending about the principal axes, and the minimum capacity for bending about the diagonal axes.

Chang and Ferguson [13] presented a method of obtaining the column deflected shape under axial loading and uniaxial bending, using an integration procedure based on Simpson's rule. The method required formulae for moment thrust strain relations. The method was restricted to columns with equal end moments, that is, to columns with symmetrical bending about the midpoint. The method was shown to give satisfactory results when compared with a series of six tests on slender reinforced concrete columns.

A procedure for the ultimate load analysis of biaxially loaded slender reinforced concrete columns was proposed by Farah and Huggins [20], in 1969. Equilibrium was satisfied at a selected number of points along the length of the column. By assuming that the column profile between any two stations is parabolic, the deflections at successive points are obtained by ensuring that the curvature at each point matches the applied loading. The method suffered from the disadvantage that the column had to be in symmetrical bending, in both the bending planes, with respect to the column midpoint. The internal equilibrium at each point was established by moment thrust curvature calculations based on the Newton-Raphson method for convergence. The integrations involved were obtained by first discretising the section into several small rectangles. The strain, and then the stress, at the centroid of each incremental rectangle was obtained, and the forces and moments calculated by assuming that the stress so obtained was uniform over the rectangle in question. Good correlation was shown with a test on a single column.

At about the same time, Warner [49] also presented a method for obtaining the moment thrust curvature relations for rectangular columns loaded with biaxial eccentricities. Warner's procedure for integrating the forces and moments across the section was remarkably similar to that adopted by Farah and Huggins, although Warner did not suggest any procedure for iteration, nor for determining the column deflected profile. A useful technique for

nondimensional representation of moment thrust curvature relations was presented.

Cranston published an extensive work [16] under the imprimatur of the Cement and Concrete Association. The work was undertaken as part of the British Standards Institution's aim at publishing a unified design code for concrete. Thus, Reference [16] forms the basis of many of the clauses relating to reinforced concrete columns in CP110 [15], and by the same token, in BS5400:Part 4 [8]. A large number of known test results were analysed using a computer program developed by Cranston [17], and it was shown that Cranston's analysis gave sufficiently accurate results. Parametric studies were reported on rectangular and circular columns. The range of parameters included percentage of steel varying from 1% to 6%, end eccentricities of 0.1 and 0.5 times the column depth, and five values of column slenderness expressed as the column length to column depth ratio (10, 15, 25, 40, and 60). A design method was proposed which used the concept of 'additional moment'. The notion is that at the critical section sufficient capacity should be designed to resist the applied thrust together with moments that account for the applied end moments (or end eccentricities), additional moments due to destabilising deflections, as well as any restraining moments.

In 1978 CEB-FIP published a manual of Buckling and Stability [12] of reinforced concrete columns. Both the cases of an isolated column and a column in a frame were considered. The manual included three methods of analysis, with varying degree of complexity. The most general method used accurate assessment of the moment thrust curvature calculations, adopting a procedure similar to that used by Warner [49]. Bending about both axes is considered. Columns of constant cross section as well as varying cross section along the length were included. The procedures given appear to be applicable only to columns fixed at the base and free at the top (cantilever columns). The 'general method' is

followed by a simplified method based on the equilibrium state. Equilibrium is satisfied only at the base (clamped end), using an approximate formula for the column deflection at the top. Finally, an approximate method is given to calculate the supplementary moment at the base, and the capacity of the base section for the total moment and axial thrust is checked using a specified strain diagram at the section. In this respect the method is similar to that suggested by Cranston [16], and which forms the basis of the clauses in CP110 [15] and BS5400:Part 4 [8]. Included in the manual is a design procedure based on the 'general method' of analysis mentioned earlier, but the procedure is not rapid enough for use in design offices. This is so inspite of the fact that for certain types of sections, nondimensional moment thrust curvature relations are supplied in the form of tables. The manual also includes a flow chart to aid the writing of computer program to solve the problem. The 'general method' has been compared with a large number of tests, many from laboratories in European countries, and the agreement is shown to be excellent.

Warner's method of calculating moment thrust curvature relations was adopted by Virdi and Dowling [45],[46], in an analytical method for determining the ultimate load of composite columns, such as steel stanchions encased in concrete. The first paper used a sine wave approximation to the column deflected profile, and good correlation was obtained with 9 tests on biaxially loaded short, medium length, and slender columns, with small, intermediate and large end eccentricties. In the second paper, a more general method for determining the deflected profile of a column with arbitrary end loading and end rotational restraints was presented. Use was made of the generalised Newton-Raphson method for a system of simultaneous nonlinear equations. The applicability of the method to reinforced concrete columns, although mentioned in these two papers, was demonstrated in a later paper by Virdi [48]. Here, although the procedure for calculating the deflected shape by the generalised Newton-Raphson method was retained, a more general method of calculating the

moment thrust curvature relations was adopted. This was based on the use of Gauss quadrature formulae, and makes it possible to apply the procedure to columns of arbitrary, polygonal shape. Load deflection response upto and beyond the peak collapse load was obtained. It is this method which forms the basis of the computer program VARCOLS, used for comparison with test results in Chapter 2 of this thesis.

In 1975, Suryanarayana and Basu [44], published a method for the analysis of biaxially restrained reinforced concrete columns. The equilibrium for increasing values of the applied load upto very near collapse, and for increasing values of nodal strain thereafter, was obtained by a procedure similar to the one proposed by Newmark [34] for elastic columns. The load deflection response beyond the peak collapse load was obtainable. The results were compared with two tests, one symmetric and one nonsymmetric restrained column. Good correlation between theory and experiments was obtained.

1.2.3. PUBLISHED METHODS OF DESIGN

In 1960, Bresler published a paper [6] in which he examined the problem of biaxially loaded reinforced concrete columns of short length (no slenderness effects). The idea of an interaction surface was introduced and two types of interaction formulae derived to approximate the interaction surface were examined. The first, a formula patterned on the well known Merchant-Rankine formula, has eventually found favour in the design of biaxially loaded composite columns [45]. However, the interpretation of the various terms appearing in the formula is altered to allow for slenderness effects. Bresler's original formula states that:

$$\frac{1}{P_i} = \frac{1}{P_x} + \frac{1}{P_y} - \frac{1}{P_o}$$

where,

P_i = the design failure load

P_o = failure load under axial compression only

P_x = failure load under axial compression and x-eccentricity

P_y = failure load under axial compression and y-eccentricity

The second formula, a variation on the moment ellipse, now appears in several national and international codes of practice, including CP110 [15] and BS5400:Part 4 [8].

$$(M_x/M_{ux})^p + (M_y/M_{uy})^q < 1.0$$

where,

M_x and M_y are the applied moments about the major axis and minor axis respectively,

M_{ux} and M_{uy} are the moment capacities in the major axis and minor axis respectively, in the presence of the applied axial load, and

p and q are constants with values ranging from 1.0 to 2.0 in different codes.

Both formulae were shown by Bresler to agree well with a series of 8 tests on short reinforced concrete columns. For the second formula, Bresler obtained a range of values for p=q varying from 1.15 to 1.55.

A similar interaction formula was suggested, by Furlong [23], involving the applied moments in the x and y directions together with the uniaxial moment capacities in the x and y directions in combination with the applied thrust.

In a very comprehensive paper, Mattock, Kriz, and Hognestad [32] illustrated the use of the rectangular stress block in the analysis of reinforced concrete members, including columns. Formulae were derived for the strength of columns in uniaxial and biaxial bending. Both the rectangular and circular shapes were considered. These formulae have survived, in some form or the other, in most codes dealing with the ultimate capacity of reinfored concrete columns. As in the case of most other contemporary publications, slenderness effects were not considered. Comparison with 84 tests on eccentrically loaded rectangular columns and 30 tests on eccentrically loaded circular columns, all conducted by Hognestad [26], and with ten rectangular columns with biaxially eccentric loading tested by Anderson and Lee [3], showed good correlation with the design formulae given in the paper.

A similar approach was adopted by Fleming and Werner [21]. The difference in the two approaches was mainly in the procedure for determining the depth of neutral axis for the case of biaxially loaded columns. Design charts, in nondimensional form, were provided for square columns loaded with biaxial eccentricity. The procedure for generating design charts for rectangular columns was also indicated.

A critical review of various design methods available upto about 1965 was published by Martin, MacGregor, Pfrang, and Breen [30]. This review, however, concentrated on research and practice in the USA, and does not adequately cover research done elsewhere.

In a paper published by Parme, Nieves, and Gouwens [39], the moment ellipse interaction formula originally proposed by Bresler, and applicable to short rectangular columns in biaxial bending, was slightly modified. Design aids based on the modified formula were presented. No comparison with any experimental data was shown, however. Also, slenderness effects were not included.

Ramamurthy [40] also examined the two formulae proposed by Bresler [6], and presented charts and formulae of his own, for the case of short rectangular columns with large biaxial eccentricities of loading. It was stated that the method is restricted to columns with 8 or more bars evenly distributed along the faces. Comparison with some 50 tests showed good agreement with the proposed interaction formulae.

In early 1970, MacGregor, Breen, and Pfrang [29] published a paper giving background to the proposed revision to the ACI Building Code 318-63. Much of the research in the previous decade or so was summarised, and the major new design proposals were spelled out. These related, in the main, to columns involved in frame action.

A similar exercise was done by the Cement and Concrete Association, in anticipation of the publication of the new British Standard Code on concrete structures, namely CP110-1972 [15]. The work was published by Cranston [16], and contained proposals, and their justification, for the design of reinforced concrete columns. The method is based principally on checking the capacity of

the critical cross section of the column, taking into account any magnification of moments due to slenderness or other effects. In this way, the strength calculations remain the same whether the column is short or long. Also, it becomes possible to make use of the large volume of research on short columns with biaxially eccentric loading. It could be stated that with this publication, the problem of uniform reinforced concrete columns, restrained or otherwise, as encountered in building frames, had been adequately assessed for the first time from the ultimate load point of view.

For a long column in uniaxial bending, Cranston proposed that the magnified moment M_t could be given by the following formula:

$$M_t = M_i + \frac{Nh}{1750} (l_e/h)^2 (1 - 0.0035\ l_e/h)$$

where,

M_i is the maximum initial moment in the length of the column,

N is the applied axial load

h is the total depth of the cross section in the plane of bending,

and,

l_e is the effective length of the column.

For columns in biaxial bending, or rectangular columns in major axis bending, this magnification of moments about both axes is calculated separately, and an interaction formula similar to the second formula suggested by Bresler, is used to calculate the column strength.

As implemented in CP110 [15] and BS5400:Part 4 [8], the above formula, together with the biaxial interaction formula mentioned, is restricted to uniform rectangular columns with aspect ratio less than 3.0.

The manual for the Buckling and Stability of Concrete columns [12] contains a design method which is close to the 'general method' of analysis included in that manual, and utilises tables of nondimensional moment thrust curvature relations. The design method appears to be unsuitable for use in design offices in view of the lengthy calculations involved.

A design method for restrained eccentrically loaded long columns was proposed by Parme [38] in 1966. Columns free to sway laterally, as well as columns not free to sway, were considered. The design aids developed in the paper enable a good estimate to be made of the moment magnification. The method was compared with tests reported by other research workers [5],[28].

Butler [9] proposed a design method for calculating the strength of restrained reinforced concrete columns. The method used the concept of reducing column flexural stiffness as it approaches its failure load. Comparisons were made with two series of theoretical results. The first was based on Cranston's approach [17], and the other was carried out using a computer program based on the method in Reference [46].

Butler's method was extended by Wood and Shaw [51], using an alternative variable stiffness design procedure for restrained reinforced concrete columns. The method for taking into account the effect of the end rotational restraints was reduced to an arithmetical procedure, in contrast with the graphical procedure suggested by Butler. Comparisons were made with the same sets of theoretical results as used by Butler [9]. Superior accuracy to the method contained in CP110 [15] was claimed.

1.2.4. TESTS ON REINFORCED CONCRETE COLUMNS

A very large number of tests on reinforced concrete columns are available in the published literature. A majority of these were on columns of short length. It appears that, in the early literature, the problem of instability of reinforced concrete columns was considered to be unimportant. It is understood that in many building structures, the slenderness of the columns is such that instability effects are likely to be small. However, this would not be true for most columns encountered in bridge structures.

Another feature common to most test results available in the literature is that the cross section is uniform along the length. Again, this is probably true for most columns in building frames, but perhaps not so for columns in bridge structures.

The following review of test data is not aimed to be comprehensive in its coverage. However, all available tests on slender columns are covered, as are any tests on variable cross section columns. Only a selected few series on short columns have been included.

The manual of stability of reinforced concrete columns [12] published by CEP/FIP contains reference to a number of tests conducted at various laboratories in Europe. Unfortunately, the references cited include matter written in diverse languages, and the test data could not be incorporated in Section 5 of this report.

Bresler [6] reported tests on 8 short columns with biaxial eccentricities. The columns were 4 ft (1220 mm) long with four 5/8 in (16 mm) diameter bars, one in each of the four corners of a 6 in x 8 in (152 mm x 203 mm) rectangular section. The end conditions were not specified, although for such short columns

the end conditions should not be of great importance.

A series of 10 tests was reported by Anderson and Lee [3]. The tests were on 4 in (102 mm) square reinforced concrete columns, each with 4 bars of reinforcement varying in diameter from 1/4 in (6 mm) to 5/8 in (16 mm). The loading was biaxially eccentric. The columns were of short length, eliminating instability. The results are more readily accessible in Reference [32].

Hognestad [26] conducted 84 tests on eccentrically loaded rectangular columns varying in length. The cross sections were 10 in x 10 in (254 mm x 254 mm). The columns had uniaxially eccentric longitudinal load. Hognestad also tested 30 columns with circular sections, all of 12 in (305 mm) diameter. A more easily accessible source of information on the columns tested by Hognestad is the paper by Mattock, Kriz, and Hognestad [32], where all the tests by Hognestad, along with tests by several others, are summarised. It is worth noting that all the columns tested by Hognestad were of sufficiently short length to virtually eliminate the effects of lateral instability.

Chang and Ferguson [13] reported 6 tests on slender columns. The length for the columns was 3200 mm in all cases. The cross section was rectangular 4-1/16 in x 6-1/8 in (103 mm x 155 mm). Four longitudinal bars of 3/8 in (10mm) diameter were placed in each corner. The ends of the columns were hinged, and the applied loading was concentric in the case of three of the six columns and uniaxially eccentric for the remaining columns.

Tests on 54 slender columns were reported by Saenz and Martin [42]. The same cross section, namely 3-9/16 in x 5 in (90 mm x 127 mm), was used for all specimens, but the column length varied from 76.9 in (1953 mm) to 152.2 in (3867 mm). Two different diameters of longitudinal reinforcement bars were used - 1/4 in (6 mm) and 3/8 in (10 mm). The ends were effectively clamped.

Meek [33] conducted tests on 9 reinforced concrete columns, all of size 5 in (127 mm) square. The columns were loaded through a ball seating at each end, simulating pin ended conditions. The columns had, unusually, transverse loads applied at two points, 12-1/2 in (317 mm) apart symmetrically placed, resulting in more or less uniform moment for about a fifth of the column height. The axial load was applied first upto the specified value without any lateral loads. The lateral bending moments were then applied keeping the axial load constant. The two biaxial moments were increased proportionately.

Martin and Olivieri [31] tested two columns with concentric loading, and another 6 with uniaxially eccentric loading. The columns were of rectangular cross section, having dimensions of 3-1/2 in x 5 in (90 mm x 127 mm). Four longitudinal bars, 3/8 in (10 mm) diameter, were used for all columns. The columns were all loaded so as to bend in double curvature, through beams connected at the ends of the columns.

A series of 8 tests on slender columns, also subjected to double curvature bending, were reported by MacGregor and Barter [28]. The specimens were of rectangular cross section 2.5 in x 4.4 in (64 mm x 112 mm). Four of the columns were pin-ended, while the other 4 had beam restraints at both ends. The reinforcement consisted of 4 bars of 3/8 in (10 mm) diameter.

Ramamurthy [40] tested 50 short reinforced concrete columns under biaxially eccentric loading. All specimens had 8 bars of reinforcement distributed evenly along the four faces of each column. The size of the bars varied from 3/8 in (10 mm) to 5/8 in (16 mm). The applied eccentricities were, in relation to the tests reported until then, large in terms of eccentricity/column width ratio. The columns were all very short, and had specially enlarged ends to ensure that the failure occured towards the middle of the column height.

Slender columns were also the subject of a series of tests on 17 reinforced concrete columns reported by Pannell and Robinson [35],[36],[37]. The columns had the dimensions 2.5 in x 3.75 in (64 mmx 95 mm). Four bars of 5/16 in (16 mm) diameter were placed in each corner. The test rig was stated to be similar to that used by Meek [33].

Tests on 8 reinforced concrete columns were reported by Cranston and Sturrock [18]. The cross section of the columns was 100 mm x 400 mm, representing virtually an extreme aspect ratio. In the context of bridge structures, these specimens approximate the behaviour of piers rather than columns. All columns had the same length of 5000 mm, and were pin ended. The reinforcement consisted of 4 bars of 1/2 in (12 mm) diameter. The applied longitudinal loading had biaxial eccentricities.

Tests conducted by Aas-Jakobsen and Aas-Jakobsen [1] on 20 columns of size 70 mm square have been quoted by Cranston [16]. The length/depth ratio of the columns varied from 21.9 to 42.8. The columns had their ends effectively pinned, and the load applied was uniaxially eccentric.

Furlong [24] reported tests on 23 columns, 9 of which had rectangular cross section of 5 in x 9 in (127 mm x 229 mm). The other 14 specimens had round ended cross section with overall dimensions of 5 in x 11 in (127 mm x 280 mm). The rectangular section had 10 bars of size 3/8 in (10 mm) diameter, while the round ended cross section had 12 bars of the same diameter. These sections, as with Cranston and Sturrock's sections, are more likely to be found in bridges than in buildings. All specimen had a length of 72 in (1829 mm). The ends were effectively pinned.

Two other series of interest, only in as much as they dealt with constantly tapered columns, were reported by Butler and Anderson [10] and Salter, Anderson,

and May [43]. The columns in both series were steel I-sections, with taper about one or both axes. These tests have been included in this review since the computer program VARCOLS has already been verified for the case of columns of variable sections [47].

Tests on columns with stepped sections were reported by Riad [41]. The cross sections of these columns were rectangular. Three of the columns had abrupt change in cross section at 3/4, 1/2, and 1/4 height. The specimens were all 6000 mm long, and were loaded with unequal eccentricities at the two ends. Two other specimens had uniform sections, and were loaded with equal eccentricities at both ends.

It may be noted that a majority of the test results reviewed relate to small scale models of rectangular cross section. There is a dearth of test results on full scale specimens with realistic imperfections, so that any uncertainty introduced by the scaling effects can be excluded. Similarly, a shortage of test results on cross sections other than uniform rectangular or uniform circular sections also becomes evident. Many bridge structures are built with, for example, sections that taper in one or both the bending planes from one end to the other. Similarly, octagonal columns are sometimes adopted in bridge structures, but no test results were obtainable for this type of construction in the published literature.

CHAPTER 2

THEORY AND VALIDATION OF THE COMPUTER PROGRAM "VARCOLS"

2.1. INTRODUCTION

The program VARCOLS has been [48] written for the inelastic stability analysis of restrained pin-ended columns having an axial load and biaxial end moments. The column cross-section may consist of a combination of several materials, with known stress-strain characteristics, acting compositely. Provision has been made to vary the cross-section along the length. Bare metal columns, concrete encased steel stanchions, concrete filled steel tubular columns, as well as reinforced concrete columns can all be analysed. The end eccentricities of the applied load, or the applied end moments, in the two bending planes can be all different. The restraints at the ends are applied in the form of moment-rotation characteristics which can be nonlinear. Lateral loads on the column are specified in the form of an initial simply supported bending moment profile in each of the two bending planes.

A variety of load paths can be traced by specifying any one of the four end moments or the axial load as the principal variable with the other four components of loading either remaining constant or varying in the same proportion as the principal variable.

The analysis essentially consists of obtaining equilibrium shapes corresponding to increasing values of the principal variable up to, and if desired beyond, the peak of the applied load versus deflection response curve. Second order iteration methods, particularly Newton Raphson technique, are employed together with advanced integration algorithms so that the rather large amount of computing involved is done rapidly and efficiently.

The output contains all the information necessary to describe the state of deflection, strain, and stress at points along the column length, for increasing values of the principal variable, up to, including, and beyond the collapse load.

2.2. THEORETICAL BASIS OF COMPUTER PROGRAM VARCOLS

2.2.1. GENERAL

The method is based on calculating the equilibrium deflected shape of the column, in the form of deflections at a discrete number of points, for increasing values of the applied loading. With increasing amount of inelastic stresses developing within the column, the stiffness of the column progressively reduces until, just before collapse, it completely vanishes. The load corresponding to the final deflected shape so obtained is taken as the ultimate load.

The calculation of the deflected shape of the column in equilibrium with some applied loading requires two basic algorithms. The first relates to the stress resultants within the section for an assumed strain distribution over the cross section. This phase is often referred to as the calculation of the moment-thrust-curvature relationship. The second algorithm deals with improving the values of the assumed deflections, which directly relate to the section strain distributions, so that internal stress resultants approach equilibrium with the external forces and moments at convergence. For this phase a rapidly converging NEWTON-RAPHSON procedure has been adopted.

2.2.2. MOMENT-THRUST-CURVATURE RELATIONSHIP

The biaxial curvatures ϕ_x and ϕ_y, together with d_n, the distance from the neutral axis to the most highly stressed corner-compression strain, can be used to establish the strain distribution in a cross section. The total curvature is given by

$$\phi = (\phi_x + \phi_y)^{\frac{1}{2}} \qquad \ldots(1)$$

The neutral axis lies at an angle θ with the y-axis, such that

$$\theta = \tan^{-1} \frac{\phi_y}{\phi_x} \qquad \ldots(2)$$

The resulting strain distribution can be used to obtain the stress distribution in the section using material stress-strain curves represented by

$$\{\sigma\} = \{\sigma(\varepsilon)\} \qquad \ldots(3)$$

where ε is the strain at any distance d from the neutral axis. From the assumption that plane sections remain plane upon flexure, it follows that

$$\varepsilon = \phi.d \qquad \ldots(4)$$

The stress resultants can then be established as

$$P = \int_A \sigma.dA \qquad \ldots(5)$$

$$M_x = \int_A \sigma.x.dA \qquad \ldots(6)$$

$$M_y = \int_A \sigma.y.dA \qquad \ldots(7)$$

Equations 1, 2, 5, 6 and 7 represent the moment - thrust - curvature relationships. In order to obtain the values of parameters corresponding to the required value of P, a Newton type convergence technique has been used. A Gaussian cubature technique has been adopted by Virdi (47) resulting in demonstrably rapid evaluation of the integrals (5) - (7). The Gauss cubature process is used to replace an integral by a weighted double summation of the values of the integral:

$$I = \int_{-1}^{1} \int_{-1}^{1} f(\xi,\eta)d\xi d\eta = \sum_{i=1}^{n} \sum_{i=j}^{n} H_i H_j f(a_i,b_j) \qquad \ldots(8)$$

where, H_i and H_j are the weighted coefficients and a_i and b_j are the coordinates of the points where the function f is evaluated.

These equations apply to a square area between the limits -1 and 1. Any quadrilateral area in Cartesian coordinates can be transformed from the (ξ , η) coordinate system to the Cartesian system (Fig. 2.1), thus:

$$x=\tfrac{1}{4}(1-\xi)(1+\eta)x_p+\tfrac{1}{4}(1+\xi)(1+\eta)x_q+\tfrac{1}{4}(1+\xi)(1-\eta)x_R+\tfrac{1}{4}(1-\xi)(1-\eta)x_s$$

$$y=\tfrac{1}{4}(1-\xi)(1+\nu)y_p+\tfrac{1}{4}(1+\xi)(1+\eta)y_q+\tfrac{1}{4}(1+\xi)(1-\eta)y_R+\tfrac{1}{4}(1-\xi)(1-\eta)y_s$$

The elemental area of $d\xi$ and $d\eta$ can also be transformed to dx dy, such that

$$dxdy = |J| \; d\xi d\eta$$

where, [J] = Jacobian = $\frac{1}{4}\begin{bmatrix} -(1+\eta) & (1-\eta) & -(1-\eta) & (1-\eta) \\ -(1-\xi) & -(1+\xi) & (1+\xi) & (1-\xi) \end{bmatrix}\begin{bmatrix} x_p & y_p \\ x_q & y_q \\ x_R & y_R \\ x_s & y_s \end{bmatrix}$

Thus, an integral in cartesian coordinates may be evaluated as follows

$$\int_A g(x,y)dxdy = \int_{-1}^{1}\int_{-1}^{1} g(x,y)\ |J|\ d\xi d\eta = \qquad \ldots(9)$$

$$= \sum_{i=1}^{m}\sum_{j=1}^{m} H_i H_j g(x_i,y_i)\ |J|$$

where x_i and y_i are the Gauss Points (a_i, b_j) in cartesian coordinates.

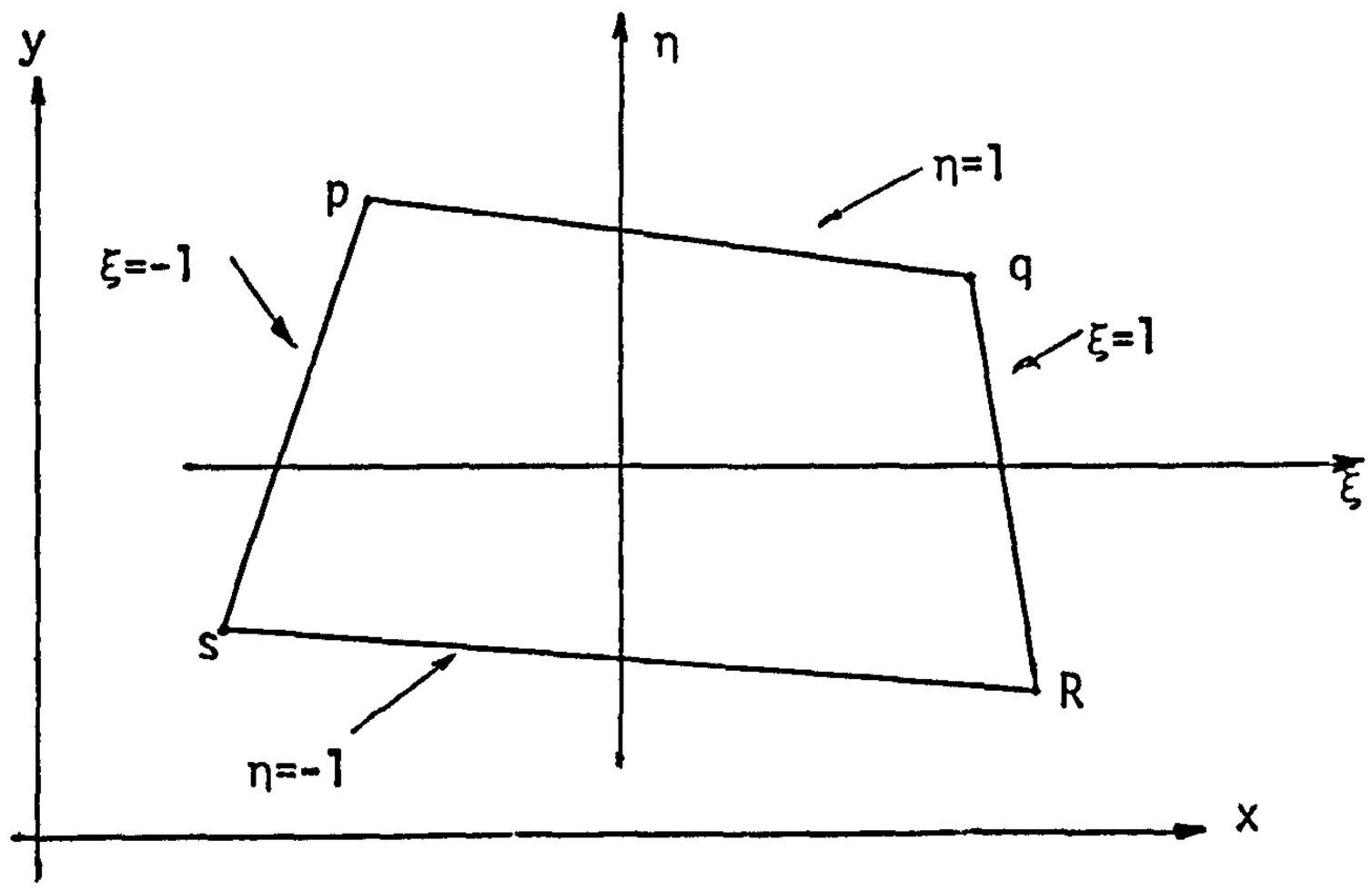

Fig. 2.1 shows the coordinate system used for the GAUSS cubature

The above procedure can be used to analyse columns of any cross section provided it can be subdivided into a series of quadrilaterals. For example, an octagonal cross section can be treated as made up from three quadrilaterals.

2.2.3. EQUILIBRIUM DEFLECTED SHAPE

Fig. 2.2 shows a column under the action of thrust P applied at end eccentricities e_A and e_B at ends A and B respectively,

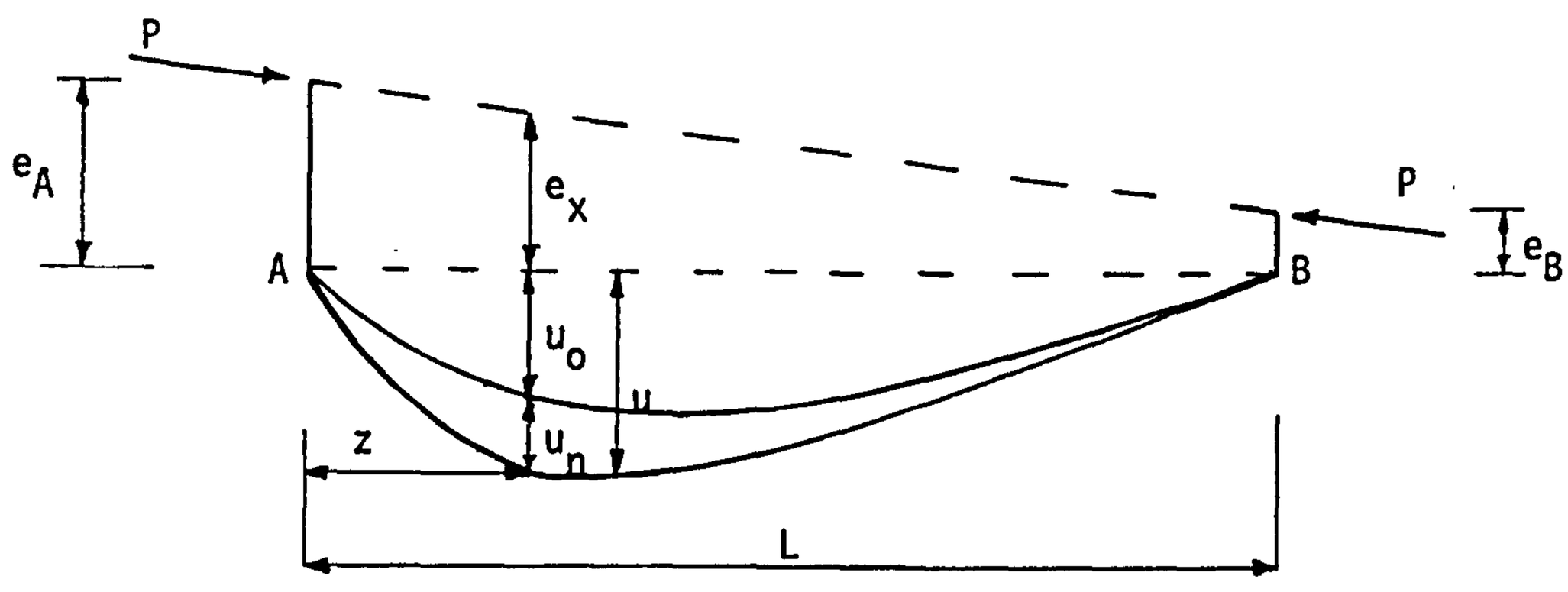

Fig. 2.2 Column under the Thrust P applied at end eccentricities.

At any stage of loading, the initial deflected shape represented by u_o at a distance Z from the node A, undergoes a change to enable equilibrium to be maintained. Hence the total bending moment M_x at point Z, becomes

$$M_x = P\ (e_x + u_o + u_n) \qquad \ldots(10)$$

$$u = \frac{M_x}{P} - e_x \qquad \ldots(11)$$

Similar equations can be written for deflections in the y-direction.

The biaxial curvatures ϕ_x and ϕ_y can be approximated as follows:

$$\phi_x = -\left(\frac{d^2u}{dz^2} - \frac{d^2uo}{dz^2}\right) \qquad \ldots(12)$$

$$\phi_y = -\left(\frac{d^2u}{dz^2} - \frac{d^2uo}{dz^2}\right) \qquad \ldots(13)$$

It follows that the bending moment M_x is a non-linear function of u and v, assuming P to be a constant at any stage of loading. The generalised Newton-Raphson method was adopted to calculate the system of non-linear equations involved.

The procedure is based on sub-dividing the column into n equal segments, each of length h. At any station s, the curvature can be calculated using the finite difference approximation.

If $\{w^k\}$ represents the vector of deflections close to the exact solution and the superscript k denotes the number of iterations, it follows that

$$\phi^k_{xs} = \frac{1}{h^2}\left(-w^k_{2s-3} + 2w^k_{2s-1} - w^k_{2s+1}\right) \qquad \ldots(14)$$

similarly

$$\phi^k_{ys} = \frac{1}{h^2}\left(-w^k_{2s-2} + 2w^k_{2s} - w^k_{2s+2}\right) \qquad \ldots(15)$$

using equations (10) and (11)

$$W^k_{2s-1} = \frac{M^k_{xs}}{P} - e_{xs} \qquad \ldots(16)$$

$$W^k_{2s} = \frac{M^k_{ys}}{P} - e_{ys} \qquad \ldots(17)$$

The calculated deflections may be considered to be functions of the assumed deflections. Thus

$$\{W^k\} = \{W^k \quad (w_1, w_2, \ldots w_{2n+2})\} \qquad \ldots(18)$$

Equations of this type may be solved using the Newton-Raphson iteration technique for a system of non-linear equations. Thus

$$\{w^{k+1}\} = \{w^k\} - ([I] - [J])^{-1}\{w^k - W^k\} \qquad \ldots(19)$$

in which [I] is a unit matrix and the Jacobean [J] needs to be evaluated numerically. Virdi [47] has shown that this can be achieved with a minimum of computation, providing certain features of the finite difference formulae are used to advantage.

For the next iteration $\{w^k\}$ is replaced by $\{w^{k+1}\}$ and the processess repeated until satisfactory convergence is obtained.

2.2.4. STABILITY ANALYSIS

If α is defined as a load factor on the initial loading $\{F_o\}$, the structure is analysed for varying end loads $\{F_\alpha\}$ given by

$$\{F_\alpha\} = [(\alpha - 1)G + I]\{F_0\} \qquad \ldots(20)$$

where [I] is an identity matrix, and [G] is a diagonal matrix, the elements of which are 1 or 0 depending upon whether the corresponding load component changes with α or not. The highest value of α for which an equilibrium shape can be obtained would be the load factor corresponding to the limit state of collapse.

The computer program VARCOLS, written on the basis of the above formulation, thus provides a means of calculating the ultimate loads of reinforced concrete columns including the material and geometric non-linear effect and for an arbitrary cross-sectioned shape, as long as it can be represented by a series of quadrilaterals.

2.3. COMPARISON OF TEST RESULTS WITH RESULTS FROM PROGRAM "VARCOLS"

Several of the test series inserted in the previous chapter have been used to validate the computer program "VARCOLS" and which has been used as the basis of subsequent studies in this project.

In carrying out the comparison between the experimental results and the theoretical results as predicted by the program VARCOLS, it has been assumed that the strength of concrete in the column is 0.67 times the reported cube strength, or 0.85 times the cylinder strength if cylinders rather than cubes were used. These factors are recommended in CP110 [15] and BS5400:Part 4 [8], as well as in CEB Recommendations [11], and are based on research carried out for CEB. A similar factor (0.64) was obtained for the case of composite columns as reported by Virdi and Dowling [45], by comparing the strength of concrete obtained from stub composite columns with the corresponding cube strength. A similar exercise was carried out at The City University for stub reinforced concrete columns and a value of 0.64 was obtained. The details and results of these tests are reported in chapter 4 of this thesis.

The results for the comparison are given in Tables 2.1 to 2.9. The Tables are labelled by their authors' names, and arranged in alphabetical order of the first author's name.

The last column in each Table gives the ratio between the experimental failure load and the calculated failure load. The average value of this ratio for the 132 tests listed is 1.32 with a standard deviation of 0.26. A summary of the comparisons is given in the Table 2.10.

A close examination of the tables reveals that only in one case the results given by the computer program appear to be on the unsafe side, namely four of the eight tests reported by MacGregor and Barter [28]. These four columns were reported to be restrained at the ends, but were otherwise identical with the other four columns, which were pin ended. Since the ultimate test loads obtained for the restrained columns were not too different from the pin ended columns in two cases, and in the other two cases the failure was reported to have occurred at the joint between the column and the restraining beam, it appears that the theoretical restraint assumed in the present computer analysis was in fact not realised. This readily explains the nonconservative nature of the results for the four columns in question.

On the other extreme are the results reported by Cranston and Sturrock [18]. The computer results obtained for their tests are on average conservative by 97 percent. One possible explanation may be found in the excessive friction reported in the end bearings used in the tests, so that the nominally pin ended columns were in fact rotationally restrained. This should result in higher than expected experimental failure loads. It is worth noting that Cranston's own theoretical results are even more conservative than obtained from using the computer program VARCOLS.

The next most conservative set of results is that reported by Pannel and Robinson [37]. These tests were all carried out on small scale models, and it is likely that the test results reflect discrepancies due to scale effect.

In the light of the above, the correlation between the test results collected from the literature and the computer results from the program VARCOLS should be regarded as satisfactory, since the theory used is shown to be safe overall inspite of a wide variety of test procedures spanning almost three decades of research on reinforced concrete columns.

2.4. CONCLUSIONS

(1) The analytical method developed by Virdi [45]-[48], on which the computer program VARCOLS is based, appears to be the most general method of analysis of reinforced concrete columns available in literature. The method caters for realistic material properties, geometrical imperfections, end conditions, and different load paths. The method is capable of analysing columns of a variety of cross sections that can be built up from quadrilateral blocks or circular arc segments.

(2) A comparison with test data collected on 132 columns shows that, on the whole, the computer program VARCOLS gives results that are conservative without being unduly so. In the isolated case of four restrained columns for which non-conservative computer results were obtained, the explanation lies in the evidence that the beam restraints were found to be ineffective in the tests, rendering them effectively pin ended. Thus, on this evidence, the computer program VARCOLS can be used, with confidence, for parametric studies on reinforced concrete columns of most types encountered in bridge structures.

(3) A vast majority of test results available in literature relate to specimens of short length for which slenderness effects would be small. The few tests on slender columns were carried out on small scale specimens of rectangular cross section. Further, very few of the tests available relate to columns of variable cross section, or columns of non-rectangular section, such

as octagonal or other shapes frequently encountered in bridge structures. Need, therefore, existed for tests on full scale specimens of rectangular, octagonal, and other practical cross sectional shapes, including columns in which the section along the length does not remain uniform for architectural or structural reasons. The tests described in Chapters 4, 5 and 6, are aimed to fill this need.

(4) Design criteria for the serviceability limit state do not appear to have received much attention in the published research work. This is probably due to the fact that requirements for serviceability can perhaps be best assessed by monitoring real structures rather than models in a laboratory.

CHAPTER 3

EXPERIMENTAL PROGRAMME

3.1. INTRODUCTION

A total of 21 tests were carried out on reinforced concrete columns of variable cross section, under the sponsarship of Department of Transport and Transport and Road Research Laboratory. 19 of these tests are described in this thesis, the other two were outside the scope of this thesis. The tests reported here were divided into four Series, namely A, B, C and D, and are described in Chapters 4, 5, and 6.

This chapter describes the manufacture of the specimens tested, the general instrumentation used, the loading rig and the test procedure adopted. All specimens were designed, manufactured and tested in the Laboratories of the Civil Engineering Department. A special loading rig had to be designed and constructed since no such rig to test full scale models was available. Considering the length of the columns tested, namely 6m and 9m, it was decided to carry out the tests in a horizontal position. Hence, an additional rig had to be designed and constructed to counter-balance the self-weight of the specimens. The measurement recorded included, deflections, concrete and reinforcement strains, the level of load applied and the monitoring and marking of surface cracks.

3.2. MANUFACTURE OF SPECIMENS

All the specimens were cast horizontally in timber moulds. Four hooks for the case of medium length columns and six hooks for the case of long length columns, were cast along with the column positioned in such a way that the level of strain caused by the lifting and haulage of the specimens was as low as

possible, usually within 10 microstrains.

Investigation of the accuracy of manufacture of the specimens showed that the overall dimensions of the cross section were kept to a tolerance of 5mm. Also, the longitudinal reinforcement bars were positioned to a tolerance of 5mm, showing that the overall straightness of the specimens did not vary by more than 5mm from the centre line. In the light of these observations, no further specific measurements of positioning of reinforcements were made.

A clear cover of 30mm was used for all specimens. Plastic spacers were used to ensure that the space between the outside face of stirrups and the mould had the designated cover.

The side forms were struck at 72 hours. The column specimen and the cubes were kept moist for the same period, and were allowed to cure under ambient conditions until the day of the test.

The transportation of the specimens from the curing location to the loading rig was made by lifting and haulage using cranes. The hooks cast in the columns ensured that the maximum dead weight strain induced in the specimens during transportation was less than 10 microstrains.

3.3. INSTRUMENTATION

For all columns, electrical resistance strain gauges were positioned at pre-selected sections along the column length. For the first two specimens tested, namely MCU0-02 and MDU0-03, six gauges were pasted at each section. It was found that if one of the corner gauges was lost due to any reason, the strain distribution in the section could not be reliably established. For this reason, for all subsequently cast specimens, at each section, the strain gauges were pasted one at each of the eight reinforcement bars, ensuring that the strain distribution at each section would be fully defined even if any one

strain gauge was lost or damaged.

For the case of medium length columns, the five sections, where the strain gauges were pasted, were located at quarter height, midheight, three-quarters height and one section close to each of the two ends. For the case of long length columns, seven sections were selected and positioned at every L/8.

To ensure satisfactory working of the gauges, it was necessary to adopt the following procedure:

1. The reinforcement bars were ground to a smooth finish at the position of each gauge. Care was exercised to ensure that the loss of steel area was only superficial.

2. An adhesive resin was applied on to the ground reinforcement bar, and the strain gauge was then pasted in the position. Next, the gauges were coated with Araldite Quick Setting epoxy resin, in order to protect them from moisture when cast.

3. The strain gauge circuits were tested using an electrical measuring meter.

The length of each strain gauge was 10.0mm with an average gauge factor of 2.11 (supplied by the manufacturer). The strain measuring circuit included dummy strain gauges fixed to an unstressed concrete specimen.

During the testing period, strain gauges were scanned through a computerised data logger, COMPULOG FOUR, with a nominal capacity to read 200 channels at a speed of 33 channels/sec. A program developed in the Civil Engineering Department of The City University, was used to scan, process, store and print the data collected.

The concrete strains were measured using demountable mechanical gauges between Demec studs. The studs were fixed on to the sides of each column at

selected points, by means of a quick hardening resin. A gauge length of 4 in (101.6mm) was used in all columns. The sections where the Demec studs were fixed, were the same as the strain gauges.

The deflection of the specimens under loading was measured using dial gauges. These gauges were supported on a rig isolated from the loading rig, so that the deflections measured were absolute. Deflections were measured at pre-selected sections, with two gauges per section, one for the horinzontal and the other for the vertical plane. An additional gauge was placed where the column was predicted to fail, so that the maximum failure deflection could be recorded. The gauges used had an accuracy of 0.01mm and travel of 20mm for Series A and 50mm for the other Series.

In addition to these measurements, a close watch for any cracks was maintained and any cracks appearing were marked with a black pen and the load recorded.

The magnitudes of the axial loads were monitored by a bonded strain gauge load cell (DS-1800, having capacity up to 5000kN), complete with a loading plate capable of tilting with the column.

The axial loading was applied by a double-acting hydraulic cylinder jack with a capacity of 5000kN maximum.

The columns were tested in a horizontal position to enable close scrutiny of the column as the test advanced. This necessitated a "Christmas Tree" arrangement to support the self weight of the column. A Dartec M1000 servo-hydraulic actuactor with a capacity of 250kN, together with a Dartec M1000/S static control panel were used to program and control the actuactor electronically, maintaining a constant load, equal to the self weight of the column, irrespective of the deflected position of the column under load.

3.4. LOADING RIG

No rig to test columns of lengths 6m and 9m was available in the Departmental laboratories. A rig was specially designed for the purpose. It was decided to use the strong floor, testing the columns in a horizontal position, to simplify the monitoring of various gauges, and therefore to keep the entire column length under observation throughout the duration of the test. A general arrangement of the rig together with some equipment used during the tests, is shown in Fig 3.1. The rig was fabricated in the workshops of the Structures Laboratory, Civil Engineering Department, at The City University.

A substantial steel reaction block was designed and constructed to support a maximum horizontal load of 5000kN at a height of 1 m. Due to the high level of the load, many difficulties arose from the very beginning. Some of these are listed below:

1. The holes in the strong floor had to be enlarged and reinforced to enable positioning of the high strength Macalloy bars used to hold the rig to the strong floor.

2. To resist the rather high bending moment resulting from the 1m lever arm, two sets of long Macalloy bars were used to stabilise the tops of the steel anchor blocks. Thus the reaction was supplied partly by the strong floor and partly by these long Macalloy bars. These bars also helped to prevent the rig from deflecting too much in relation with the strong floor, ensuring that the loading applied remained horizontal throughout the test.

3. To test the columns horizontally requires some mechanism for counter-balancing the dead weight of the specimens. Reference has already been made to the "Christmas tree" scheme employed for this purpose. The arrangement of the self weight rig is shown in Fig. 3.2. The self weight rig was controlled and supported by a 250kN servo-actuactor and a static control pannel, enabling

the dead weight of the specimen to be counter-balanced even after the column had deflected under the applied axial load.

The longitudinal load was applied by means of a double-acting hydraulic jack. The jack was reacted off the steel reaction block. The column was placed in the rig with the jack at the eccentrically loaded end and the load cell at the concentrically loaded end. For the first specimens, a ball and socket type bearing was used at the jack end. For the remaining specimens, a Glacier bridge bearing of the rotational, non-tranlational type was used. It was hoped that this would add to the realism of the full scale tests. At the load cell end, freedom of rotation was provided by a tilting plate with a concave surface, and the load cell itself had a matching close fitting convex head, coated with PTFE.

The axial loading was measured by a digital voltmeter connected to the load cell, and also by a meter in the pump circuit which had been used to activate the jack. The load cell was calibrated prior to the test using a compression load machine (AVERY-DENISON 200 tons) and using the same voltmeter as was used during the tests.

3.5. TEST PROCEDURE

Firstly, the specimens were placed in the self-weight rig. The self weight suspender supports were adjusted in order to balance the weight and to have the ends at the exact positions for the desired eccentricity. Templates were bolted on to the ball bearing at the jack and to the outside dish of the load cell. It was found to be easier to bolt the templates at the design eccentricity. Since the templates were of the same size as the column end in each case, the next step was to fasten these to the column ends using the Araldite Resin. This procedure ensured that the correct placing of the specimens in the loading rig would be anchieved.

Before recording any measurements, it was imperative to apply a small load to ensure that the specimens were adequately stabilized in the loading rig. The "zero" load readings were recorded. The loading was then increased in small increments up to complete failure.

Deflections and strains were recorded at each increment of load. For the strain gauges, four scans were specified to the data logger, so that the strain gauge readings reported are the average between these four readings. This procedure also enable an estimate of the drift in the readings to be made, thereby identifying defective gauges or circuits.

The load level was read at both its instantaneous value and also at the end of a load stage (usually 5-10 minutes). This was necessary as some leakage from the jack was noticed and also due to a small percentage of slip at the end reaction blocks.

When the applied longitudinal load reached about 80-85% of the expected failure load value (attainment of this stage was also indicated by somewhat larger creep deflections at a constant level of load), the dial gauges were removed. From that point on, only the strains measured by the data logger were recorded until the failure load was reached. One last set of strain readings was taken, after the column had already failed and the axial load allowed to drop to zero.

CHAPTER 4

SERIES A AND B - MEDIUM COLUMNS

4.1 INTRODUCTION

AS part of Series A and B, tests were carried out on 7 reinforced concrete columns, all 6.0 m long. The first 3 specimens were part of Series A while the remaining 4 specimens formed Series B. All specimens, except column MCUO-02, were tested under uniaxially eccentric loading at the stronger end and nominally concentric at the other end.

The five sections where the deflections and the concrete and reinforcement strains were measured, were located at quarter height, midheight, three-quarters height and one section close to each of the two ends.

A set of measurements for each column is provided as well as the comparisons between test results and the failure loads obtained from VARCOLS and the Limit State loads according to BS5400:Part 4 [8].

4.2. DETAILS OF TESTS

Four of the seven columns in Series A and B had tapering rectangular cross sections. Another two of the columns had octagonal cross sections, uniform along the length. The remaining specimen had a uniform rectangular shape. In all cases, the percentage of reinforcement was kept as close as possible to that in some of the actual columns designed by various Road Construction Units. The details of several such columns were supplied by the Department of Transport.

In the specimens tested, eight longitudinal reinforcement bars were placed symmetrically in the cross section of each column. The links, 8mm diameter, were

positioned at 200mm centers. In arriving at suitable details of reinforcement at the column ends to deal with the concentrated load applied at the end, guidance was obtained from the clauses relating to end blocks for prestressed concrete beams.

All specimens, except one, were tested with a concentric load at the weaker of the two ends. In all cases, at the other end, a uniaxially eccentric load was applied. For the single case of the uniform rectangular column, unequal uniaxial eccentricities were applied at the two ends.

The cross section and reinforcement details for the specimens tested are shown in the Figs. 4.1 to 4.4.

4.2.1 SPECIMENS OF SERIES A

In order to facilitate, as far as possible, the use of the same formwork for subsequent specimens of similar dimensions but perhaps with different levels of eccentricity, it was decided to have the first three columns in the Series, all with different shape enabling work on the fabrication of the three specimens to proceed in parallel.

The first specimen, Column MCUO-02, had a square uniform cross section of dimensions 400mm x 400mm. Eight longitudinal reinforcement bars of 16mm diameter were placed in the two-thirds of the length of the specimen. In the remaining length, eight longitudinal bars of 20mm diameter were used to allow for increasing moments. This particular column had uniaxially eccentric loading at both ends. At the stronger end, a uniaxial eccentricity of 110mm was applied and at the weaker one, of 55mm.

The second specimen, Column MDUO-03, was tapered in both planes. It had a square cross section of 300mm x 300mm at the stronger end and 200mm x 200mm at the other. Eight longitudinal reinforcement bars of 16mm were placed all along

the length. At the stronger end an eccentricity of 60mm was applied, while the loading was nominally concentric at the other end.

The third specimen, Column MTUO-04, had a taper in one plane only, with a rectangular cross section of 300mm x 250mm at one end and 200mm x 250mm at the other. As in the previous specimen eight longitudinal bars of 16mm diameter were used. The load was applied at an eccentricity of 25mm at the stronger end, and concentrically at the weaker one.

4.2.2. SPECIMENS OF SERIES B

The second series of tests covered four columns. Two of the columns with rectangular cross section were identical to two of the specimens in the previous Series. Thus, Column MDUO-05 was identical to Column MDUO-03, while Column MTUO-06 was the same as Column MTUO-04. Both columns were tested with nominally concentric loading at the weaker end and uniaxial eccentricities at the stronger end, as before. The magnitudes of the eccentricities were much higher than those for the Series A columns.

The other two columns in the Series, Column MGUO-07 and MGUO-08, were identical with each other. Again, these columns were tested with a nominally cconcentric load at one end and uniaxially eccentric load the other. The end eccentricity for Column MGUO-07 was half that used for Column MGUO-08. Both columns had a uniform octagonal cross section along the length with a depth of 250mm. Eight longitudinal reinforcement bars of 16mm were used and again the ends were strengthened in accordance with the clauses relating to end blocks.

Fig. 4.5 shows a view of reinforcement cage for one of the octagonal section columns, in the formwork, ready to be cast.

4.2.3. MATERIAL PROPERTIES AND MANUFACTURE OF SPECIMENS FOR SERIES A AND B

The concrete used for casting the specimens was designed to have a 28-day cube strength of 35.0N/mm^2 using Ordinary Portland Cement and 20mm maximum aggregate size.

All specimens were manufactured from the same batch of materials (sand,aggregate,cement,reinforcement bars, etc) and similar casting and curing procedures were adopted. Generally, nine or twelve cubes were cast with each column and tested on the same day as the column. The observed cube strengths for each column are given in Table 4.1.

Short lengths of steel, cut at random from the lengths used in the tests specimens, were subjected to standard tensile tests. A very consistent set of yield strength values were obtained. Table 4.2 shows the values obtained for Series A and B specimens.

4.3. TEST RESULTS

The failure load in all cases, except for Column MCUO-02, followed an almost parallel course, that is, instability failure occurred by compression combined with flexural stresses after the column had been subjected to large lateral displacements. The pattern of the lateral displacements was similar in all seven specimens and agreed with the expected mode, so that the displacements continued to increase slowly with load increments until just before failure, at which stage the column continued to show increase in deflections without any load increment. At this stage, the concrete started to spall on the concave side of the bent column. Almost immediately, the concrete cracked on the tension side, followed by buckling of the longitudinal reinforcement bars outwards. The final failure was, in general, sudden, indicating compression failure of concrete, rather than tensile failure of steel. In the ligth of the above, it

may be considered that the columns tested satisfied the usual serviceability requirements of cracking up to the collapse load.

In the case of Column MCUO-02, when the applied longitudinal load reached about 80% of the expected failure load, the pump started leaking intensively, due to the failure of a joint in the pipework. As the values of strains measured were very near to the yield strain of steel, the test was not continued and the readings recorded up to that load were taken as the failure values.

Complete failure was obtained in the case of all other columns. A typical view of a failed column in the rig is given in Fig. 4.6, which highlights the bend in the column.

Fig. 4.7 gives a typical view of the mode of failure. The characteristic tension cracks and compression crushed concrete are both illustrated. Similar pattern was observed for all the other columns tested to failure. A close up of the failure section is shown in Fig. 4.8.

In all cases, no notable tensile craks were developed until just before the failure load was reached. When the column failed, the tension cracks were very accentuated and localised at the failure section only. One of the reasons why the cracks did not develop early might be due to the fact that the level of eccentricity in these specimens was relatively low. Also, the slenderness ratio of these columns was not sufficiently high. Both these factors combine to explain the compression type sudden failure obtained in the tests. The next Series of tests had a slenderness about 50% higher than the columns described in this Chapter. It was hoped that the mode of failure would involve a more even spread of tensile cracking.

4.4. COMPARISON of PROGRAM VARCOLS and TEST RESULTS

4.4.1. GENERAL

Theoretical results were obtained using the computer program, VARCOLS, capable of computing ultimate load of a column based on realistic imperfections, loading, as well as nonlinear material properties. A description of the program and its theoretical basis, was described in Chapter 2.

The computed results were obtained on the basis of a crushing strain of concrete having a value of 0.0035 and a maximum concrete stress of 0.67 times the observed cube strength. A parabolic- rectangular stress block, as specified in BS5400:Part 4 [8], was adopted for concrete. For steel, a trilinear curve, in accordance with the same code, was assumed. An initial lack of straightness of 0.001 times the column length was assumed as standard. However, results were also obtained on the basis of initially straight columns, and these are discussed in Section 4.3.6 below. In what follows, the test results are presented for each column separately. Maximum deflections and strains for selected points are plotted against load for each specimen.

4.4.2. ULTIMATE LOADS

Table 4.3 gives the ultimate loads for the 7 specimens tested. The last column in the table gives the ratio between the experimental failure load and the calculated failure load obtained from the computer program VARCOLS. The mean value of this ratio for the seven tests listed is 1.35 with a standard deviation of 0.22. The test results reveal that only in one case, Column MTUO-04, the result given by the computer program is marginally (by about 5%) on the unsafe side. Hence, the correlation between the test results and computed results should be considered satisfactory.

4.4.3. LOCATION OF FAILURE ZONE

The section where the column failure occurred was very similar for each pair of columns (that is, MTUO-04 and MTUO-06, MDUO-03 and MDUO-05, MGUO-07 and MGUO-08). In the case of rectangular tapered columns, failure was located at about two-thirds of the column length from the end where the eccentric load was applied, whereas for the octagonal cross section it occurred at about one-third the column length from the eccentrically loaded end. These locations agree with the theoretical positions obtained from the program VARCOLS, as shown in Table 4.4.

4.4.4. LOAD vs DEFLECTION CURVES

A set of graphs showing the maximum deflections against load for each column, together with the results computed from the program VARCOLS is given in Figs. 4.9 to 4.15.

Generally, the computed and measured deflections are in good agreement. This is particulary true for columns MDUO-03, MTUO-04, and MDUO-05. In only one case, Column MGUO-08, the computed deflections were much bigger than the experimental one. This could possibly be due to the fact that the concrete mix for this column resulted in very low cube strength values, whereas the concrete strength in the column may have been higher. A series of squash load tests on specimens cut off from the undamaged parts of each of the columns were tested later and are reported in Chapter 5 of this thesis.

4.4.5. LOAD vs STRAIN CURVES

The load vs strain graphs were obtained by plotting the maximum measured strains against the load applied. For each column, a similar curve is also plotted using the values computed by the program VARCOLS. The set of curves is

given in Figs. 4.9 to 4.15. Once more a reasonable agreement between the tested and computed strains has been obtained for most of the columns. However, the marked difference noted for the deflections of Column MGUO-08 is also reflected in the strain values for this column.

It is interesting to note that the maximum strain measured from the specimens tested, was in all cases less than 0.0025. This value is considerably less than the value of 0.0035 that is specified in many Codes of Practice for reinforced concrete. In order to examine the effect of this difference in the crushing strain of concrete on the design strength predicted by the Limit State Code for Bridges BS5400:Part 4 [8], a separate study was done and it is included in the Appendix A.

4.4.6. STRAIN PROFILES

A set of strain profiles were obtained by plotting the computed strains from program VARCOLS as well as the measured strains for each column for certain levels of loads. For each column, two sections were selected for this purpose. These were located at mid length, and either at three quarters length for rectangular cross sections or at one quarter length for octagonal cross sections, measured from the eccentrically loaded end. The strain profiles are shown in Figs. 4.16 to 4.22.

For the standard case, run using an initial imperfection of L/1000, and shown in the Figs. 4.16 to 4.22 using continuous lines, good agreement is obtained for the maximum compressive strains for nearly all cases. For the case of the strains at the opposite face, and hence for the strain distribution as a whole, however, a good agreement was obtained only for columns MDUO-03, MDUO-05, MTUO-06, and MGUO-07. For the remaining columns the agreement was not very good, particularly at higher load levels. It was noted that the measured profiles showed a near absence of tensile strains, even at high loads. This indicated

that possibly the assumption of an initial lack of straightness of L/1000 was too pessimistic. Comment has already been made of the rather small imperfections measured in the columns prior to casting. Accordingly, analytical results were also obtained for the case of zero imperfection. The strain profiles for this case are shown in the Figures using dashed lines. The agreement between the measured and analytical strain profiles improves significantly for all specimens confirming the absence of initial imperfections.

The ultimate failure loads obtained for the case of zero imperfections are given in Table 4.5, along with the test results and the results for the case of L/1000 imperfection. It is notable that the mean value of the ratio of experimental to theoretical failure loads reduces to 1.25 with a standard deviation of 0.21. This indicates better agreement for all cases, except column MTUO-04.

4.5. COMPARISON OF BS5400:Part 4 AND TEST RESULTS

For the calculation of the strength of rectangular tapered reinforced concrete columns and for the case of octagonal cross sections, a similar procedure was adopted, that is, the assumptions usually made for rectangular sections were also used for the octagonal cross section columns. In all cases, the failure loads were calculated at the mid-length, while checks were made for the resistance at the two ends as well.

When using BS5400:Part 4, two sets of values of the partial safety factors were used. For the first case, the partial safety factors for concrete and steel were both adopted as 1.0, on the grounds that laboratory conditions would result in minimum variability of concrete strength. The experimentally observed values of steel and concrete strengths were used. For the second case, the partial safety values specified in BS5400:Part 4, namely 1.5 for concrete and 1.15 for steel, together with the design characteristic strengths for the two materials were used.

For all cases, the failure section was assumed to be at mid-length. The eccentricity used at this section was taken as the actual eccentricity applied at the stronger end corrected by a factor of 0.6, in accordance with Equation (22) of BS5400:Part 4.

Table 4.6 shows the calculated failure loads for the specimens along with the test results. The last two columns in the table give the ratio between the experimental failure load and the calculated failure load for the two sets of partial safety factors, 1.0 and the values specified by BS5400:Part 4, respectively. The mean value of the ratio for the first case (partial safety factor values 1.0) is 1.57 with a standard deviation of 0.10. The mean value of the ratio using the partial safety factors specified in BS5400:Part 4 is 2.10, with a standard deviation of 0.11.

4.6. CONCLUSION

This Chapter describes 7 tests on reinforced concrete columns of variable cross section, including tapered rectangular columns and uniform octagonal columns. In all cases the failure was sudden, and was triggered by the crushing of concrete. No tensile cracks were observed, except just before the collapse, indicating that crack width serviceability criteria would be met with these columns almost upto collapse.

It was observed that the crushing of concrete occured at a strain of around 0.0025 which is considerably below the normally accepted value of 0.0035. The effect of this difference on the design strength of the slender columns when using BS5400:Part 4, is assessed and presented in Appendix A of this thesis.

A comparison between the test results and the results obtained from the computer program VARCOLS has been shown to give good agreement in terms of the ultimate failure loads, defections, and strains, for the majority of the columns tested. The results show close agreement for five columns, marginally unsafe

agreement for one column, and very conservative (by 68%) agreement for another.

The procedure given in BS5400:Part 4, applies mainly to uniform rectangular columns. When applying the steps to the case of octagonal columns, the formulae given in the Code had to be slighty modified, to account for the change of section from rectangular to octagonal.

The test results were compared with two set of calculations based on BS5400:Part 4. When the partial safety factors as specified in the Code together with the design material strength values are used, a mean ratio of test failure load to design failure load of 2.14 was obtained, with a standard deviation of 0.23. When observed steel and concrete cube strength values combined with a partial safety factors of 1.0 for both steel and concrete are used, as is usual for laboratory conditions, the mean ratio of test failure load to design failure load obtained was 1.57, with a standard deviation of 0.10. Clearly the procedure in BS5400:Part 4 is very conservative and there is scope for further improvement.

4.7. ASSESSMENT OF CONCRETE REDUCTION FACTOR

4.7.1. INTRODUCTION

In BS5400:Part 4[8] the strength of concrete in a member is taken as $0.67f_{cu}$, where f_{cu} is the characteristic cube strength obtained from tests on 28-day-old cubes. This value is of course, further divided by the partial safety factor. In the case of laboratory tests the partial safety factor is usually taken as unity. An attempt was made to assess the value of the reduction factor as realised in the current Series of tests. For this purpose, stub column tests were carried out on specimens cut from the undamaged lengths of the original test columns of Series A and B, after the specimens had been loaded to the failure.

4.7.2. DETAILS OF TESTS AND INSTRUMENTATION

Eight stub columns were cut from four specimens tested in Series A and B. The cutting machine used was a Clipper Masonary Saw which is often used for cutting bricks. It was necessary to make some adjustments to the machine in order to enable the saw to cut throughout the column sections. Following the practice for steel sections as recommended in the Column Research Council guide [54], it was decided to have stub columns with the ratio of l/b equal to 3.0, where l is the length of the stub column and b the depth at midlength of the stub column.

The stub columns were tested axially in a vertical position. A compression testing machine with a nominal capacity of 300 tons was used for the tests. The specimens were capped with a thin layer of plaster of Paris to ensure that the faces of the stub columns were parallel to the planes of the platens of the testing machine. Three dial gauges were used to monitor the vertical movement of the upper platen relative to the lower platen of the stub columns during the test. The load was increased in 15 tons (150KN) increments and was monitored by a pressure gauge capable of reaching 10000psi (3000 N/mm^2).

4.7.3. STUB COLUMN TEST RESULTS

The results of the axial compressive test on stub columns are shown in Table 4.7. The reduction factor for a given case was determined by first subtracting from the stub column ultimate load the contribution of steel, taken as the total area of steel bars times the experimentally obtained tensile strength of the bars. The result is taken as the contribution of concrete. The concrete strength is then obtained by dividing the concrete contribution to the ultimate load with the area of concrete. This value of the strength of concrete is then compared with the cube strength obtained in Series A and B. It may be

observed that the average strength of concrete in the stub columns is 0.64 times the average cube strength with a standard deviation of 0.07, which is very near to the reduction factor of 0.67 and recommended by BS5400:Part 4 used throughout this Thesis. It was also observed that in all cases the failure coccurred by general crushing of concrete. Interestingly, the spread of spalling was more or less uniform on all faces. This indicates that the casting of the specimens in a horizontal position did not introduce any significant weakening of the concrete on the side facing the top at the time of casting.

In the light of the above, it was decided to adhere to the recommended strength reduction factor of 0.67 in all theoretical and design calculations for the entire project.

CHAPTER 5

SERIES C

LONG COLUMNS - UNIAXIALLY ECCENTRIC LOADING

5.1. INTRODUCTION

Four of the six columns in this Series had tapering rectangular cross sections. The other two had octagonal cross sections, uniform along the length. All columns had the same length of 9.0m along the length.

All six columns had the same number of longitudinal reinforcement bars, eight each, as in the previous Series A and B. The bars were placed symmetrically in the cross section of each column. The links, 8mm diameter, were positioned at 200mm centres.

The cross section and reinforcement details for the specimens tested are shown in Figs. 5.1 and 5.2.

All specimens were tested with a concentric load at the weaker of the two ends. In all cases, at the other end, a uniaxially ecccentric loading was applied. The loadings applied were systematically increased in increments of 50KN up to about 90% of the failure load.

5.2. SPECIMENS OF SERIES C

The six columns in the Series were subdivided into three pairs. The two columns in a pair were identical with each other, except for the level of end eccentricity applied.

The first pair, Columns LDUO-09 and LDUO-10, were tapered in both planes. Both had a cross section of 400mm x 400mm at one end and 300mm x 300mm at the other. These dimensions correspond to a l/h_t (length to midheight depth) ratio of 26, where h_t is the midheight depth of the cross section. Eight longitudinal reinforcement bars of 16mm were placed, continuous along the length. At the stronger end, Column LDUO-09 had an eccentricity of 100mm whereas Column LDUO-10 had a corresponding eccentricity of 235mm. These eccentricities correspond to $0.30h_t$ and $0.67h_t$ for Columns LDUO-09 and LDUO-10 respectively, where h_t is the midheight depth of the cross section.

The second pair, Columns LDUO-11 and LDUO-12, were also tapered in both planes, having a cross section of 300mm x 300mm at the stronger end and 200mm x 200mm at the other. These dimensions correspond to a l/h_t (length to midheight depth) ratio of 36. As for the previous pair, eight longitudinal reiforcement bars of 16mm diameter were used. The axial load was applied at an eccentricity of 65mm for Column LDUO-11 and 175mm for Column LDUO-12 at the stronger end, whilst it was concentric at the weaker end in both cases. These eccentricities correspond to $0.25h_t$ and $0.70h_t$ for Columns LDUO-11 and LDUO-12 respectively, where h_t is the midheight depth of the cross section.

The other two columns in the Series, Columns LGUO-13 and LGUO-14 had a uniform octagonal cross section along the length with a depth of 300mm. Eight longitudinal reinforcement bars of 16mm were used. Column LGUO-13 had an eccentricity of 90mm and for Column LGUO-14, the eccentricity was equal to 120mm, with a nominally concentric load at the other end for both specimens. These dimensions correspond to a l/h_t (length to midspan depth) ratio of 30 whilst the eccentricties applied correspond to $0.30h_t$ and $0.40h_t$ for Columns LGUO-13 and LGUO-14 respectively, where h_t is the cross section depth.

Table 5.3 shows details of each column together with the level of eccentricity applied.

5.3. MATERIAL PROPERTIES AND MANUFACTURE OF SPECIMENS FOR SERIES C

The target concrete strength used for casting the specimens was the same as described in Chapter 4 for Series A and B namely 30N/mm^2. The observed cube strengths obtained from 12 cubes, size 150mm, for each column are given in Table 5.1. It will be observed that the target strengths was achieved in all cases, with a small margin of safety. Table 5.2 shows the values obtained from the standard tensile tests on short lengths of steel, cut at random from the lengths used in the test specimens. Six hooks were cast, positioned along the columnn in such a way that the level of strain caused by the lifting and haulage of the specimens was within 10 microstrains.

5.4. INSTRUMENTATION

The instrumentation used was similar to that for Series A and B tests, except for the type of bearing at the jack end. A Glacier Spherical Free Sliding Structural Bearing, as used in bridges, was procured. The bearing had a nominal capacity of 500 tons. A cross section of the bearing is shown in Fig. 5.3.

For all columns, electrical resistance strain gauges and Demec studs were positioned at seven sections along the length. The strain gauges were pasted one on each of the eight reinforcement bars, ensuring that the strain distribution at each section would be fully defined even if any one strain gauge was lost or damaged. Fig. 5.4 shows the strain gauge and Demec stud locations along the column length for all specimens.

In this Series, surface width of cracks at various stages of loading, were monitored using a microscope capable of a five times magnification.

5.5. TEST RESULTS

5.5.1. GENERAL

Columns LDUO-09 and LDUO-10 produced a very large lateral displacement under loading. Column LDUO-09 had a mode of failure that differed from that of the other five columns in the Series. At the stage where the column continued to show increase in deflections without any increase in load, the concrete started to spall on the concave side of the bent column. The final failure was sudden, indicating compression failure of concrete with the longitudinal reinforcement bars buckled outwards. No tensile cracks were observed prior to the failure load. This mode of failure may be attributed to the rather small level of the applied end eccentricity, or possibly to locally weak strength of concrete.

Column LDUO-10, due to the higher level of eccentricity applied, showed a typical flexure failure with plainly visible tension cracks. The cracks started to develop when the load applied was about 40% of the experimental failure load. From the stage when the tensile cracks first developed to the ultimate load stage, the deflections increased consistently. The maximum deflection measured was about twice the maximum deflection recorded for Column LDUO-09.

Columns LDUO-11 and LDUO-12 displayed a very accentuated bow upon loading, particulary Column LDUO-12 with the greater eccentricity of applied load.

The failure load for both these columns followed an almost parallel course, that is, instability failure occurred with very high deflections. The displacements continued to increase gradually with every load increment until the point where the tensile cracks started to develop. From this point, the increase in lateral displacements accelerated for each increment of load right up to the ultimate load, at which stage the lateral displacements were still increasing without any increment of load. Soon after this point the concrete

displayed very wide cracks on the tension side and almost at the same time the concrete started to spall on the concave side of the bent column.

The first tensile cracks were observed when the applied load was about 35% for Column LDUO-11 and 40% for Column LDUO-12,of the experimental failure load. Both columns failed at a section about two-thirds along the length, measured from the eccentrically loaded end.

The two octagonal cross section specimens, Columns LGUO-13 and LGUO-14, showed more accentuated lateral displacements in the first third of the length from the eccentrically loaded end. The tensile cracks were very noticeable from about 40% of experimental failure load for both columns.

The modes of failure for these columns were very similar to the previous pair, i.e. showed a flexure type failure with many tensile cracks developed on the convex side of the bent specimens.

Figs. 5.5 and 5.6 show a typical mode of failure for long length tapered columns subjected to uniaxial bending.

5.5.2. CRACKING BEHAVIOUR

The tensile cracks in all cases, except for Column LDUO-09, followed an almost parallel course, that is, the first tensile cracks appeared at about 35%-40% of the failure load. For the subsequent increments of loading, the cracks spread more or less evenly along the length, with a closer spacing in the region where the eventual failure section was located.

According to BS5400:Part 4[8], the surface width of cracks should not exceed the values specified in Table 1 of the Code, depending upon the conditions of the environment. In the case of laboratory tests, moderate conditions have been adopted and the design crack widths be limited to the

value of 0.25mm according to Table 1. Furthermore, the subclause 6.5.8 of BS5400:Part 4 states that "cracks due to bending in a column, designed for an ultimate axial load greater than $0.20f_{cu}A_c$ are unlikely to occur. A more lightly loaded column subjected to bending, should be considered as a beam for the purpose of crack control". Table 5.4 gives the value of $0.20f_{cu}A_c$, the ultimate load calculated from BS5400:Part 4 using safety factors 1.5 and 1.15 for concrete and steel respectively, the load which had been applied at the time when the first cracks were observed, and the region along the length where the first cracks were developed for each column tested.

It is worth noting that the first tensile cracks had a measured surface width of between 0.03mm and 0.05mm. According to BS5400:Part 4, the design width allowed under the exposure condition similiar to the laboratory enviroment can not be greater than 0.25mm. Generally, this crack width was reached only when the load applied was greater than 80-85% of the experimental failure load.

5.6. COMPARISON OF PROGRAM VARCOLS AND TEST RESULTS

5.6.1. GENERAL

The computed results were obtained using the computer program VARCOLS, validated and described briefly in Chapter 2 of this thesis. The theoretical results were obtained on the basis of a crushing strain of concrete having a value of 0.0035 and a maximum concrete stress of 0.67 times the observed cube strength. A parabolic rectangular stress block, as specified in BS5400:Part 4[8], was adopted for concrete. For steel, a trilinear curve in accordance with the same code, was assumed. An initial lack of straightness of 0.001 times the column length was assumed as standard.

5.6.2. ULTIMATE LOADS

Table 5.3 gives the experimental failure loads for the six specimens tested, together with the calculated failure loads obtained from the computer program VARCOLS. The ratio between the experimental failure load and the calculated failure load from VARCOLS is also given and the mean value for the six columns listed is 1.48 with a standard deviation of 0.24. The minimum value of this ratio was 1.18, obtained for Column LGUO-14. It can be seen that in all cases the results given by the computer program are on the safe side.

5.6.3. LOCATION OF FAILURE ZONE

Table 5.5 gives the location of failed section from the eccentrically loaded end for each column tested, as well as the corresponding values obtained from the theoretical analysis. It may be observed that the two values agree with each other very closely in each case.

In the case of rectangular tapered cross section columns, the failed section was located between one-third and one-half of the column length, from the end where the eccentric load was applied, for Columns LDUO-09 and LDUO-10 and between one-half and two-thirds, for Columns LDUO-11 and LDUO-12.

For the octagonal cross sections, Columns LGUO-13 and LGUO-14, with the section being uniform along the length, the failed section occurred at about one third of the column length from the eccentrically loaded end. The location is given in Table 5.5 for both theoretical and experimental results.

5.6.4. LOAD vs DEFLECTION CURVES

Generally speaking, the measured deflections followed the same pattern for all specimens tested, that is, small deflections until about the stage when the first tensile cracks were developed, and later, larger deflections for subsequent increments of load.

Figs. 5.7 to 5.12 give a set of graphs showing the maximum deflections at column midheight against load for each column, together with the theorectical deflections obtained from the computer program VARCOLS. The agreement between computed and measured deflections is generally good, and is excellent for Columns LDUO-11 and LGUO-14.

5.6.5. LOAD vs STRAIN CURVES

A set of load vs strain curves are given in Figs. 5.7 to 5.12. The graphs were obtained by plotting the maximum compressive strains at predetermined sections, against the load applied. The section chosen was the monitored section closest to the failed section. For each column, a similar curve is also plotted for the corresponding station along the length, using the values computed by the program VARCOLS.

It is interesting to note that for all columns tested, the maximum compressive strain recorded was never greater than 0.0025. Hence, the maximum concrete strain recommended by BS5400:Part 4, namely 0.0035, was not reached in any case of the specimens tested. These results agree with tests results reported by Pancholi and Wilby [53], who carried out tests on slender reinforced concrete uniform columns. They reported a very similar pattern for the load vs strain curves based on their tests and the maximum concrete strain measured was, often, no greater than 0.001. The effect of this observation is discussed and presented in the Appendix A of this thesis.

The experimental and theoretical curves obtained showed a consistently good agreement for all columns, specially for Columns LDUO-12 and LGUO-14.

5.6.6. STRAIN PROFILES

A set of strain profiles are given in Figs. 5.13 to 5.18 for each column. Two sections were selected, at mid length and either at two-thirds of the length for rectangular cross sections or at one-third of the length for octagonal cross sections, measured from the eccentrically loaded end. The profiles were obtained by plotting the computed strains from program VARCOLS as well as the experimental measured strains for each column for certain levels of loads.

The agreement between the theoretical and experimental curve, is good for almost all cases. Some difference can be observed for the octagonal cross section Column LGUO-13, mainly for the tensile strains.

5.7. COMPARISON OF BS5400:PART 4 AND TEST RESULTS

The column clauses in BS5400:Part 4[8], are mainly concerned with the design of uniform cross section columns in bridges. No guidance is given on the design of tapered columns. Hence, a procedure to design columns with tapering sections and columns with sections other than rectangular and circular shapes has had to be adopted. The assumptions usually made for rectangular sections were retained for the octagonal cross section columns, that is, the stress block for strength is based on a crushing strain of concrete, having a value of 0.0035 on a maximum concrete stress of 0.67 times the observed cube strength.

When using BS5400:Part 4, two sets of values of the partial safety factor were used. For the first case, the partial safety factors for concrete and

steel were both adopted as 1.0, on the grounds that Laboratory conditions would result in minimum variability of concrete strength. The experimentally observed values for the strength of steel and concrete were used. For the second set of calculation, the partial safety factor values specified in BS5400:Part 4, namely 1.5 for concrete and 1.15 for steel, together with the design characteristic strengths for the two material, rather than the experimentally observed values, were used.

For all cases, the failure was assumed to be at mid-length. Due to the fact that the eccentricity had been applied only at one end, the eccentricity used at mid-length section was taken as the actual eccentricity applied at the stronger end, corrected by a factor of 0.6, in accordance with Equation (22) of BS5400:Part 4.

Table 5.6 shows the calculated failure loads for the specimens along with the test results. The last two columns in the Table give the ratio between the experimental failure load and the calculated failure load for the two sets of partial safety factors, 1.0 and the values specified by BS5400:Part 4, respectively. The mean value of the ratio for the first case (partial safety factor values 1.0) is 1.67 with a standard deviation of 0.20. The mean value of the ratio using the partial safety factors specified in BS5400:Part 4 is 2.14 with a standard deviation of 0.24. The agreement for the first case, i.e. the partial safety value as unity is reasonably good whereas for the second case the agreement is rather far on the safe side.

5.8. CONCLUSION

This chapter described six tests on long reinforced concrete columns including tapered rectangular columns and uniform octagonal columns. All specimens were subjected to uniaxial bending.

A comparison between the test results and the results obtained from the computer program VARCOLS has been shown to give good agreement in terms of the ultimate failure loads, deflections and strains, for all cases of the columns tested. The load deflection comparisons were particularly good for Columns LDUO-11 and LDUO-14 and the load strain comparisons for Columns LDUO-12 and LDUO-14.

It was observed that the maximum compressive concrete strain was limited to 0.0025, well below the value of 0.0035 used by BS5400:Part 4 (and the same figure used by CP110). The codes mentioned use theories based on material failure for very slender columns.

For the cracking behaviour, the loads for which the first cracks appeared were all less than the value specified in subclause 6.5.8 of BS5400:Part 4. However, this is not as serious a problem as may appear at first. The maximum surface crack width allowed by the Code, namely 0.25mm, was reached when the applied load was greater than about 80-85% of the experimental failure load. It can also be seen from the previous sections that the calculated failure loads for both BS5400:Part 4 and computer program VARCOLS are smaller than 85% of the experimental failure load. Hence, it can be concluded that in all the tests the serviceability limit state load has been achieved without undue cracking, and that the clauses relating to crack control in BS5400:Part 4[8] are satisfactory.

CHAPTER 6

SERIES D

LONG COLUMNS - BIAXIALLY ECCENTRIC LOADING

6.1. INTRODUCTION

The six columns forming the Series D of the experimental programe, had the same geometrical sizes and details as columns of series C reported in Chapter 5. The two Series differed in the types of loading applied at the stronger end, that is, biaxially eccentric loading for Series D compared with uniaxially eccentric loading for Series C. The magnitude of the eccentricities applied in Series D was of the same order as the eccentricities applied in Series C, now applied about both the principal axes.

6.2. DETAILS OF TESTS

6.2.1. GENERAL

Four of the six columns in this series had tapering rectangular cross sections. The other two had octagonal cross sections, uniform along the length. All columns in this series had the same length of 9.0m. The columns tested had the same number of reinforcement bars, that is eight each. The bars were placed symmetrically in the cross section of each column. Shear links, 8mm diameter were positioned at 200mm centres.

All specimens were tested with a concentric load at the weaker of the two ends. In all cases, at the stronger end, a biaxially eccentric loading was applied.

Due to the high level of eccentricities applied in both the vertical and the horizontal directions, the loaded end of the columns had to be strengthened by the addition of an enlarged end block, in order to allow the load be applied sastifactory.

The cross section and reinforcement details for the specimens tested are shown in Figs. 6.1 and 6.2.

6.2.2. SPECIMENS OF SERIES D

The six columns in the Series were subdivided into three pairs. The two columns forming a pair were identical with each other, except for the level of end eccentricities applied.

The first pair, Columns LDBO-15 and LDBO-16, was tapered in both planes. Both had a cross section of 400mm x 400mm at the stronger end and 300mm x 300mm at the other. These dimensions correspond to a l/h_t (length to midheight depth) ratio of 26. Eight longitudinal reinforcement bars of 16mm were placed continuous along the length. At the stronger end, Column LDBO-15 had an eccentricity of 105mm in both the principal axes, whereas Column LDBO-16 had corresponding eccentricities of 150mm. These eccentricities correspond to $0.30h_t$ and $0.45h_t$ for Column LDBO-15 and LDBO-16 respectively, where h_t is the midheight depth of the cross section.

The second pair, Columns LDBO-17 and LDBO-18, were also tapered in both the bending planes, having a cross section of 300mm x 300mm at the stronger end and 200mm x 200mm at the other. These dimensions correspond to a l/h_t (length to midheight depth) ratio of 36. As for the previous pair, eight longitudinal reinforcement bars of 16mm diameter were used. The biaxial load was applied at eccentricities of 65mm in both the horizontal and the vertical directions, for Column LDBO-17 and 120mm for Column LDBO-18. In both cases the biaxially

eccentric loading was applied at the stronger end, whilst it was concentric at the weaker end. These eccentricities correspond to $0.25h_t$ and $0.48h_t$ for Columns LDBO-17 and LDBO-18 respectively.

The remaining two columns in the series, Columns LGBO-19 and LGBO-20, had a uniform octagonal cross section along the length with a depth of 300mm. Eight longitudinal reinforcement bars of 16mm were used, one in each corner. Column LGBO-19 had biaxial eccentricities of 90mm with respect to both the principal axes and for Column LGBO-20, the eccentricities were equal to 180mm. For both specimens, the other end had a nominally concentric load. These eccentricities correspond to values of $0.30h_t$ and $0.60h_t$ for Columns LGBO-19 and LGBO-20 respectively. The slenderness ratio represented by the l/h_t value was 30 for both columns.

Table 6.3 shows details of each column together with the level of eccentricities applied.

6.2.3. INSTRUMENTATION, MATERIAL PROPERTIES AND MANUFACTURE OF SPECIMENS

The instrumentation for increasing strain and deflections, and the loading rig used, were the same as used in Series A, B, and C described earlier in this Thesis. Figs. 6.3 shows details and general view of the rig and instrumentation used for the tests.

The concrete used for casting the specimens and the procedure for the manufacture of the specimens was the same as described for Series A and B in Chapter 4. The observed cube strengths obtained from 12 cubes, size 150mm, for each column are given in Table 6.1. It will be seen that the target strength was achieved in almost all cases with only a small margin of error. The values obtained from the standard tensile tests of short lengths of steel, cut at random from the lengths used in the test specimens are shown in Table 6.2. Six

hooks were cast, positioned along the column length in such a way that the level of strain caused by the lifting and haulage of the specimens was as low as possible, usually within 10 microstrains.

6.3. TEST RESULTS

6.3.1. GENERAL

In all the tests, the load was applied in increments, the size of which depended on the estimated ultimate strength of the column. At each stage of loading, surface strains in concrete and the deflections of the column about the principal axes were recorded.

For all the six specimens tested, the course followed was almost the same, that is, for each increment of load, the strains and the deflections of the column about the principal axes increased.

Column LGBO-20 had a premature failure at the end where the eccentricities were applied. This is explained by the high level of eccentricities applied, making the initial bending moment applied predominant in relation to the total bending moment.

Figs. 6.4 and 6.5 show a typical view of the mode of failure. The characteristic tension cracks and compression crushed concrete are both illustrated. By comparing the length of the widest tensile crack in Fig. 6.4 and the spread of compressive spalling in Fig. 6.5, it is clear that the inclination of the neutral axis is very close to an angle of 45 degrees.

6.3.2. CRACKING BEHAVIOUR

Table 6.4 gives the value of the load which had been applied at the time the first cracks were observed as well as the width of the cracks at this stage. Also, the region along the length where the first cracks were observed for each specimen tested is identified.

For all the columns tested in the Series, the first tensile cracks naturally appeared at the farthest corner from the applied load. It will be seen that at this stage the measured surface width was between 0.03mm and 0.05mm. As the load applied increased, the cracks progressively developed into the core of the column and widened for each increment of load. When the applied load reached about 85-90% of the experimental failure load the measured surface width was still less than 0.25mm, and the cracks had spread more or less evenly along the length on the tension sides of the column. The cracks appeared with a closer spacing in the region where the experimental failure section was eventually located.

6.4. COMPARISON OF PROGRAM VARCOLS AND TEST RESULTS

6.4.1. GENERAL

The computed results were obtained using the computer program VARCOLS, validated and described briefly in Chapter 2 of this Thesis. The theoretical values were obtained on the basis of crushing strain of concrete having a value of 0.0035 and a maximum concrete stress of 0.67 times the observed cube strength. A parabolic rectangular stress block, as specified in BS5400:Part 4 [8] was adopted for concrete. For steel a trilinear curve, in accordance with the same code, was assumed. An initial lack of straightness of 0.001 times the column length was adopted as standard. The reasons for the choice of these constants were discussed in Section 4.4.

6.4.2. ULTIMATE LOADS

Table 6.3 gives the experimental failure loads for the six specimens tested, together with the calculated failure loads obtained from the computer program VARCOLS. The ratio between the experimental failure loads and the calculated failure loads from VARCOLS is also given in each case. The least value of this ratio was 1.0 for Column LGBO-20. The mean value for this ratio for the six columns listed was 1.39 with a standard deviation value of 0.25. It may be seen that in all cases the results given by the computer program are on the safe side and the margin of error is small and consistent with that for Series A, B, and C.

6.4.3. LOCATION OF FAILURE ZONE

Table 6.5 gives the location of the failed section for each column, measured from the eccentrically loaded end, as well as the corresponding value obtained from the computer program. It may be observed that the two values agree well with each other, except for the case of Column LGBO-20 for which the failed section was located at the end where the eccentricities were applied.

In the case of rectangular tapered cross section columns, LDBO-15 to 18, the failed section was located between on-half and one-third of the column length from the end where the biaxially eccentric loading was applied. These locations differ from the uniaxially eccentric loading cases, where the failed section was usually located between one-half and two-thirds of the column length from the stronger end.

For the octagonal cross section column, namely LGBO-19, the failed section occurred at about one-third of the column length from the biaxially eccentrically loaded end. This location was similar to the location of the failed section for the octagonal cross section columns tested under uniaxially eccentric loading.

6.4.4. LOAD vs. DEFLECTION CURVES

Figs. 6.6 to 6.11 give a set of graphs, showing the maximum deflections about the principal axes against load for each of the columns in this Series. In the graphs, the theoretical deflections about the principal axes obtained from the computer program VARCOLS are also shown. It can be seen that the agreement between computed and measured deflections is consistently good.

Generally, the measured deflections followed the same pattern for all specimens tested, that is, small deflections until the first tensile cracks were developed, and later, larger deflections for each increment of load.

The vertical deflections, in all cases, were slightly greater than the horizontal deflections, although the eccentricities applied about the principal axes were nominally the same. This is possibly explained by the way in which the rig, for counter-balancing the self-weight, worked. The suspending links allowed a proper movement of the jack cross-head in line with the vertical movement of the column, at the same time as keeping the force in the jack equal to the weight of the column. However, while the rig allowed a force movement of the column in the horizontal direction, the jack itself remained stationary. Thus the tension in the links would cause a slight reduction of the horizontal deflections. This is evidenced by the relative position of the curves corresponding to horizontal and vertical deflections in Figs. 6.6 to 6.11.

6.4.5. LOAD vs. STRAIN CURVES

A set of Load vs. Maximum Compressive Strains curves is given in Figs. 6.6 to 6.11 for each column. The graphs were obtained by plotting the maximum measured strains at the closest monitored section to the actual failed section, against the load applied. For each column, a similar curve is also plotted using the values computed by the program VARCOLS.

The plotted strains were in all cases measured at the closest corner from the line of the biaxially eccentric load applied. As observed in the previous tests, the maximum compressive strains just before crushing of concrete were never greater than 0.0025. Hence, the maximum concrete strain recommended by BS5400:Part 4, namely 0.0035, was not reached for any of the specimens tested.

6.4.6. STRAIN PROFILES

Figs. 6.13 to 6.18 show the strain profiles for each of the columns tested. Two sections were selected, one at mid-length and the other at one-third length, measured from the eccentrically loaded end. The profiles were obtained by plotting the computed strains from program VARCOLS as well as the measured strains for each column for certain levels of loads. For this comparison, the inclination of the neutral axis in the experimental results was assumed to be the same as that given by the program VARCOLS, for selected levels of loads. This assumption was necessary because of the difficulty of assessing the orientation of the neutral axis from the test results in the case of biaxially loaded columns. Fig. 6.12 shows the way in which the strains, measured at each reinforcement bar, were plotted.

It can be seen from Figs. 6.13 to 6.18 that the agreement between the theorectical and the experimental strain profiles is consistently good for all cases, particulary for column LDBO-18.

6.5. CONCLUSION

This chapter described six tests on slender reinforced concrete columns, including tapered rectangular columns and uniform octagonal columns. All specimens were subjected to biaxially eccentric loading.

A comparison between the test results and the results obtained from the computer program VARCOLS has been shown to give good agreement in terms of the ultimate failure loads, deflections and strains, for almost all columns tested. The comparison between the experimental and theorectical strain profiles was made, assuming that the experimental value of the inclination of the neutral axis was the same as the theorectical value. Subject to this assumption, the comparison shows good agreement between the observed and the computed values. In this connection, it may be observed that the angle of the neutral axis with the horizontal plane was very close to the theorectical value of 45 degrees at failure for all cases, justifying the above assumption.

As observed for the uniaxially eccentric loading specimens, the maximum comppressive concrete strain for this Series, also was not greater than 0.0025, significantly less than the value of 0.0035 assumed in the Code.

For the cracking behaviour, it was found that in all six tests the serviceability limit state load had been achieved without exceeding the surface crack width values in the relevant clauses in BS5400:Part 4[8].

CHAPTER 7

DESIGN METHOD

7.1. INTRODUCTION

In Chapter 2, it was shown that the design procedure as contained in BS5400:Part 4 [8] is very conservative when compared with a large number of test results on reinforced concrete columns gathered from the published literature. Most of these tests were carried out on columns with uniform cross-section along the length.

In bridge structures, tapered columns are often used. As part of the current project, tests were conducted on columns of variable cross-sections, including columns with taper in one or both bending planes. In Chapters 4, 5 and 6 the method given in BS5400:Part 4 was adapted for use with tapered sections and found to be very conservative. There appeared to be scope for an improved method of design for tapered columns.

A rigorous method of analysis, embodied in the computer program VARCOLS, has also been shown to give good, marginally conservative, results when compared with the tests reported in this Thesis.

The objective of this Chapter is to explain an alternative method of design for rectangular uniform and tapered reinforced concrete columns. The method was developed by employing the computer program VARCOLS for calculating 'exact' failure loads of pin-ended columns. Computer results for about a thousand column cases were obtained for this purpose. The initial development was restricted to the case of rectangular uniform reinforced concrete columns, but was subsequently extended to the case of rectangular tapered reinforced concrete columns. Design charts are presented for both uniform and tapered cross-sections. The method is suitable for use in design offices.

7.2. DESIGN PRINCIPLES

7.2.1. GENERAL

All relevant limit states have to be considered in design, but in reinforced concrete structures the three most important ones are the ultimate limit state and the serviceability limit states of deflection and cracking. The criteria with which the limit states have to comply are as follows:

1. In the ultimate limit state, or collapse limit state, the strength of the structure should be sufficient to withstand the design loads.

2. In the serviceability limit state of deflection, the deflections should not be excessive, having regard to the particular structure.

3. In the serviceability limit state of cracking, where the assessed surface width of cracks should not exceed 0.25mm.

The usual approach is to design on the basis of the most critical limit state and then check that the remaining limit states will not be reached. On the whole, the design will be for the ultimate limit state. The procedure is to analyse the structure and check the critical section for strength.

For columns, it is commonly believed that the serviceability limit states of deflection and of cracking will rarely be critical, since for most columns the tensile stresses in the reinforcement will be less than those for beams.

7.2.2. SAFETY FACTORS

The British Code for reinforced concrete bridges BS5400:Part 4[8], suggests that, in designing for a particular limit state, two safety factors should be used: a partial factor applied to the loads, and another partial factor applied to the strength of the materials. The values to be considered for loads are

defined in BS5400:Part 2. For the strength of materials, BS5400:Part 4 defines the safety factors 1.5 and 1.15 for concrete and steel, respectively.

Safety factors are, of course, adopted to cover those variations in loading, in design approach, or in construction which are likely to occur after the designer and the constructor have each used their skill and knowledge.

For the purpose of the failure loads calculated by computer programs and for the method of design developed in this report, only the characteristic strengths of concrete and steel are used, that is, the safety factor value is taken as unity for both concrete and steel.

The characteristic strength to be assumed for concrete in design is 0.67 f_{cu}, where f_{cu} is the characteristic cube strength. The yield strength to be assumed for steel is 0.87 f_y, where f_y is the characteristic yield strength of reinforcement bars.

The factor of 0.67 for concrete takes account of the ratio between the bending strength in a flexural member and the characteristic cube strength. The applicability of this value has been reviewed as part of this project. The details of the tests are given in Chapter 4 of this thesis and it can be seen that the mean value obtained (0.64) is very close to the factor of 0.67 recommended in BS5400:Part 4.

7.3. ASSUMPTIONS

The problem of buckling by flexure of slender reinforced concrete columns would not be solved without recourse to certain simplifications and idealisations. The major assumptions made in the method of analysis used in this report are given below.

1.Perfect bond is assumed between concrete and steel.

2. The strain distribution across the section is assumed to be linear, varying in proportion to the distance from the neutral axis, i.e., it is derived from the assumption that plane sections remain plane after the application of the loads.

3. The stresses distribution in the concrete in compression is derived from the stress-strain curve shown in Fig. 7.1. The strain at the outermost compression fibre at failure is taken as 0.0035. This curve is recommended in BS5400:Part 4 [8] for any rigourous calculations. However, it has been shown in Chapters 4, 5 and 6 of this thesis that, for slender reinforced concrete columns, the collapse mode is by instability failure and that the maximum concrete strain does not reach the ultimate strain specified in BS5400:Part 4, namely 0.0035. Nevertheless, in order to make allowance for long term effects under service conditions, the value of 0.0035 for the maximum concrete strain has been retained.

4. The stresses in the reinforcement bars are derived from the stress-strain curve shown in Fig. 7.2. This curve, again, is derived from BS5400:Part 4 [8].

5. The tensile strength of concrete and the strain hardening in steel are neglected.

6.Shear stresses are small, therefore their effect on deflection and on strength can be neglected.

7.4. DESIGN METHOD

7.4.1. INTRODUCTION

The design method is developed by obtaining ultimate loads of a range of column cross-sections with various combinations of slenderness and type of loading and, additionally, the angle of taper for tapered columns. Since consideration of all possible combinations would have led to a very large number of cases, a selective approach was adopted. The selection of particular values for various parameters is now discussed.

7.4.2. SELECTION OF COLUMN CROSS SECTIONS AND MATERIAL PROPERTIES

For rectangular uniform section columns, three dimensions of cross-section were analysed, namely 100mm x 200mm, 100mm x 300mm and 200mm x 200mm. Two levels of reinforcement, 1% and 6%, were used, complying with the limits in the range recommended in BS5400:Part 4.

In the case of tapered columns, the mid-height cross section was assumed to be the section adopted for defining slenderness ratio. Accordingly, three mid-height cross sections were selected and analysed. The dimensions were 250mm x 250mm, 300mm x 300mm and 400mm x 400mm. The percentage of reinforcement for these columns was assumed to be 2% at the mid-height cross section. This obviously meant that at the narrow ends, the percentages were higher and at the wider ends, these were lower. In all cases these were within the specified range of 1% to 6% [8].

The concrete characteristic strength f_{cu} used in the derivations was 30 N/mm^2 and for steel, a characteristic strength f_y of 425 N/mm^2 was adopted.

7.4.3. SELECTION OF COLUMN END CONDITIONS AND LOADING

In all cases, the columns were assumed to be pinned at both ends and the failure was assumed to occur in the plane of the applied eccentricities.

The columns were analysed for four levels of uniaxial eccentricities, namely 0.05h, 0.10h, 0.20h and 0.40h. The value for h was defined as the depth of cross section at the mid-length of the column. The eccentric loading adopted was equal at both ends for uniform cross section columns, whilst for tapered columns an end eccentricity was applied at the stronger end while the loading was concentric at the other end.

7.4.4. SELECTION OF COLUMN SLENDERNESS AND TAPER

For each level of eccentricity analysed, ten different column lengths were considered, corresponding to l/h ratios of 4, 8, 10, 12, 15, 20, 30, 40 and 60 where l is the effective length of the column and h is the depth of cross section at the mid length in the plan of bending.

For the case of tapered columns, it was necessary to include the angle of taper as an additional parameter. Three values for the angle of taper were adopted, namely, 1:120, 1:100 and 1:80.

With the range of variables outlined so far, the number of columns analysed by computer was about 600. A summary of the results obtained is given in Appendix C.

7.4.5. PROCEDURE FOR THE DEVELOPMENT OF THE DESIGN METHOD

The design method was developed by first obtaining ultimate loads of a range of column cross sections with various combinations of slenderness and type of loading, and additionally, the angle of taper for the case of tapered

columns. The results obtained were nondimensionalised in various ways, to reduce the number of design parameters.

The analytical ultimate loads, N, obtained from the computer program VARCOLS were first divided by N_{uz} which is the ultimate axial capacity of the section in the absence of moments, that is, the column "squash load". Since the material safety factors have been kept equal to 1.0 (see Subsection 7.2.2. above), the squash load is given by:

$$N_{uz} = 0.67 f_{cu} A_c + f_y A_s$$

where,

A_c = Area of concrete in the mid-height section and

A_s = Area of steel in the mid-height section.

For each combination of cross section and percentage of reinforcement, graphs were obtained by plotting the values of N/N_{uz} against 1/h for each level of e/h, where e is the eccentricity applied and h is the depth of the cross section at mid-height. In the case of tapered columns, the angle of taper was varied in combination with the cross section.

Figs. 7.3 to 7.8 show the 1/h vs. N/N_{uz} curves for each combination of cross section and a percentage of reinforcement for uniform columns. Figs. 7.9 to 7.11 show similar curves for each angle of taper and three different cross sections for tapered columns.

When the graphs in Figs. 7.3 to 7.8 were superimposed, for each percentage of reinforcement in the case of uniform columns, a family of curves falling within narrow bands was obtained. For the case of tapered columns, similar results were achieved, when graphs in Figs. 7.9 to 7.11 were superimposed for each angle of taper.

Figs. 7.12 and 7.13 show the family of curves obtained for uniform cross sections, while Fig. 7.14 shows the family of curves for the tapered columns. The narrowness of the bands suggests that simple relationships for describing the column behaviour could be obtained by making them independent of the column size.

To explore an alternative form of presentation of the results, it was observed that for a constant value of N/N_{uz}, different ratios of l/h can be obtained for different levels of e/h. Based on this observation, a curve of l/h against e/h can be drawn for a constant value of N/N_{uz}. To achieve this, it was necessary to employ an interpolation technique on the original data obtained from the computer program VARCOLS. For this purpose, Lagrangian interpolation for irregularly spaced data was adopted. The interpolation was carried out for a number of values of N/N_{uz}, namely, 0.10, 0.20, 0.30, 0.40, 0.50, 0.60 and 0.70. The curves obtained show a simple, but not necessarily linear, relationship between the parameters l/h and e/h for a constant N/N_{uz}. The shape of these curves is such that a linear approximation could be established for use in design.

In order to determine any further common parameters, these curves were again superimposed and a new family of curves was obtained. Figs. 7.15 and 7.16 show the results for uniform columns, and Fig. 7.17, for tapered columns. The superimposition shows that the resulting curves are very nearly straight lines and once more falling within narrow bands. Hence, a linear regression of l/h on e/h was applied by using least squares curve fitting. The lower bound curve, being on the safe side, was obtained and for of this curve a single equation was found, relating the two parameters l/h and e/h for a given value of N/N_{uz}. Figs. 7.18 and 7.19 show the curves corresponding to the above equations for uniform columns and Fig. 7.20 for tapered columns.

The novel way in which the computed results were analysed and finally presented, that is, plotting the curves e/h against l/h for each value of N/N_{uz} makes the design method very simple and easy to be use for both uniform and tapered slender reinforced concrete columns. The essential feature of the method is that the slenderness effect has already been considered in the graphs. A more detailed presentation of the design procedure is given in the Section 7.6 below.

7.4.6. EFFECT OF MATERIAL PROPERTIES

The above derivation was based on specific characteristic strengths of concrete and steel, namely 30 N/mm^2 and 425N/mm^2 respectively. The influence of material properties was next examined by considering a number of cases with concrete strengths of 20N/mm^2 and 50N/mm^2 in combination with a steel strength of 475N/mm^2. Figs. 7.21 and 7.22 show the family of curves obtained where these values were used. It was found that the relationships between l/h and e/h for a constant N/N_{uz} were very close to the previously plotted curves. The new curves also had a near-linear characteristic and fell within the envelope of curves plotted for the initially assumed characteristic strength values. Hence, the conclusion is that the graphs obtained for the initially chosen strengths of steel and concrete can be used for any other characteristic strength of concrete or steel without further modification.

7.5 DESIGN PROCEDURE

In the light of the above, a procedure for the design of slender uniform and tapered reinforced concrete columns using the design curves formulated above, is now outlined. The values of the applied thrust N, end bending moments M, the concrete characteristic strength f_{cu}, the steel characteristic strength f_y and the column effective length l are known. The key steps in the

procedure are as follows:

1.Calculate the value of eccentricity at each end by dividing the end bending moment M by the thrust N.

2.Calculate the eccentricity at the critical section as follows

$$e = (e_1 + e_2)/2$$

where,

e_1 and e_2 are the eccentricities at the two ends. For the case of tapered columns e_1 is the eccentricity applied at the stronger end while e_2 is the eccentricity applied at the weaker one. This implies that at the critical section, the average of the two end eccentricities is to be used. If a more conservative results are required , the following formula, which is to be found in many Codes, including BS5400:Part 4, may be used

$$e = 0.6e_1 + 0.4e_2$$

3.Select values for b and h at the critical section. In the case of tapered columns b and h are to be taken at the mid-height. At the two ends, the sections chosen should be checked for strength, without buckling effects, for combination of N and e_1 and N and e_2, respectively.

4.Select a trial arrangement for the longitudinal reinforcement at the critical section.

5.Calculate the value of N_{uz} according to

$$N_{uz} = (0.67f_{cu}A_c)/f_{mc} + (f_yA_s)/f_{ms}$$

where f_{mc} and f_{ms} are the safety factors for concrete and steel respectively.

6.Calculate the value of N/N_{uz}

7.Calculate e/h and l/h

8.Using the design charts, evaluate the value of N/N_{uz} using the values of e/h and l/h.

9.Compare the evaluated N/N_{uz} value obtained from the design charts with the required design value of N/N_{uz}.

10.If necessary, modify the cross-section and the reinforcement arrangement and repeat steps 3-9 until equality of the value N/N_{uz} is obtained.

The proposed method of design for slender rectangular uniform and tapered reinforced concrete columns seems very simple to be used, since the ultimate buckling load can be obtained quickly for a given column length, level of eccentricity applied and by trial and error, the dimensions of the cross section and the longitudinal reinforcement arrangement.

For cases where biaxial bending is involved, the existing interation formulae in BS5400:Part 4[8] could be used after calculating the uniaxial strength about the two principal axes.

A worked example for the application of the method of design just summarized, is given in the Appendix B of this Thesis.

7.6. COMPARISONS BETWEEN THE PROPOSED METHOD OF DESIGN AND TEST RESULTS

The comparisons have been restricted to the case of pin ended columns. From various test series described in Chapters 2, 4, 5 and 6, a few have been selected for this purpose. In the assessment of the strength of sections, when using the program VARCOLS, the stress-strain curves given in Figs. 7.1 and 7.2 have been used. It has been assumed that the strength of concrete in the column is 0.67 times the reported cube strength. Where individual authors have reported cylinder strength, the cube strength has been assumed to be 1.25 times these strengths. In all cases the safety factors have been taken as 1.0 for both concrete and steel.

The comparison between the test results and the calculated design loads, N, are given in tables 7.1 to 7.5. The last column in each table gives the ratio between the experimental failure load and the calculated design load. In the case of uniform columns, the mean value of this ratio for the 64 tests listed is 1.31 with a standard deviation of 0.16. A summary of the comparisons is given in Table 7.6. In the case of tapered columns, the mean value for that ratio is 1.34 with a standard deviation of 0.15. Table 7.7 shows the details of the test results reported in chapters 4 and 5 of this thesis and the comparison between those results and the results calculated by the proposed method of design. The correlation between the test results collected and the results obtained when using the method of design can be regarded as satisfactory since the method used is shown to be on the safe side for all cases.

7.7. CONCLUSION

An alternative method of design for slender reinforced concrete columns with either uniform or tapered cross sections has been presented. The method has so far been developed to cover the design of columns subjected to compression and uniaxial bending. The way in which the graphs were presented, that is, e/h against l/h for each level of N/N_{uz}, making them non-dimensional, resulted in a design method that is very simple and easy to be used. Comparison with a number of test results show it to be reasonably safe as well as accurate, for both uniform and tapered slender reinforced concrete columns.

The method has been shown to be very satisfactory when compared with a wide range of test results published. Particularly satisfying is the agreement for tapered columns, for which very few test data are available and for which, in consequence, few comparisons have been made to date. Taking this point in conjunction with the demonstrated simplicity of the approach, the method is recommended for general use.

CHAPTER 8

CONCLUSIONS

8.1. GENERAL

The analytical method developed by VIRDI [45]-[48], on which the computer program VARCOLS is based, appears to be the most general method of analysis of reinforced concrete columns available in literature.

A comparison with test data collected from the literature on 132 specimens shows that, on the whole, the computer program VARCOLS gives results that are conservative without being unduly so. A mean value of 1.32 for the correlation between experimental and theoretical failure loads was obtained, with a standard deviation of 0.26.

8.2. CONCLUSIONS RELATING TO THE EXPERIMENTS

The thesis describes a total of 19 tests on slender reiforced concrete columns of uniaxially or biaxially loaded rectangular tapered columns as well as octagonal columns. The 19 tests were grouped into four Series - A, B, C, and D.

For the 7 tests on reinforced concrete columns of length 6.0m forming Series A and B, and subjected to uniaxial bending, including tapered rectangular columns and octagonal columns, the failure mode was sudden in all cases, indicating compression failure of concrete.

No tensile cracks were observed, indicating therefore that the serviceability limit state load would be met with these columns almost up to collapse.

It was observed that the crushing of concrete occurred at a strain of around 0.0025 which is considerably below the normally accepted value of 0.0035, also specified in many Codes of Practice.

Comparisons between experimental and theoretical results obtained from program VARCOLS has been shown to give good agreement for the majority of the 7 columns forming Series A and B.

The experimental results were compared with two sets of calculations based on BS5400:Part 4 [8]. One was based on the use of experimentally observed strengths for steel and concrete together with partial factors of safety of 1.0 for both the materials. The second set was based on target strength of concrete, the design characteristic strength of steel, as well as the specified factors of safety for concrete and steel, namely 1.5 and 1.15 respectively. It was shown that the procedure in the Code is very conservative and there is scope for further improvement.

The mode of failure for the 6 long columns (9.0m) forming Series C, tested under uniaxially eccentric loading followed an almost parallel course, that is, instability failure occurred with very high deflections.

The first tensile cracks appeared at about 35%-40% of the failure load with a surface crack width of around 0.03-0.05mm. The maximum design surface crack width allowed by BS5400:Part 4[8], under the exposure condition similar to the laboratory environment, namely 0.25mm, was not reached before 80-85% of the experimental failure. Hence, it can be concluded that in all the tests the servicability limit state load had been achieved without undue cracking according to BS5400:Part 4 [8].

The comparisons between the tests results and the results obtained from the computer program VARCOLS has been shown, in most of the cases, to give good agreement in terms of the ultimate failure loads, deflections and strains.

The comparison between the test results and the calculations based on BS5400:Part 4[8] shows that when the partial safety factor values are assumed to be unity the agreement is good. However, for the case where the partial safety factor values are adopted as the values specified in BS5400:Part 4, namely 1.5 for concrete and 1.15 for steel, the agreement was rather far on the safe side.

For the case of columns with biaxial bending forming Series D, the six long columns (9.0m) tested show a very similar mode of failure to the long columns tested under uniaxial bending.

For all the columns tested the serviceability limit state load for cracking, as recommended by BS5400:Part 4 had been achieved. In the light of this evidence it is recommended that the use of the clauses concerned with crack control in columns in the BS5400:Part 4[8] are satisfactory.

The maximum compressive concrete strain measured for all long length columns (9.0m) for both uniaxial and biaxial bending was not greater than 0.0025. It is suggested that the value 0.0035 specified in the Limit State Code for Bridges BS5400:Part 4[8] will have to be reviewed for the case of slender columns.

8.3. CONCLUSIONS RELATING TO THE DESIGN PROCEDURE

The method of design was derived by producing ultimate loads from the computer program VARCOLS for a range of column cross sections with various combinations of slenderness and type of loading, and additionally, the angle of taper for the case of tapered columns. The results were nondimensionalised by dividing the ultimate loads by the "squash load" (N_{uz}). The nondimensional values of N/N_{uz} were subsequently used to plot graphs having the values of N/N_{uz} against 1/h. Hence, a family of curves were obtained falling within

narrow bands. Furthermore, a family of near-straight lines were obtained when the values of l/h were plotted against e/h. As a consequence of that, the lower bound curves, being on the safe side, were found relating the two parameters l/h and e/h for a given N/N_{uz}. These curves, it was found, could be approximated by straight lines and form the basis of the design method developed in this thesis.

The straight lines approximation for the lower bound curves makes the method very simple and easy to be used.

The alternative method of design for slender reinforced concrete columns with either uniform or tapered cross sections is shown to give a good agreement when compared with a reasonably wide range of test results published, as well as with the test results described in this thesis. In the light of the above, the method of design is recommended for general use.

APPENDIX A

A.1. INTRODUCTION

The design of slender columns in BS5400:Part 4[8] as well as in CP110, is based on the principle of checking a critical section for the applied force and a total moment, which includes additional moments to account for buckling. Columns are considered slender if the length/depth (L/h) ratio exceeds 12. A formula for calculating the additional moments due to slenderness effects is given in both codes, and is in fact based on the work done by Cranston [16].

In CP110, another factor, K_1, is used to reduce the additional moments due to slenderness effects, with the objective of narrowing the margin of conservatism. This parameter is not used in BS5400:Part 4[8].

In the two codes, the strength of a section is checked by first establishing a strain distribution in the section. In all cases the strain of the extreme fibre in compression is taken as 0.0035. This value corresponds to the short term crushing strain of concrete multiplied by a suitable factor to allow for creep effects. Also, the formula for additional moment is derived using the same concept of a strain distribution with an extreme fibre strain corresponding to the crushing strain of concrete. Originally, CEB Recommendations [11] included a value of 0.003 for the crushing strain of concrete. Cranston [16] introduced a factor of 1.25 for long term effects resulting in a value of 0.003 x 1.25 = 0.00375. This value forms the basis for the actual additional moment formula included in both BS5400:Part 4[8] and CP110[15].

As mentioned in Chapters 4,5 and 6, the short term crushing strain of concrete observed was no greater than 0.0025. In the literature, other

investigations have also reported a short term crushing strain of concrete for slender reinforced concrete columns, well below the Code figure of 0.0035. For example, Pancholi and Wilby[53] reporting tests on slender reinforced concrete columns, found that the observed short term crushing strain of concrete was only 0.001.

In the light of this evidence, it appears necessary to examine the influence of a smaller value of the crushing strain of concrete and hence the influence of this value on the formula for additional moments. The value chosen for this study is 0.0025.

A.2. Additional moment due to slender column effect

The strength of a slender column is significantly reduced by the transverse deflections induced by the axial force. At the critical section the lateral deflection e_{add} causes an increase in the total moment

The additional eccentricity e_{add} depends on the curvature $1/r_u$ of the column and on the distribution of this curvature. Hence, Taking the triangular curvature distribution and rectangular curvature distribution diagrams and integrating these to give the deflection,

$$a_u = \frac{l^2}{8r_u} \qquad \text{(Triangular distribution)} \qquad \ldots(1)$$

$$a_u = \frac{l^2}{12r_u} \qquad \text{(Rectangular distribution)} \qquad \ldots(2)$$

CRANSTON [16], based on the then recent CEB Recommendations [11] estimated the deflection a_u as the average value. Hence,

$$a_u = \frac{l^2}{10 r_u} \qquad \ldots(3)$$

As the additional bending moment, M_a is the product of the design axial load times the additional eccentricity, it follows

$$M_a = N e_{add} = \frac{N\, l^2}{10}\left(\frac{1}{r_u}\right) \qquad \ldots(4)$$

where,

M_a = additional moment

N = design axial load

l_e = effective length of the column determined from elastic theory

l/r_u = curvature due to loading at the centre of the effective length

CEB recommends [11] that the curvature, l/r_u should be assessed by the following expression:

$$\frac{1}{r_u} = \frac{0.003 + \frac{f_y}{E_s} - \frac{le}{5000h}}{h} \cdot K_1 \qquad \ldots(5)$$

where,

f_y = design strength of the reinforcement

E_s = modulus of elasticity of the reinforcement

h = overall depth of the section

k_1 = a factor depending upon the intensity of axial load and is explained in sub-section A.3 of this Appendix

k_1 is given by the expression

$$K_1 = \frac{N_{uz} - N_u}{N_{uz} - N_{bal}} \qquad \ldots(6)$$

where,

N_{uz} = the "squash load" of the section.

N_{bal} = the axial load corresponding to "balanced condition", i.e. when the tension steel has just reached its design strength simultaneously with the maximum or ultimate strain in the outermost concrete compression fibres.

N_{bal} may be computed from

$$N_{bal} = (0.67/\delta_{mc})\ f_{cu}\ bd_c + (f'_{s1}/\delta_{ms})A'_{s1} + (f_{s2}/\delta_{ms})A_{s2} \qquad \ldots(7)$$

where,

the steel stresses f'_{s1} and f_{s2} and the stress block depth d_c are to be determined from the strain diagram for the balanced condition.

At a tensile strain of 0.002, fs_2 may be taken as -0.72 fy, similarly $f'_{sl} = 0.72\ f_y$ and $d_c = 0.636\ (h-d_2)$. Hence,

$$N_{bal} = 0.254\ f_{cu} b(h-d_2) - 0.72 f_y (A'_{sl} - A_{s2}) \qquad \ldots(8)$$

A.3. ADDITIONAL MOMENT EQUATION ACCORDING TO BS5400:PART 4

In the basic equation for curvature, Eqn. 5, the maximum concrete strain recommended by CEB, is adopted as 0.003. The design strength f_y for the steel has been taken as 360N/mm^2 with a modulus of elasticity E_s of 200 N/mm^2. Using these values in Eqn. 5, the expression for curvature $1/r_u$ becomes,

$$\frac{1}{r_u} = \frac{1}{208h}\left(1 - 0.00415\,\frac{l_e}{h}\right) K_1 \qquad \ldots(9)$$

substituting Eqn. 9 into Eqn. 4 gives:

$$M_a = \frac{Nh}{2080}\left(\frac{l_e}{h}\right)^2\left(1 - 0.00415\,\frac{l_e}{h}\right) . K_1 \qquad \ldots(10)$$

Cranston [16] has suggested that

$$e_{add} = \frac{h}{1750}\left(\frac{l_e}{h}\right)^2\left(1 - 0.0035\,\frac{l_e}{h}\right). K_1 \qquad \ldots(11)$$

$$M_a = \frac{Nh}{1750}\left(\frac{l_e}{h}\right)^2\left(1 - 0.0035\ \frac{l_e}{h}\right).K_1 \qquad \ldots(12)$$

Equations (11) and (12) were obtained by using the same maximum concrete strain recommended by CEB, but here multiplied by a factor dependent upon the age of loading, at atmospheric conditions and the ratio of the moment. Thus the concrete strain was taken as 0.003 x 1.25 = 0.00375. The remaining values were taken to be the same as in Eqn. 5. Obviously, Equations 11 and 12 are more conservative than Equations 9 and 10.

To compensate this conservatism, Cranston (and hence CP 110) recommended that the additional moment in slender columns may be adjusted by the factor k_1 earlier referred to in equation 6. To calculate the value of k_1 each time becomes tedious, especially as the amount of reinforcement has to be known or estimated before the values can be found.

BS5400:Part 4 adopts Equations 11 and 12 but assumes K_1 to be equal to 1.0 in all cases at the expense of conservatism.

The strain diagram shows that the curvature depends on the strain ε_{s2} of the reinforcement A_{s2} (ε_{cu} being taken always as 0.0035 at failure). The curvature expression is in fact intended for the particular balanced condition of ε_{cu} = 0.0035 and ε_{s2} = 0.002 (tensile). As the failure load N_u increases, the tensile strain in A_{s2} reduces becoming zero for $d_c = h - d_2$, i.e. as N_u approaches the axial capacity N_{uz} the column curvature at failure becomes progressively less, and is theoretically zero for $N_u = N_{uz}$. Therefore the purpose of using k_1 is to enable the designer to take advantage of this phenomemnon reducing the total moment M_t. the factor k_1 enables a corresponding reduction to be made in the total moment M_t.

A.4. AMENDMENT TO BS5400:PART 4 ADDITIONAL MOMENT EQUATION

Tests reported in this thesis have shown that the maximum compressive strain in the concrete was no greater than 0.0025 for slender column. Hence, the curvature is less than the curvature obtained for the balanced condition for the value of $\varepsilon_{cu} = 0.0035$ and $\varepsilon_{s2} = 0.002$. If the value of $\varepsilon_{cu} = 0.0025$ is used in Equation 5 a new expression for the curvature $1/r_u$ can be obtained

$$\frac{1}{r_u} = \frac{1}{225h} \left(1 - 0.0045 \frac{l_e}{h}\right) \qquad \ldots(13)$$

hence,

$$e_{add} = \frac{h}{2250} \left(\frac{l_e}{h}\right)^2 \left(1 - 0.0045 \frac{l_e}{h}\right) \qquad \ldots(14)$$

and

$$M_a = \frac{Nh}{2250} \left(\frac{l_e}{h}\right)^2 \left(1 - 0.0045 \frac{l_e}{h}\right) \qquad \ldots(15)$$

It can be seen from equation 6 that k_1 is always smaller than 1.0 when N_u is greater than N_{bal}, i.e. for design axial loads bigger than the axial load corresponding to "balanced" condition. Hence, Eqn. 15 may be used to calculate the additional moment for slender columns for the case where N_{uz} is greater than N_{bal}, which in fact occurs in most of the cases.

The graph in Fig. A.3 shows the curves for Equations (12) and (15). The main difference between the new equation and the existing one is the setting of a lower limit on the additional eccentricity, once the upper limit was already set by Equation 12.

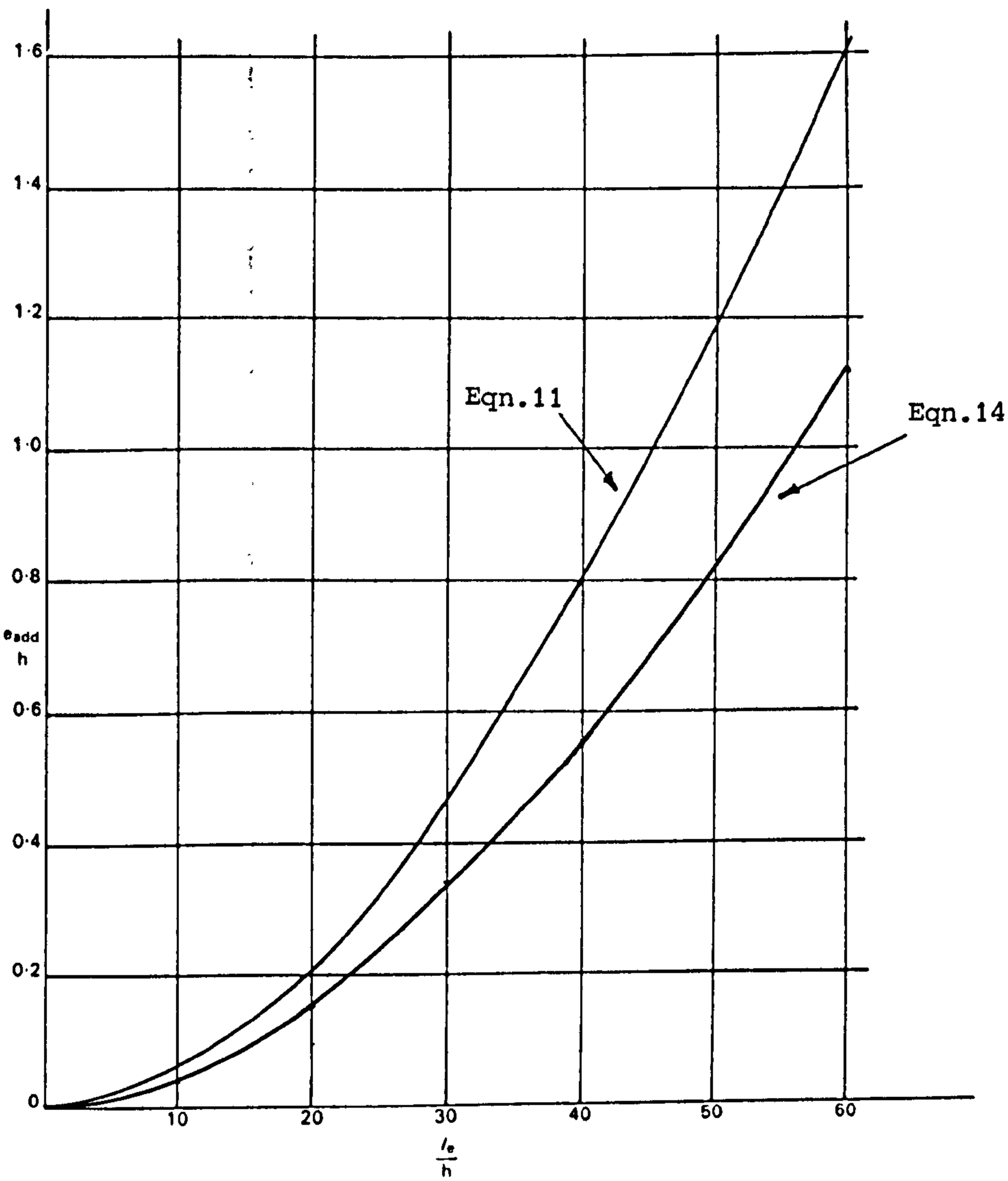

Fig. A.3 - Curves for calculating additional moment in slender column

APPENDIX B

B.1. UNIFORM COLUMN

Design the longitudinal reinforcement for the column section b = 150mm and h = 300mm if N = 400 KN and M_x = 50KNm. Given f_{cu} = 30N/mm^2, f_y = 425N/mm^2 and L = 6000m.

$$e = \frac{M}{N} = \frac{50000}{400} = 125$$

assuming A_{sc} = 6%

$$N_{uz} = \frac{0.67}{1.5} \times 30 \times 300 \times 150 + \frac{425}{1.15} \times 0.06 \times 300 \times 150$$

N_{uz} = 1600 KN

$\frac{N}{N_{uz}}$ = 0.25

e/h = 0.42

l/h = 20

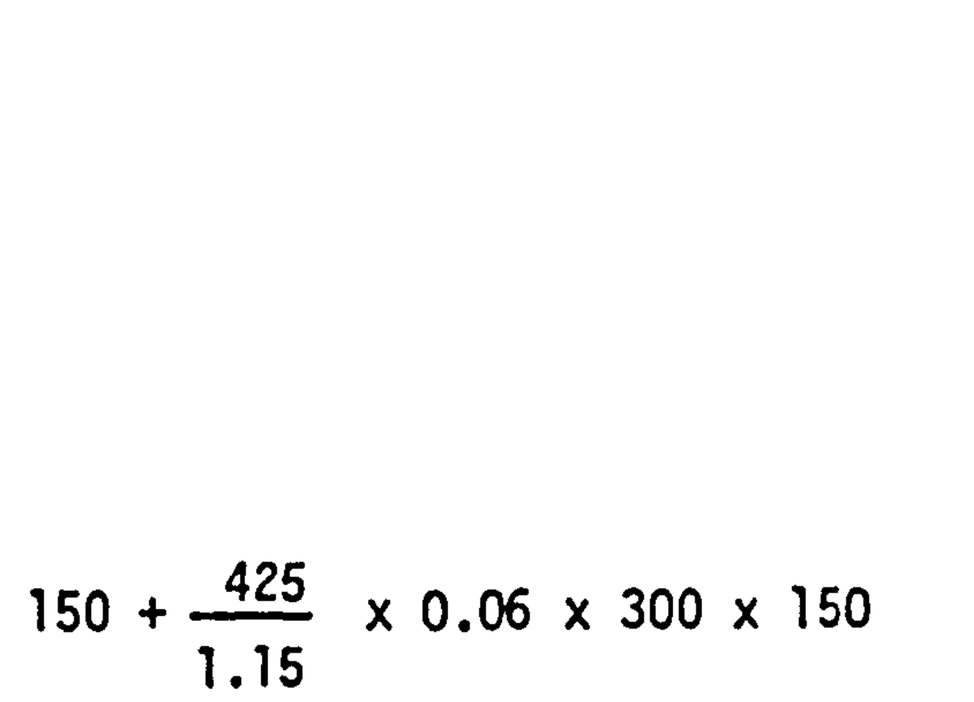

from Fig. 7.19.

Hence,

$$\frac{N_{calc}}{N_{uz}} = 0.28 > \frac{N}{N_{uz}} = 0.25 \quad \checkmark$$

USE six 20 mm bars (1889mm^2)

B.2. TAPERED COLUMN

Design the longitudinal reinforcement for the tapered column having $b_1 = h_1 = 400mm$ and $b_2 = h_2 = 200mm$ at each end respectively, if N = 470 KN and M_{x1} = 80 KNm. Given $f_{cu} = 30N/mm^2$, $f_y = 425N/mm^2$, and L = 9.0 m.

at the end 1

$$e_1 = \frac{M_{x1}}{N} = \frac{80000}{470} = 170$$

at the end 2

$$e_2 = 0$$

at the mid-height section

$$e_t = 0.5 \times 170 = 85$$

Assuming A_{sc} = 2% at the critical section

$$N_{uz} = \frac{0.67}{1.5} \times 30 \times 300 \times 300 + \frac{425}{1.15} \times 0.02 \times 300 \times 300 = 1871 \text{ KN}$$

$$\frac{N}{N_{uz}} = \frac{470}{1871} = 0.25$$

$$\frac{e_t}{h_t} = \frac{85}{300} = 0.28 \qquad \text{and} \qquad \frac{l}{h_t} = 30$$

Using Fig. 7.20 follows

$$\frac{N_{calc}}{N_{uz}} \simeq 0.25 \simeq \frac{N}{N_{uz}}$$

Check end 1 for N and M_{x1} without buckling effect (L/h = 0)

$$\frac{e}{h} = \frac{170}{400} = 0.42 \qquad \text{from Fig. 7.20 follows}$$

$N_{calc} > 0.60\ N_{uz}$ which is greater than 470 KN.

Check end 2 for the "squash load" N_{uz}.

$$N_{uz} = \frac{0.67}{1.5} \times 30 \times 200 \times 200 + \frac{425}{1.15} \times 1884$$

N_{uz} = 1232 KN N = 470 KN

A P P E N D I X C

FAILURE LOAD* CALCULATED FROM COMPUTER PROGRAM "VARCOLS"

Rectangular uniform cross section 100mm x 200mm

Percentage of reinforcement = 1%

f_{cu} = 30N/mm^2

f_y = 425N/mm^2

d/h = 00.85

e/h	0	0.05	0.10	0.20	0.40
L/h					
04	467.6	411.3	368.0	287.5	165.1
08	451.0	390.9	348.2	258.2	150.0
10	441.1	377.1	335.2	258.2	150.0
12	429.4	361.3	319.0	221.9	134.3
15	406.3	335.8	292.7	198.5	122.9
18	376.9	310.1	265.7	174.2	111.5
20	354.1	292.9	241.5	159.6	102.2
25	294.9	241.6	183.7	126.0	79.2
30	240.7	188.7	138.1	99.7	62.2
40	154.6	114.4	82.9	60.6	40.7
50	101.4	72.7	54.3	39.1	28.4
60	69.2	48.3	37.9	27.0	20.8
00	487.0	430.5	388.8	310.0	199.4

*in kN

FAILURE LOAD* CALCULATED FROM COMPUTER PROGRAM "VARCOLS"

Rectangular uniform cross section 100mm x 200mm

Percentage of reinforcement = 6%

f_{cu} = 30N/mm^2

f_y = 425N/mm^2

d/h = 00.85

e/h	0	0.05	0.10	0.20	0.40
L/h					
04	846.7	733.2	653.6	536.9	381.9
08	799.4	696.1	619.9	507.3	361.1
10	773.8	671.9	597.7	487.1	347.3
12	749.2	644.7	572.2	464.1	332.0
15	721.4	600.0	531.7	426.1	307.4
18	685.6	558.6	489.2	385.1	282.0
20	652.5	530.4	462.6	360.8	264.8
25	547.0	454.6	388.5	304.6	225.2
30	440.4	361.3	310.9	252.3	192.6
40	269.2	218.9	197.6	172.8	141.2
50	173.94		133.7	121.6	105.0
60	118.60	101.8	96.0	89.0	79.2
00		798.0	709.3	588.43	125.60

*in kN

FAILURE LOAD* CALCULATED FROM COMPUTER PROGRAM "VARCOLS"

Rectangular uniform cross section 100mm x 300mm

Percentage of reinforcement = 1%

f_{cu} = 30N/mm^2

f_y = 425 N/mm^2

d/h = 00.85

e/h	0	0.05	0.10	0.20	0.40
L/h					
04	701.43	616.99	552.0	431.21	247.67
08	676.47	586.39	522.29	387.23	224.94
10	661.60	565.65	502.79	359.51	213.24
12	644.06	541.93	478.44	332.82	201.45
15	609.37	503.73	439.02	297.79	184.37
20	531.19	439.29	362.17	239.38	153.23
30	361.00	282.97	207.21	149.51	93.34
40	231.83	171.67	124.34	90.87	60.98
60	103.81	72.49	56.85	40.42	12.25

*in kN

FAILURE LOAD* CALCULATED FROM COMPUTER PROGRAM "VARCOLS"

Rectangular uniform cross section 100mm x 300mm

Percentage of reinforcement = 6%

f_{cu} = 30N/mm^2

f_y = 425N/mm^2

d/h = 00.85

e/h	0	0.05	0.10	0.20	0.40
L/h					
04	1270.13	1099.96	980.46	805.44	572.85
08	1199.05	1044.20	929.83	760.96	541.64
10	1160.75	1007.85	896.48	730.63	521.00
12	1123.86	966.99	859.10	696.22	498.06
15	1082.12	900.02	797.56	6539.21	461.13
20	978.81	795.65	693.89	541.14	397.17
30	660.66	541.94	466.36	378.45	288.96
40	403.80	328.37	296.44	259.14	211.79
60	177.88	152.65	143.96	133.45	118.85

*in kN

FAILURE LOAD* CALCULATED FROM COMPUTER PROGRAM "VARCOLS"

Rectangular uniform cross section 200mm x 200mm

Percentage of reinforcement = 1%

f_{cu} = 30N/mm^2

f_y = 425N/mm^2

d/h = 00.85

e/h	0	0.05	0.10	0.20	0.40
L/h					
04	935.24	822.65	736.00	574.89	330.22
08	901.97	781.74	696.38	516.31	299.93
10	882.13	754.20	670.39	479.34	284.32
12	858.75	722.58	637.92	443.76	268.60
15	812.50	671.65	585.36	397.06	245.43
20	708.25	585.73	482.90	319.19	204.31
30	481.34	377.30	276.28	199.35	124.45
40	309.11	228.89	165.79	121.16	81.30
60	138.42	96.66	75.80	48.22	26.50
00	974.00	861.26	777.24	619.80	400.00

*in kN

FAILURE LOAD* CALCULATED FROM COMPUTER PROGRAM "VARCOLS"

Rectangular uniform cross section 200mm x 200mm

Percentage of reinforcement = 6%

f_{cu} = 30N/mm^2

f_y = 425N/mm^2

d/h = 00.85

e/h	0	0.05	0.10	0.20	0.40
L/h					
04	1693.51	1466.44	1307.28	1073.84	763.75
08	1598.74	1392.25	1239.79	1014.64	722.18
10	1547.67	1343.81	1195.30	974.18	694.66
12	1498.49	1289.33	1145.46	928.28	664.09
15	1442.83	1200.03	1063.41	852.29	614.85
20	1305.08	1060.88	925.20	721.53	529.56
30	880.88	722.59	621.82	504.60	385.28
40	538.40	437.83	395.25	345.52	282.38
60	237.17	203.53	191.25	177.94	158.47
00	1824.00	1595.88	1418.64	1176.52	851.16

*in kN

FAILURE LOAD* CALCULATED FROM COMPUTER PROGRAM "VARCOLS"

Rectangular uniform cross section 100mm x 200mm

Percentage of reinforcement = 1%

f_{cu} = 20N/mm^2

f_y = 425N/mm^2

d/h = 00.85

e/h	0	0.05	0.10	0.20	0.40
L/h					
04	331.15	291.81	262.07	216.08	131.30
08	321.06	281.23	252.57	202.93	118.87
10	314.11	274.09	245.41	189.47	111.94
12	306.28	266.81	238.46	173.64	105.79
15	293.03	254.15	226.58	154.27	96.65
20	265.00	229.40	192.14	126.30	82.80
30	206.32	172.17	132.26	88.69	59.77
40	153.02	118.19	85.41	61.82	41.00
60	51.61	40.91	38.83	35.30	24.71

*in kN

FAILURE LOAD* CALCULATED FROM COMPUTER PROGRAM "VARCOLS"

Rectangular uniform cross section 100mm x 200mm

Percentage of reinforcement = 1%

f_{cu} = 50N/mm^2

f_y = 425N/mm^2

d/h = 00.85

e/h	0	0.05	0.10	0.20	0.40
L/h					
04	725.72	640.30	574.49	440.88	233.58
08	704.83	613.67	548.78	383.49	213.57
10	692.20	597.55	533.01	357.75	203.64
12	675.71	578.73	514.49	334.69	193.54
15	644.00	546.10	476.74	301.03	177.25
20	578.60	486.56	406.70	248.92	133.79
30	432.02	349.81	254.46	164.66	76.04
40	303.05	226.52	156.03	101.79	48.02
60	120.42	81.40	64.29	40.00	20.03

*in kN

FAILURE LOAD* CALCULATED FROM COMPUTER PROGRAM "VARCOLS"

Rectangular uniform cross section 100mm x 300mm

Percentage of reinforcement = 1%

f_{cu} = $20N/mm^2$

f_y = $425N/mm^2$

d/h = 00.85

e/h	0	0.05	0.10	0.20	0.40
L/h					
04	505.62	443.45	397.71	327.66	196.95
08	481.59	421.85	378.86	304.39	178.31
10	471.16	413.01	368.12	284.21	169.44
12	459.42	402.42	357.70	260.46	158.85
15	439.54	381.24	339.87	231.41	144.96
20	397.51	344.09	288.20	189.45	121.79
30	309.48	258.26	198.39	133.04	90.02
40	229.53	177.29	128.12	92.74	63.54
60	79.43	63.54	58.25	51.32	37.07

*in kN

FAILURE LOAD* CALCULATED FROM COMPUTER PROGRAM "VARCOLS"

Rectangular uniform cross section 100mm x 300mm

Percentage of reinforcement = 1%

f_{cu} = 50N/mm^2

f_y = 425N/mm^2

d/h = 00.85

e/h	0	0.05	0.10	0.20	0.40
L/h					
04	1088.54	960.45	861.74	620.00	350.38
08	1057.24	920.50	823.17	575.24	320.36
10	1038.30	896.32	799.52	536.63	305.46
12	1013.57	868.10	771.73	502.03	290.32
15	966.01	819.14	715.10	451.53	265.87
20	867.90	729.84	610.05	373.38	200.69
30	648.04	524.72	381.69	246.99	127.81
40	454.58	339.78	234.05	152.69	100.00
60	250.00	124.58	100.00	80.00	40.00

*in kN

FAILURE LOAD* CALCULATED FROM COMPUTER PROGRAM "VARCOLS"

Tapered cross section columns

Percentage of reinforcement = 2%

f_{cu} = 30N/mm^2

f_y = 425N/mm^2

d/h = 00.85

Angle of Taper = 1:120

CROSS SECTION**	250mm x 250mm			300mm x 300mm			400mm x 400mm		
e/h	0.10	0.20	0.40	0.10	0.20	0.40	0.10	0.20	0.40
L/h									
04	1502.66	1226.00	782.25	2167.00	1769.00	1113.01	3830.50	3220.00	2084.19
12	1311.97	1156.47	774.58	1908.82	1699.77	1162.02	3439.50	3088.19	2167.26
20	1059.45	873.63	582.90	1545.44	1295.87	890.06	2791.00	2397.00	1692.03
30	706.00	547.09	387.10	1036.44	816.73	585.00	1910.00	1530.50	1113.25
40	423.02	322.31	244.67	620.95	481.10	370.37	1167.69	918.31	717.76

*in kN
**cross section at mid height

FAILURE LOAD* CALCULATED FROM COMPUTER PROGRAM "VARCOLS"

Tapered cross section columns

Percentage of reinforcement = 2%

f_{cu} = 30N/mm^2

f_y = 425N/mm^2

d/h = 00.85

Angle of Taper = 1:100

CROSS SECTION**	250mm x 250mm			300mm x 300mm			400mm x 400mm		
e/h	0.10	0.20	0.40	0.10	0.20	0.40	0.10	0.20	0.40
L/h									
04	1476.73	1223.14	754.19	2166.94	1815.64	1373.26	3741.34	3271.60	2128.94
12	1305.53	1163.06	790.26	1870.05	1690.00	1189.36	3344.23	3091.42	2225.18
20	1033.20	863.23	584.33	1375.51	1223.23	866.75	2747.08	2385.00	1694.49
30	677.32	527.16	373.05	1072.91	831.57	595.32	1827.30	1486.63	1085.04
40	378.45	292.51	222.59	567.59	444.47	343.33	1064.66	847.29	665.86

*in kN
**cross section at mid height

FAILURE LOAD* CALCULATED FROM COMPUTER PROGRAM "VARCOLS"

Tapered cross section columns

Percentage of reinforcement = 2%

f_{cu} = 30N/mm^2

f_y = 425N/mm^2

d/h = 00.85

Angle of Taper = 1:80

CROSS SECTION**	250mm x 250mm			300mm x 300mm			400mm x 400mm		
e/h	0.10	0.20	0.40	0.10	0.20	0.40	0.10	0.20	0.40
L/h									
04	1437.19	1184.55	726.63	2108.47	1760.10	1106.84	3700.13	3330.29	2174.49
12	1275.27	1160.88	811.85	1868.41	1701.67	1215.00	3370.00	3080.04	2270.77
20	979.52	844.32	578.23	1449.72	1263.09	884.65	2635.35	2350.69	1686.92
30	617.94	496.13	352.54	910.67	741.58	535.86	1672.98	1385.74	1022.33
40	307.50	239.89	184.23	466.31	369.55	289.29	888.40	718.04	573.55

*in kN
**cross section at mid height

REFERENCES

[1] - AAS-JAKOBSEN, A, and AAS-JAKOBSEN, K. Buckling of Slender Reinforced Concrete Columns. COMITE EUROPEEN DU BETON, Bulletin d'Information, no. 69, 1968.

[2] - ACI 318-77. Building Code Requirements for Reinforced Concrete. AMERICAN CONCRETE INSTITUTE, DETROIT, 1977.

[3] - ANDERSON, P., and LEE, H.N. A modified Plastic Theory of Reinforced Concrete. UNIVERSITY OF MINNESOTA ENGINEERING EXPERIMENT STATION, Bulletin No. 33.

[4] - AS 1480 : 1974. SAA Concrete Structures Code. STANDARDS ASSOCIATION OF AUSTRALIA, 1974.

[5] - BREEN, J.E., and FERGUSON, P.M. The Restrained Long Column as a part of a Rectangular Frame. ACI JOURNAL, Proceedings, vol. 61, no. 5, 1964, May, pp 563-588.

[6] - BRESLER, B. Design Criteria for Reinforced Columns under Axial Load and Biaxial Bending. ACI JOURNAL, Proceedings, vol. 57, no. 5, 1960, November, pp 481-490.

[7] - BROMS, B., and VIEST, I.M. Ultimate Strength Analysis of Long Restrained Reinforced Concrete Columns. ASCE TRANSACTIONS, vol. 126, 1961, Part I - pp 308-347, Part II - pp 348-366, and Part III - pp 367-400.

[8] - BS 5400:PART 4-1978. Code of Practice for Design of Concrete Bridges. BRITISH STANDARDS INSTITUTION, 1978.

[9] - BUTLER, D.J. The Strength of Restrained Reinforced Concrete Columns - A New Approach. MAGAZINE OF CONCRETE RESEARCH, vol. 29, no. 100, 1977, September, pp 113-122.

[10] - BUTLER, D.J., and ANDERSON, G.B. The Elastic Buckling of Tapered Beam-Columns. WELDING JOURNAL, vol. 42, no. 1, 1963, January, pp 29-36.

[11] - CEB-FIP. International Recommendations for the Design and Construction of Concrete Structures. CEMENT AND CONCRETE ASSOCIATION, LONDON, 1970, 80pp.

[12] - CEB-FIP. Manual of Buckling and Stability. THE CONSTRUCTION PRESS, 1978.

[13] - CHANG W.F., and FERGUSON, P.M. Long Hinged Reinforced Concrete Columns. ACI JOURNAL, Proceedings, vol. 60, no. 1, 1963, January, pp 1-26.

[14] - CHU, K-H, and PABARCIUS, A. Biaxially Loaded Reinforced Concrete Columns. ASCE, Proceedings, vol. 84, no. ST8, 1958, December, pp 1865-1 - 1865-27.

[15] - CP 110:1972. Design Charts for Singly Reinforced Beams, Doubly Reinforced Beams and Rectangular Columns. BRITISH STANDARDS INSTITUTION, 1972.

[16] - CRANSTON, W.B. Analysis and Design of Reinforced Concrete Columns. CEMENT AND CONCRETE ASSOCIATION. Research Report No. 20, 1972, 54pp.

[17] - CRANSTON, W.B. A Computer Method for the Analysis of Restrained Columns. CEMENT AND CONCRETE ASSOCIATION. TRA 402, 1967, April, 20pp.

[18] - CRANSTON, W.B., and STURROCK, R.D. Lateral Instability of Slender Reinforced Concrete Columns. RILEM INTERNATIONAL SYMPOSIUM, Buenos Aires, 1971, Theme I, pp 117-141.

[19] - ERNST, G.C., HROMADIK, J.J., and RIVELAND, A.R. Inelastic Buckling of Plain and Reinforced Concrete Columns, Plates, and Shells. UNIVERSITY OF NEBRASKA ENGINEERING EXPERIMENT STATION, BULLETIN No. 3, 1953, August.

[20] - FARAH, A., and HUGGINS, M.W. Analysis of Reinforced Concrete Columns Subjected to Longitudinal Load and Biaxial Bending. ACI JOURNAL, vol. 66, no. 7, 1969, July, pp 569-575.

[21] - FLEMING, J.F., and WERNER, S.D. Design of Columns Subjected to Biaxial Bending. ACI JOURNAL, Proceedings, vol. 62, no. 3, 1965, March, pp 327-342.

[22] - FOGEL, C.M., and KETTER, R.L. Elastic Strength of Tapered Columns. JOURNAL OF THE STRUCTURAL DIVISION, ASCE, vol. 88, no. ST5, 1962, October, pp 67-104.

[23] - FURLONG, R.W. Ultimate Strength of Square Columns under Biaxially Eccentric Load. ACI JOURNAL, Proceedings, vol. 57, no. 9, 1961, March, pp 1129-1140.

[24] - FURLONG, R.W. Concrete Columns Under Biaxially Eccentric Thrust. ACI JOURNAL, Proceedings, vol. 76, no. 10, 1979, October, pp 1093-1118.

[25] - GERE, J.M., and CARTER, W.O. Critical Buckling Loads for Tapered Columns. JOURNAL OF THE STRUCTURAL DIVISION, ASCE, vol. 88, no. ST1, 1962, February, pp 1-11.

[26] - HOGNESTAD, E. A Study of Combined Bending and Axial Load in Reinforced Concrete Members. UNIVERSITY OF ILLINOIS ENGINEERING EXPERIMENT STATION, URBANA, Bulletin No. 399, 1951, November.

[27] - JENSEN, V.P. Ultimate Strength of Reinforced Concrete Beams as Related to the Plasticity Ratio of Concrete. UNIVERSITY OF ILLINOIS ENGINEERING EXPERIMENT STATION, URBANA, Bulletin No. 345, 1943, June, 60pp.

[28] - MacGREGOR, J.G., and BARTER, S.L. Long Eccentrically Loaded Concrete Columns Bent in Double Curvature. SYMPOSIUM ON REINFORCED CONCRETE COLUMNS, ACI, SP-13, 1966, pp 139-156.

[29] - MacGREGOR, J.G., BREEN, J.E., and PFRANG, E.O. Design of Slender Concrete Columns. ACI JOURNAL, Proceedings, vol. 67, no. 1, 1970, January, pp 6-28.

[30] - MARTIN, I., MacGREGOR, J.G., PFRANG, E.O., and BREEN, J.E. Critical Review of the Design of Reinforced Concrete Columns. SYMPOSIUM ON REINFORCED CONCRETE COLUMNS, ACI, SP-13, 1966, pp 13-53.

[31] - MARTIN, I., and OLIVIERI, E. Test of Slender Reinforced Concrete Columns Bent in Double Curvature. SYMPOSIUM ON REINFORCED CONCRETE COLUMNS, ACI, SP-13, 1966, pp 121-138.

[32] - MATTOCK, A.H., KRIZ, L.B., and HOGNESTAD, E. Rectangular Concrete Stress Distribution in Ultimate Strength Design. ACI JOURNAL, Proceedings, col. 57, no. 8, 1961, February, pp 875-928.

[33] - MEEK, J.L. Ultimate Strength of Columns with Biaxially Eccentric Loads. ACI JOURNAL, Proceedings, vol. 60, no. 8, 1963, August, pp 1053-1064.

[34] - NEWMARK, N.M. Numerical Procedure for Computing Deflections, Moments and Buckling Loads. ASCE Proceedings, vol. 68, 1942, pp 691-718.

[35] - PANNEL, F.N. Design of Biaxially Loaded Columns by Ultimate Methods. MAGAZINE OF CONCRETE RESEARCH, LONDON, vol. 12, no. 35, 1960, July, pp 99-108.

[36] - PANNEL, F.N. Failure Surfaces for Members in Compression and Biaxial Bending. ACI JOURNAL, Proceedings, vol. 60, no. 1, 1963, January, pp 129-140.

[37] - PANNEL, F.N., and ROBINSON, J.L. Slender Reinforced Concrete Columns under Biaxial Eccentricity of Loading. MAGAZINE OF CONCRETE RESEARCH, LONDON, vol. 20, no. 65, 1968, December, pp 195-204.

[38] - PARME, A.L. Capacity of Restrained Eccentrically Loaded Long Columns. SYMPOSIUM ON REINFORCED CONCRETE COLUMNS, ACI, SP-13, 1966, pp 354-367.

[39] - PARME, A.L., NIEVES, J.M., and GOUWENS, A. Capacity of Reinforced Rectangular Columns Subject to Biaxial Bending. ACI JOURNAL, Proceedings, vol. 63, no. 9, 1966, September, pp 911-922.

[40] - RAMAMURTHY, L.N. Investigation of the Ultimate Strength of Square and Rectangular Columns under Biaxially Eccentric Loads. SYMPOSIUM ON REINFORCED CONCRETE COLUMNS, ACI, SP-13, 1966, pp 263-298.

[41] - RIAD, L. Eccentrically Loaded Reinforced Concrete Columns with Variable Cross Section. SYMPOSIUM ON REINFORCED CONCRETE COLUMNS, ACI, SP-13, 1966, pp 245-262.

[42] - SAENZ, L., and MARTIN, I. Tests of Reinforced Concrete Columns with High Slenderness Ratio. ACI JOURNAL, Proceedings, vol. 60, no. 5, 1963, May, pp 589-616.

[43] - SALTER, J.B., ANDERSON, B., and MAY, I.M. Tests on Tapered Steel Columns. THE STRUCTURAL ENGINEER, vol. 58A, no. 6, 1980, June, pp 189-193.

[44] - SURYANARAYANA, P., and BASU, A.K. Analysis of Restrained Reinforced Concrete Columns Under Biaxial Bending. SYMPOSIUM ON REINFORCED CONCRETE COLUMNS, ACI, SP-13, 1966, pp 211-232.

[45] - VIRDI, K.S., and DOWLING, P.J. The Ultimate Strength of Composite Columns in Biaxial Bending. PROCEEDINGS, THE INSTITUTION OF CIVIL ENGINEERS, LONDON. vol. 58, Part 2, 1973, March, pp 251-272.

[46] - VIRDI, K.S., and DOWLING, P.J. The Ultimate Strength of Biaxially Restrained Columns. PROCEEDINGS, THE INSTITUTION OF CIVIL ENGINEERS, LONDON. vol. 61, Part 2, 1976, March, pp 41-58.

[47] - VIRDI, K.S. Variable Cross Section Columns Loaded upto Failure. NUMERICAL METHODS FOR NONLINEAR PROBLEMS, Edited by TAYLOR, C., HINTON, E., and OWEN, D.R.J., Pineridge Press, Swansea, 1980, pp 553-564.

[48] - VIRDI, K.S. Biaxially Loaded Slender Reinforced Concrete Columns. ADVANCED MECHANICS OF REINFORCED CONCRETE, IABSE COLLOQUIUM, Delft, 1981, Final Report, pp 449-462.

[49] - WARNER, R.F. Biaxial Moment Thrust Curvature Relations. JOURNAL OF THE STRUCTURAL DIVISION, ASCE, vol. 95, no. ST5, 1969, May, pp 923-940.

[50] - WHITNEY, C.S. Plastic Theory of Reinforced Concrete Columns. PROCEEDINGS, ASCE, vol. 66, no. 10, 1940, December, pp 1749-1780.

[51] - WOOD, R.H., and SHAW, M.R. Developments in the Variable Stiffness Approach to Reinforced Concrete Column Design. MAGAZINE OF CONCRETE RESEARCH, LONDON. vol. 31, no. 108, 1979, September, pp 127-141.

[52] - - Report of ASCE-ACI Joint Committee on Ultimate Strength Design. ASCE Proceedings, vol. 81, no. 5, 1955, October. Also, ACI JOURNAL, Proceedings, vol. 52, no. 1, 1956, January, pp 505-524.

[53] - WILBY, C.B. and PANCHOLI, V.R. Design of Very Slender Reinforced Concrete Columns, Civil Engineering, NOV., 1978.

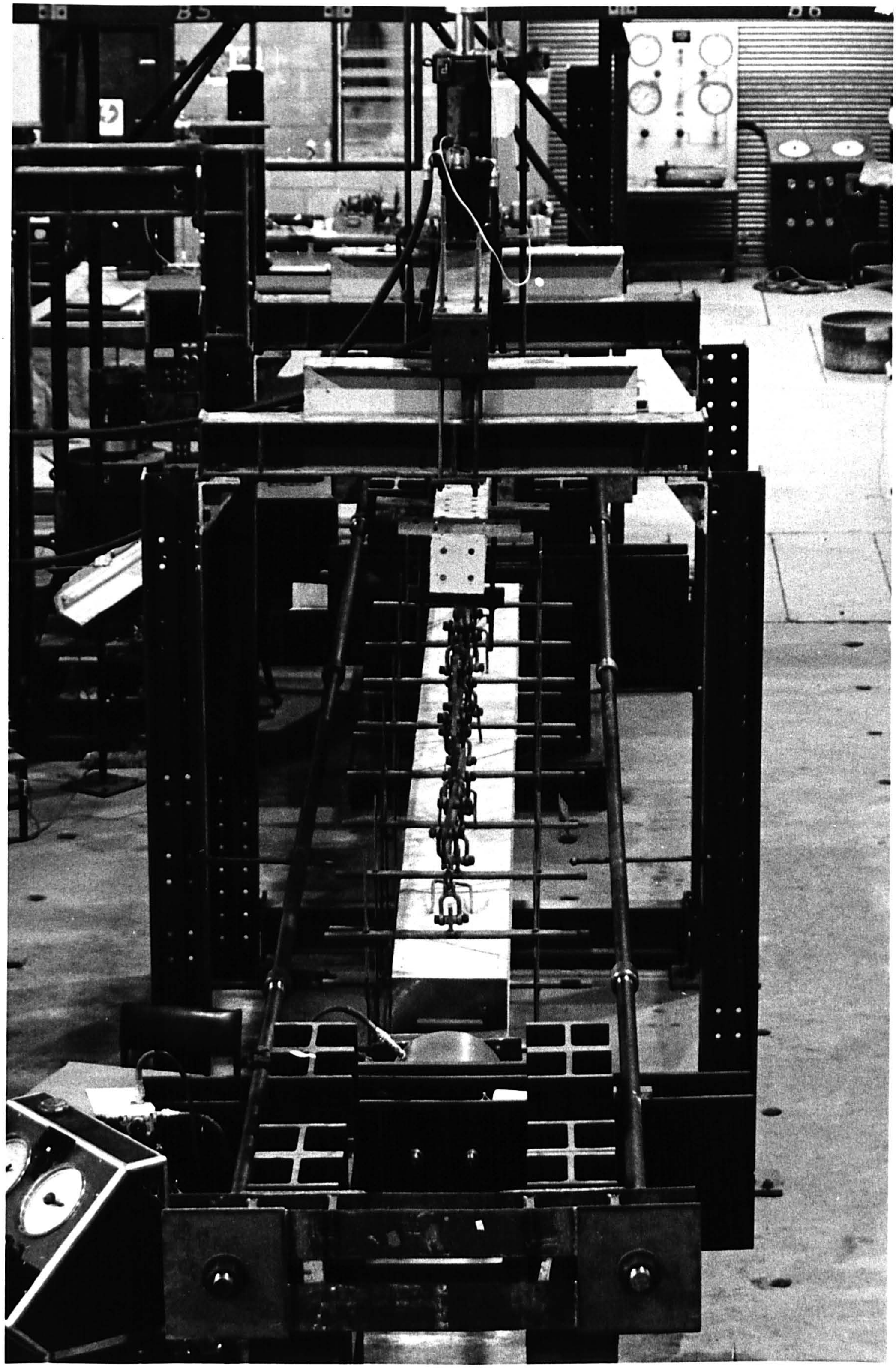

Fig. 3.1. General view of the rig

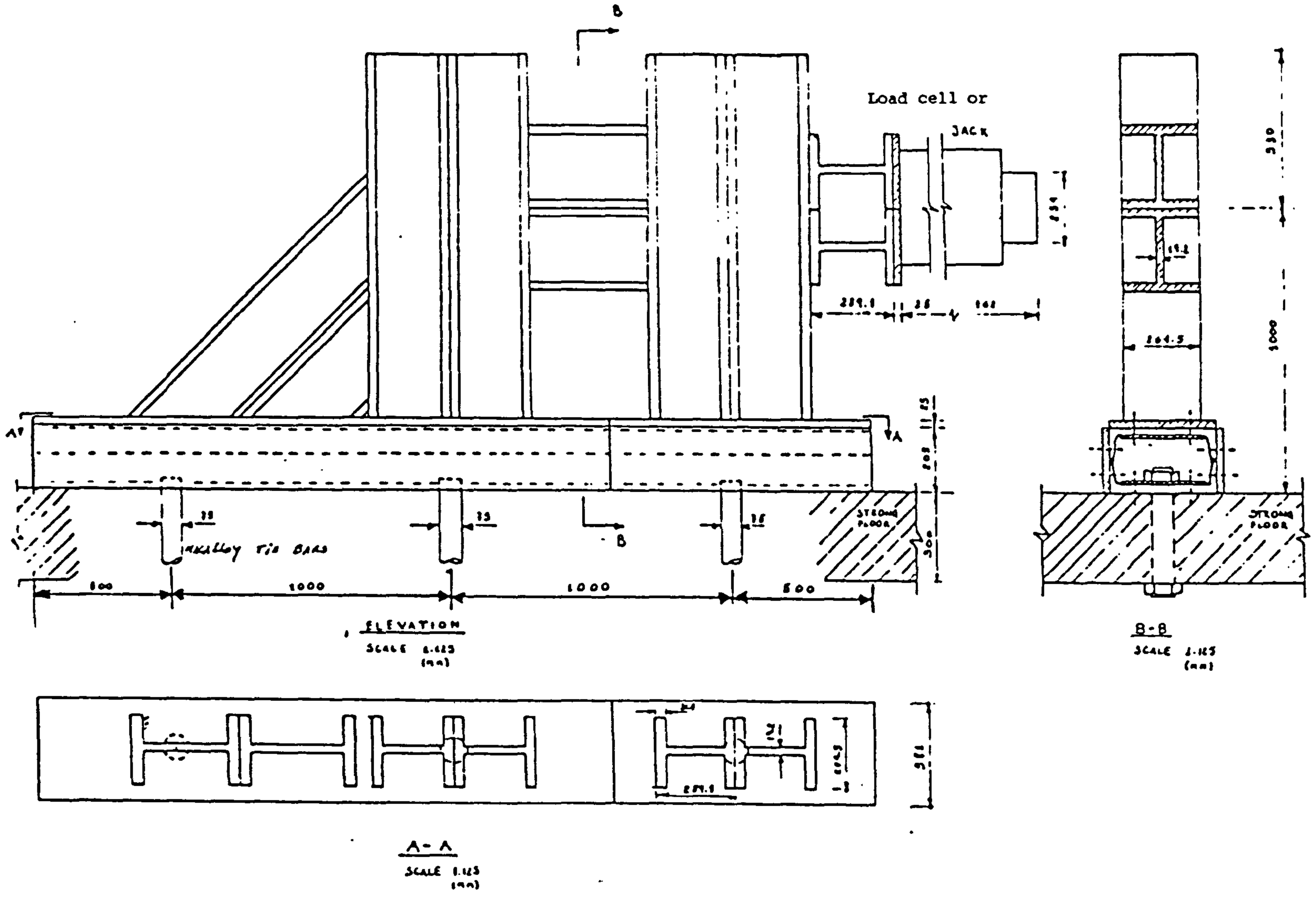

Fig. 3.1.A. - Details of the reaction block at the ends.

Fig.3.2. View of the *self-weight rig*

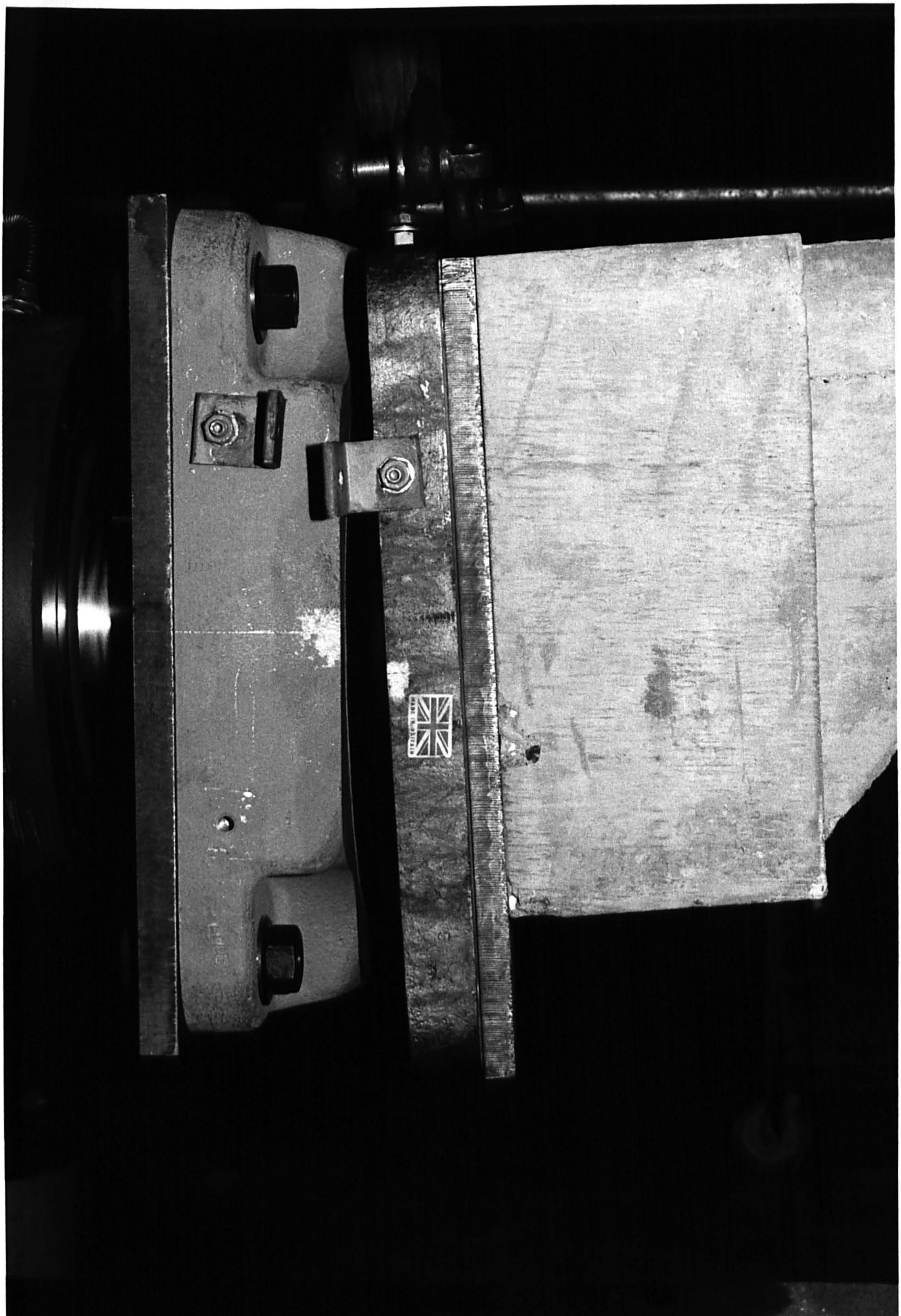

Fig. 3.3. Close-up of the Glacier Structural Bearing

COLUMN MCUO 2

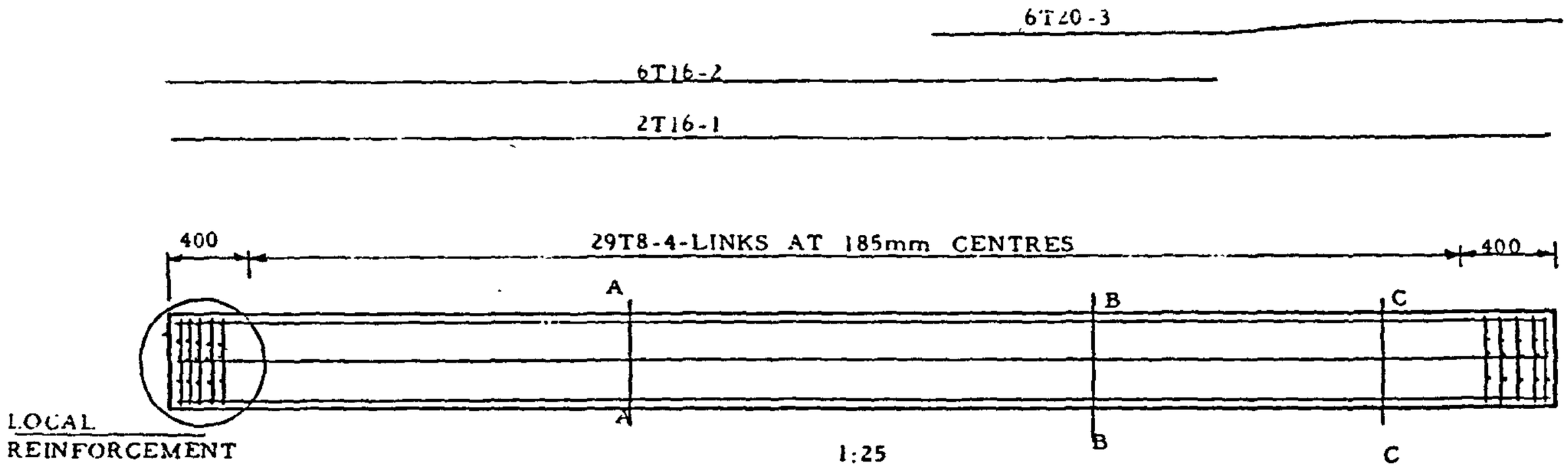

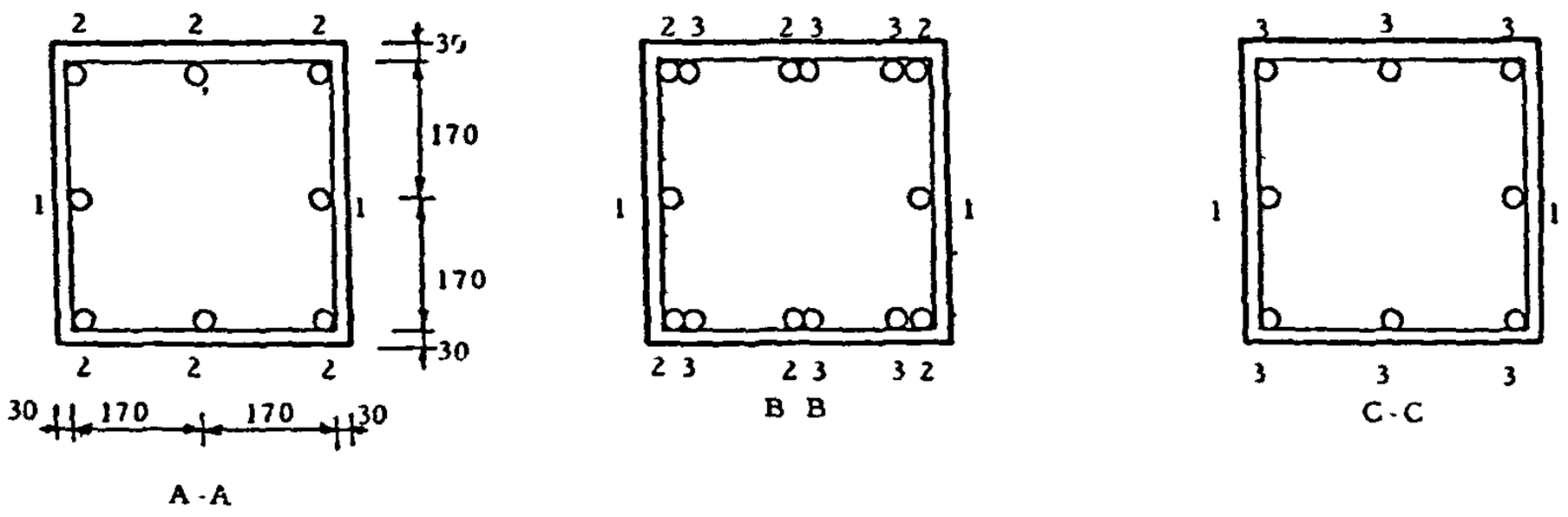

Fig. 4.1. - Reinforcement details for column MCUO-02

COLUMN MARK-03/05

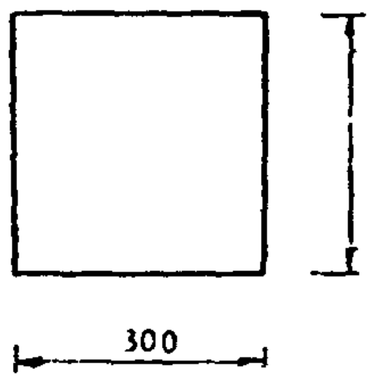

A-A

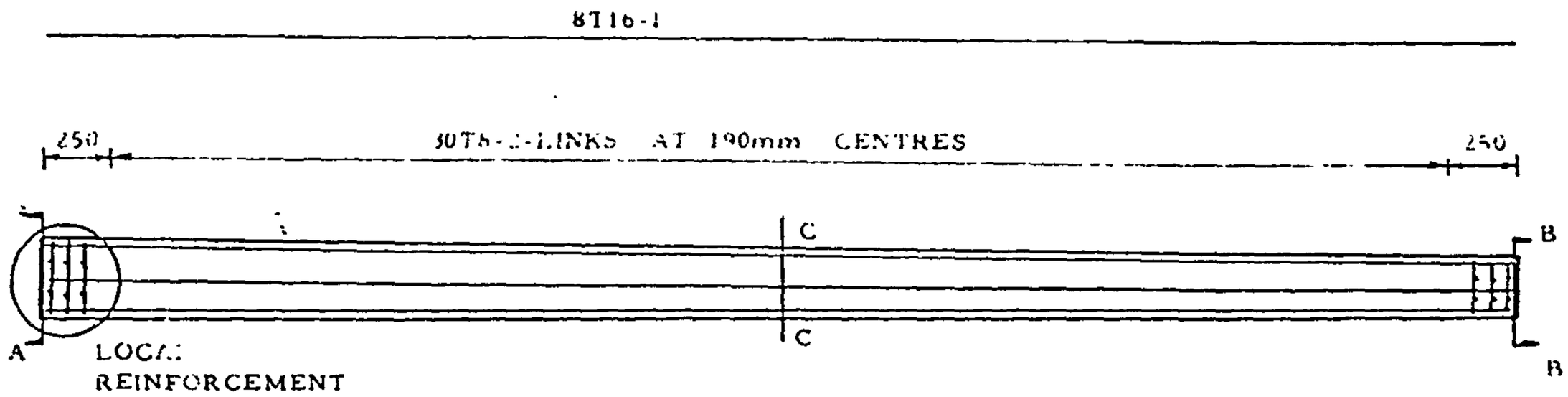

1:25

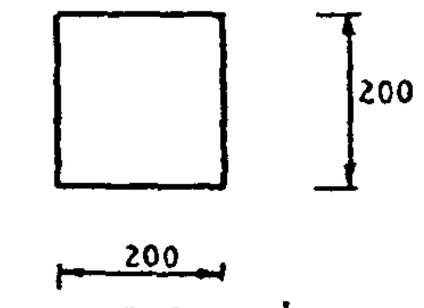

B-B

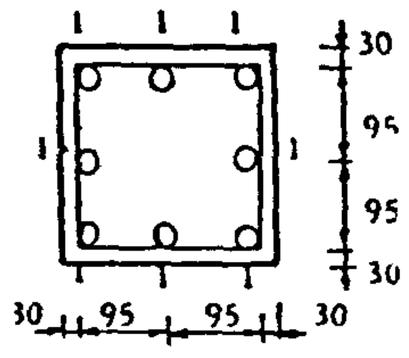

C-C

1:10

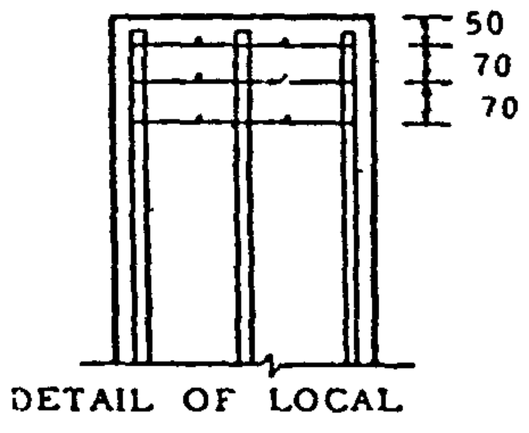

DETAIL OF LOCAL
REINFORCEMENT

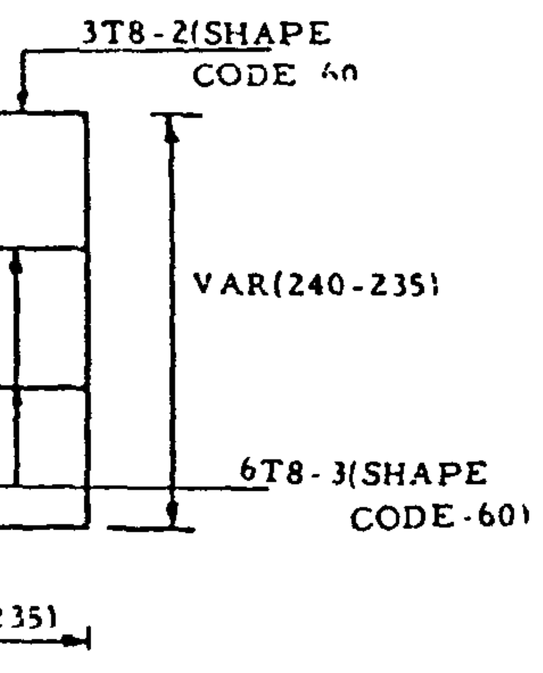

MESH-SIZE AT TOP

1:50

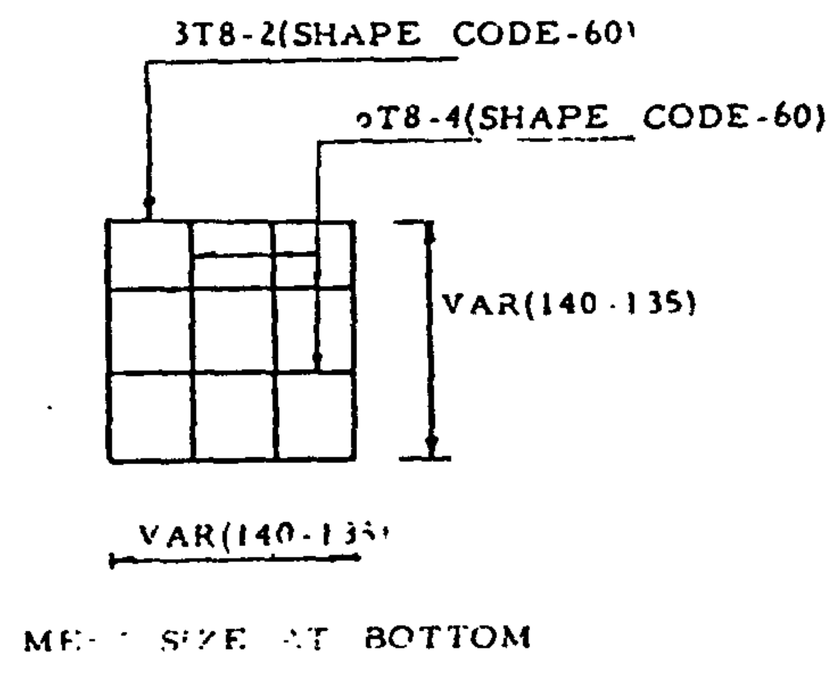

MESH SIZE AT BOTTOM

1:50

Fig. 4.2. - Reinforcement details for columns MDUO-03/05

COLUMN MTUO-04/06

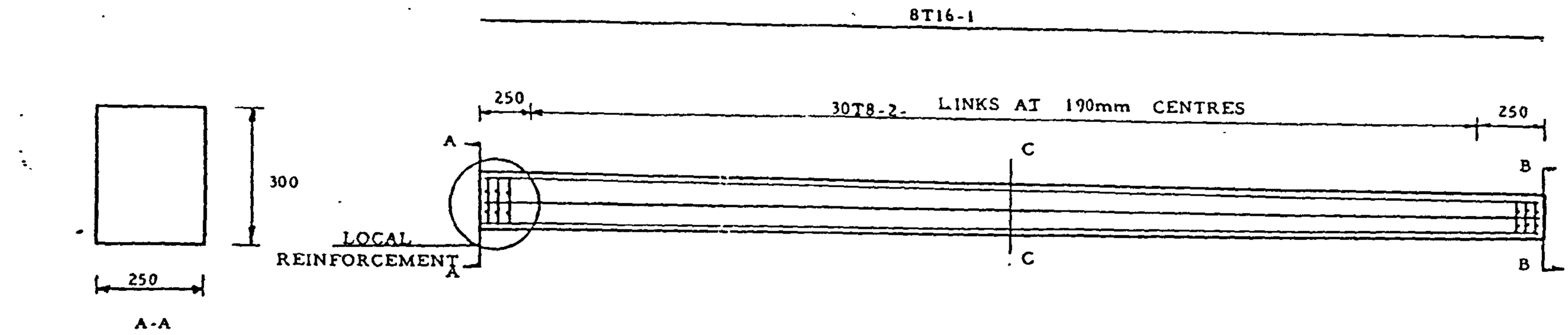

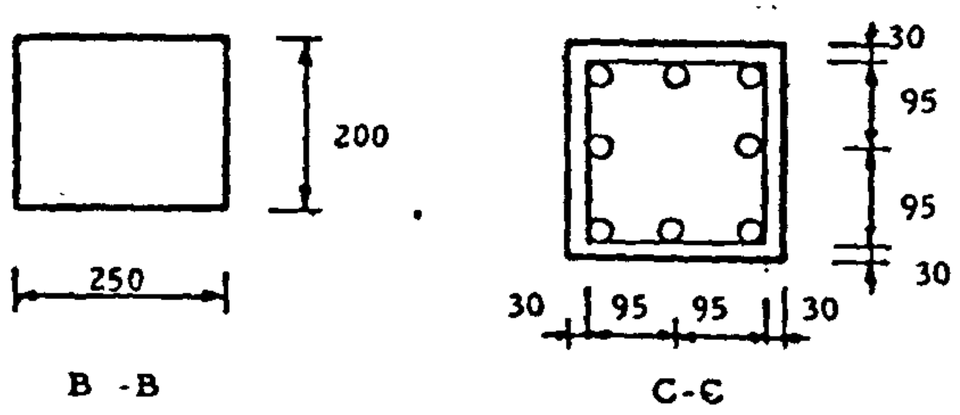

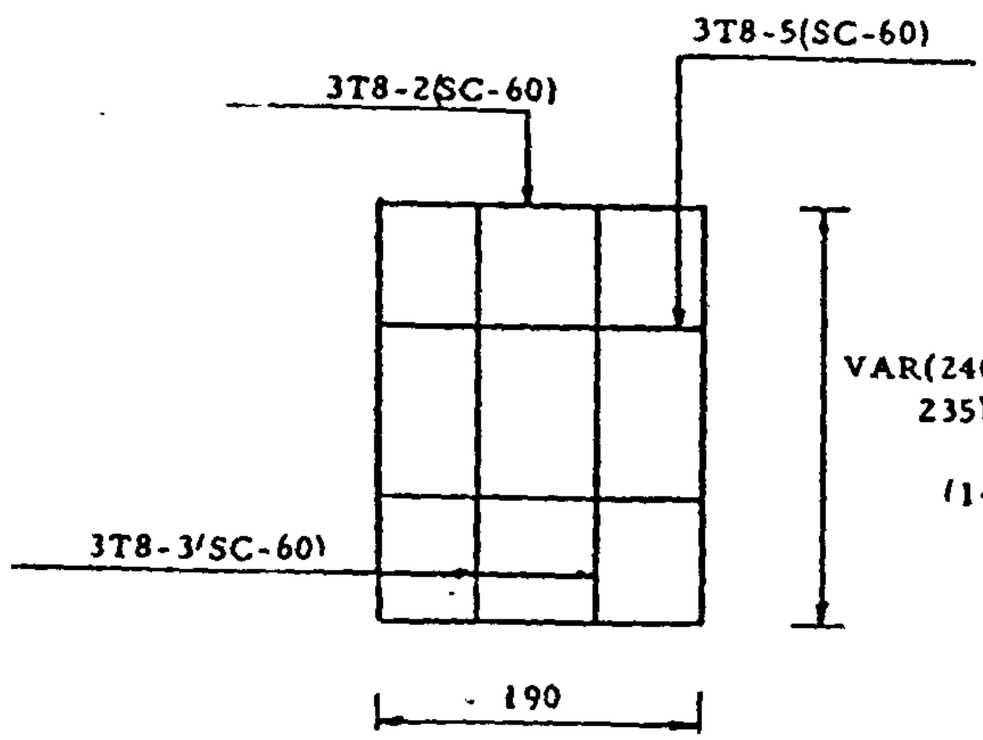

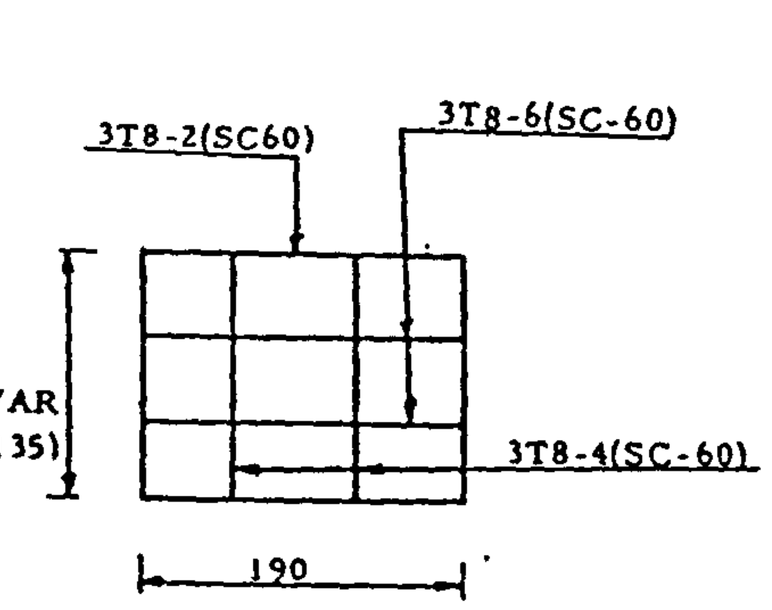

Fig. 4.3. - Reinforcement details for columns MTUO-04/06

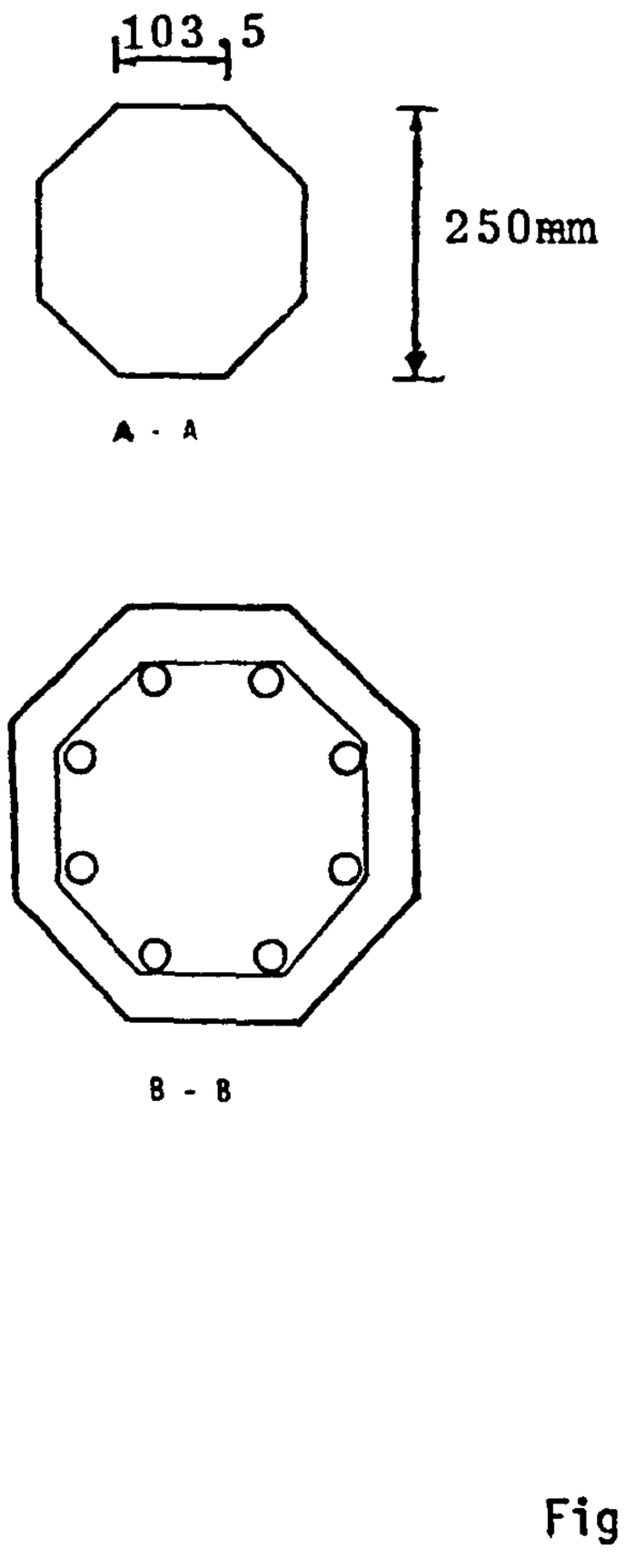

Fig. 4.4. Reinforcement details for columns MGUO_07/08

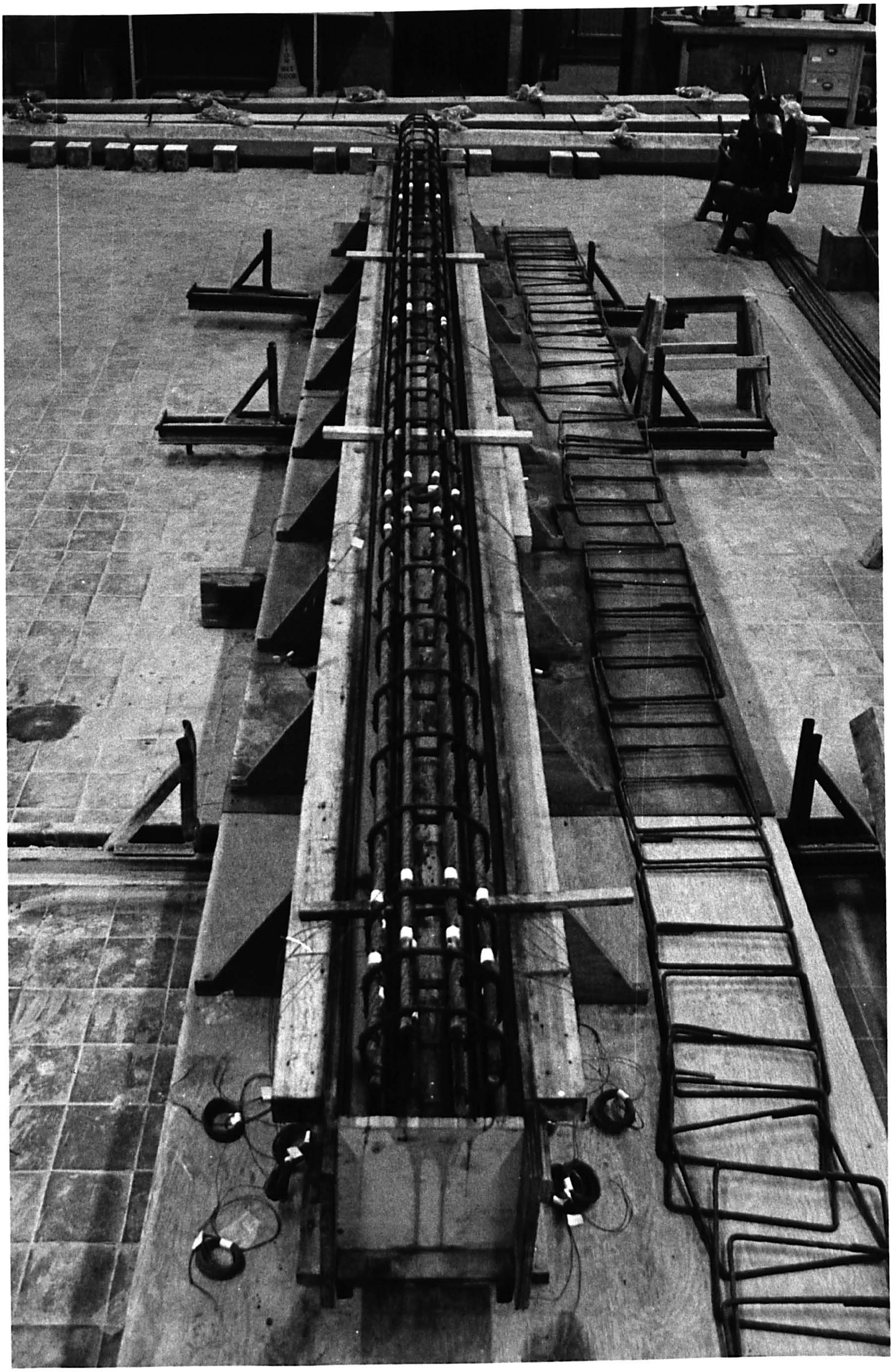

Fig. 4.5. A view of reinforcement cage for octagonal cross section columns

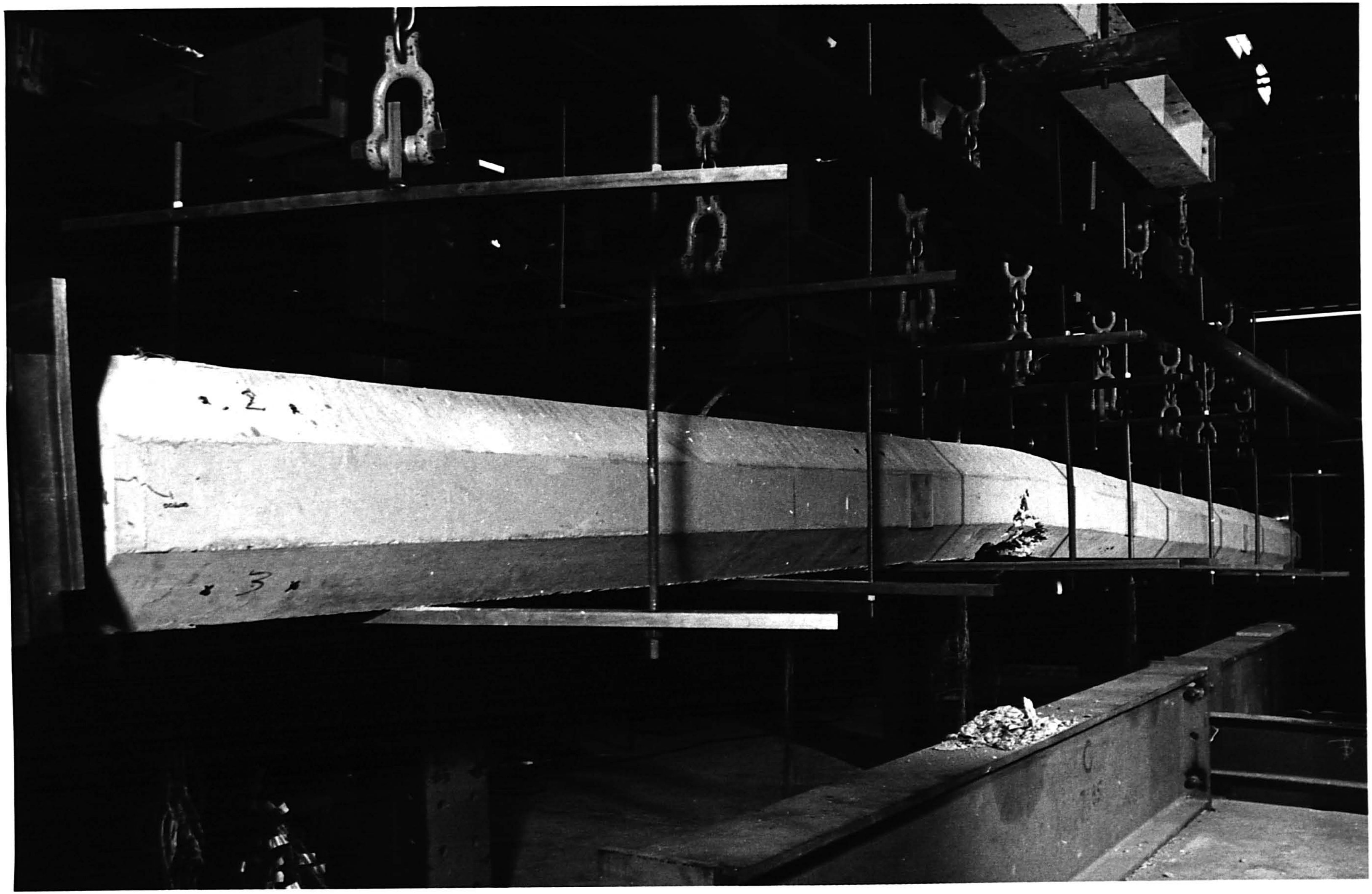

Fig. 4.6. A typical view of
failed column

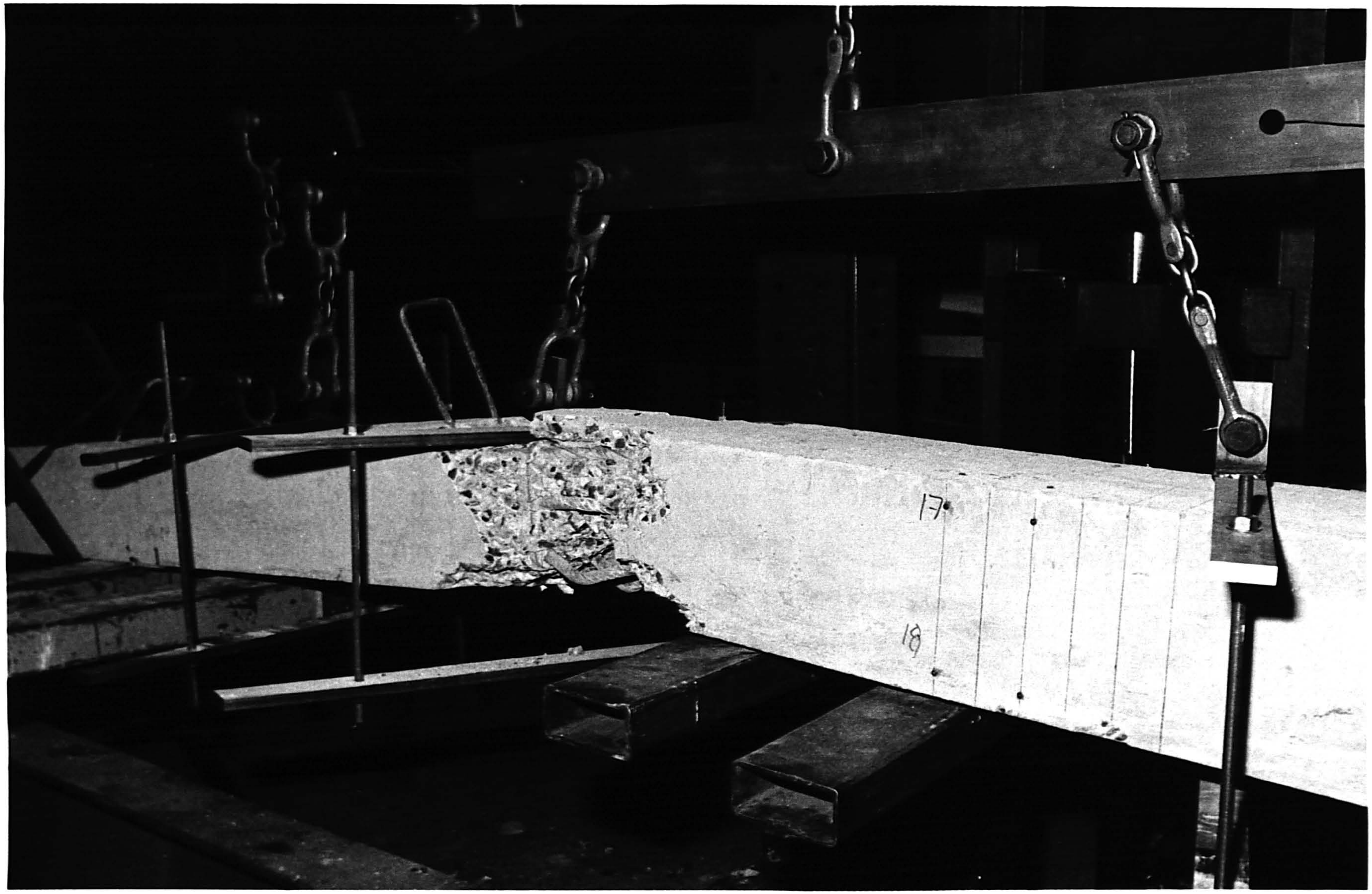

Fig. 4.7. View of the mode of failure

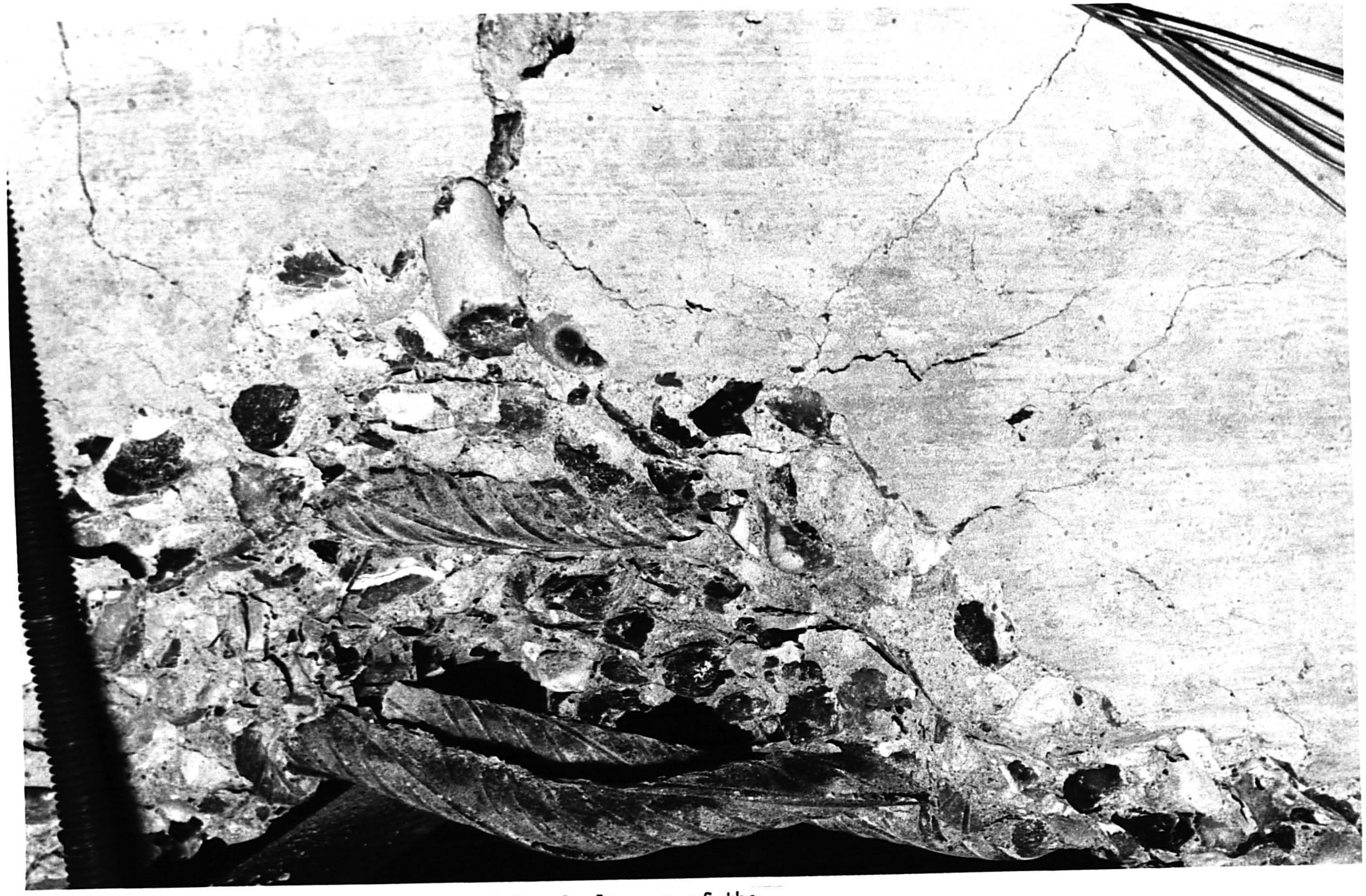

Fig. 4.8. A close-up of the failed section

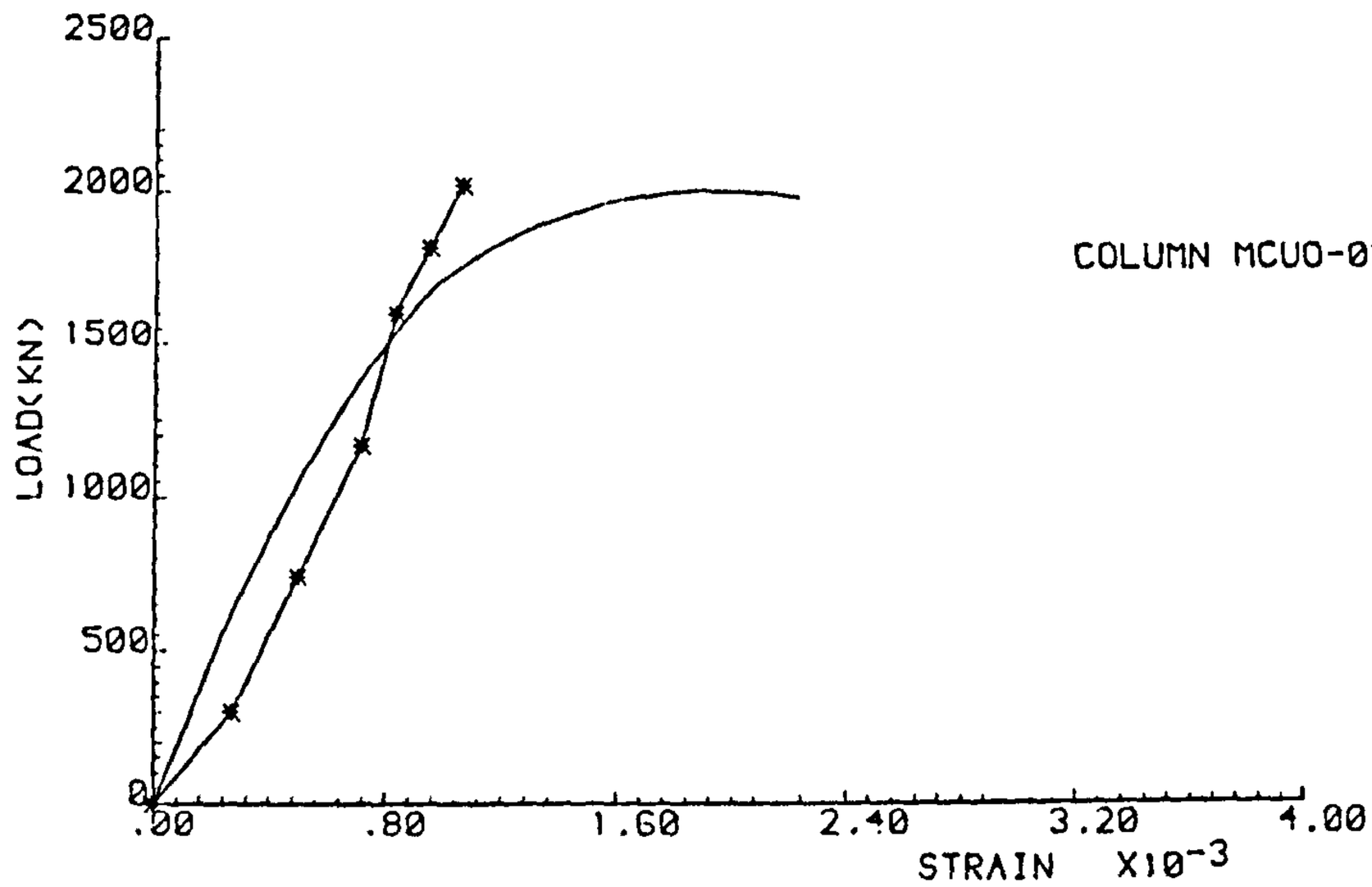

LOAD vs STRAIN

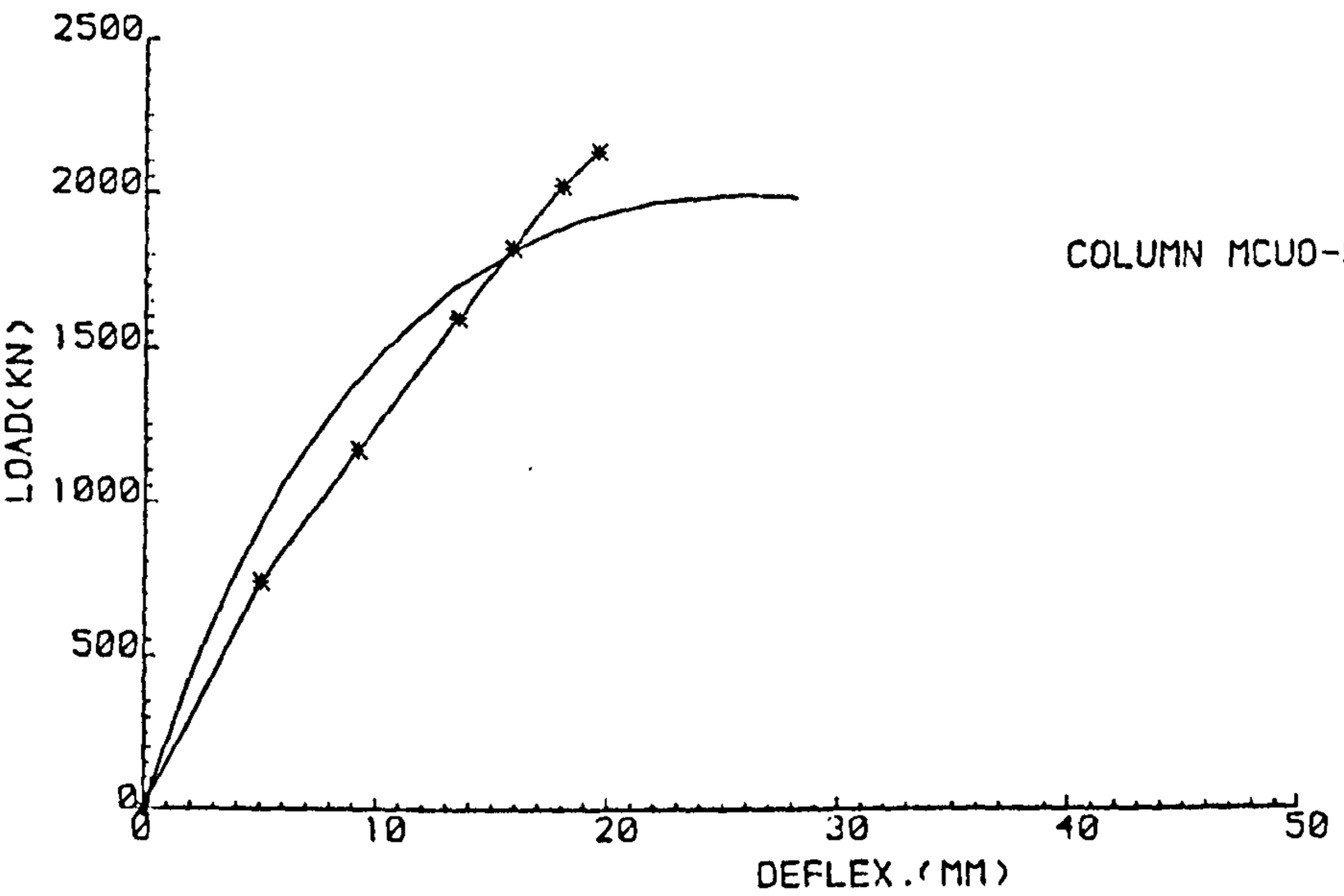

LOAD vs DEFLECTION

Fig. 4.9 - Comparison between experimental and theoretical results for column MCU0-02

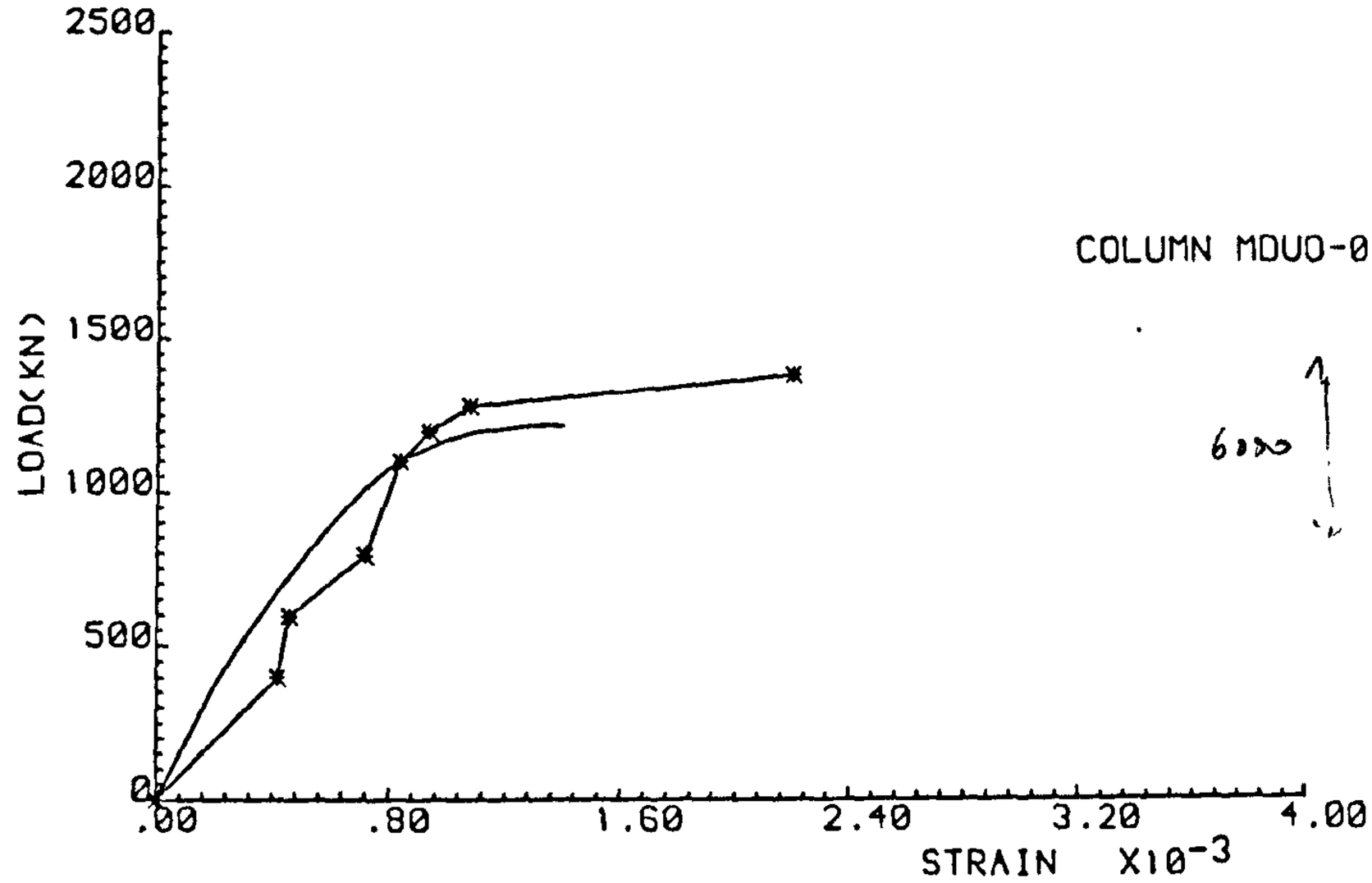

LOAD vs STRAIN

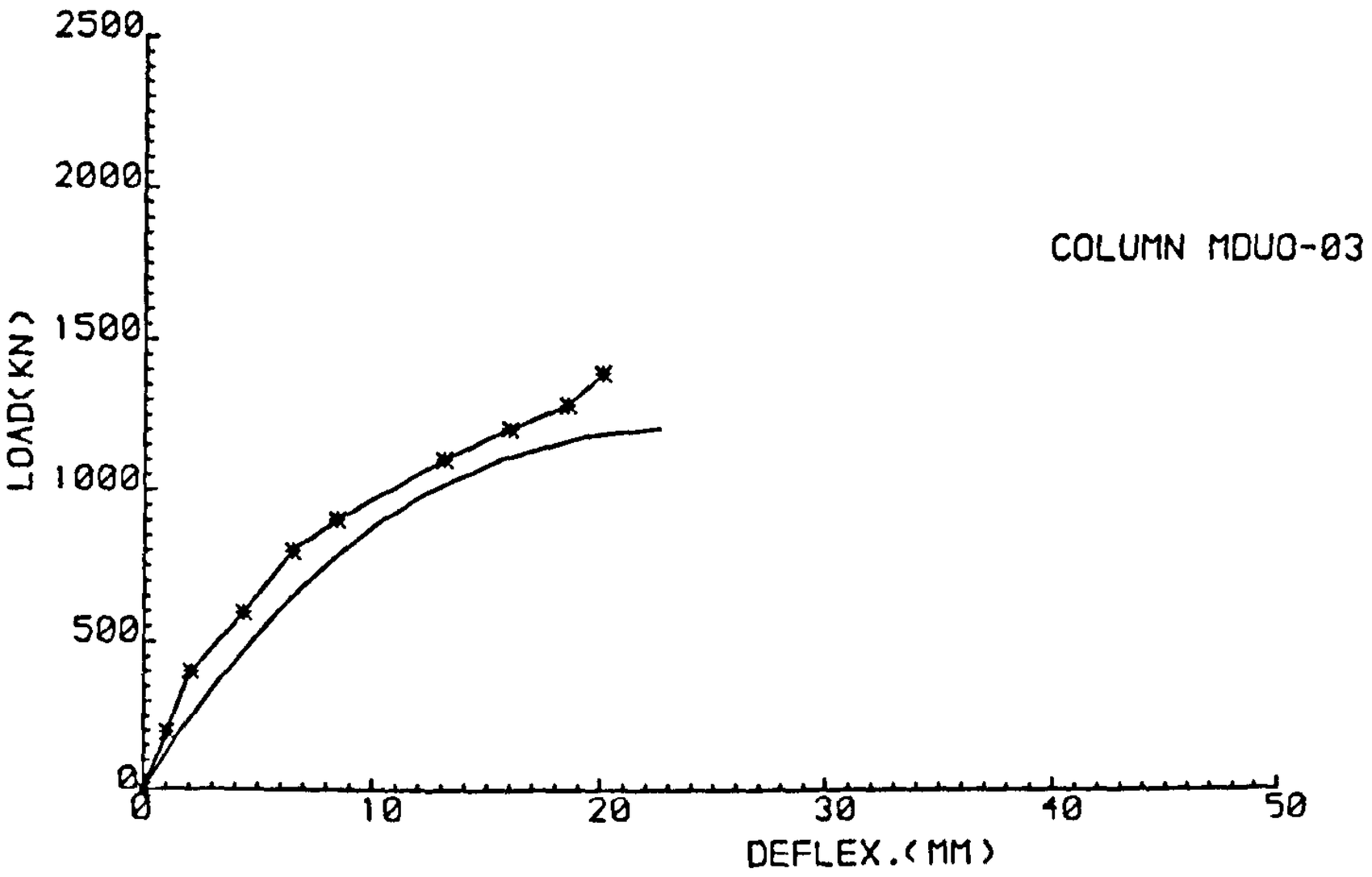

LOAD vs DEFLECTION

Fig. 4.10 - Comparison between experimental and theoretical results for column MDU0-03

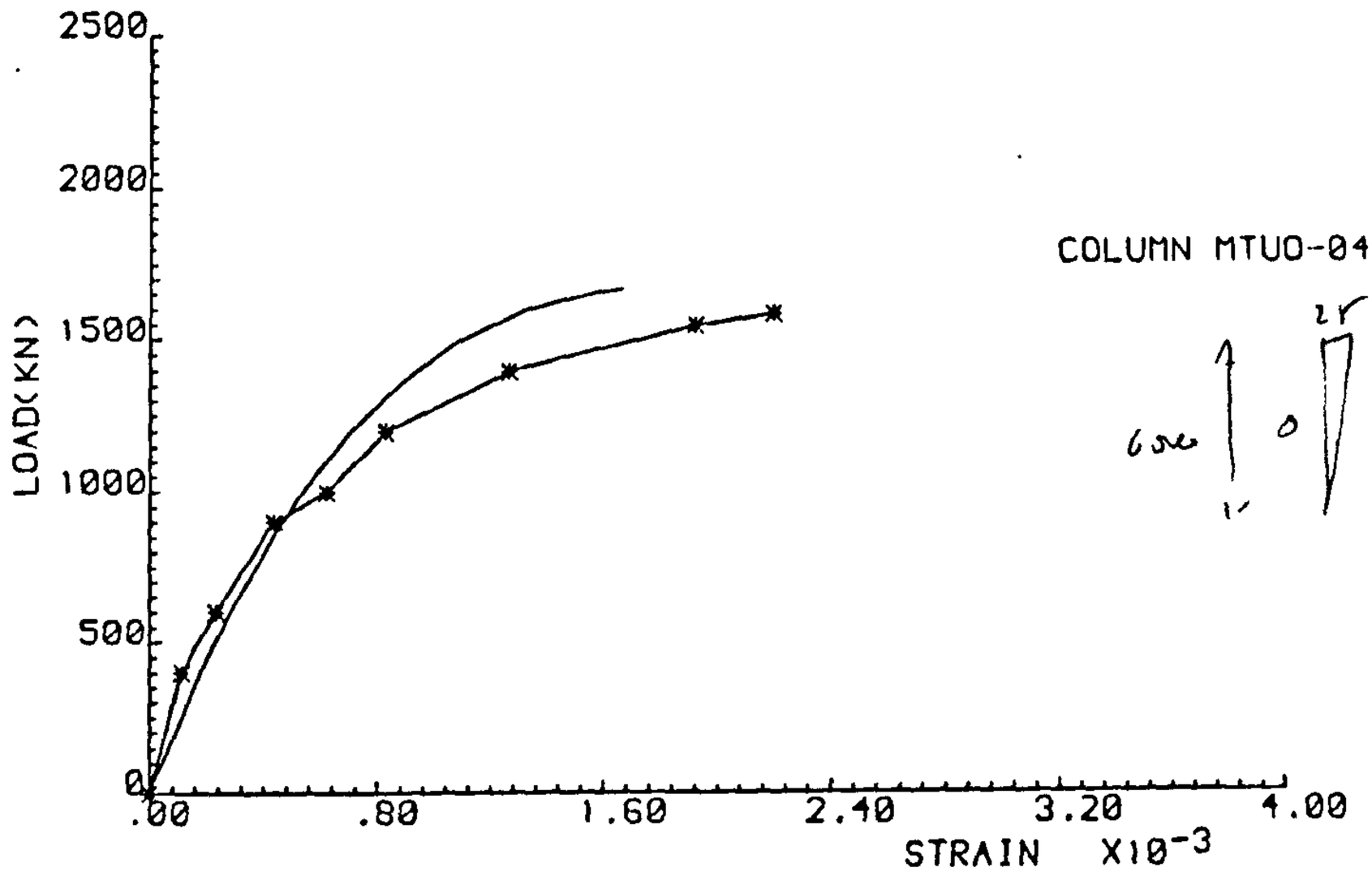

LOAD vs STRAIN

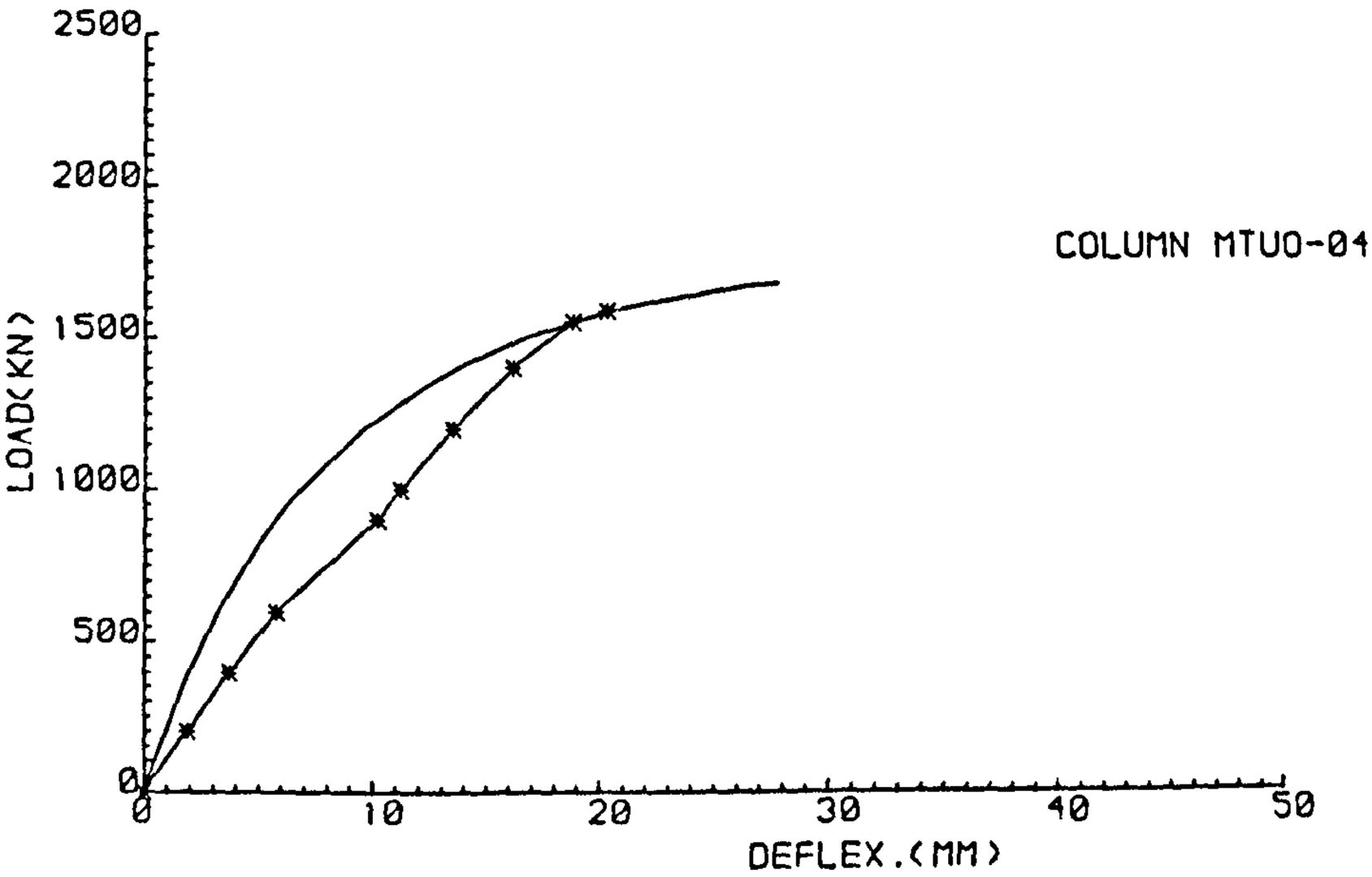

LOAD vs DEFLECTION

Fig. 4.11 - Comparison between experimental and theoretical results for column MTUO-04

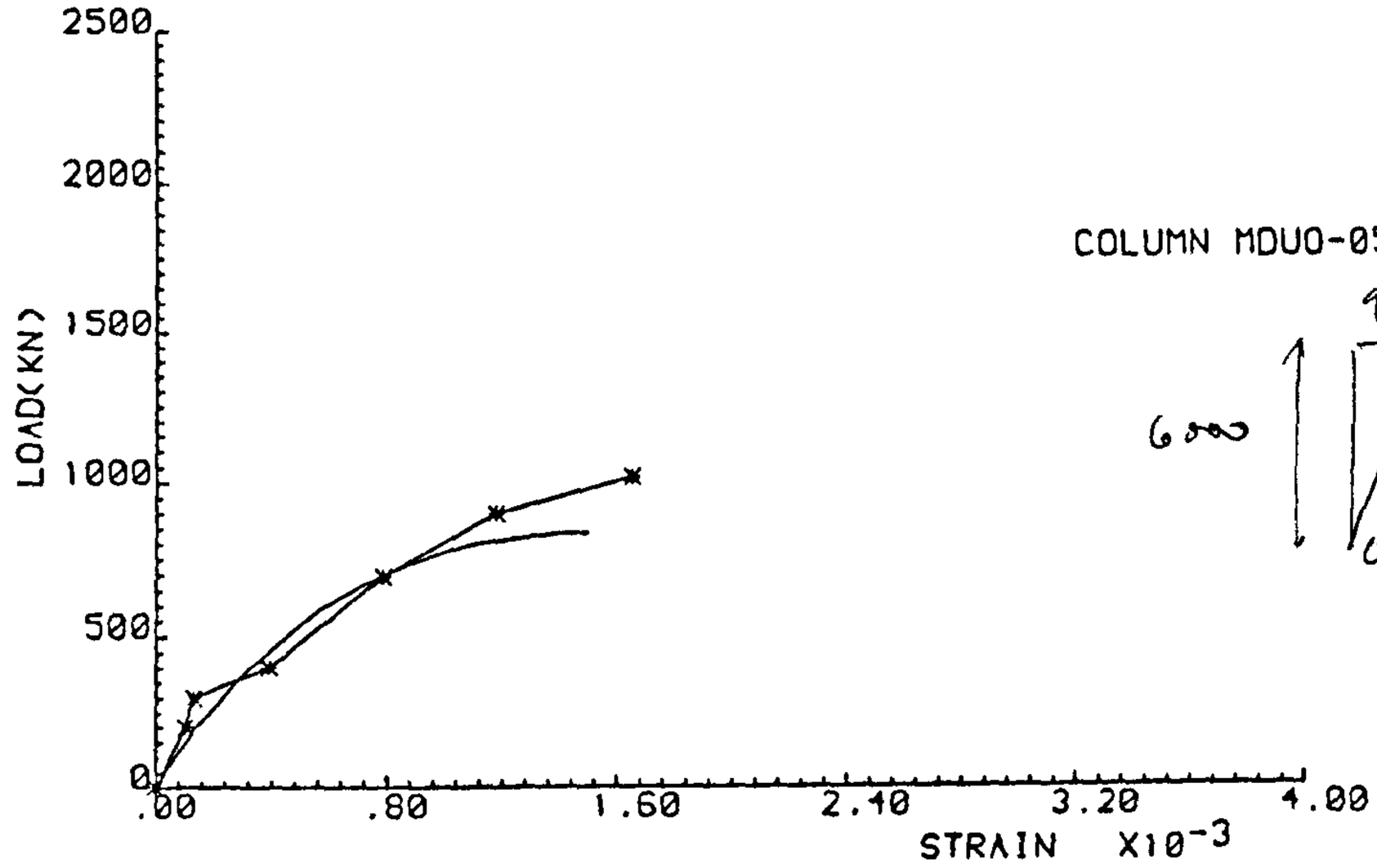

LOAD vs STRAIN

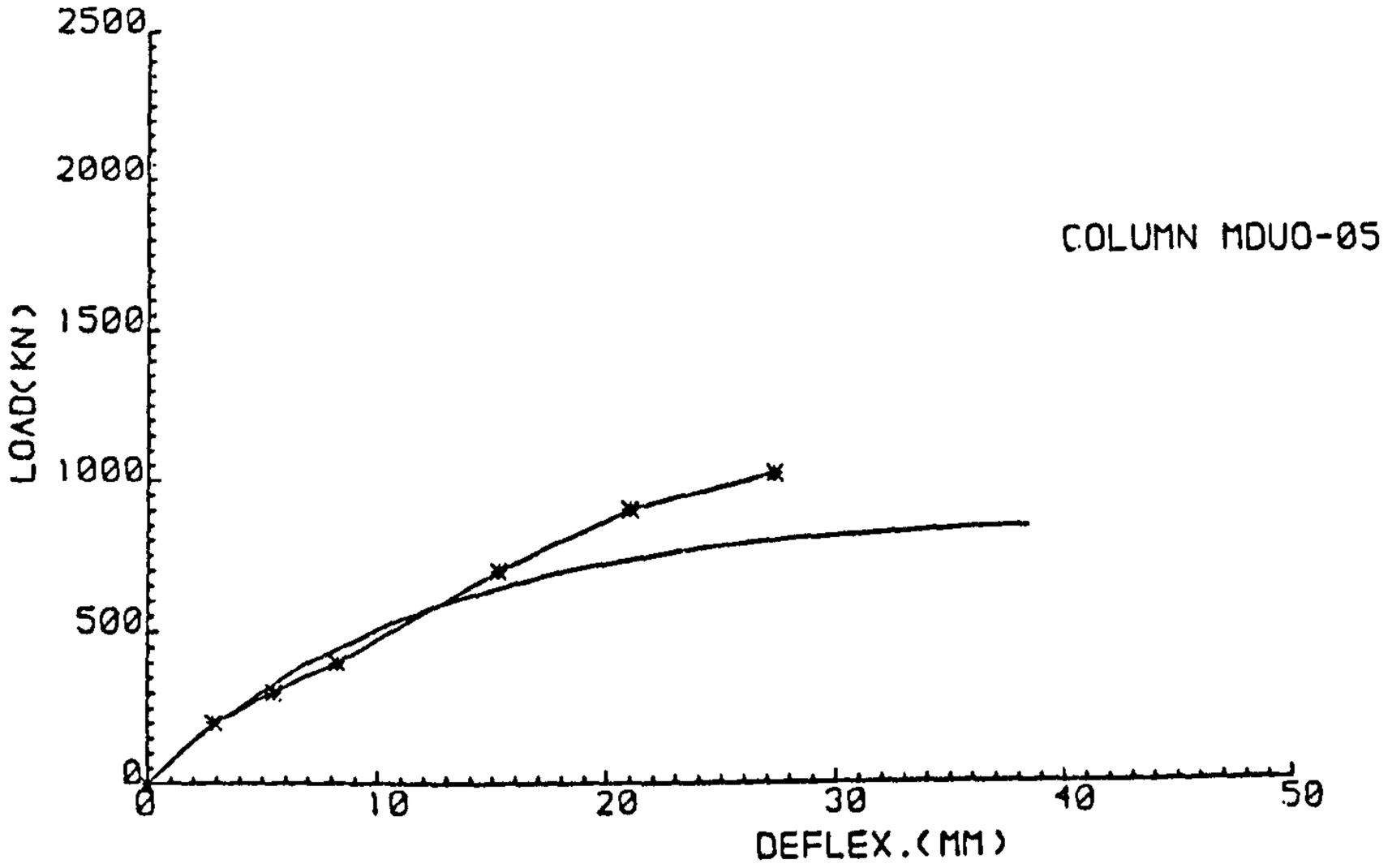

LOAD vs DEFLECTION

Fig. 4.12 - Comparison between experimental and theoretical results for column MDU0-05

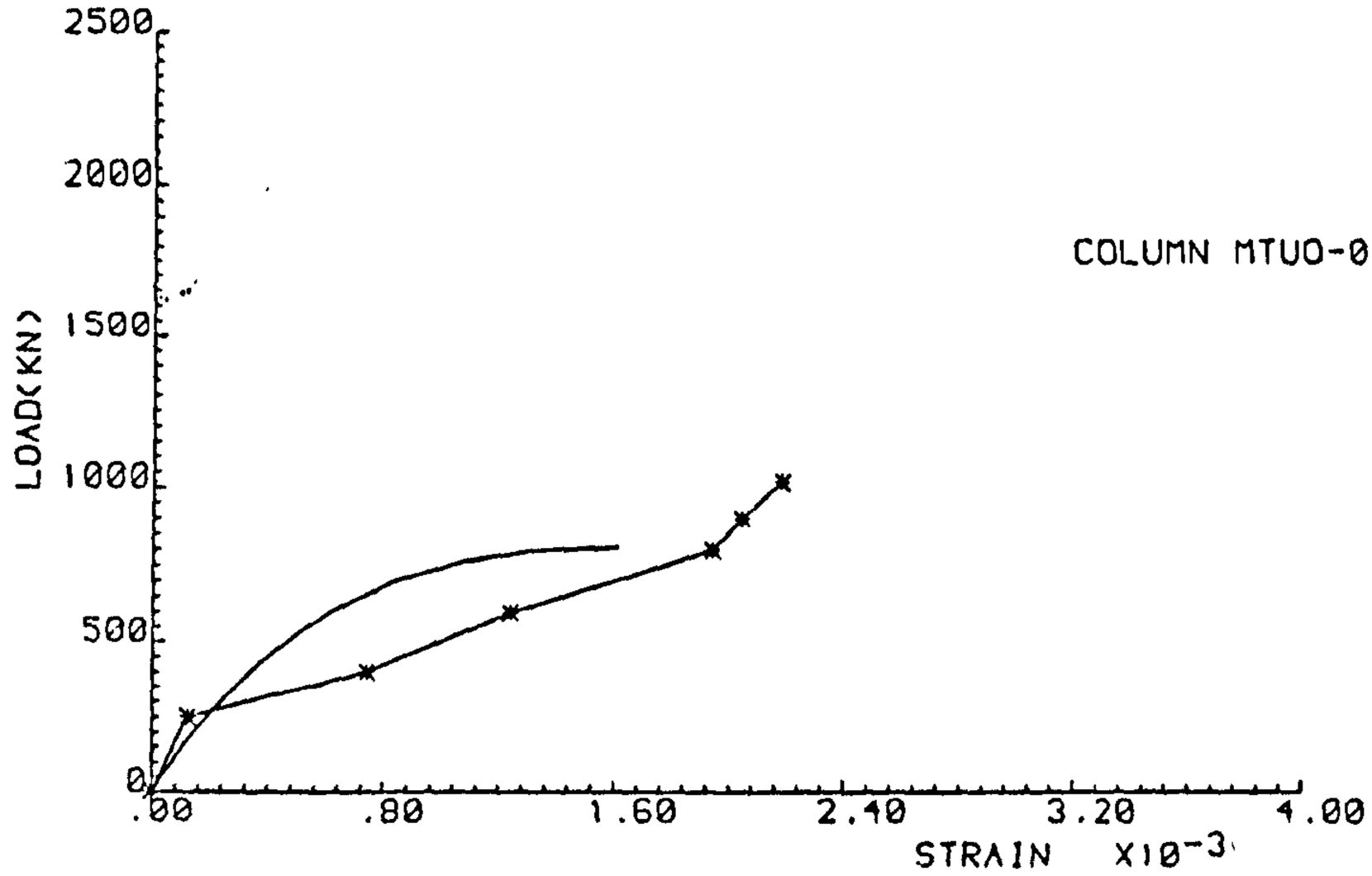

LOAD vs STRAIN

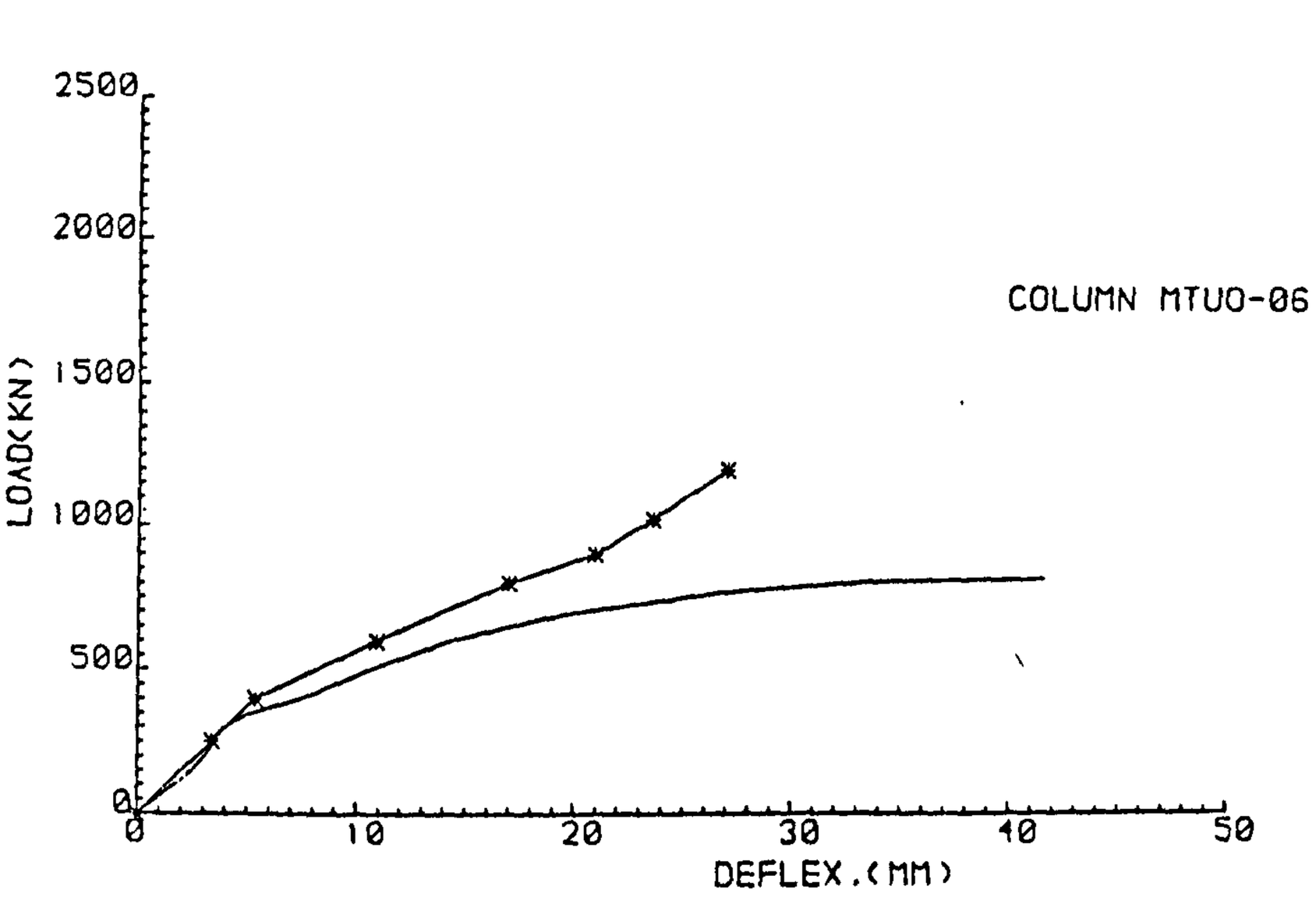

LOAD vs DEFLECTION

Fig. 4.13 - Comparison between experimental and theoretical results for column MTUO-06

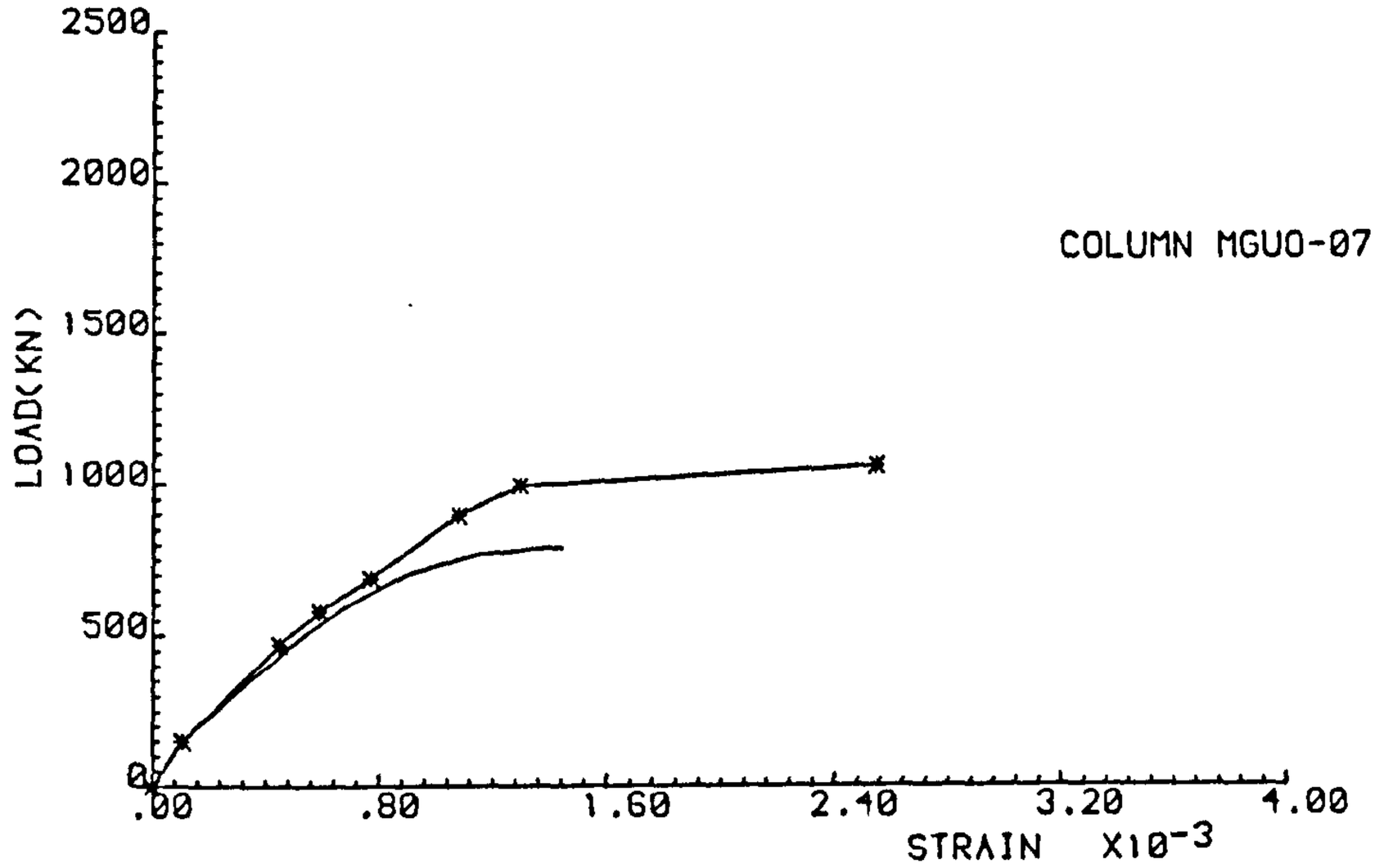

LOAD vs STRAIN

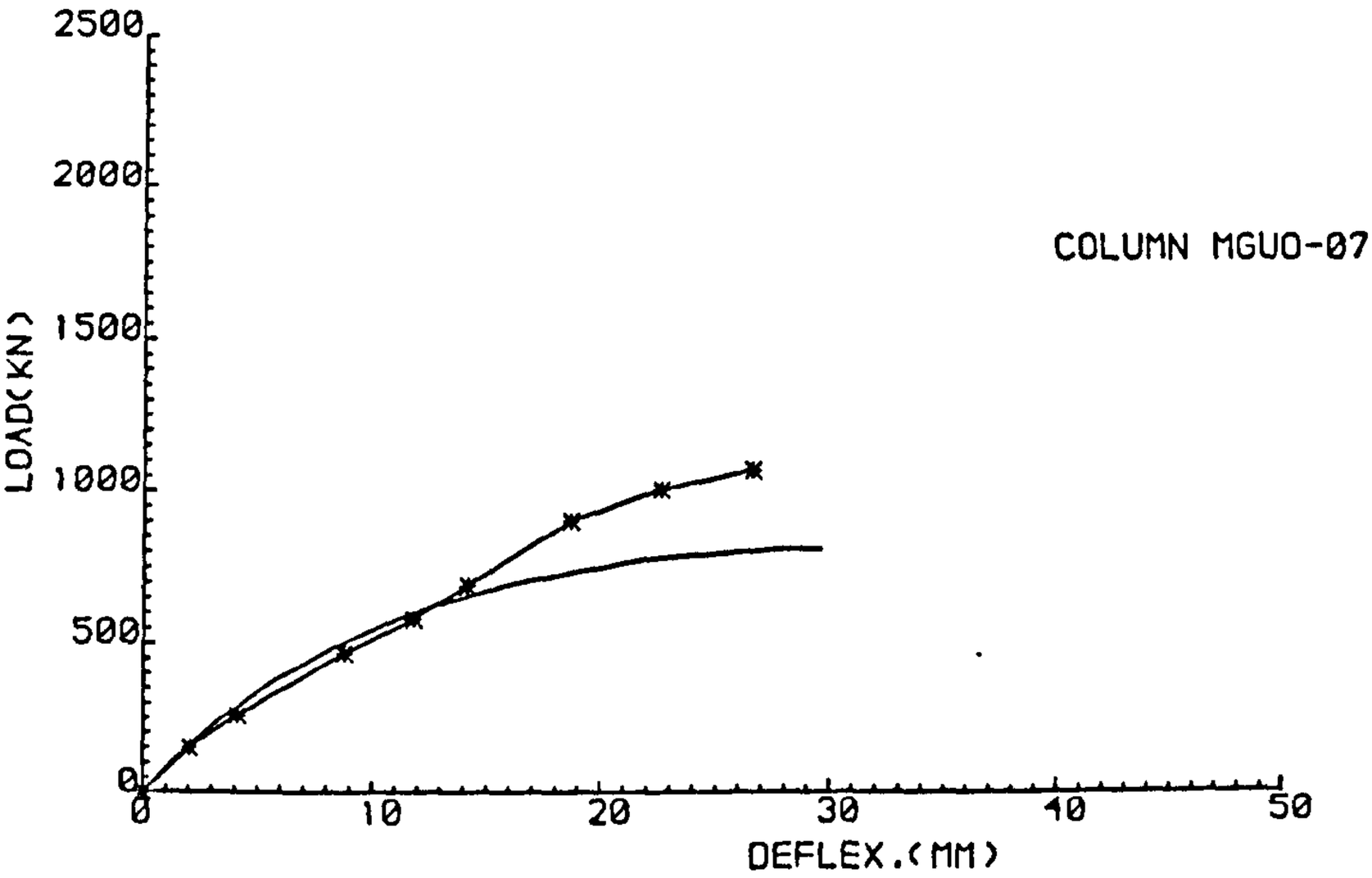

LOAD vs DEFLECTION

Fig. 4.14 - Comparison between experimental and theoretical results for column MGUO-07

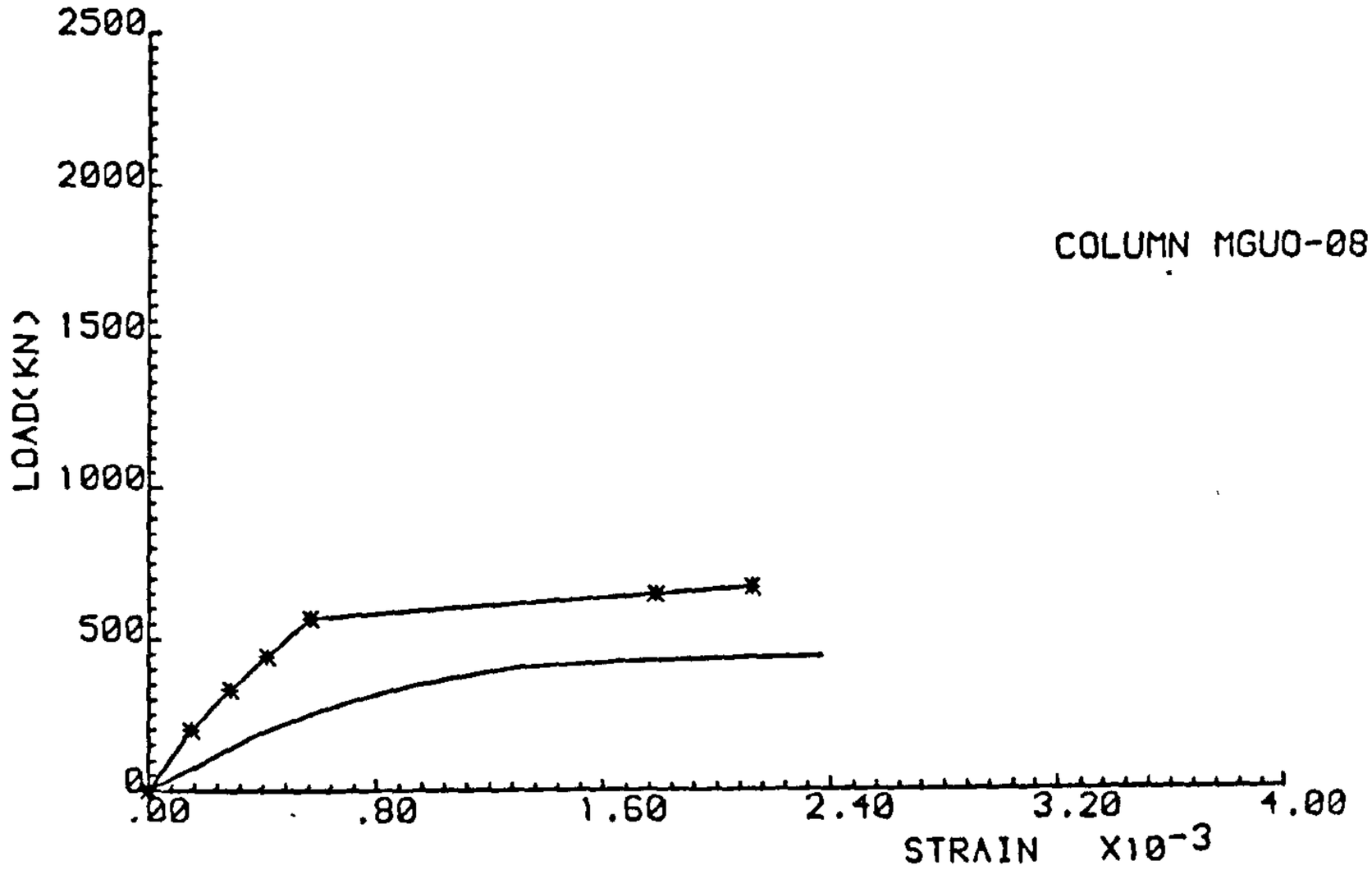

LOAD vs STRAIN

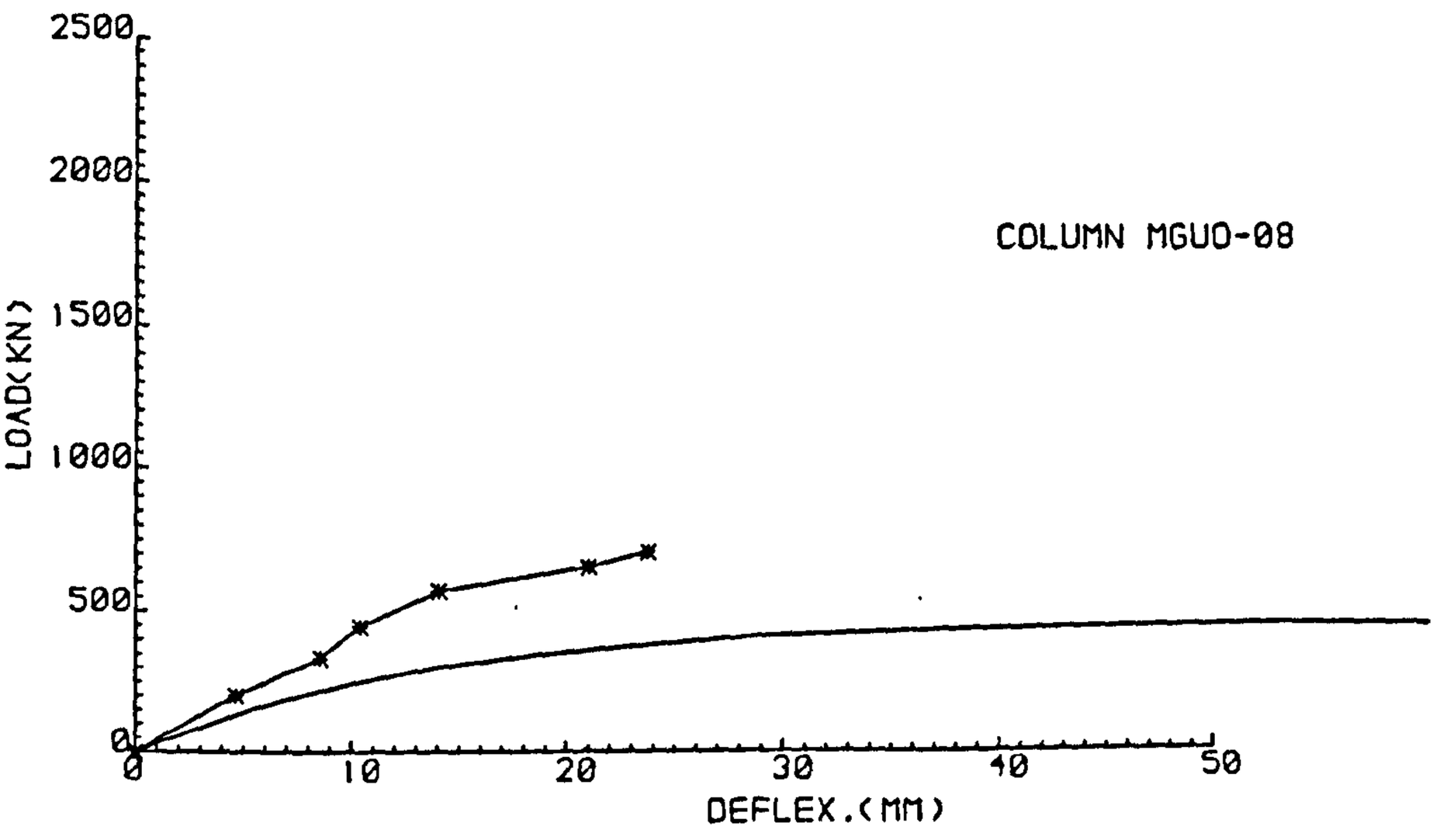

LOAD vs DEFLECTION

Fig. 4.15 - Comparison between experimental and theoretical results for column MGUO-08

SECTION at MID-LENGTH

SECTION at THREE-QUARTER LENGTH
from the ECCENTRICALLY LOADED END

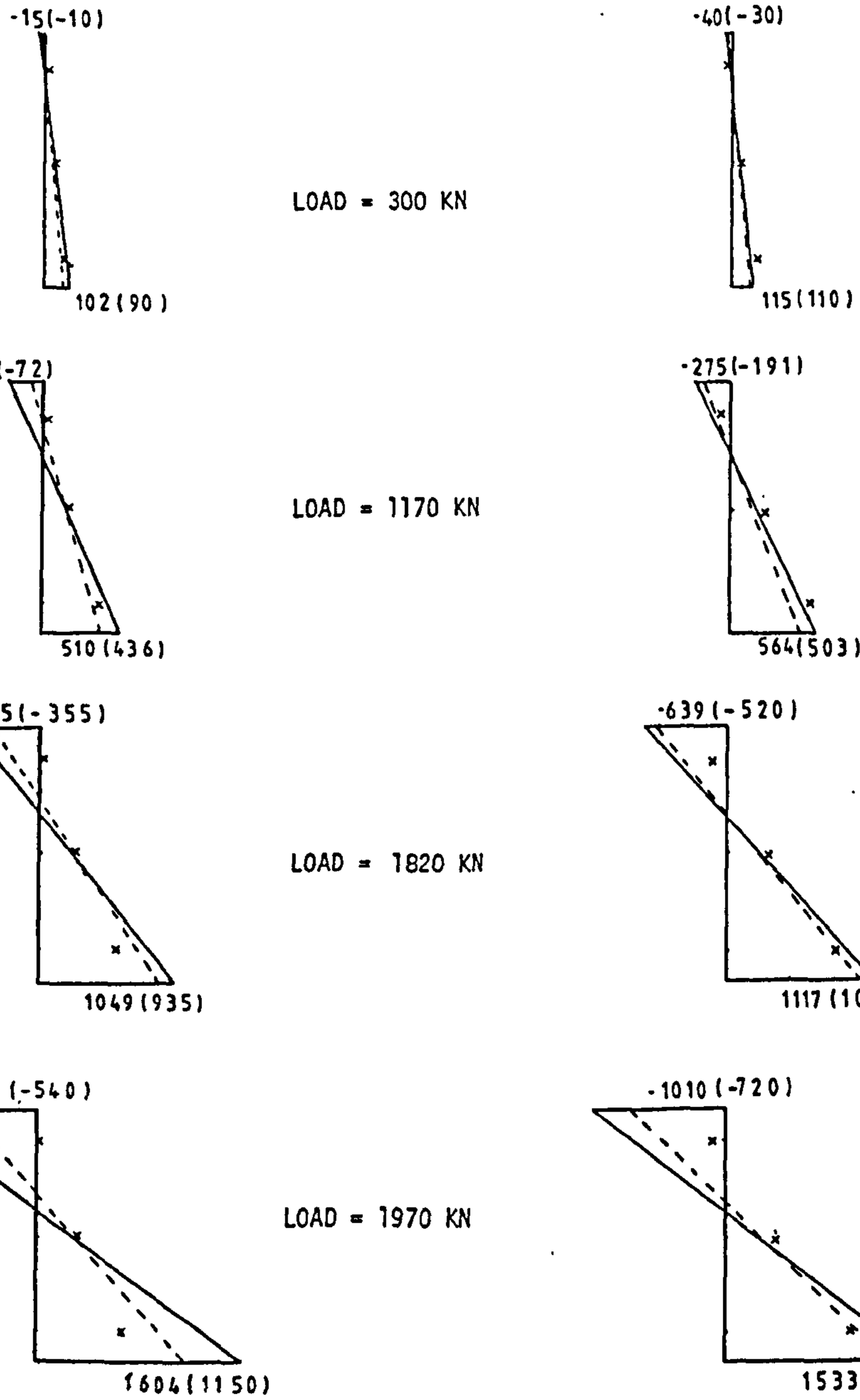

Fig. 4.16. - Strain* Profiles across the section for column MCUO-02

*strain values shown $x10^6$

SECTION at MID-LENGTH		SECTION at THREE-QUARTER LENGTH from the ECCENTRICALLY LOADED END
	LOAD = 400 KN	
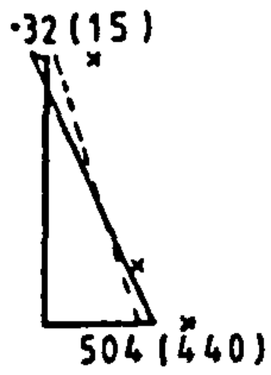	LOAD = 800 KN	
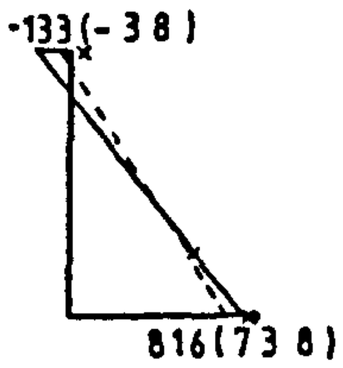	LOAD = 1100 KN	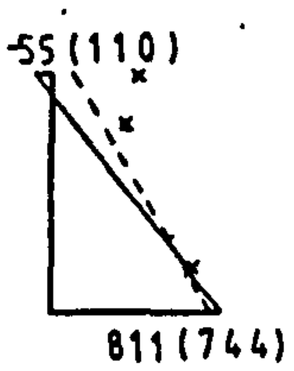
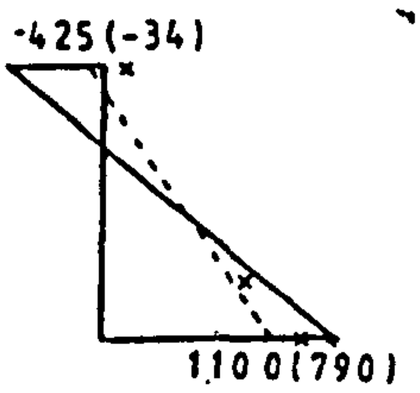	LOAD = 1200 KN	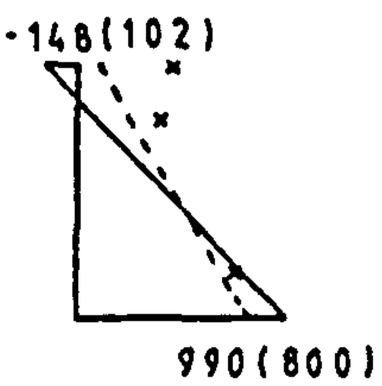

Fig. 4.17. - Strain* Profiles across the section for column MDUO-03

*strain values shown $x10^6$

SECTION at MID-LENGTH

SECTION at THREE-QUARTER LENGTH from the ECCENTRICALLY LOADED END

LOAD = 400 KN

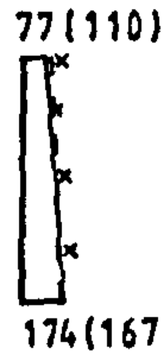

LOAD = 900 KN

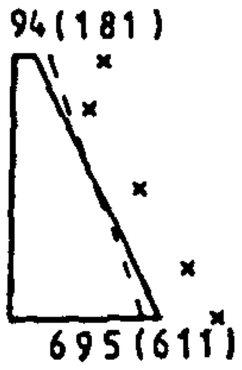

LOAD = 1200 KN

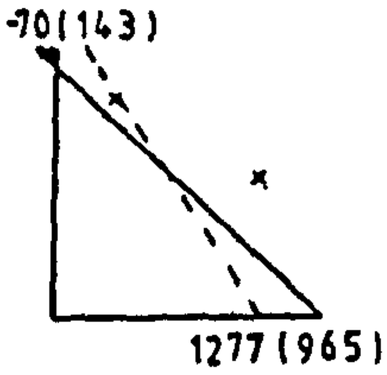

LOAD = 1580 KN

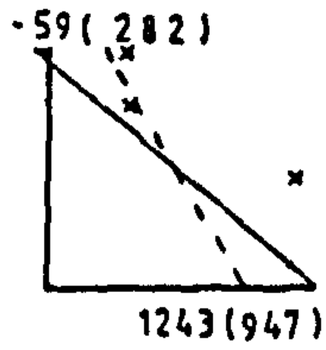

Fig. 4.18. - Strain* Profiles across the section for column MTU0-04

*strain values shown $x10^6$

SECTION at MID-LENGTH		SECTION at THREE-QUARTER LENGTH from the ECCENTRICALLY LOADED END
-52(-19)  227(204)	LOAD = 300 KN	-3(33)  207(191)
-96(-32)  324(283)	LOAD = 400 KN	-14(39)  288(265)
-436(-221) 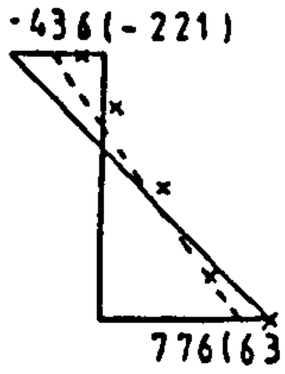 776(631)	LOAD = 700 KN	-109(18) 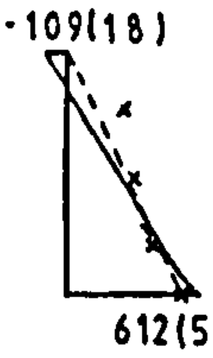 612(545)
-783(-400) 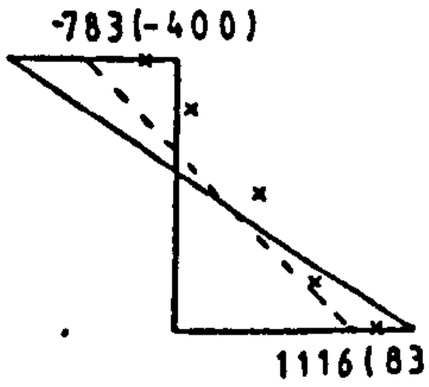 1116(836)	LOAD = 800 KN	-245(-16) 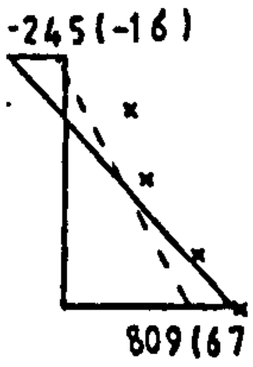 809(679)

Fig. 4.19. - Strain* Profiles across the section for column MDU0-05

*strain values shown $x10^6$

SECTION at MID-LENGTH		SECTION at THREE-QUARTER LENGTH from the ECCENTRICALLY LOADED END
-39(-15)  192(173)	LOAD = 250 KN	(27)  157(145)
-103(-33)  336(291)	LOAD = 400 KN	-12(35)  267(246)
-292(-139)  611(511)	LOAD = 600 KN	-58(30)  448(406)
-1020(-487) 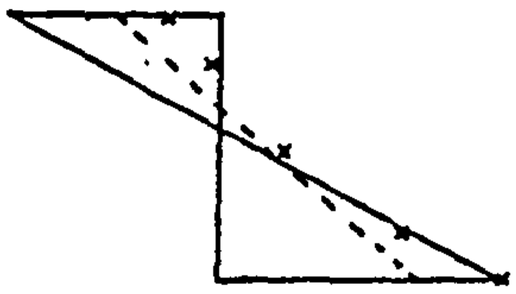 1329(918)	LOAD = 800 KN	-350(-23) 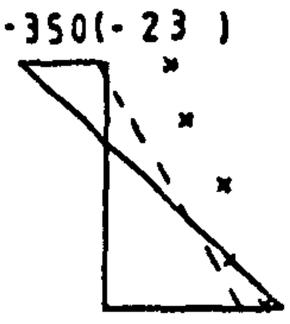 820(636)

Fig. 4.20. - Strain* Profiles across the section for column MTU0-06

*strain values shown $x10^6$

SECTION at MID-LENGTH

SECTION at ONE-QUARTER LENGTH from the ECCENTRICALLY LOADED END

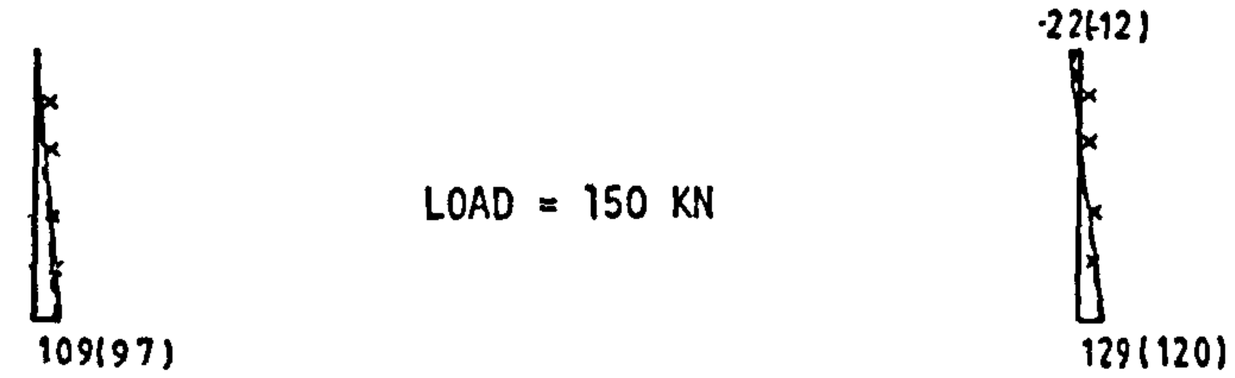

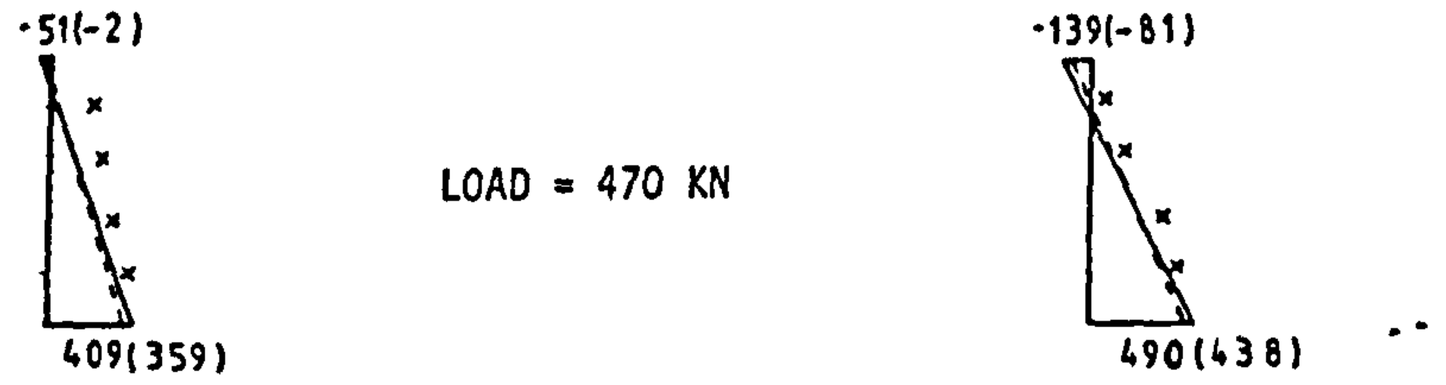

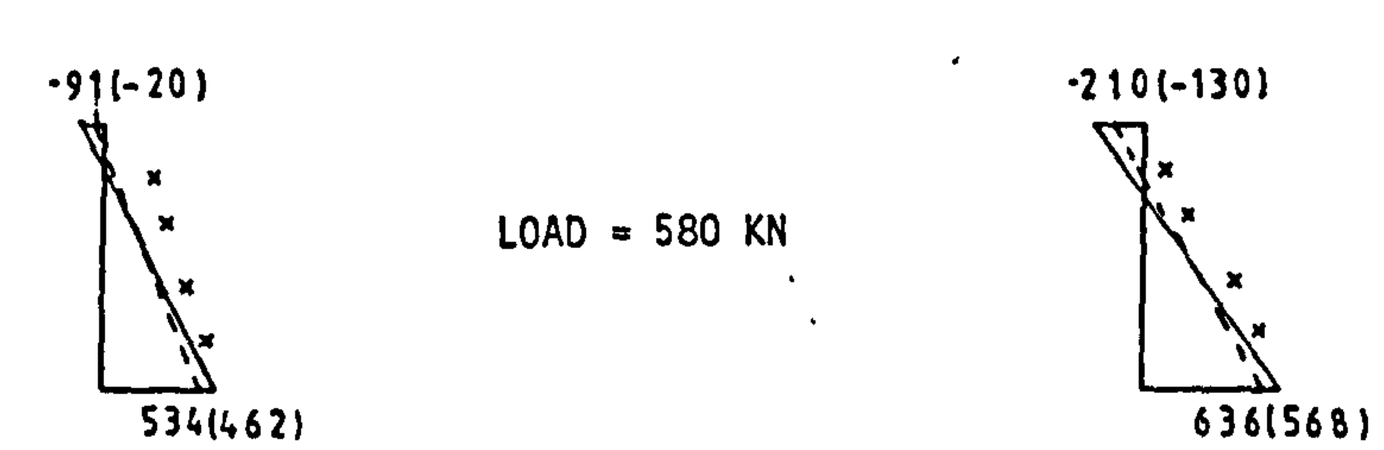

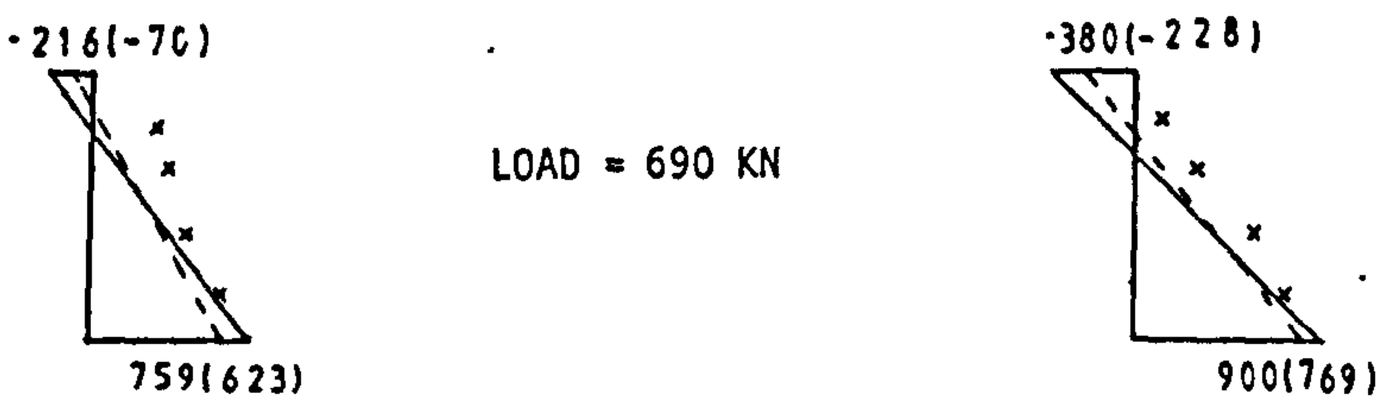

4.21. - Strain* Profiles across the section for column MGUO-07

*strain values shown $x10^6$

SECTION at MID-LENGTH

SECTION at ONE-QUARTER LENGTH from the ECCENTRICALLY LOADED END

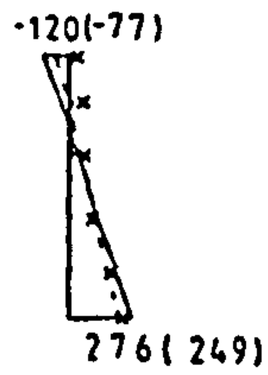

LOAD = 200 KN

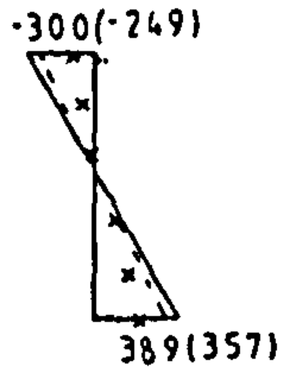

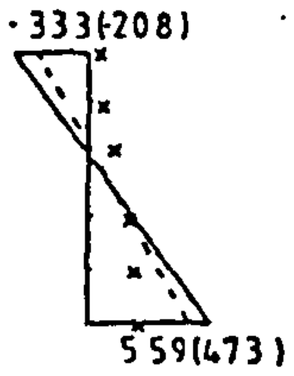

LOAD = 325 KN

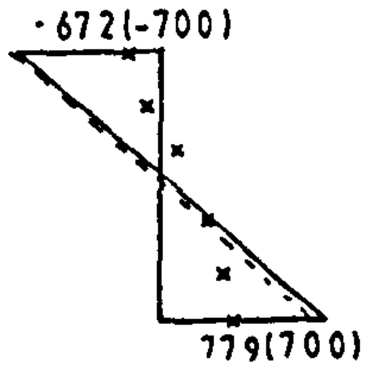

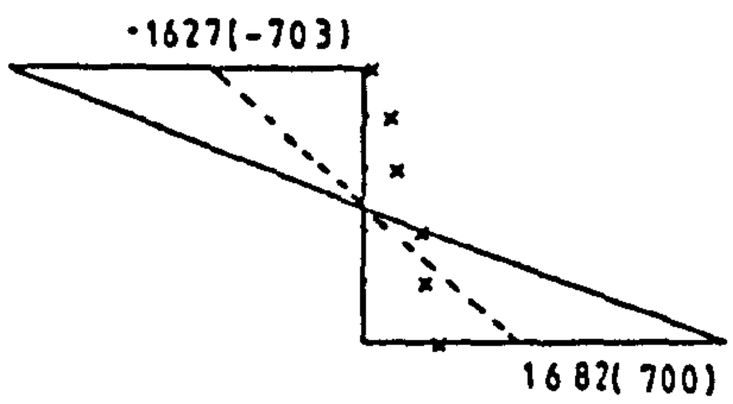

LOAD = 400 KN

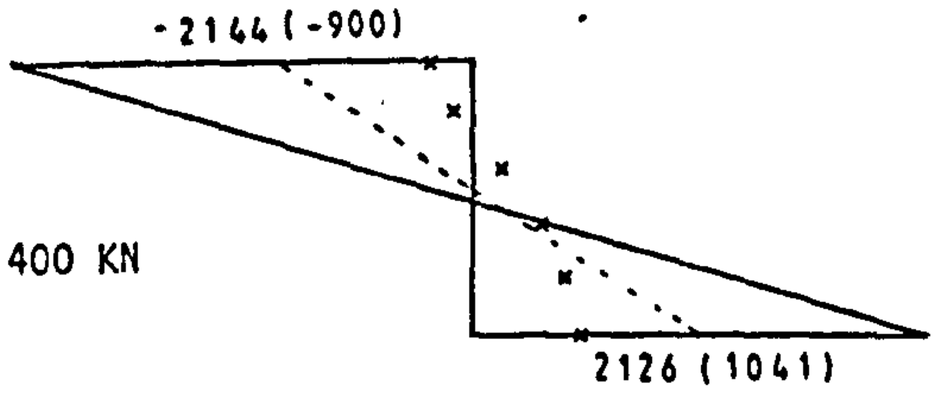

4.22. - Strain* Profiles across the section for column MGUO-08

*strain values shown $x10^6$

SERIES - C

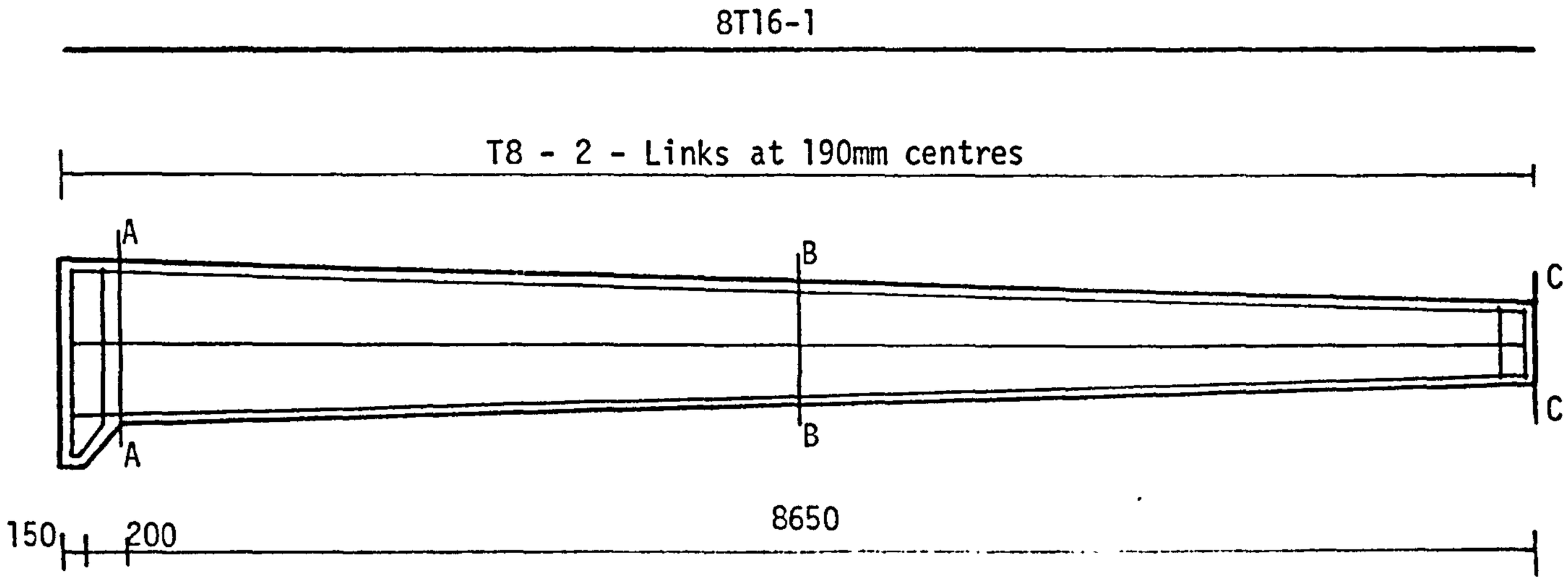

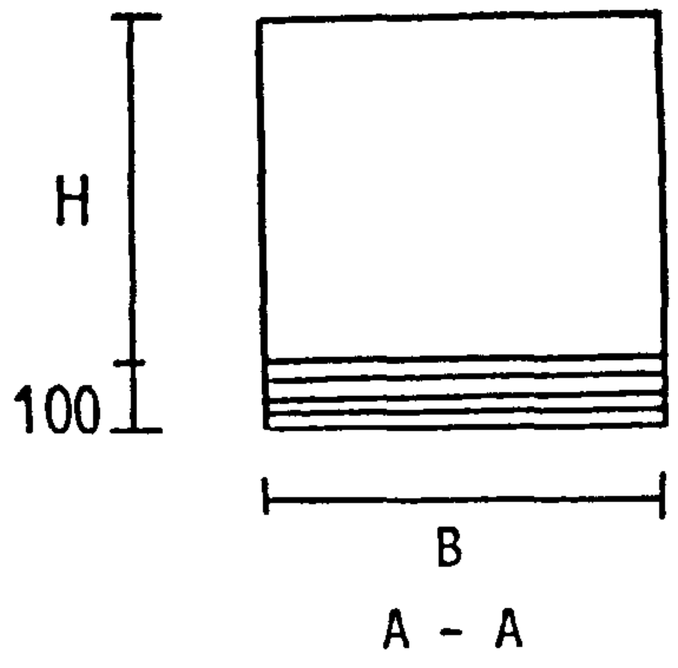

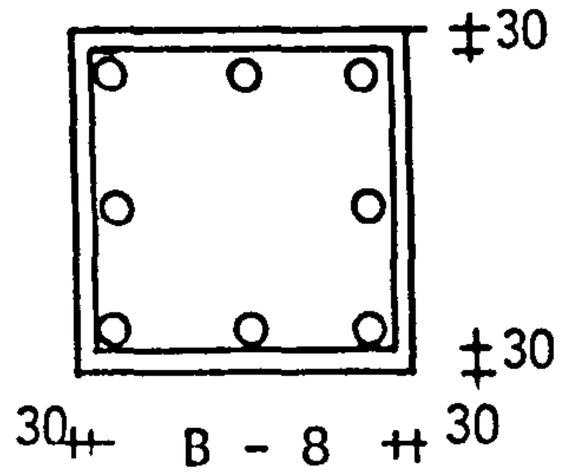

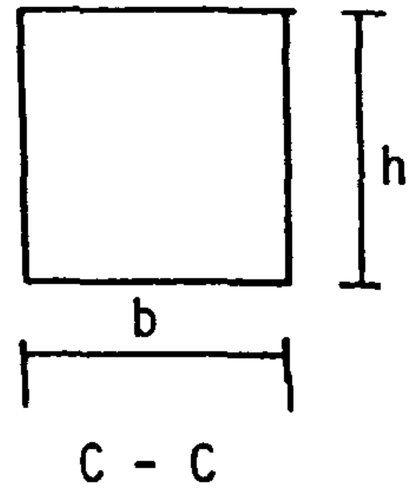

COLUMN LABEL	H (mm)	B (mm)	h (mm)	b (mm)
LDUO-09/10	400	400	300	300
LDUO-11/12	300	300	200	200

Fig. 5-1- REINFORCEMENT DETAILS AND CROSS SECTIONS OF TAPERED COLUMNS

SERIES - C

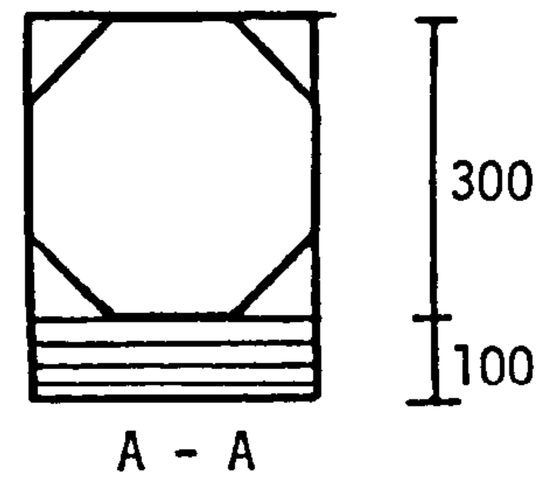

A - A

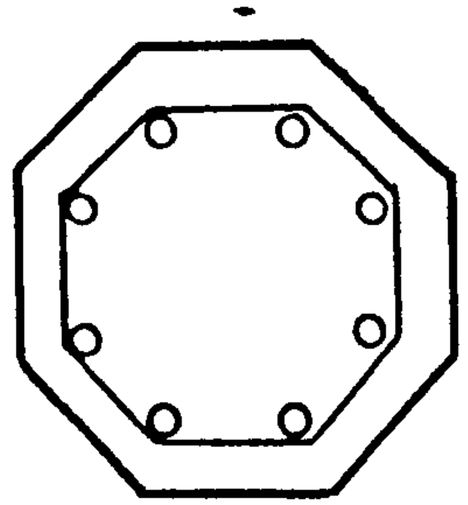

B - B

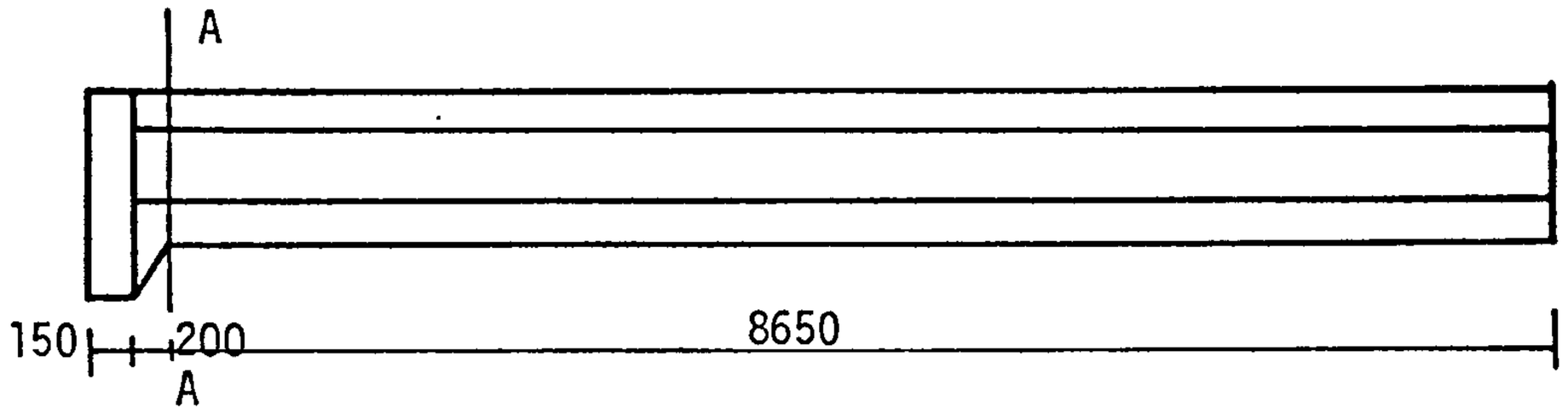

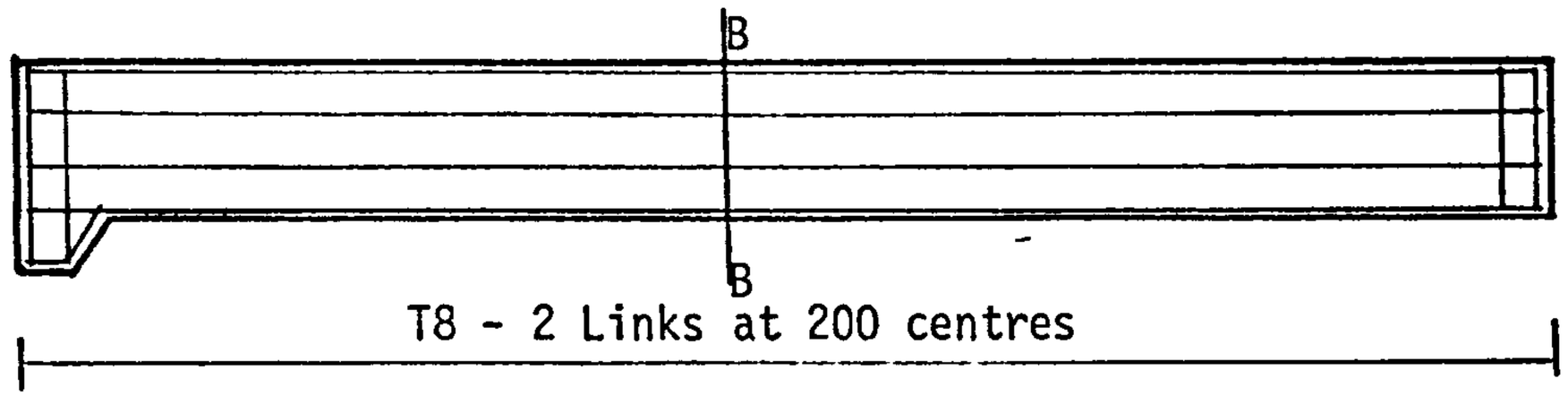

T8 - 2 Links at 200 centres

8 T16 - 1

Fig. 5.2 - REINFORCEMENT DETAILS AND CROSS SECTION OF OCTAGONAL COLUMNS

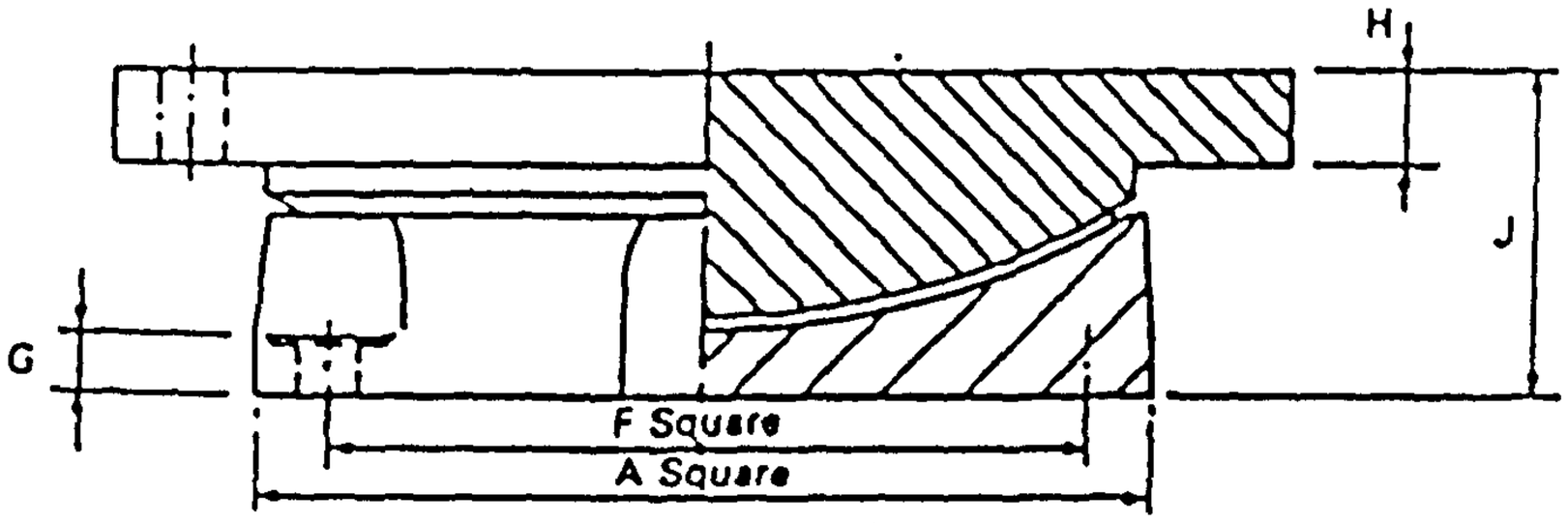

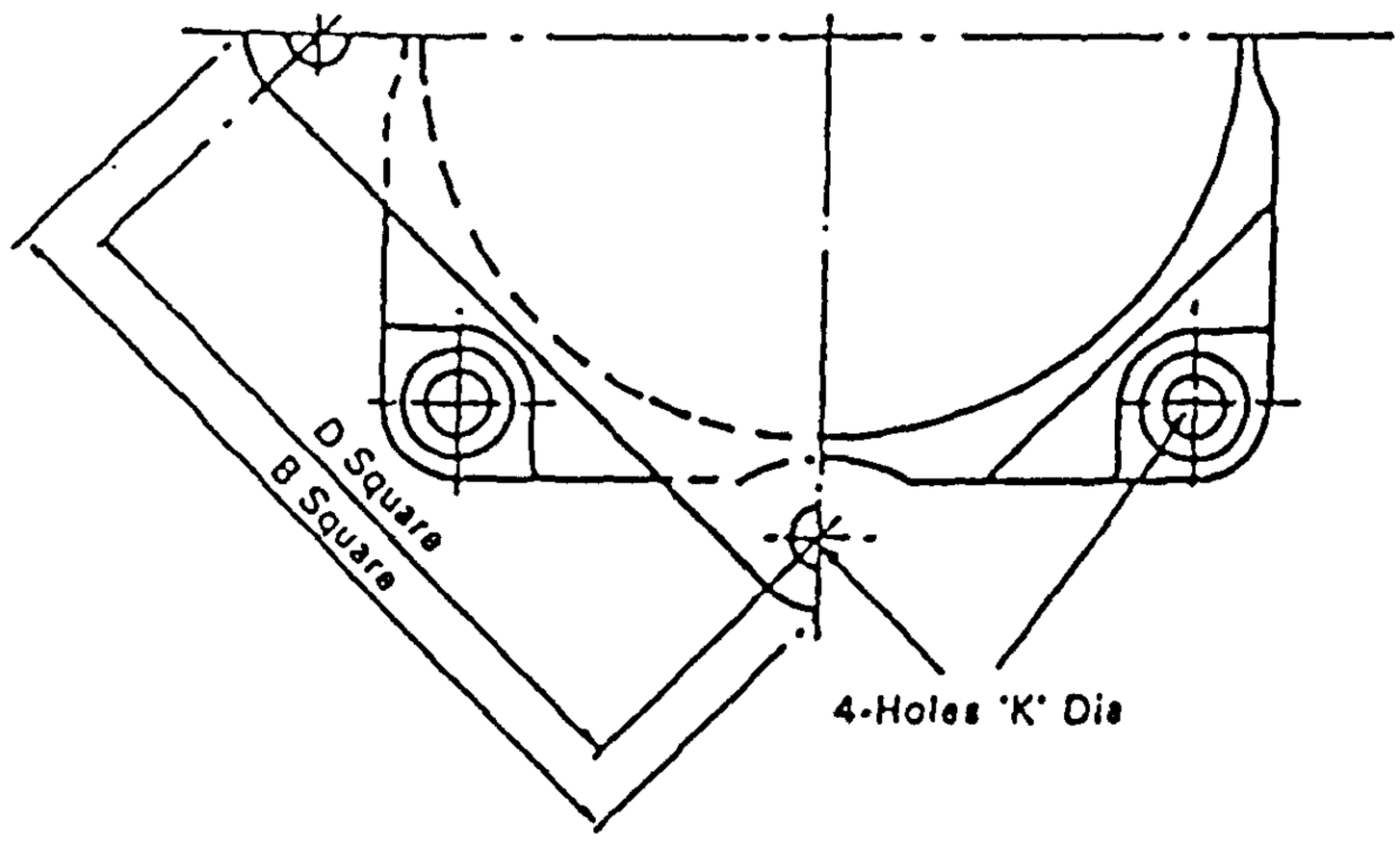

Bearing Part No.	Vertical Load Maximum Dead kN	Maximum Dead + Live kN	Horizontal Load Max. (resultant) kN	Dimensions - mm A	B	D	F	G	H	J	K
Gz 450	3150	5040	675	490	490	395	395	39	42	152	33

Fig. 5.3. Cross section of the Glacier Structural Bearing

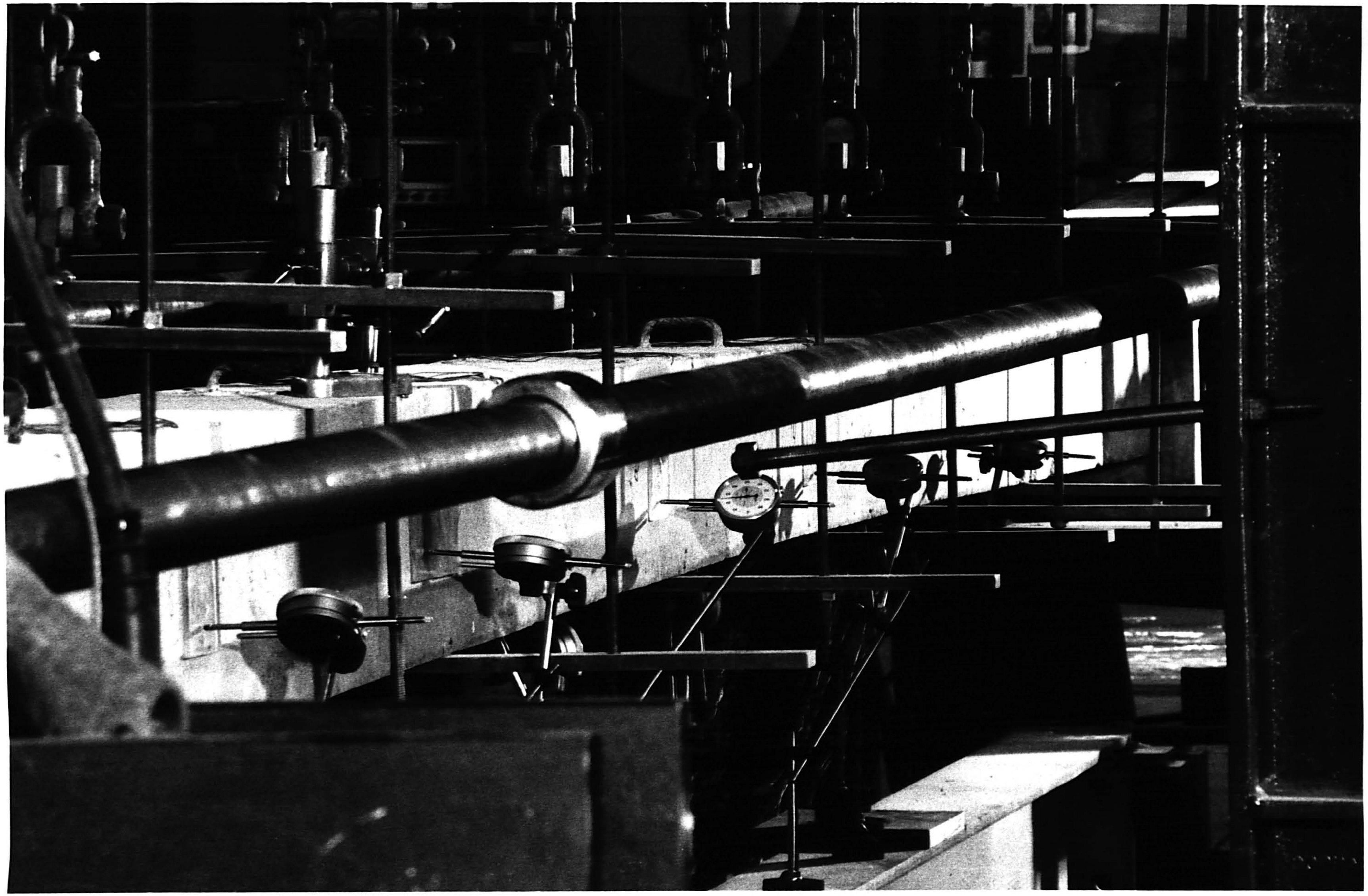

Fig. 5.4. Strain and dial gauge locations along the column length

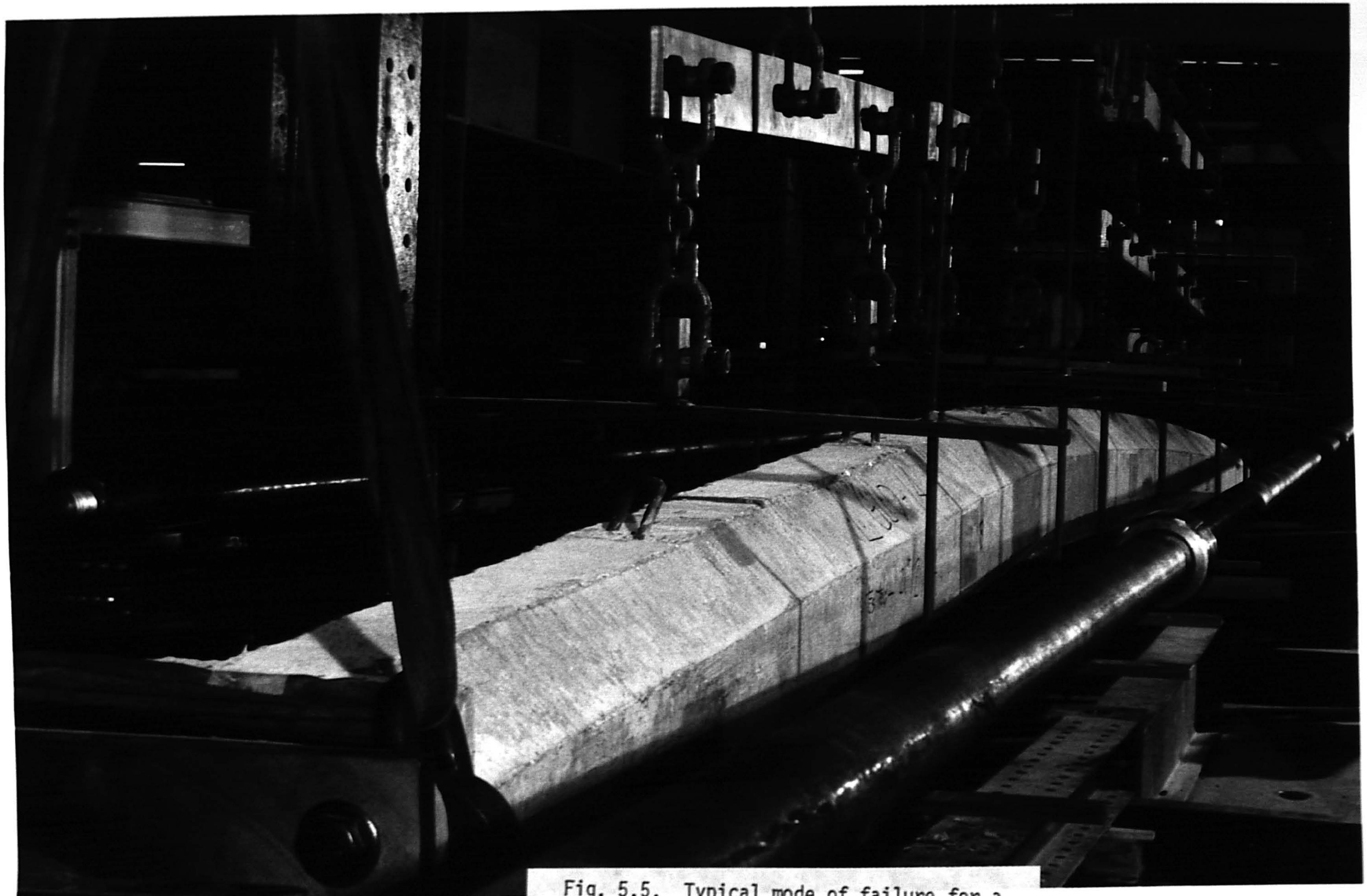

Fig. 5.5. Typical mode of failure for a long length column subjected to uniaxial bending.

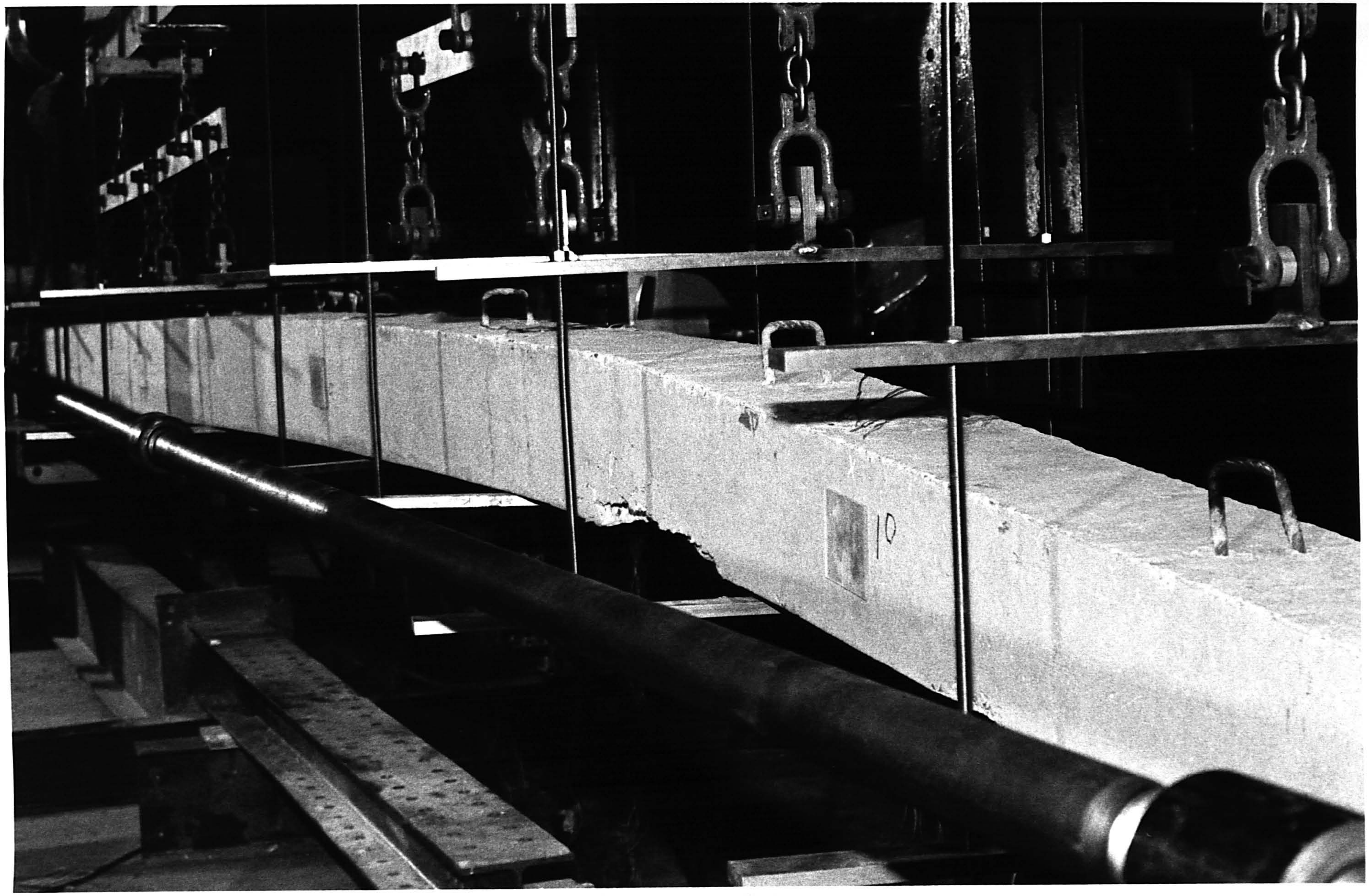

Fig. 5.6. A typical view of failed column

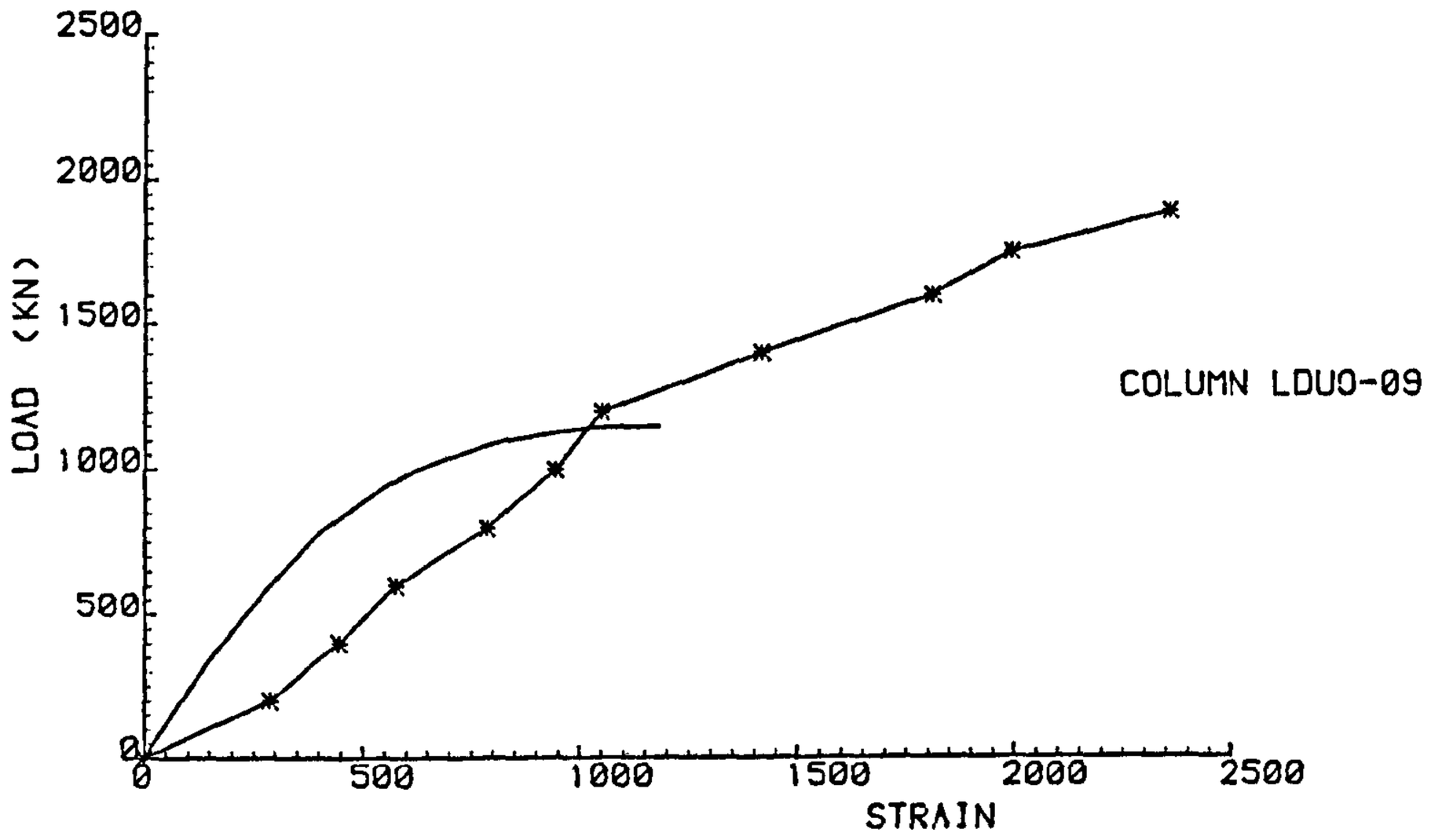

LOAD vs MAX. STRAIN

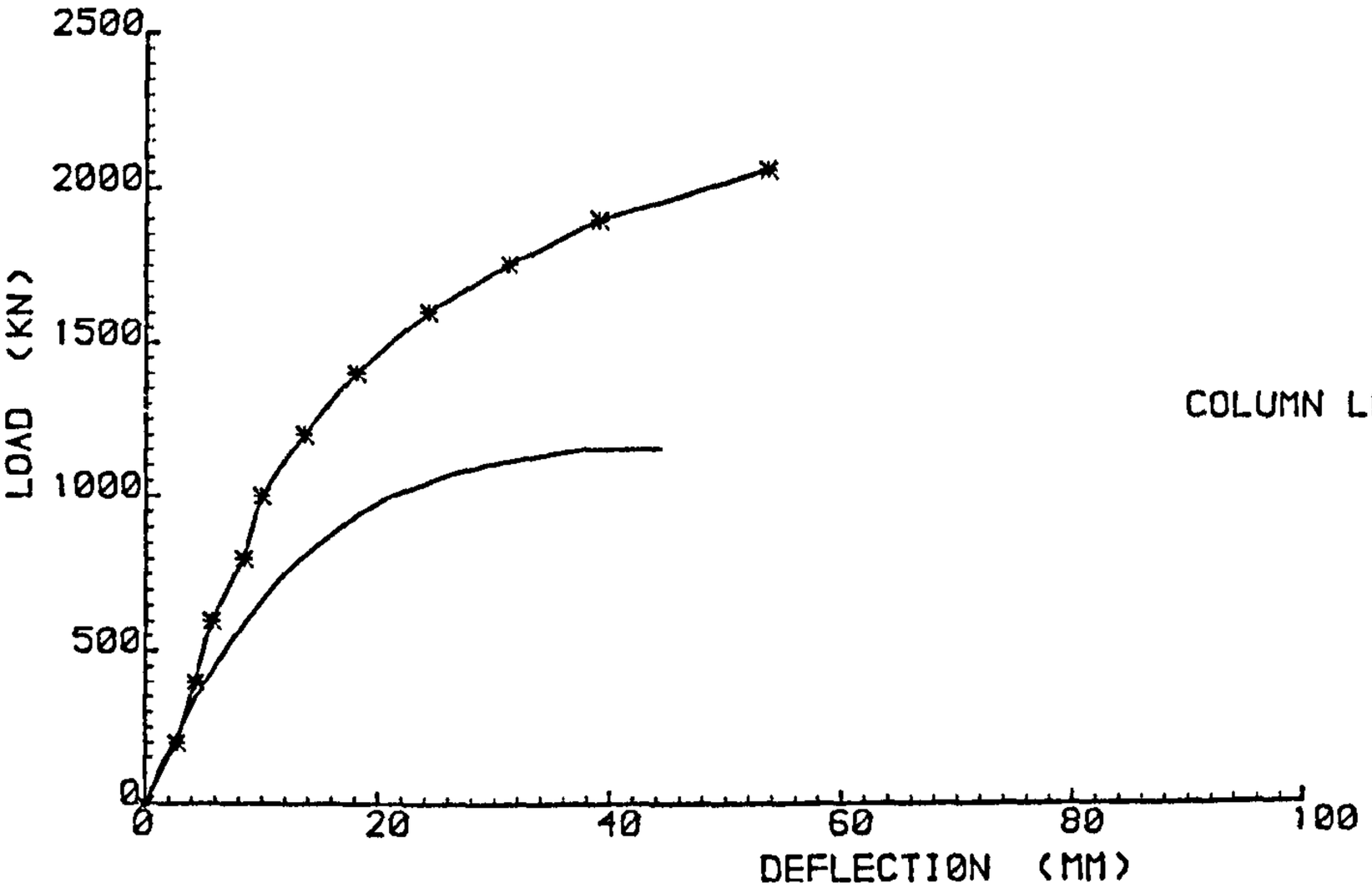

LOAD vs MAX. DEFLECTION

Fig. 5.7 - Comparison between experimental and theoretical results for column LDUO-09

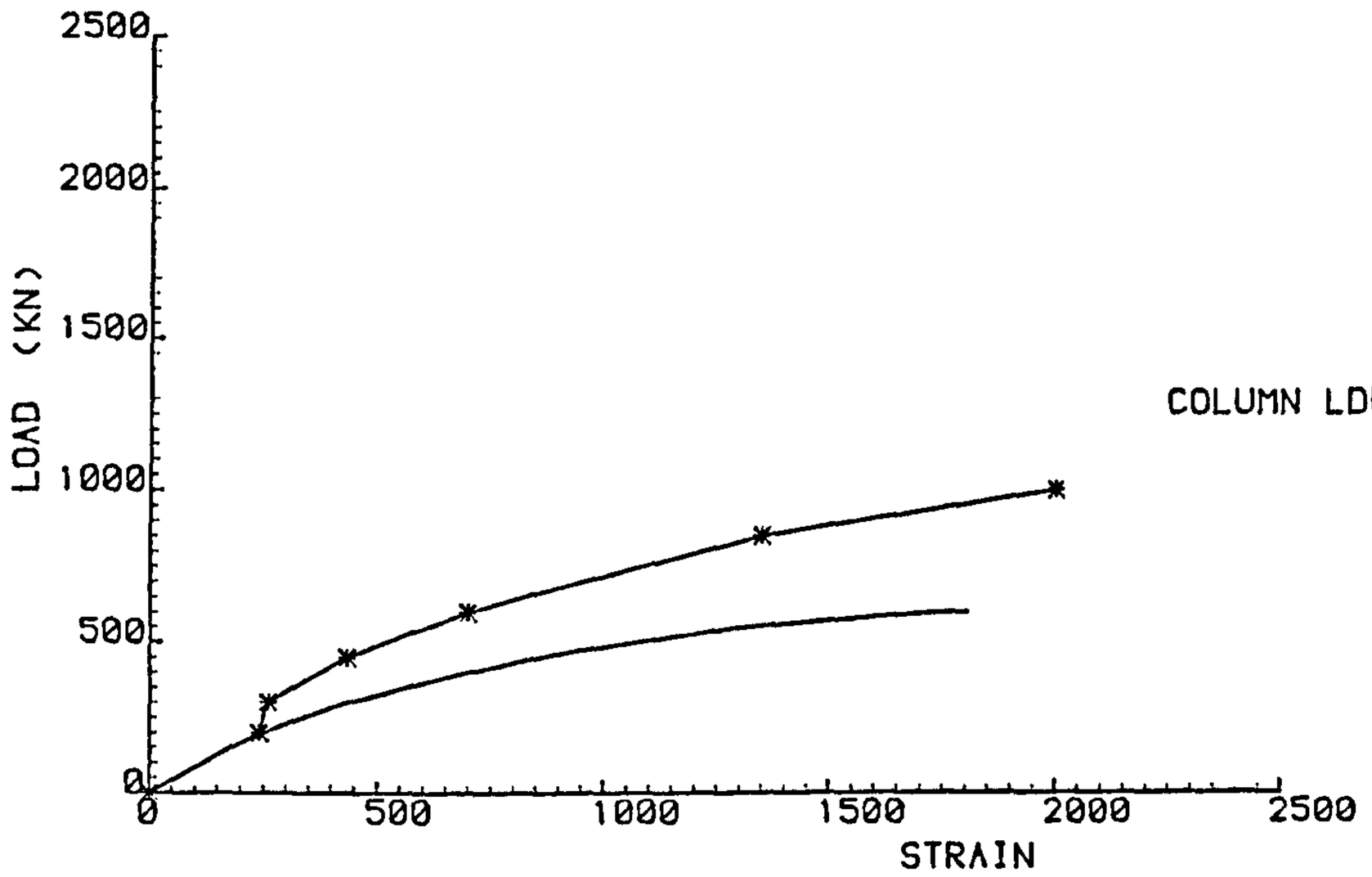

LOAD vs MAX. STRAIN

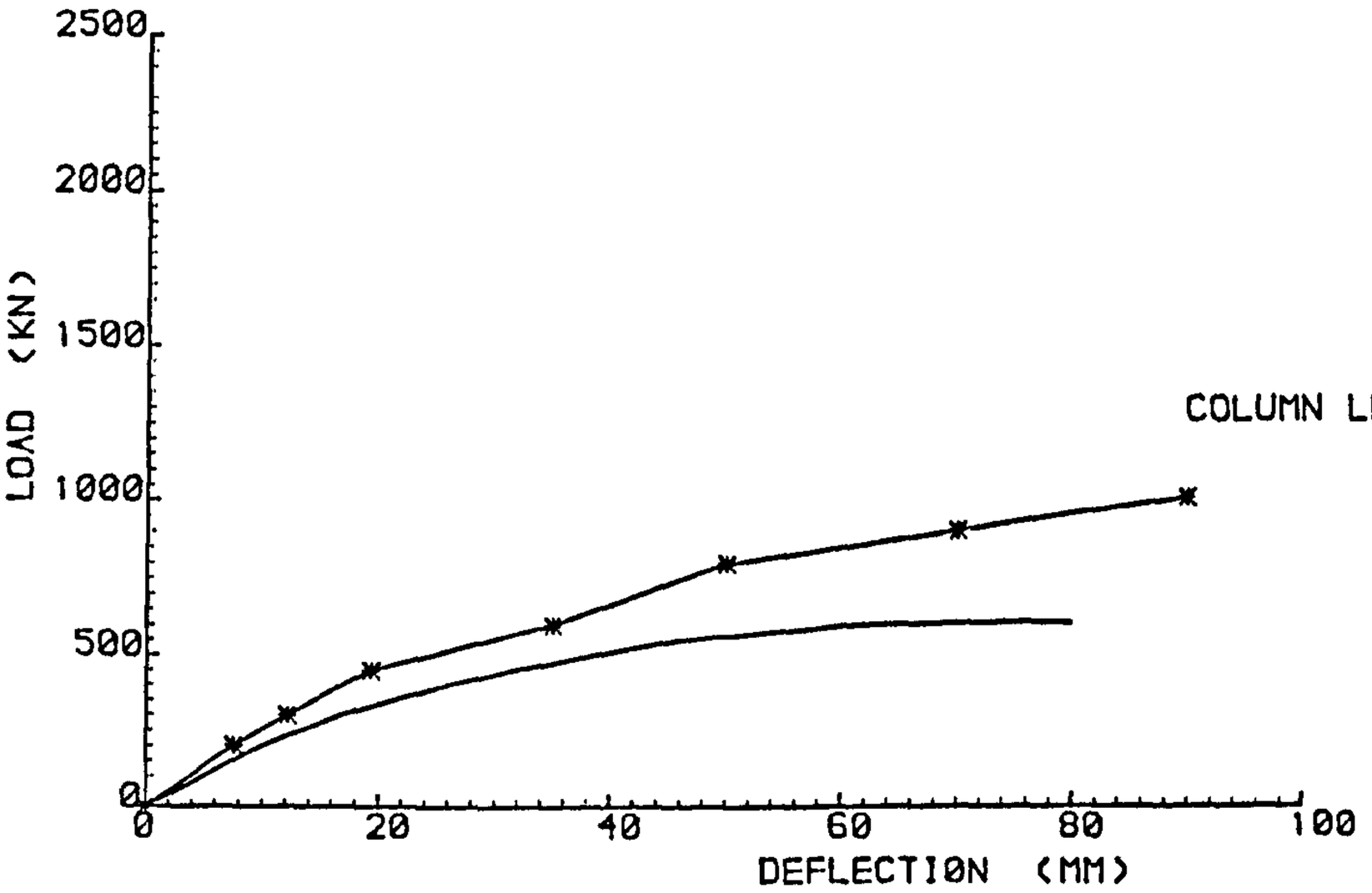

LOAD vs MAX. DEFLECTION

Fig. 5.8 - Comparison between experimental and theoretical results for column LDU0-10

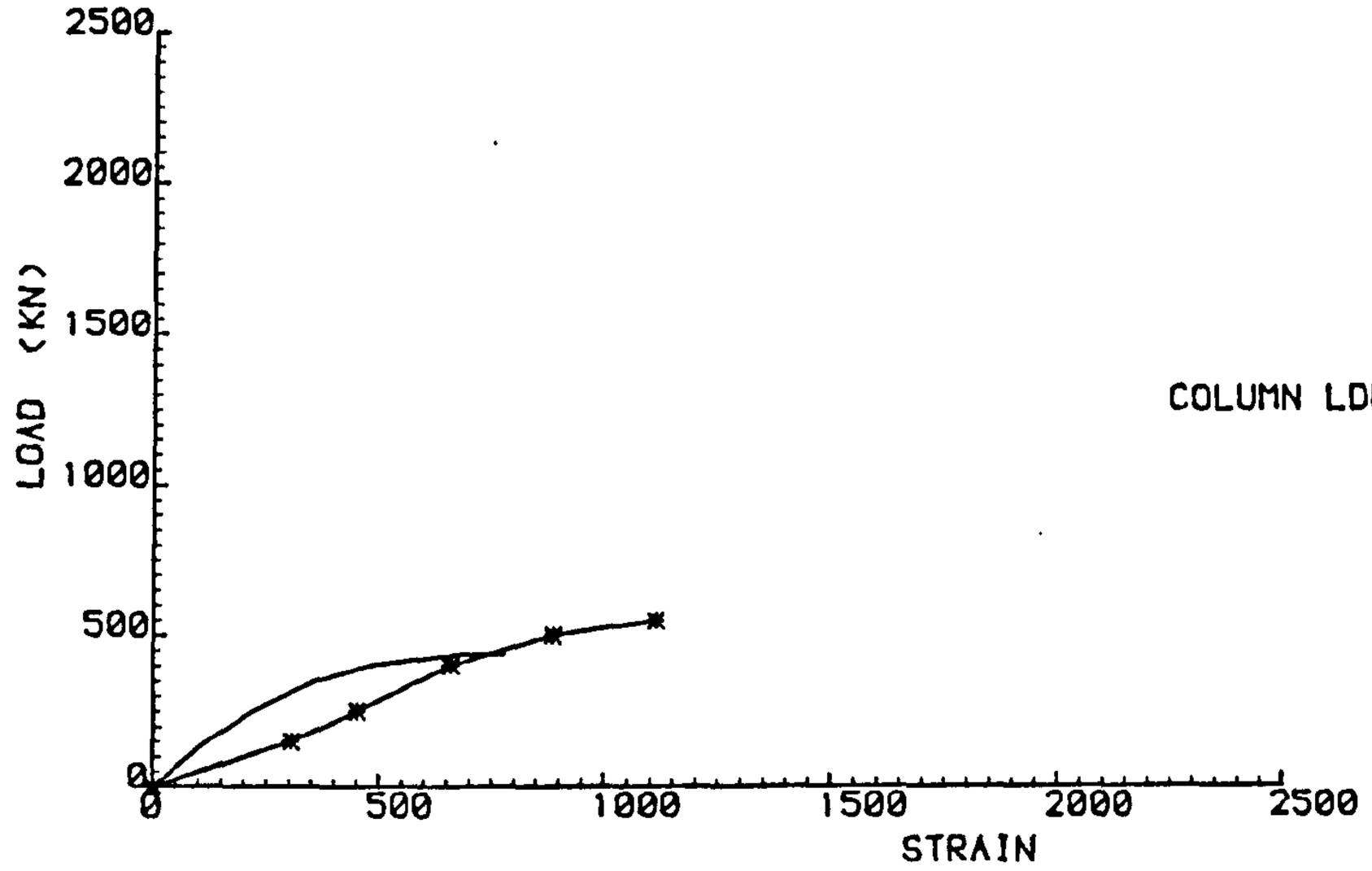

LOAD vs MAX. STRAIN

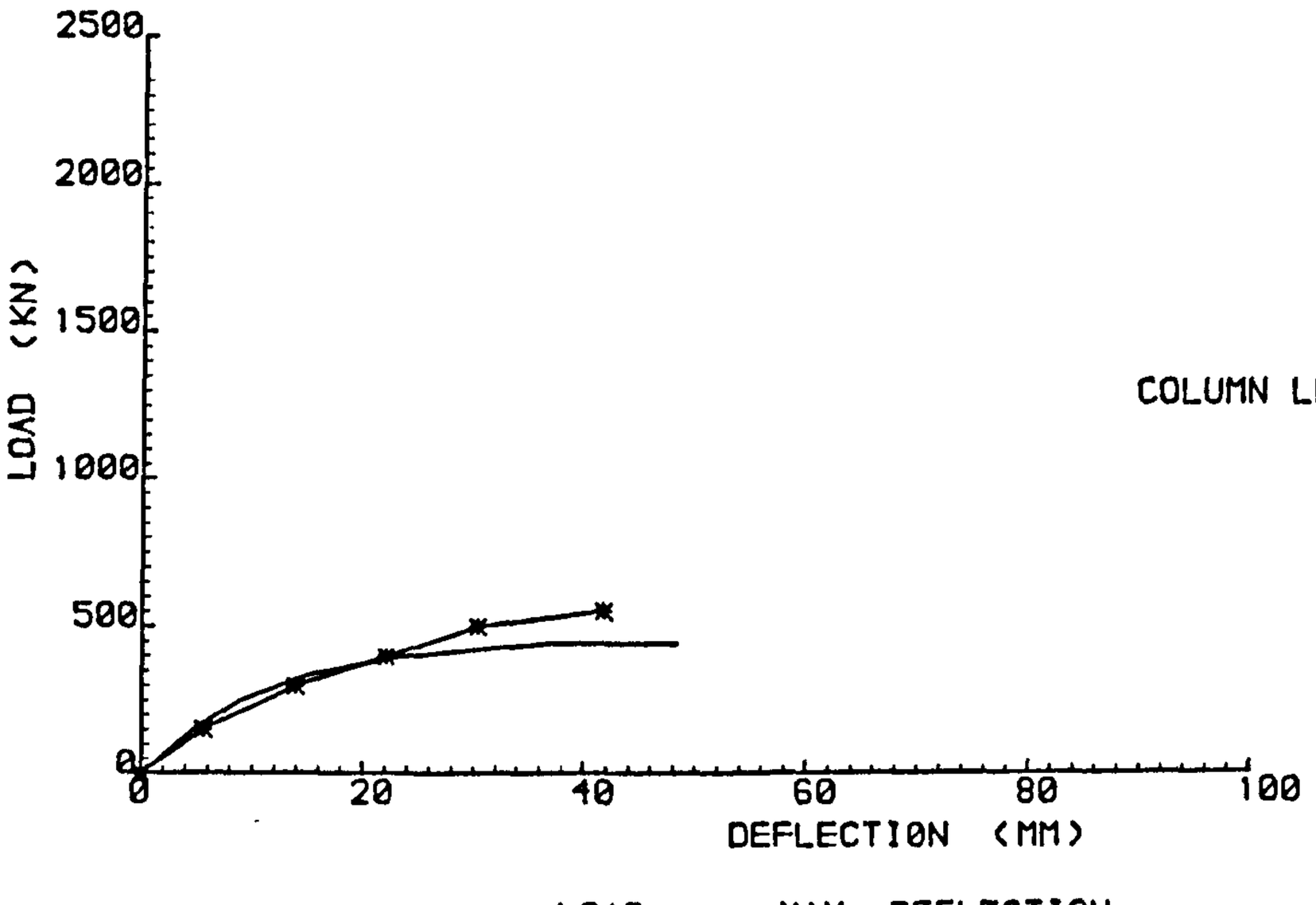

LOAD vs MAX. DEFLECTION

Fig. 5.9 - Comparison between experimental and theoretical results for column LDUO-11

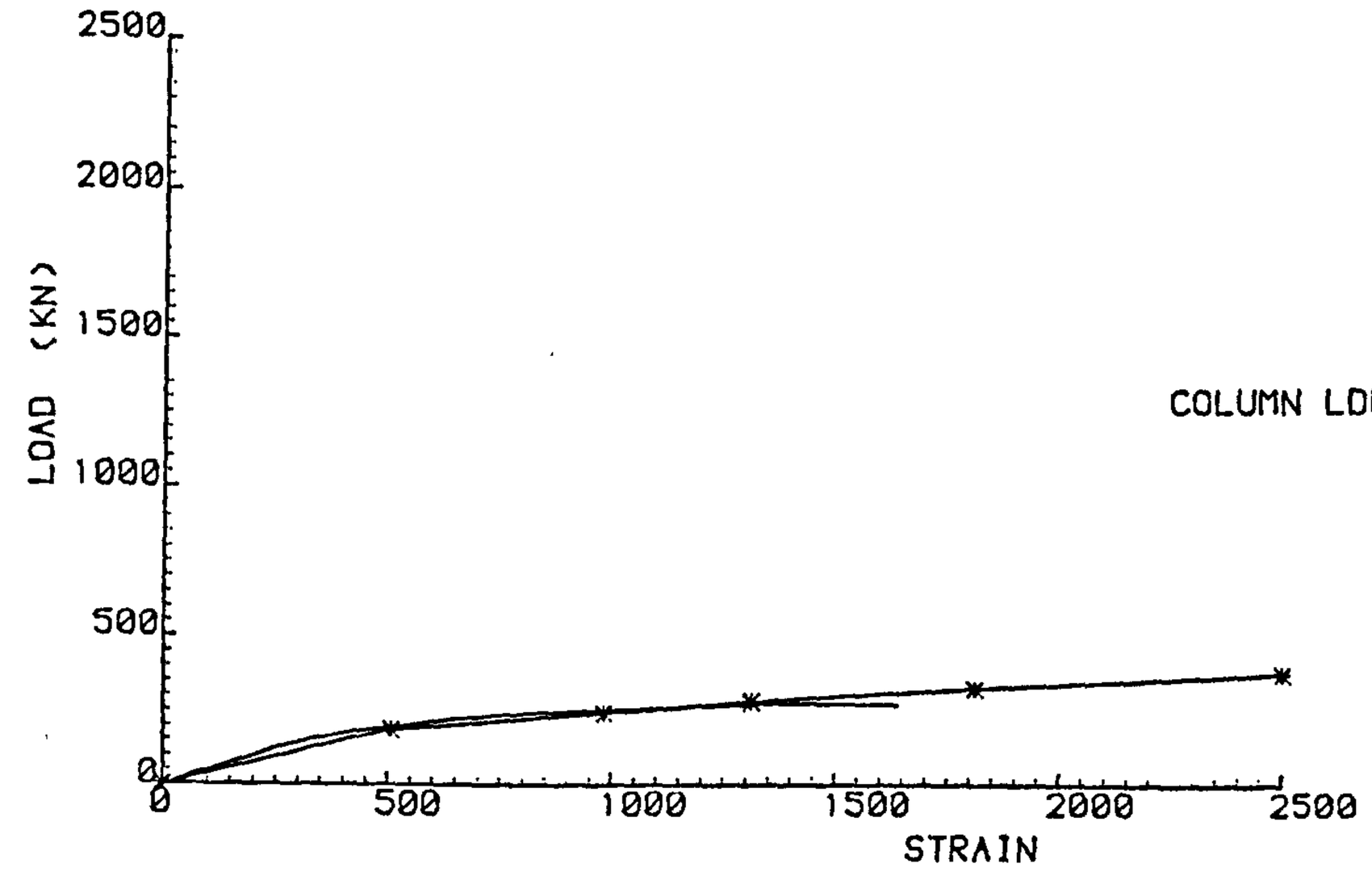

LOAD vs MAX. STRAIN

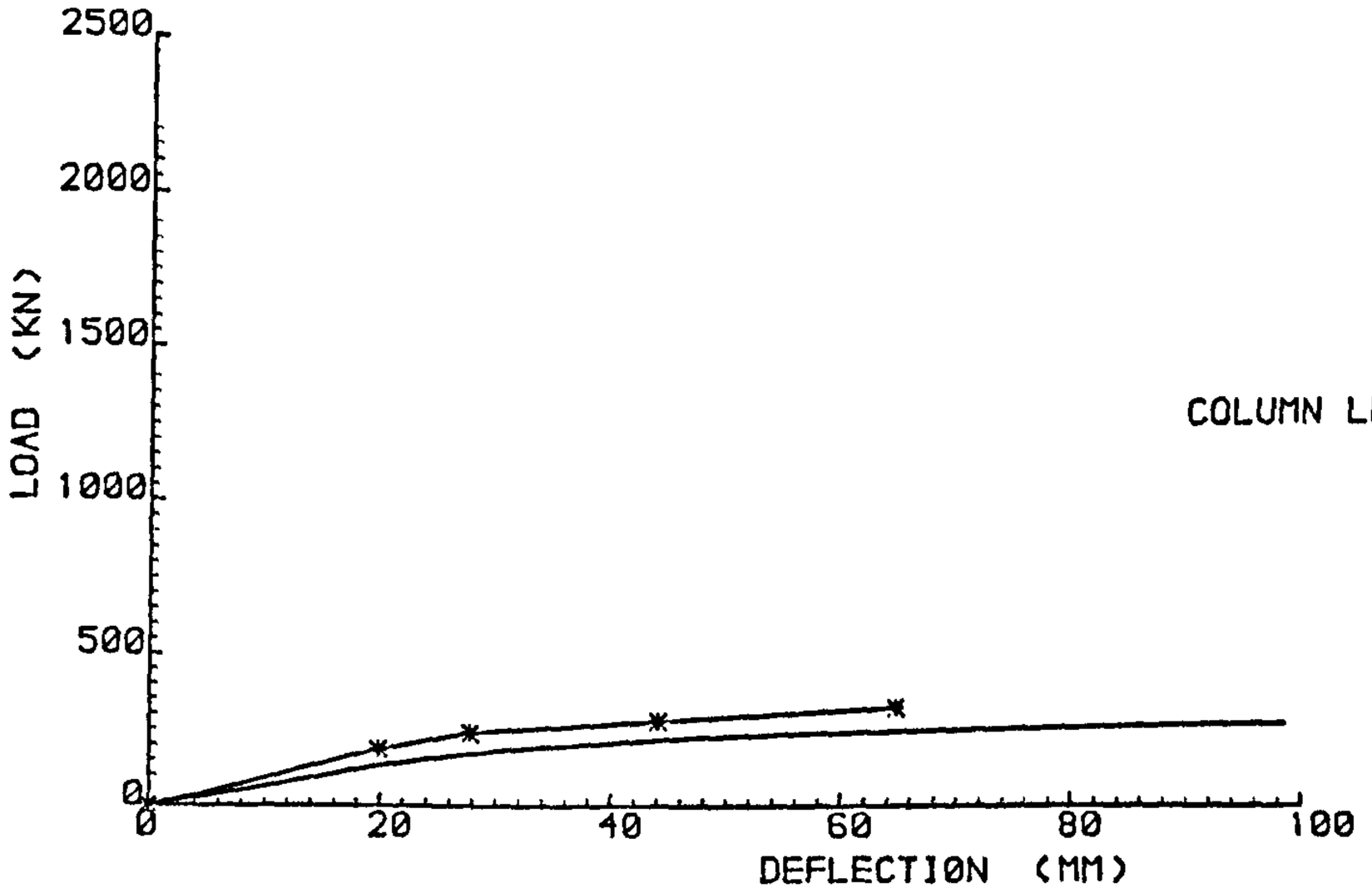

LOAD vs MAX. DEFLECTION

Fig. 5.10 - Comparison between experimental and theoretical results For column LDUO-12

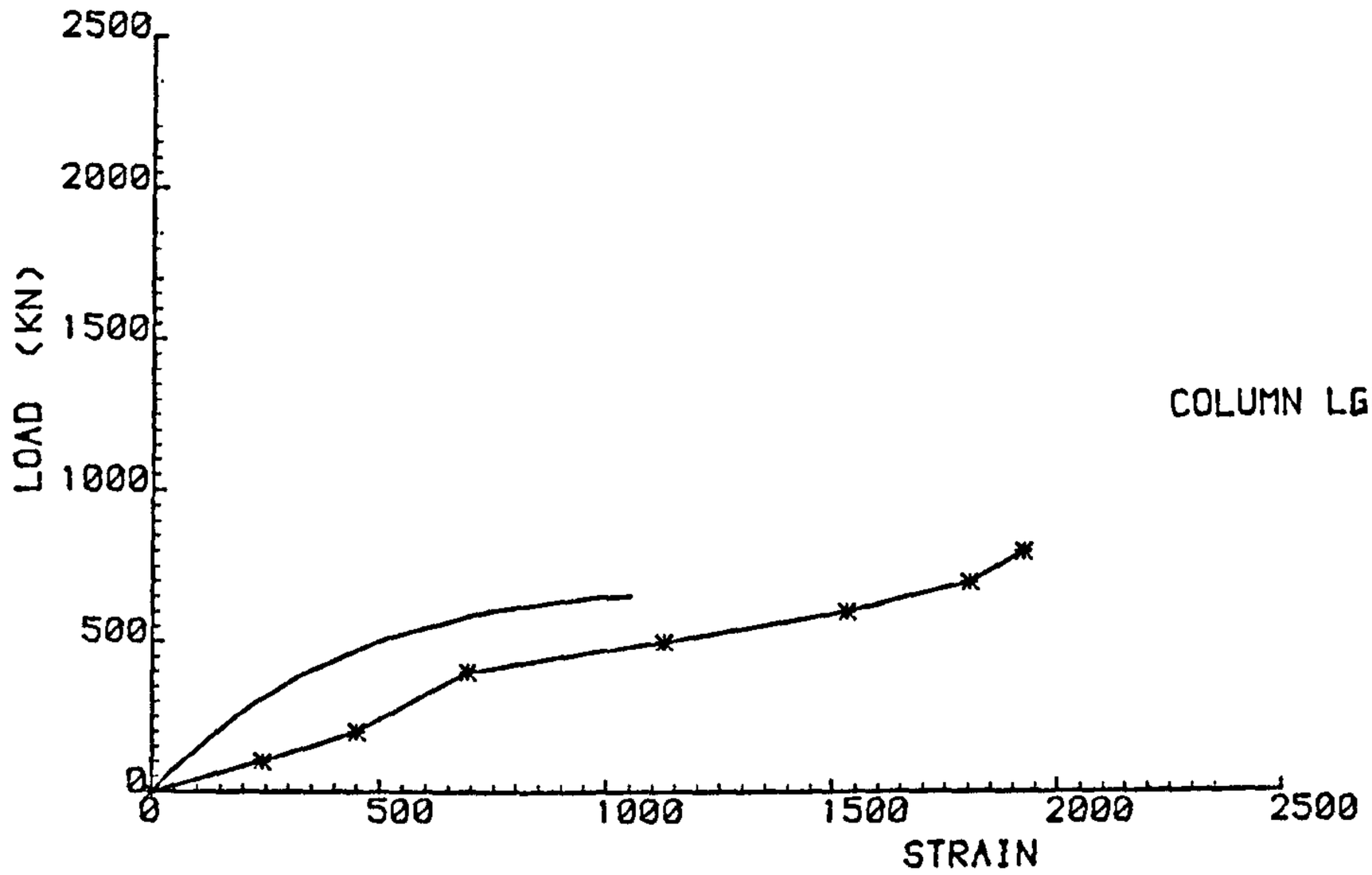

LOAD vs MAX. STRAIN

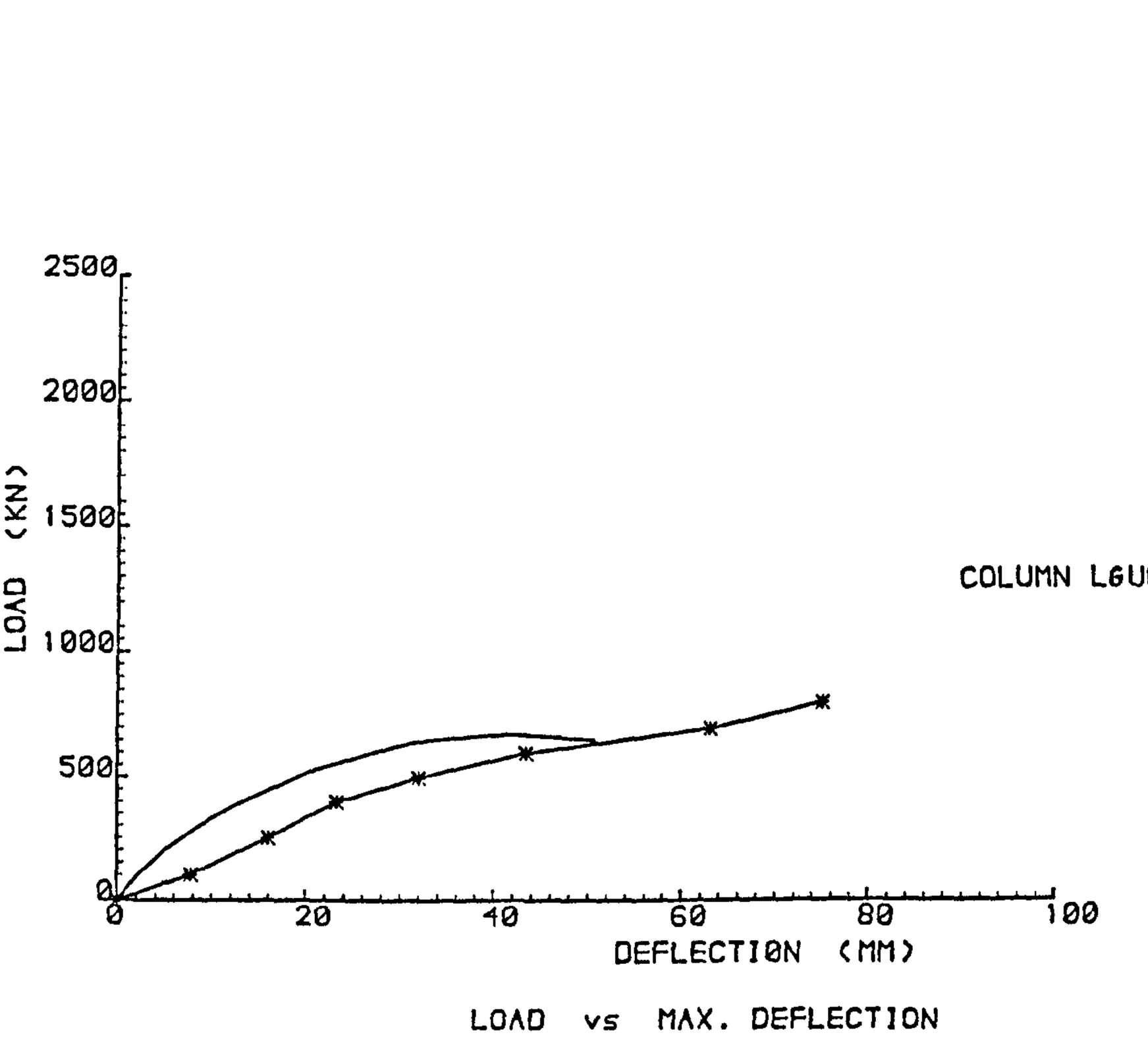

LOAD vs MAX. DEFLECTION

Fig. 5.11 - Comparison between experimental and theoretical results for column LGUO-13

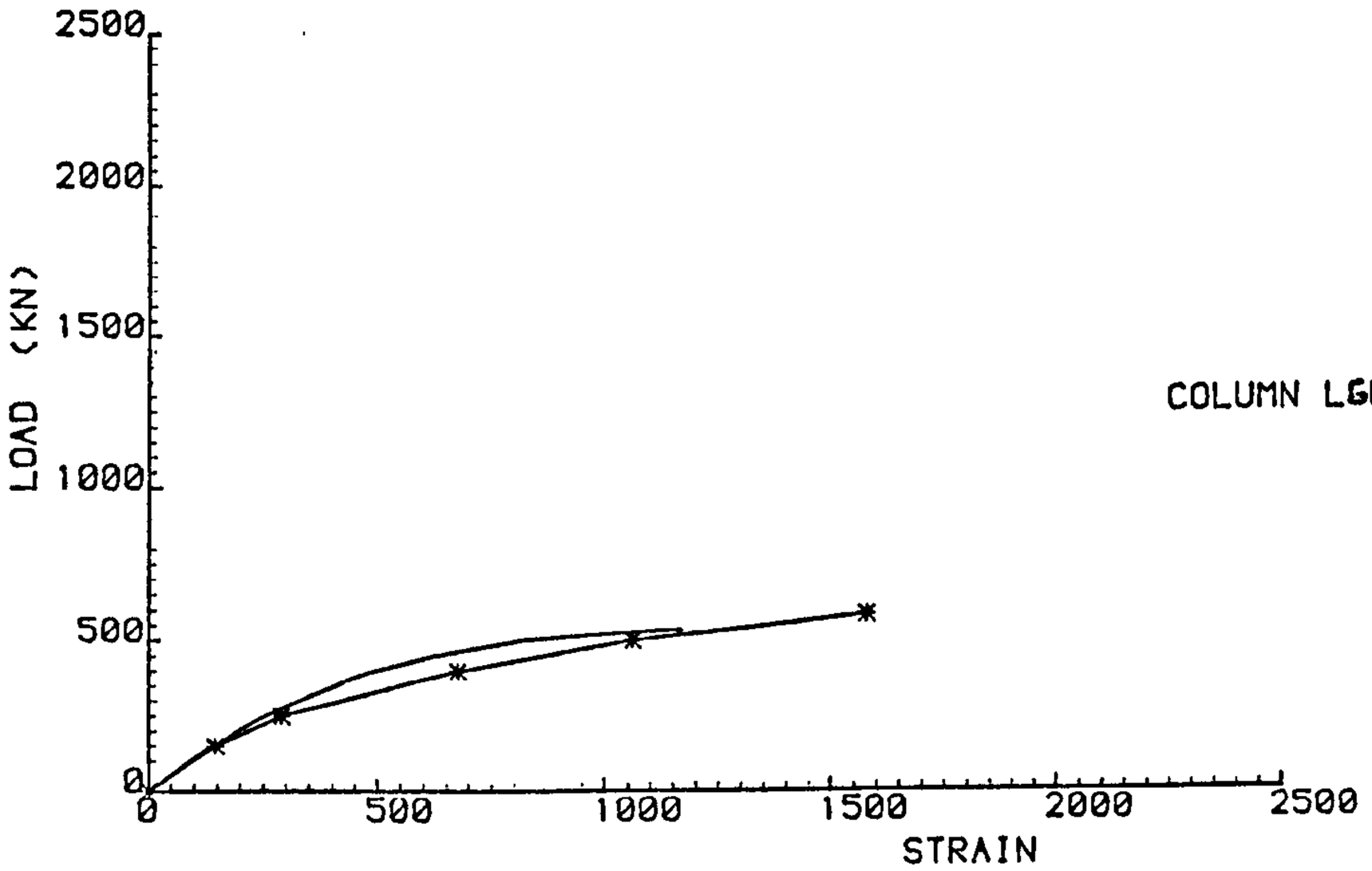

LOAD vs MAX. STRAIN

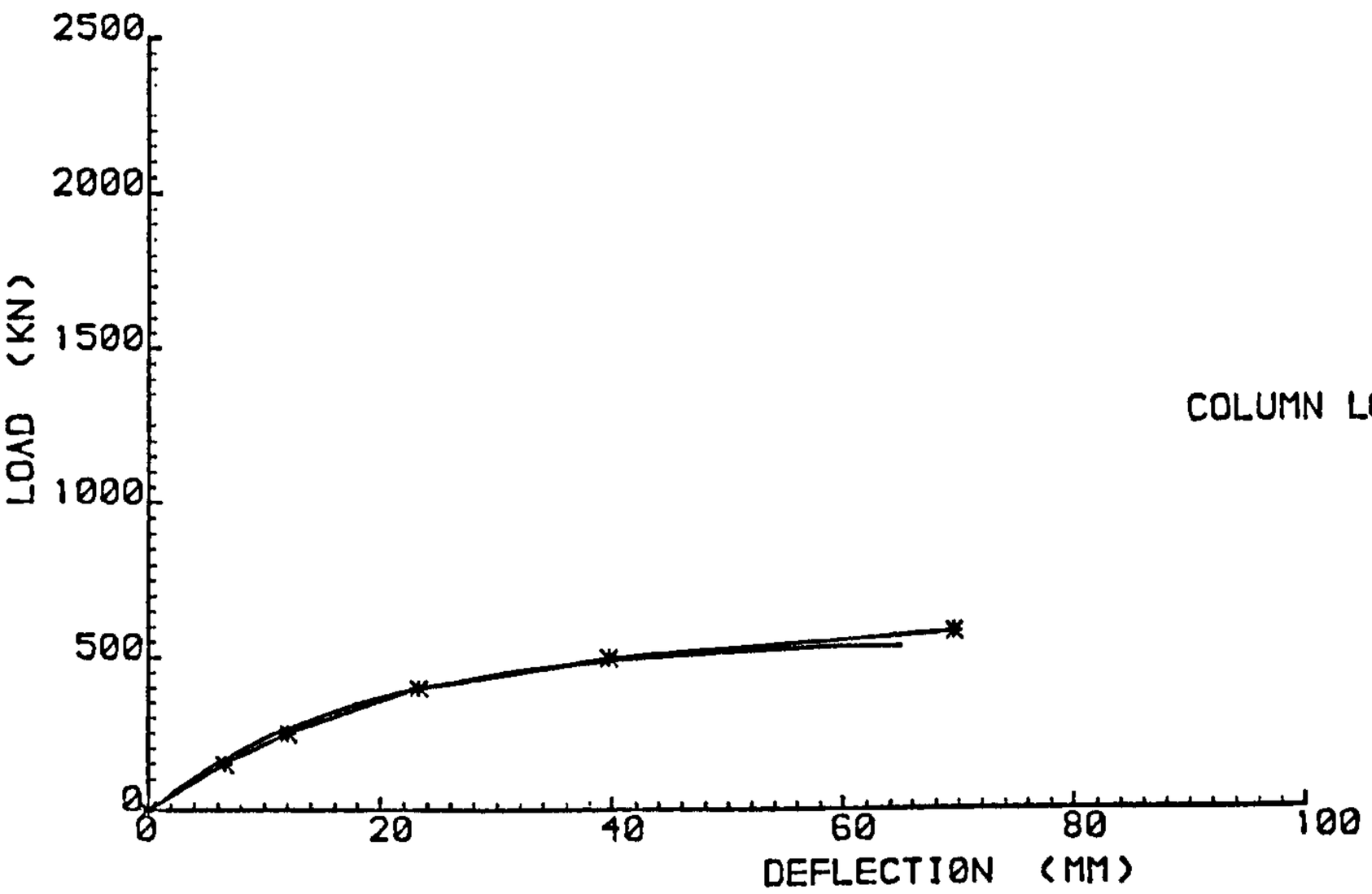

LOAD vs MAX. DEFLECTION

Fig. 5.12 - Comparison between experimental and theoretical results for column LGUO-14

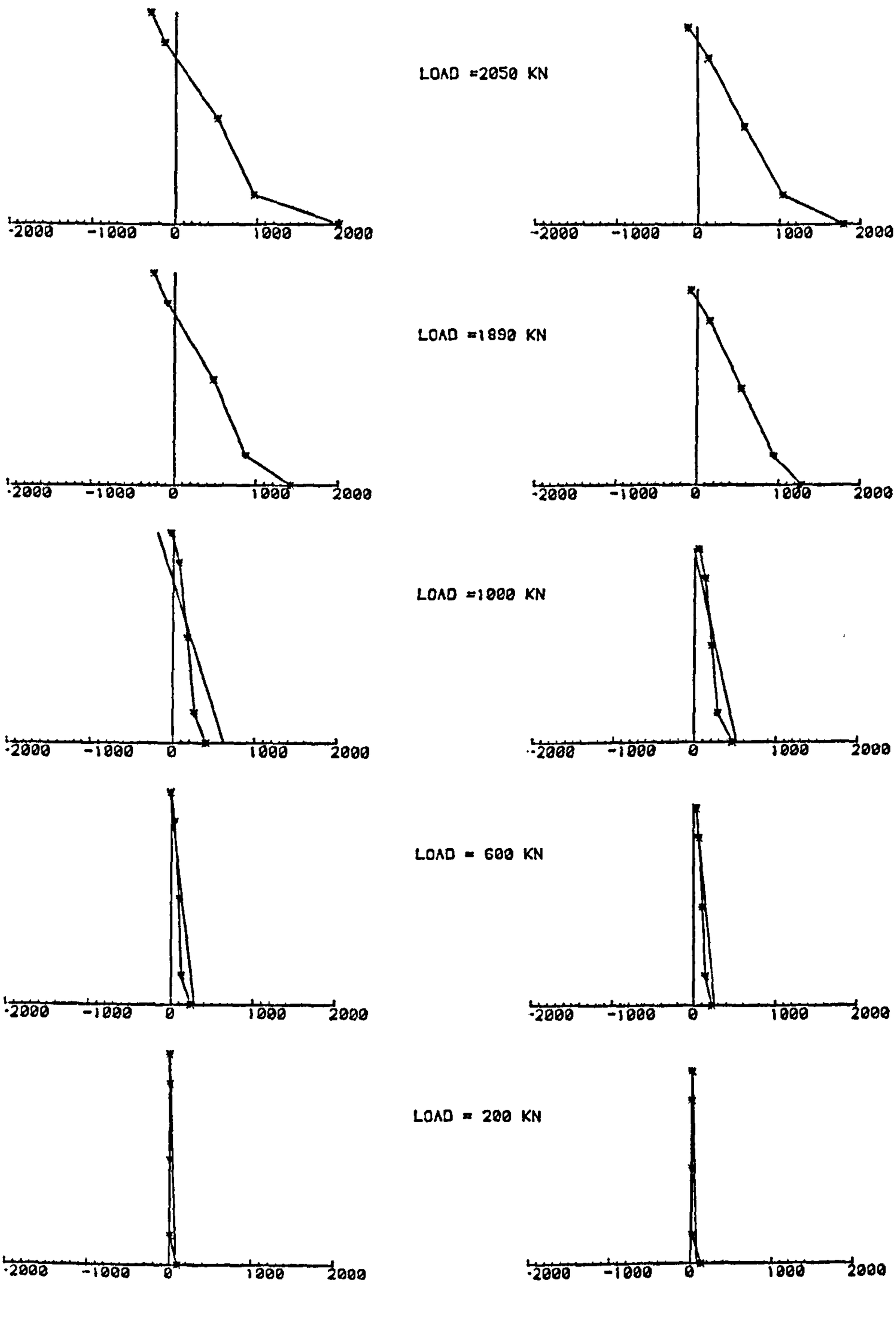

Fig. 5.13 - Strain profiles across the sectionFor column LDU0-09

* strain values shown x10^{6}

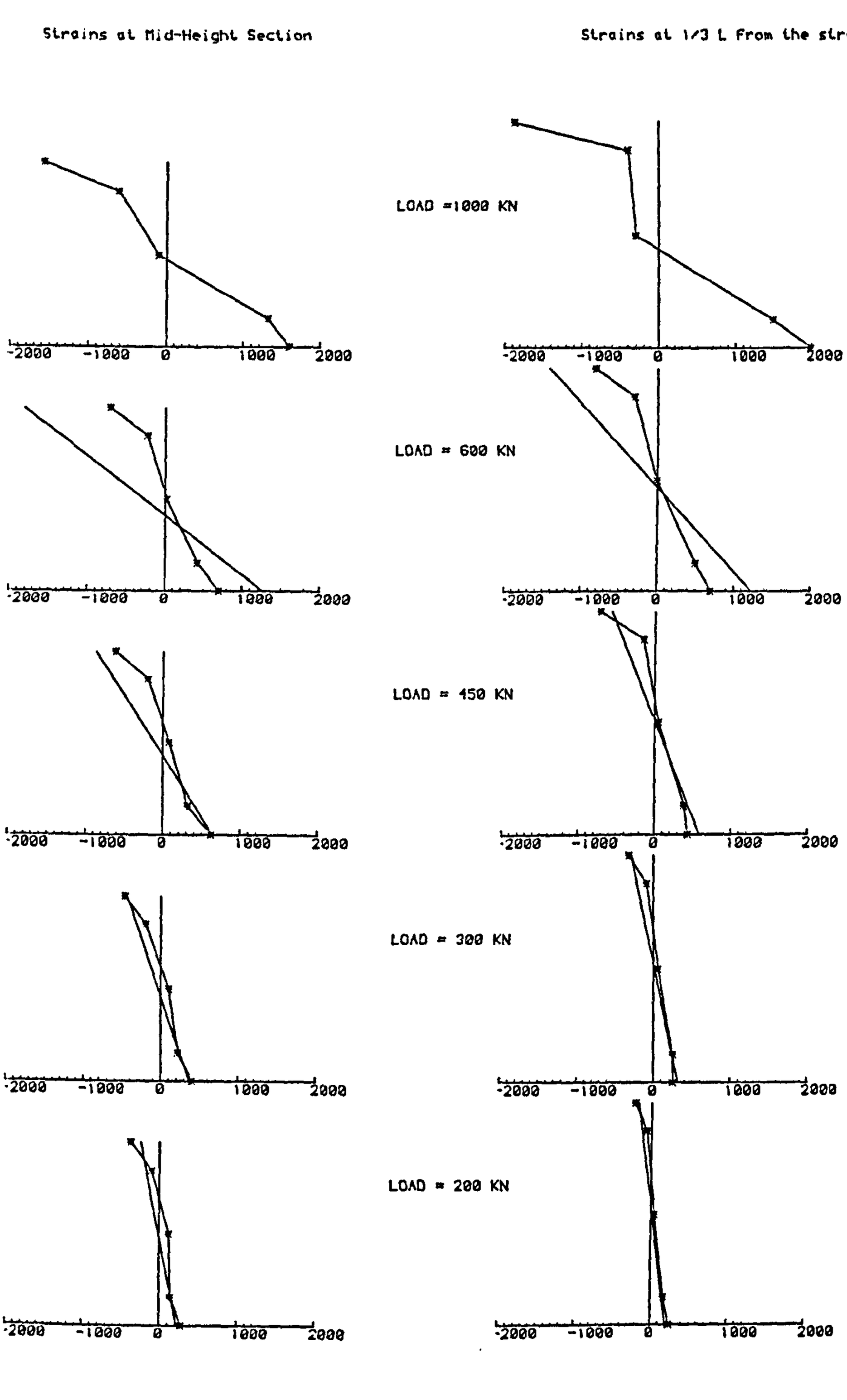

Fig. 5.14 - Strain profiles across the sectionfor column LDU0-10

* strain values shown x10^{6}

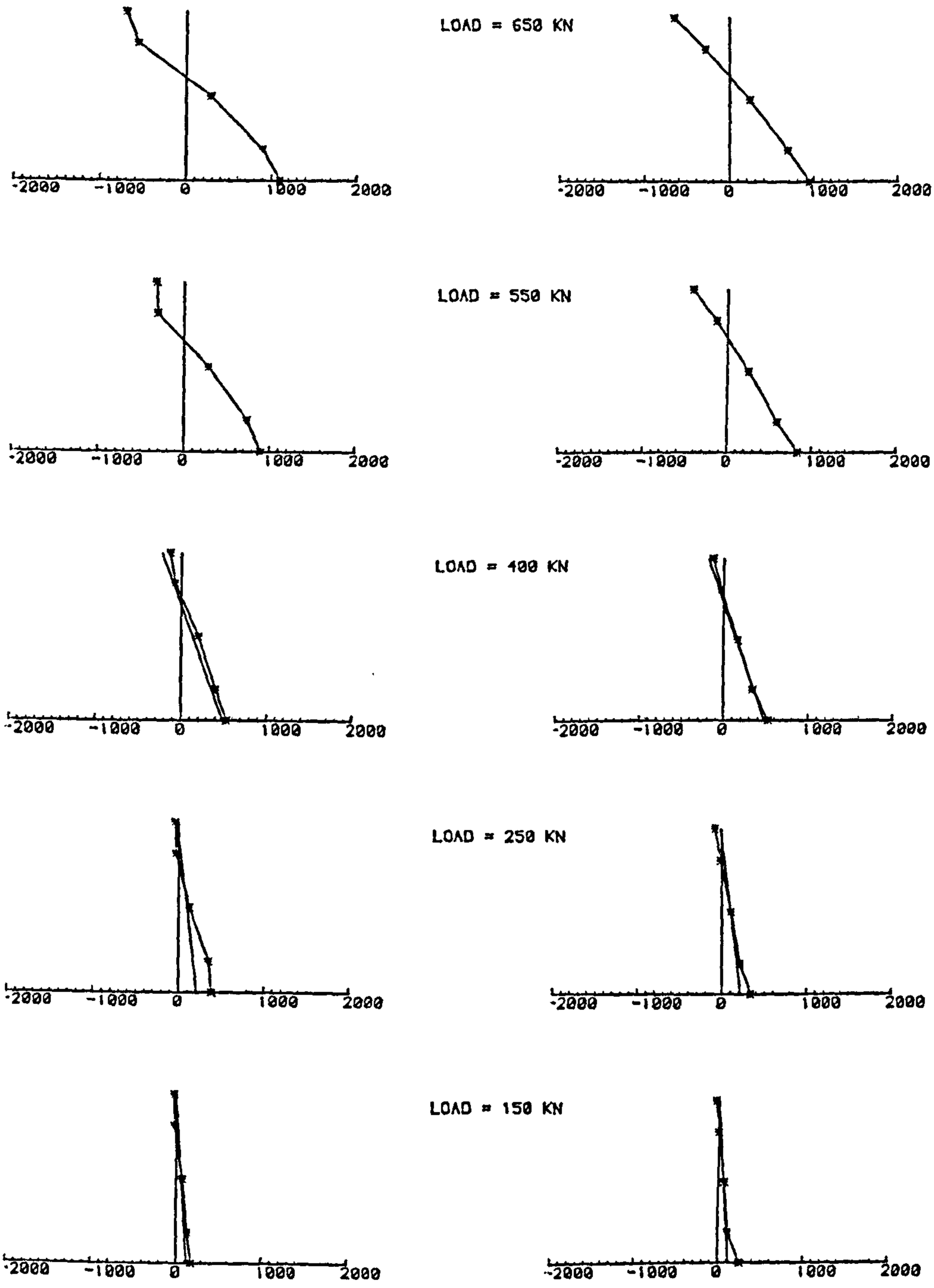

Fig. 5.15 - Strain profiles across the sectionfor column LDU0-11

* strain values shown x10^{6}

Strains at Mid-Height Section

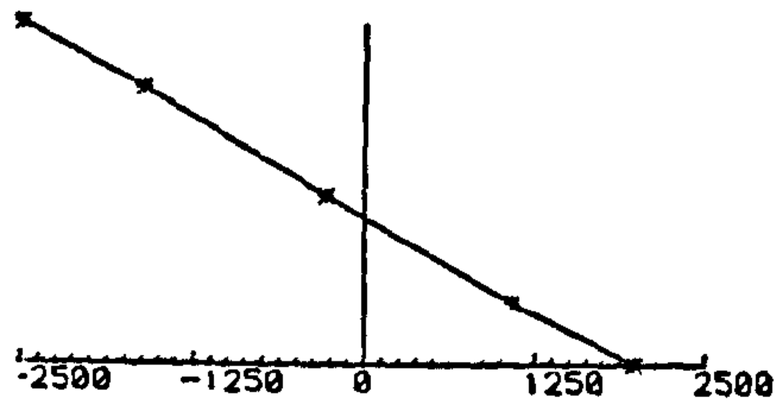

Strains at 2/3 L From the stronger end

LOAD = 370 KN

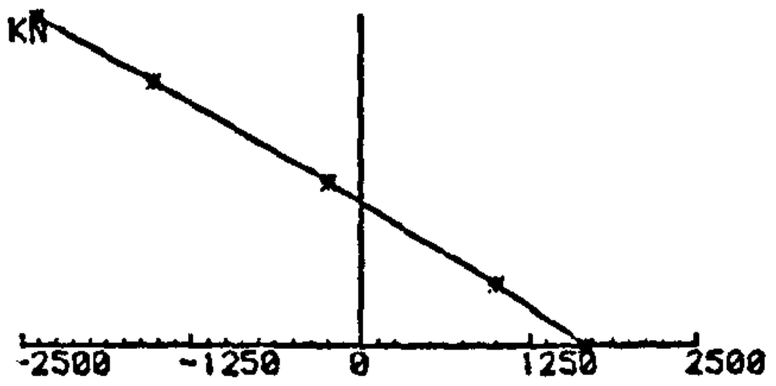

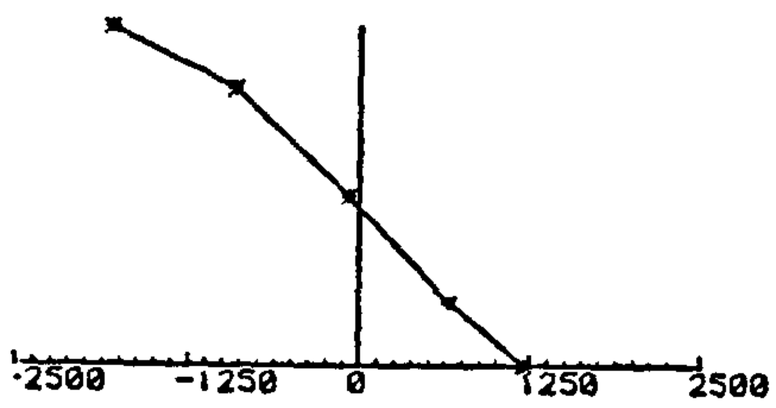

LOAD = 325 KN

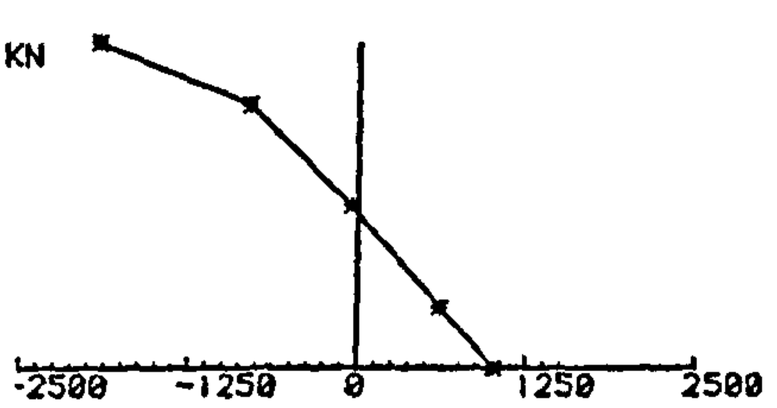

LOAD = 270 KN

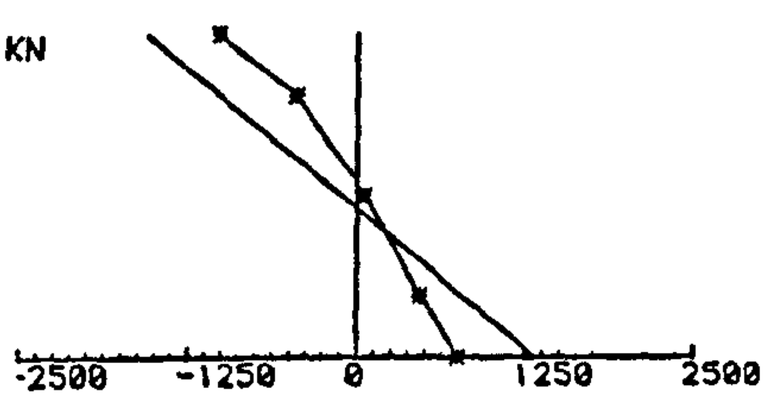

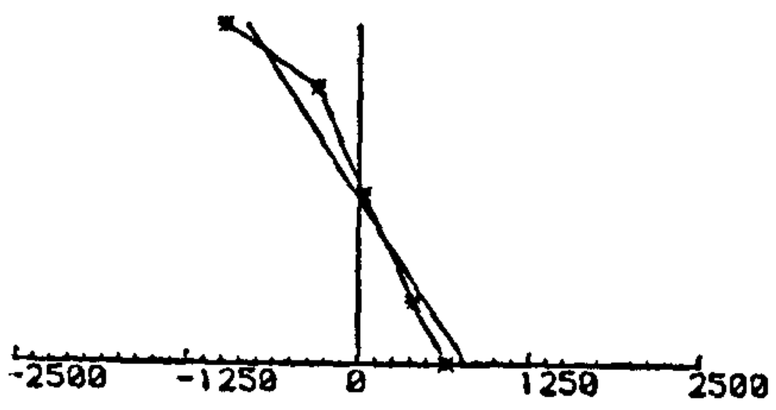

LOAD = 240 KN

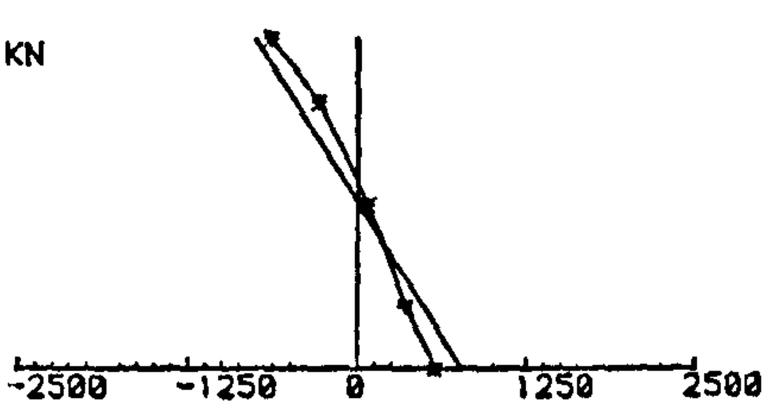

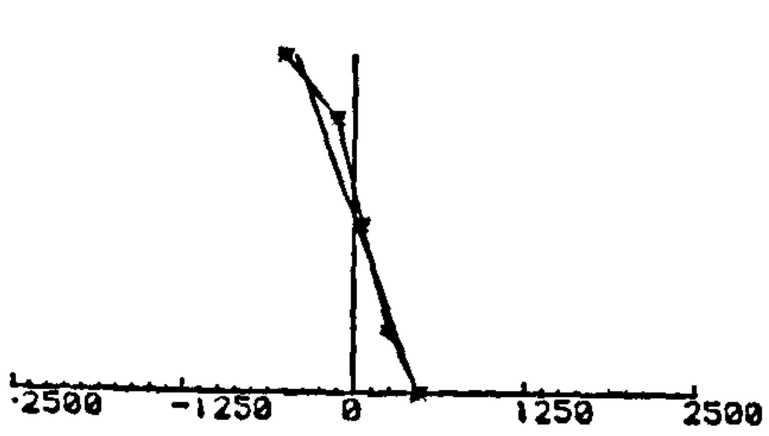

LOAD = 185 KN

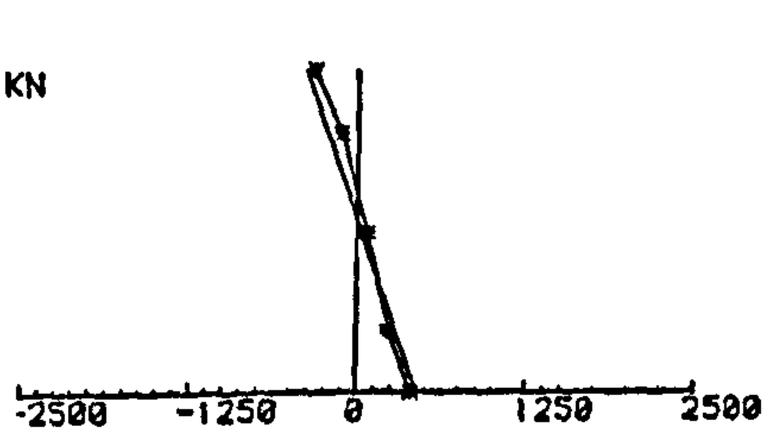

Fig. 5.16 - Strain profiles across the sectionfor column LDU0-12

* strain values shown x10^6

Strains at Mid-Height Section

Strains at 1/3 L From the stronger end

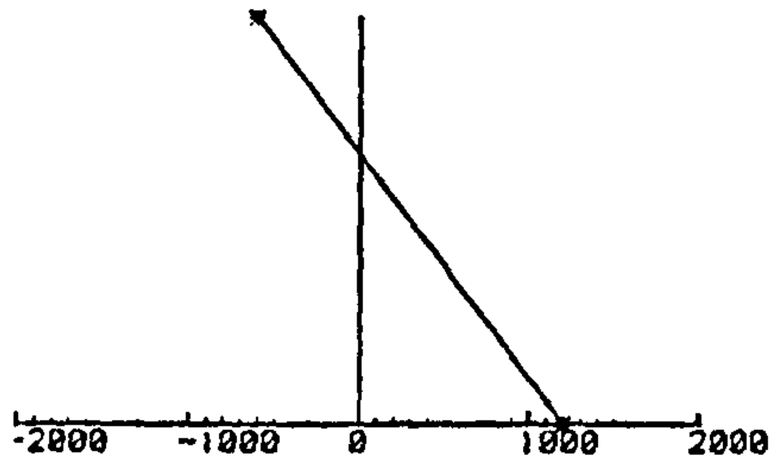

LOAD = 800 KN

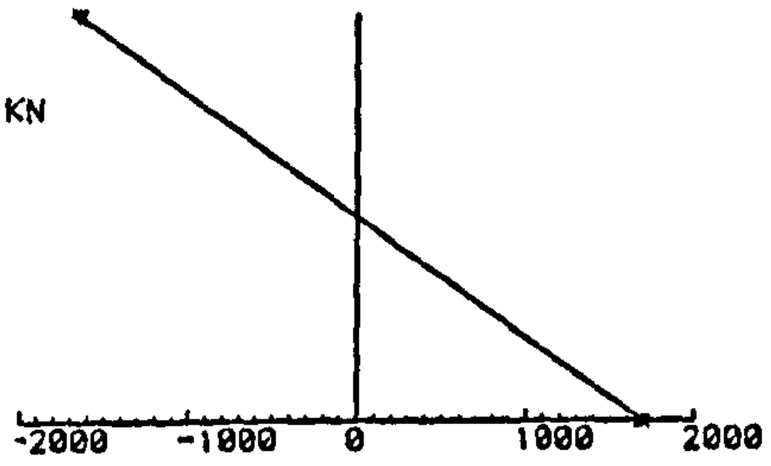

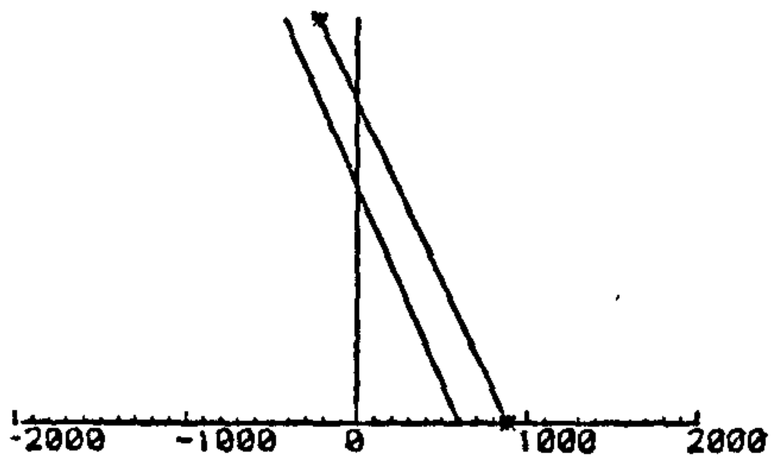

LOAD = 600 KN

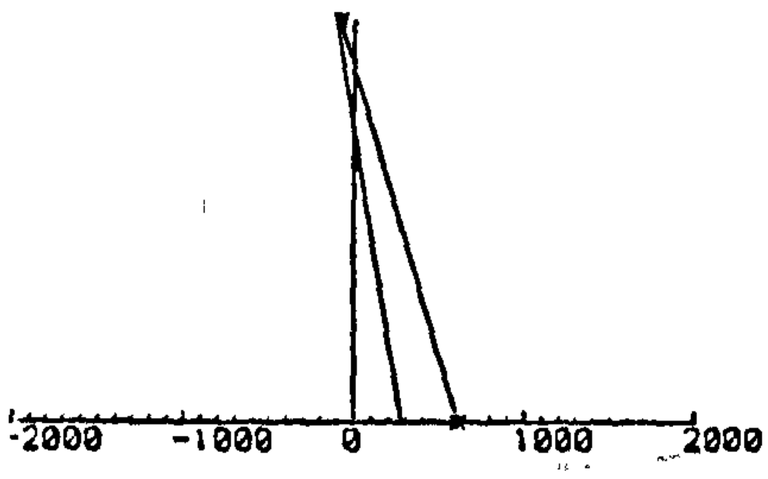

LOAD = 400 KN

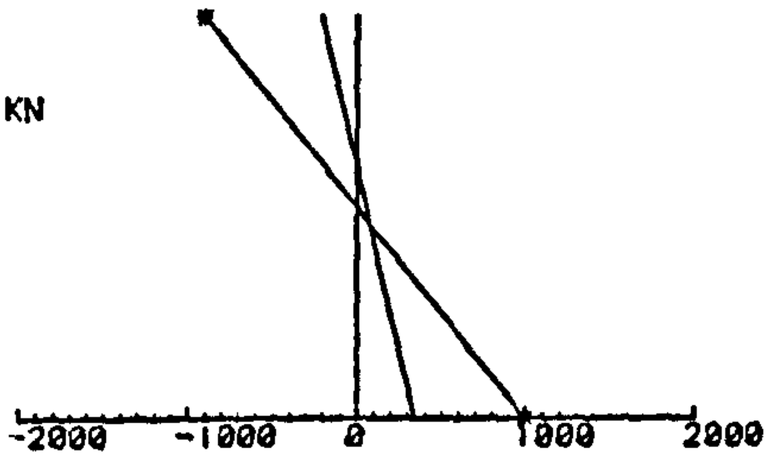

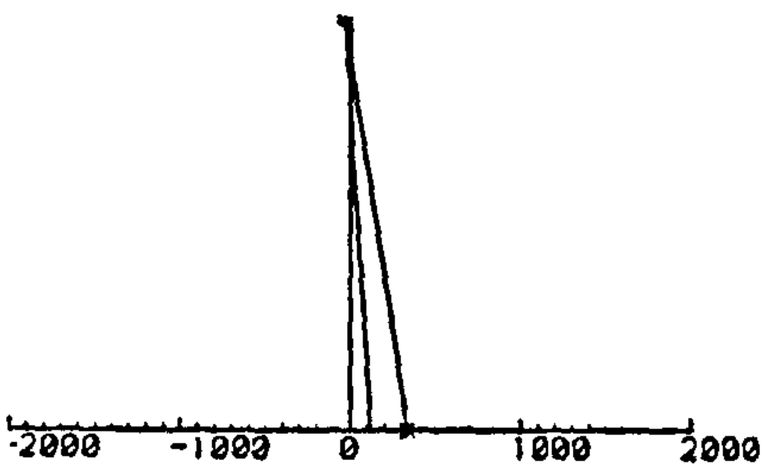

LOAD = 200 KN

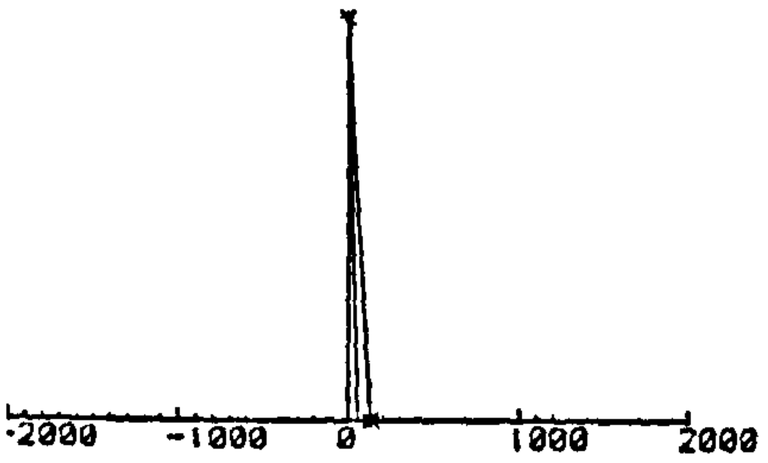

LOAD = 100 KN

F.g. 5.17 - Strain profiles across the sectionFor column LGU0-13

* strain values shown x10^{6}

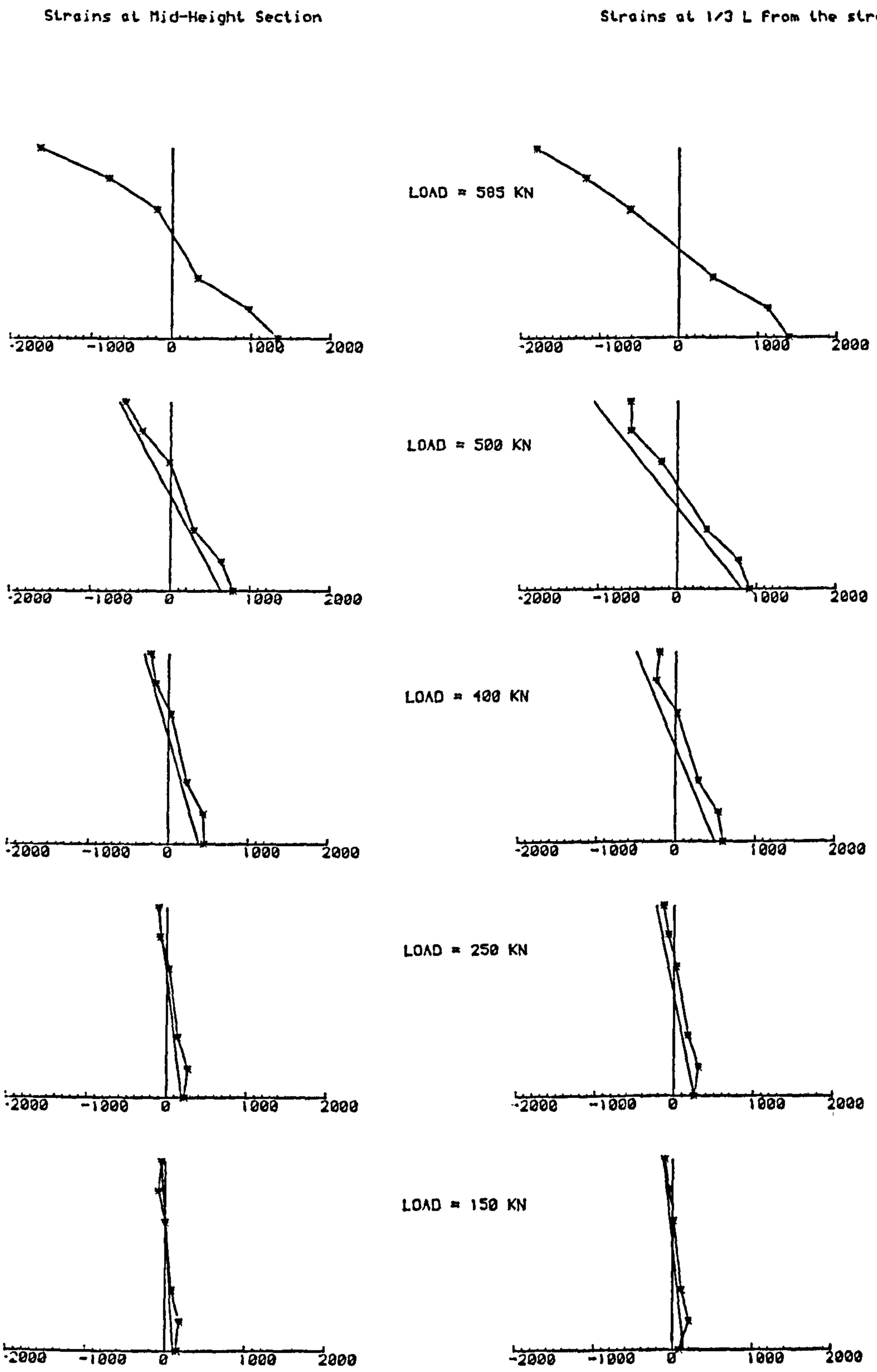

Fig. 5.18 - Strain profiles across the sectionfor column LGU0-14

* strain values shown $x10^{6}$

SERIES - D

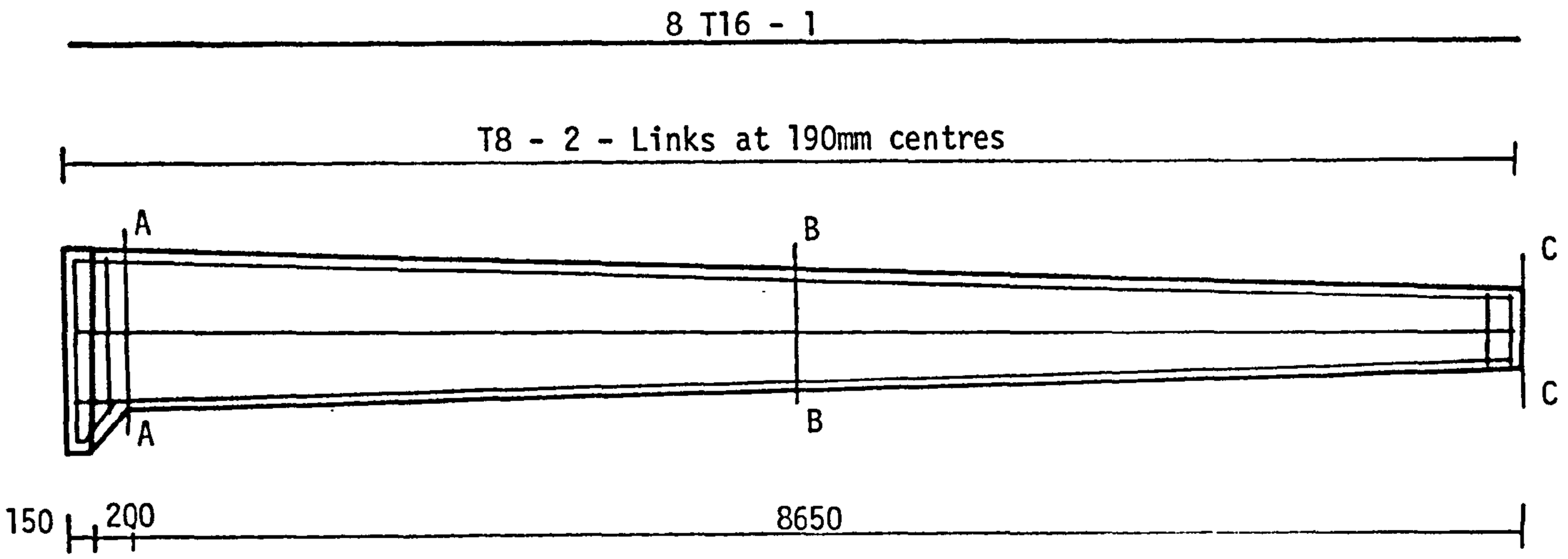

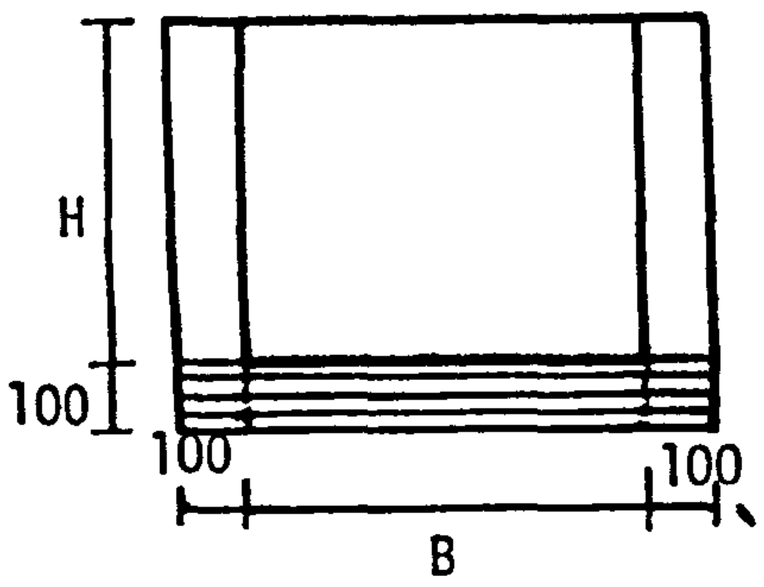

A - A

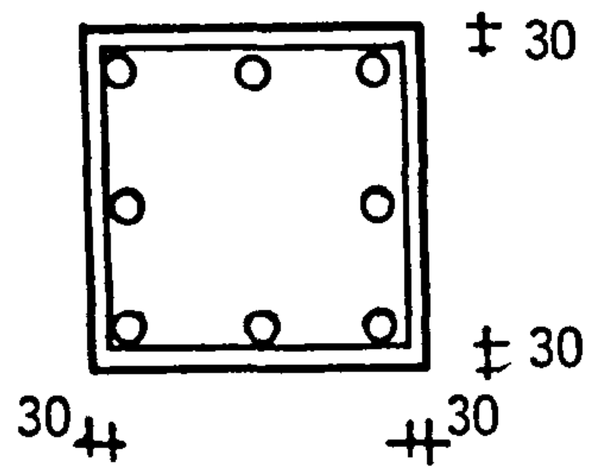

B - B

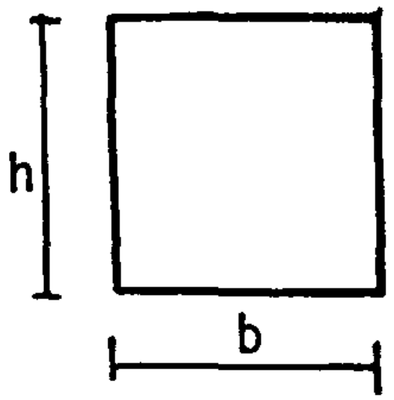

C - C

COLUMN LABEL	H (mm)	B (mm)	h (mm)	b (mm)
LDBO-15/16	400	400	300	300
LDBO-17/18	300	300	200	200

Fig. 6.1 – REINFORCEMENT DETAILS AND CROSS SECTIONS OF TAPERED COLUMNS

SERIES - D

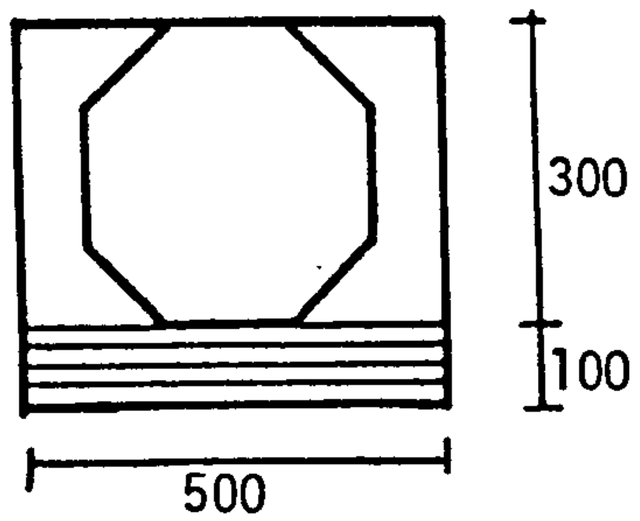

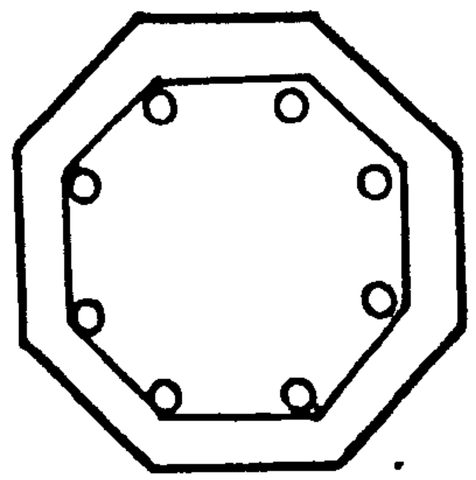

B - B

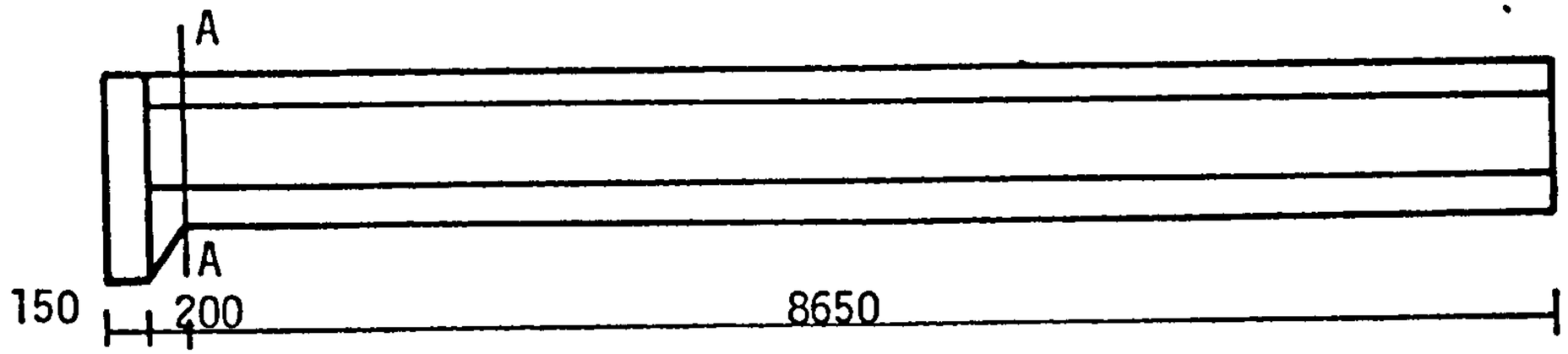

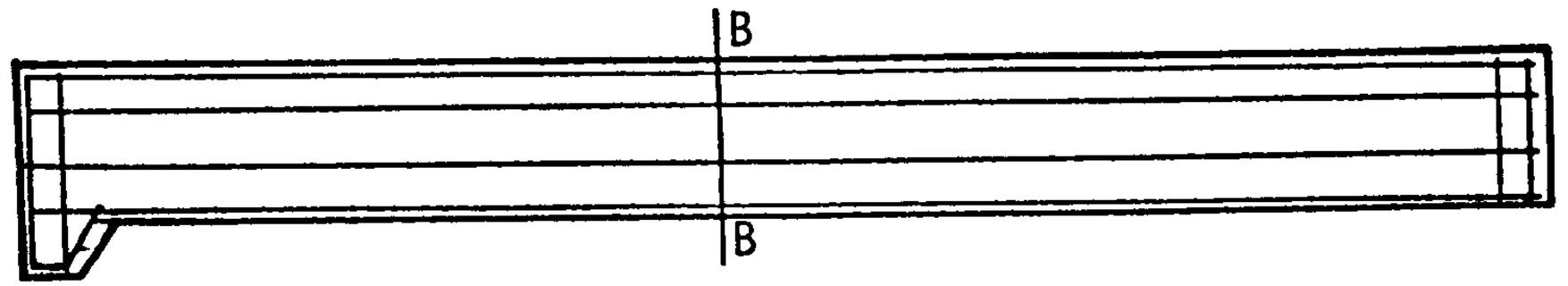

T8 - 2 - Links at 200 centres

8 T16 - 1

Fig. 6.2 - REINFORCEMENT DETAILS AND CROSS SECTION OF OCTAGONAL COLUMNS

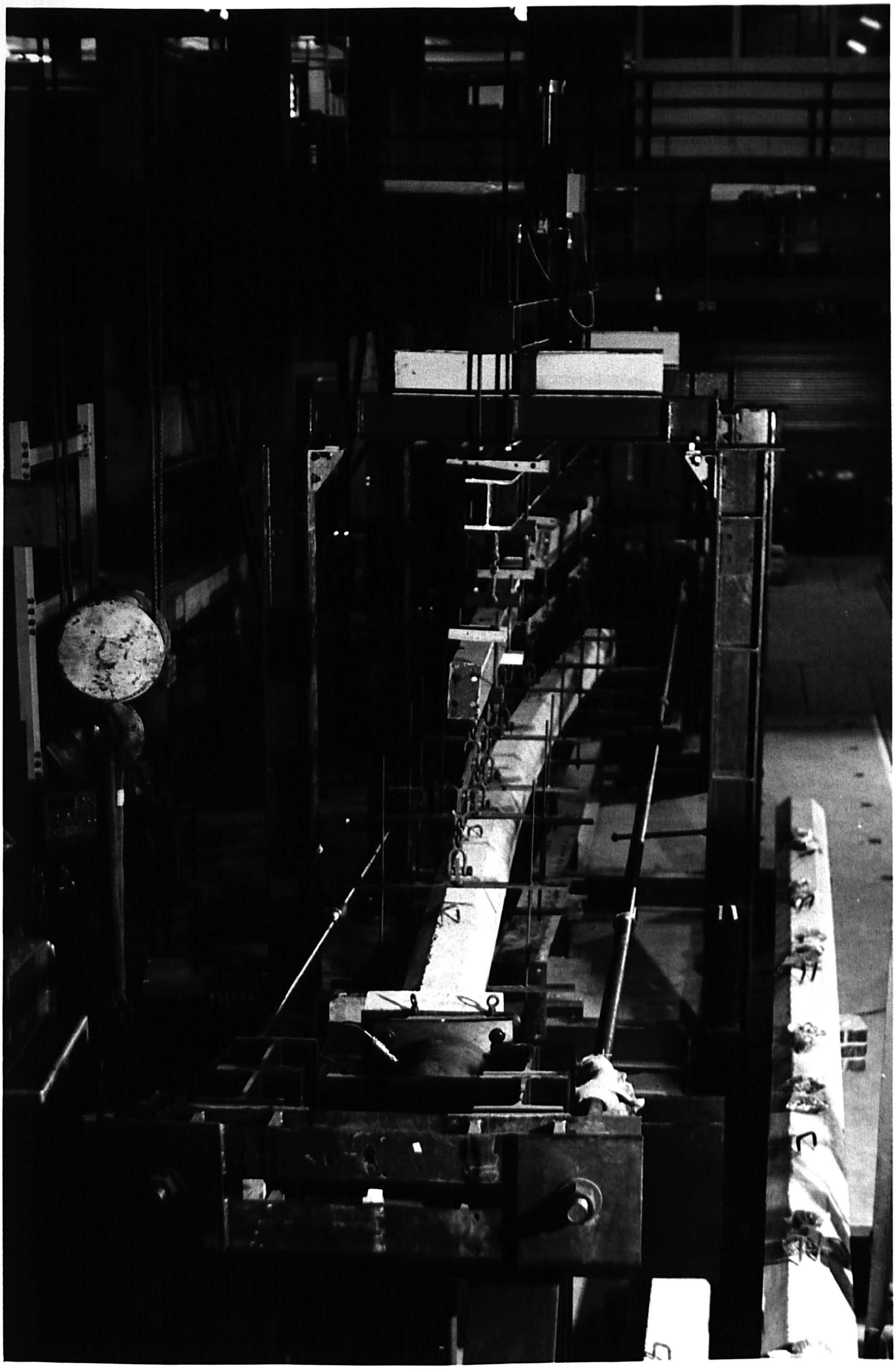

Fig. 6.3. General view of the rig and the instrumentation

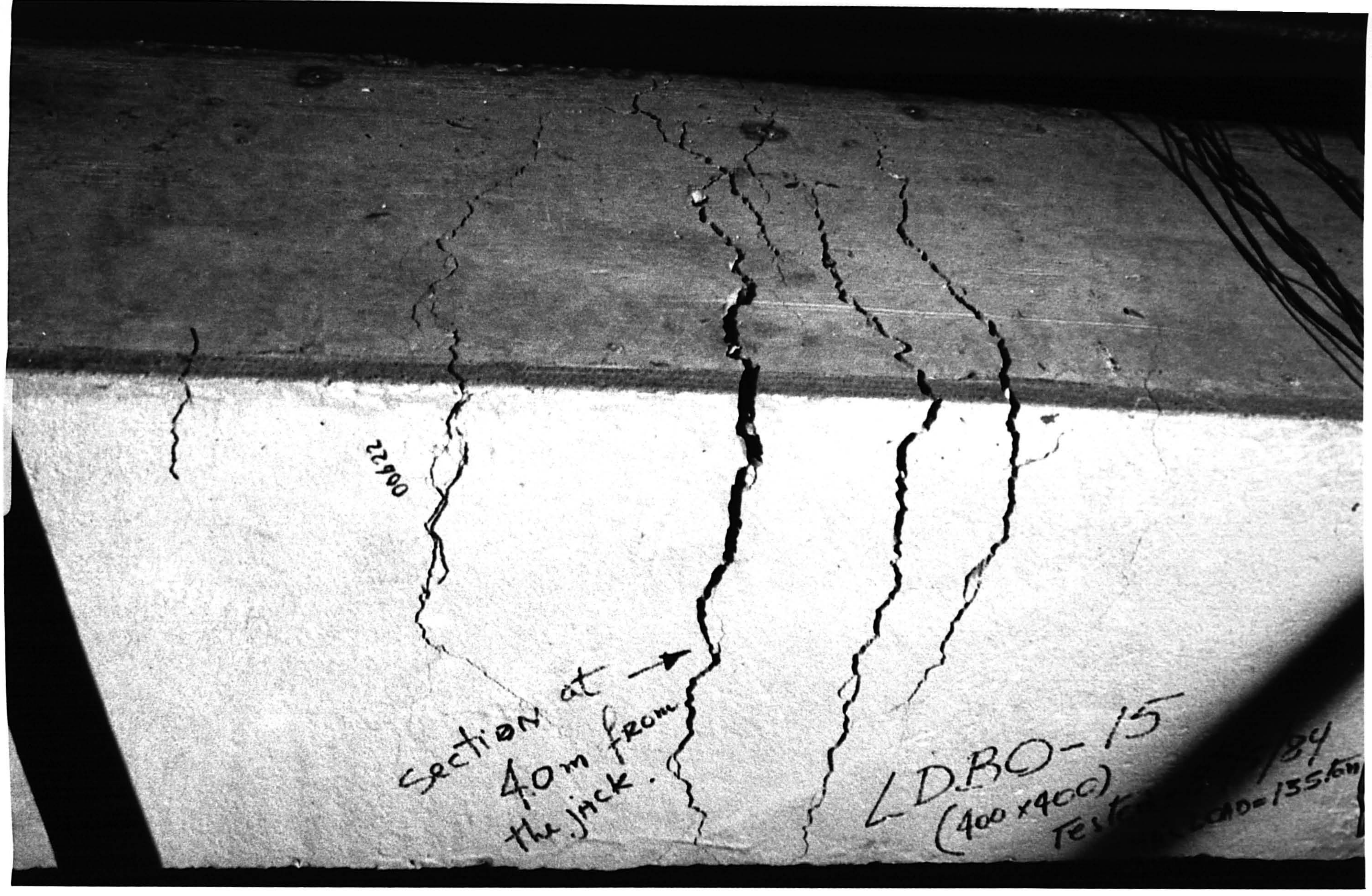

Fig. 6.4. A typical view of failed column

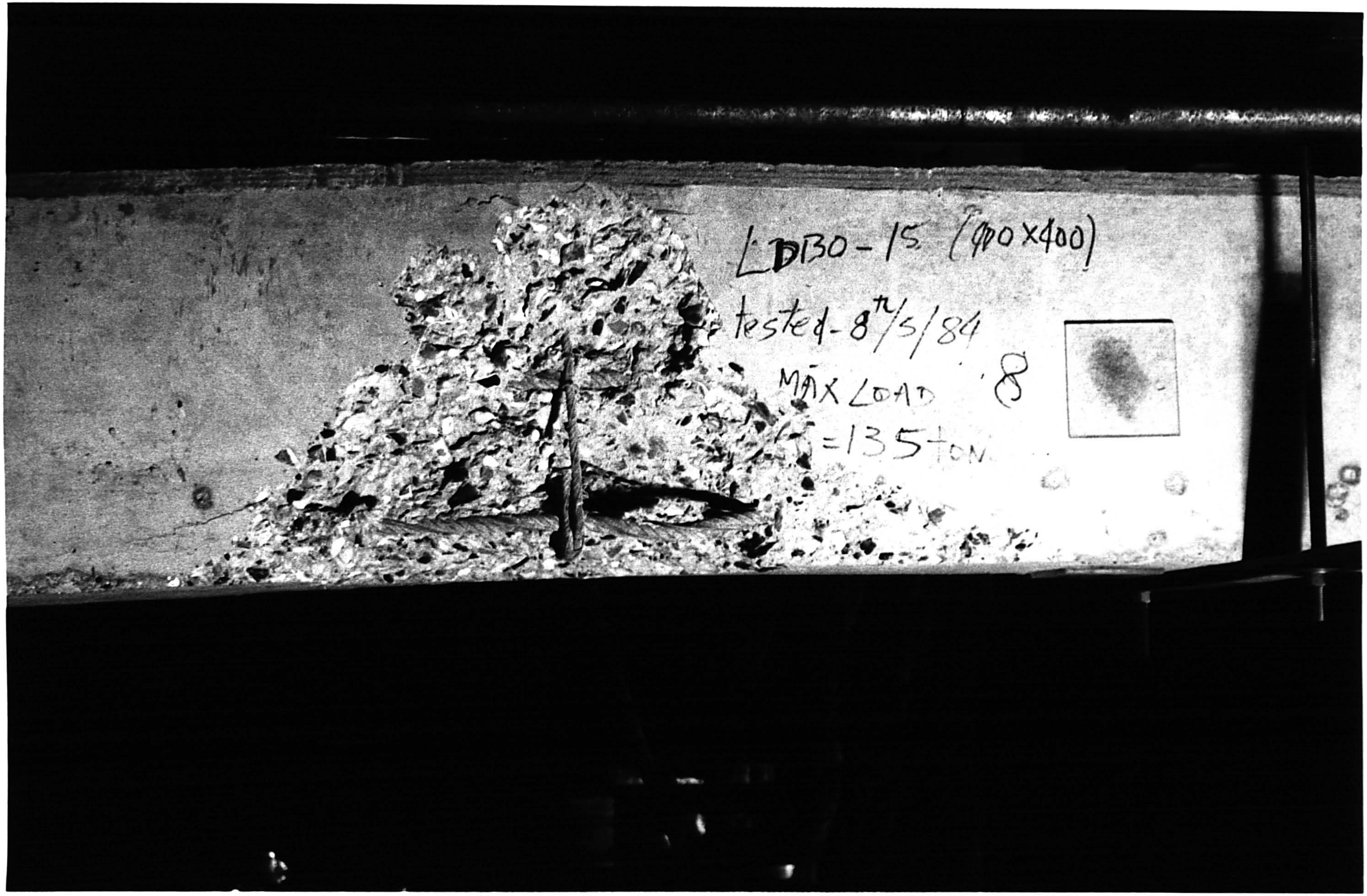

Fig. 6.5. View of the mode of failure

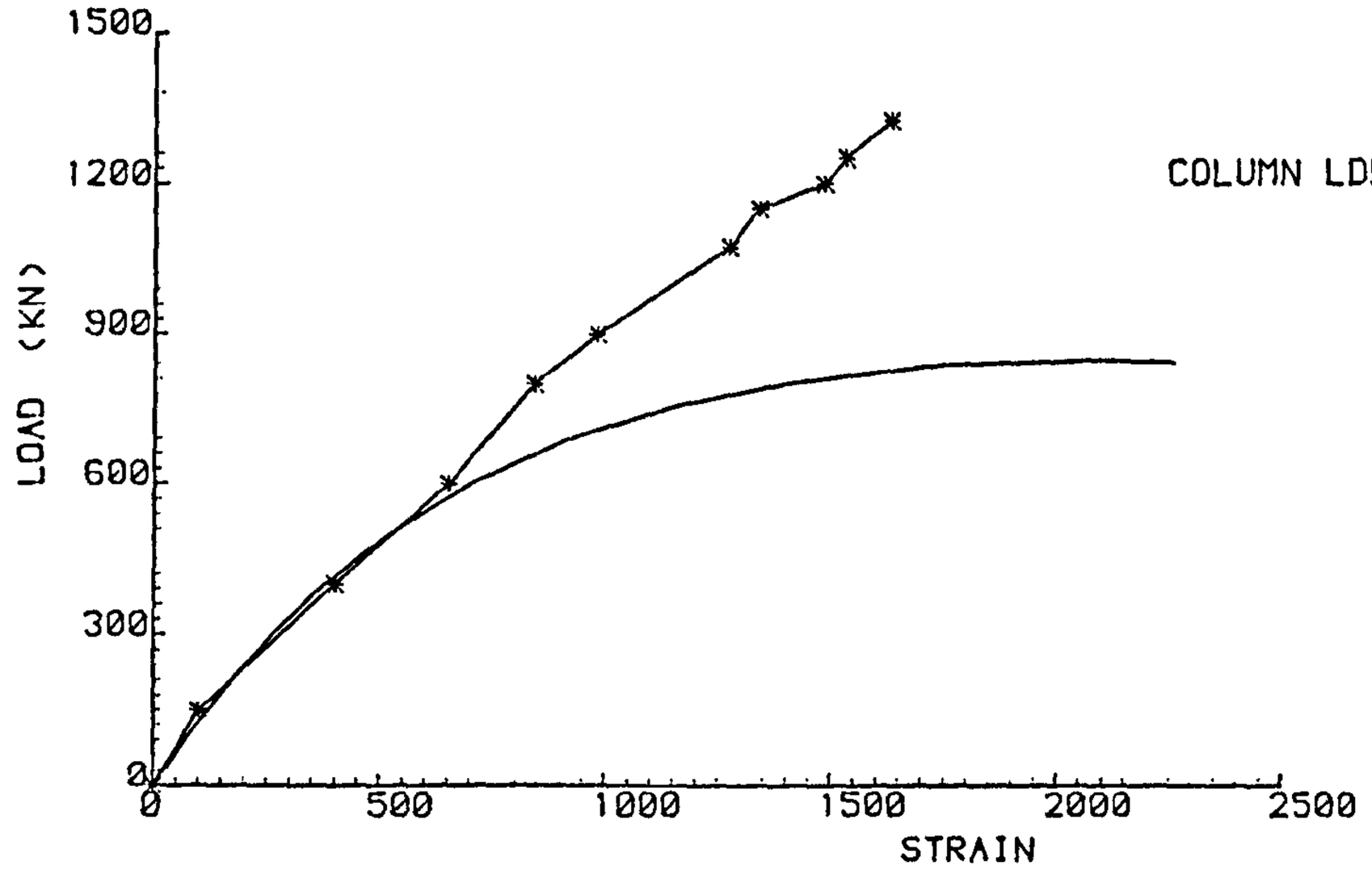

LOAD vs MAX. STRAIN

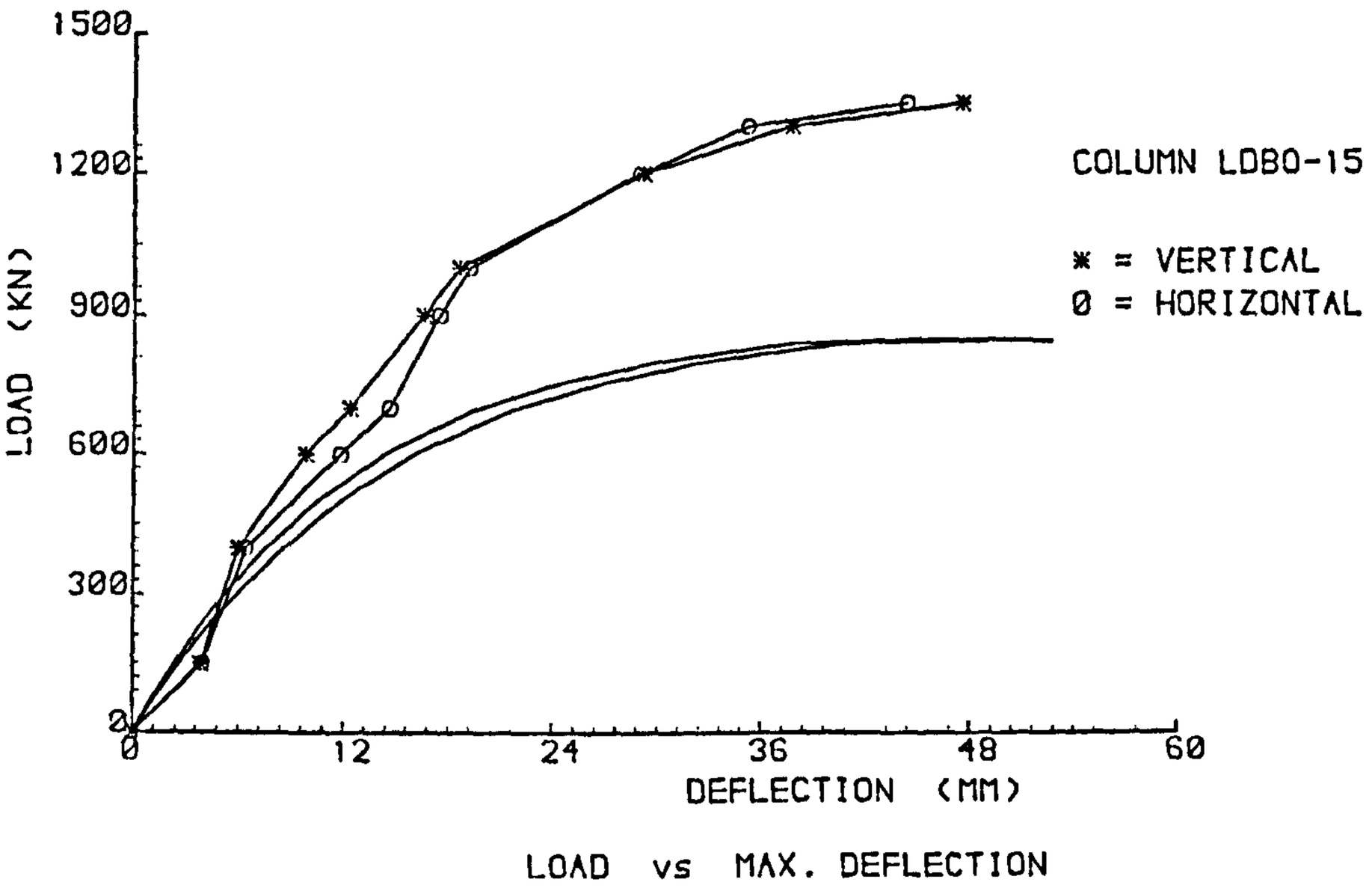

LOAD vs MAX. DEFLECTION

Fig. G.6 - Comparison between experimental and theoretical results for column LDBO-15

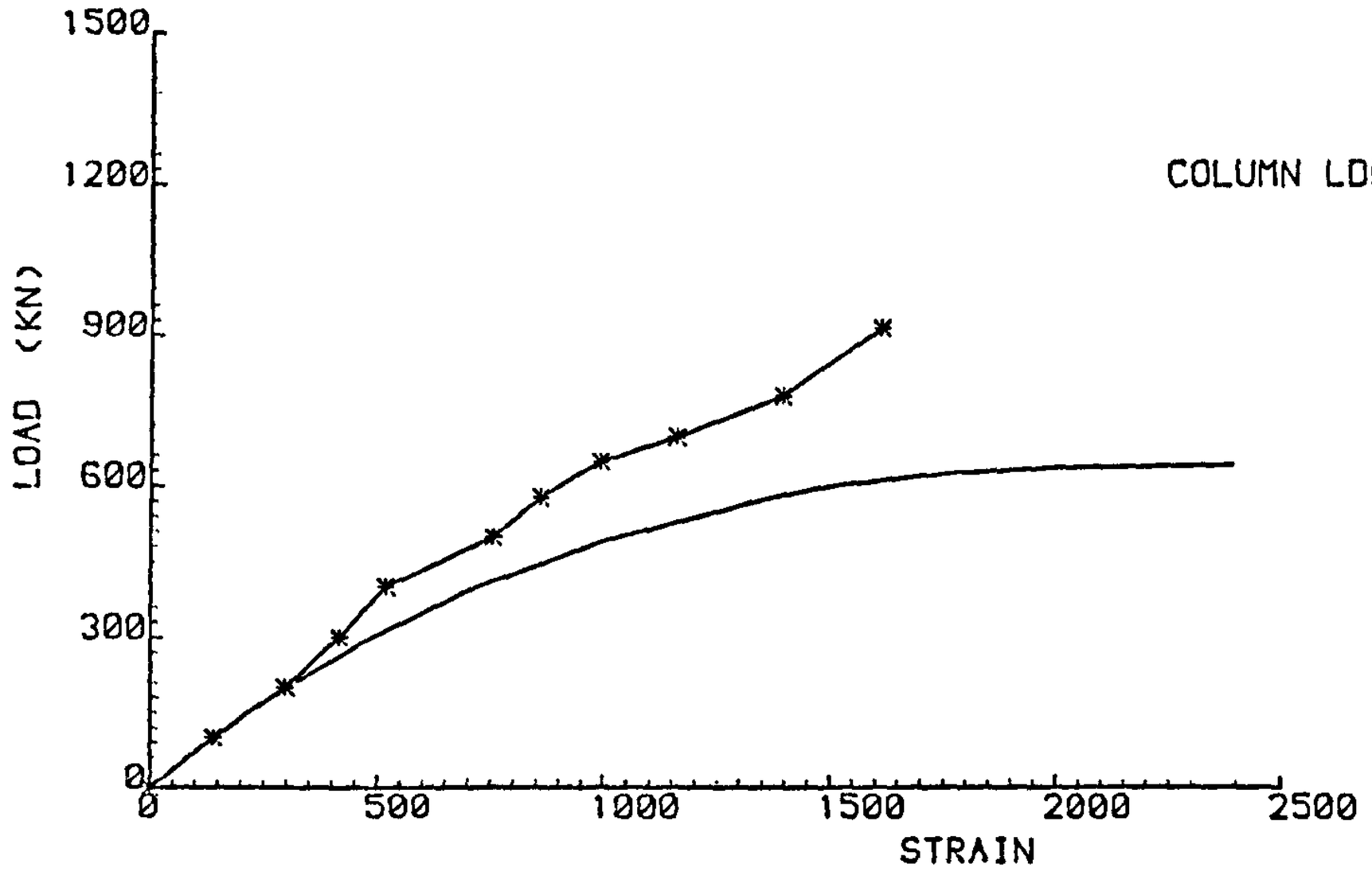

LOAD vs MAX. STRAIN

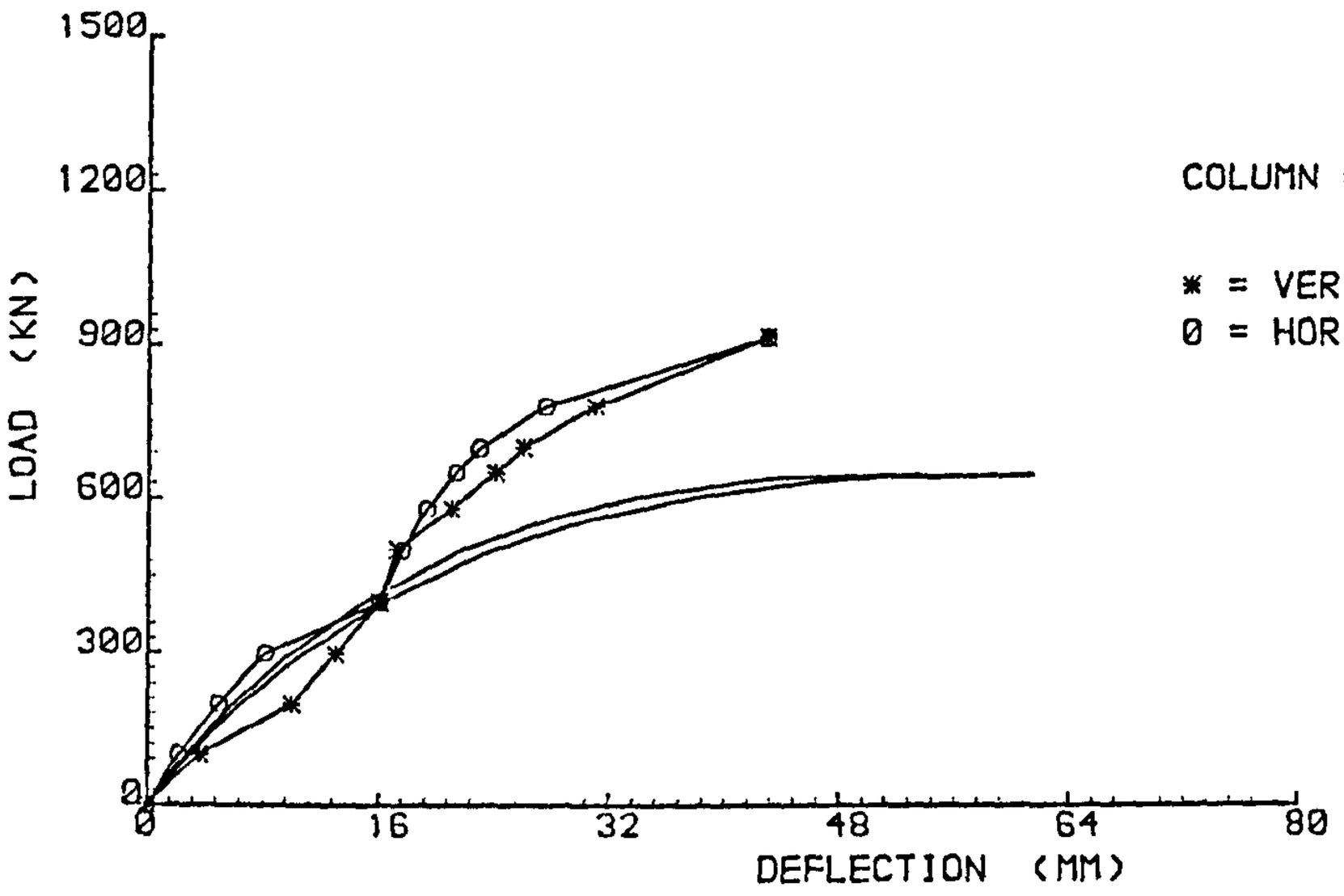

LOAD vs MAX. DEFLECTION

Fig. 6.7 - Comparison between experimental and theoretical results For column LDBO-16

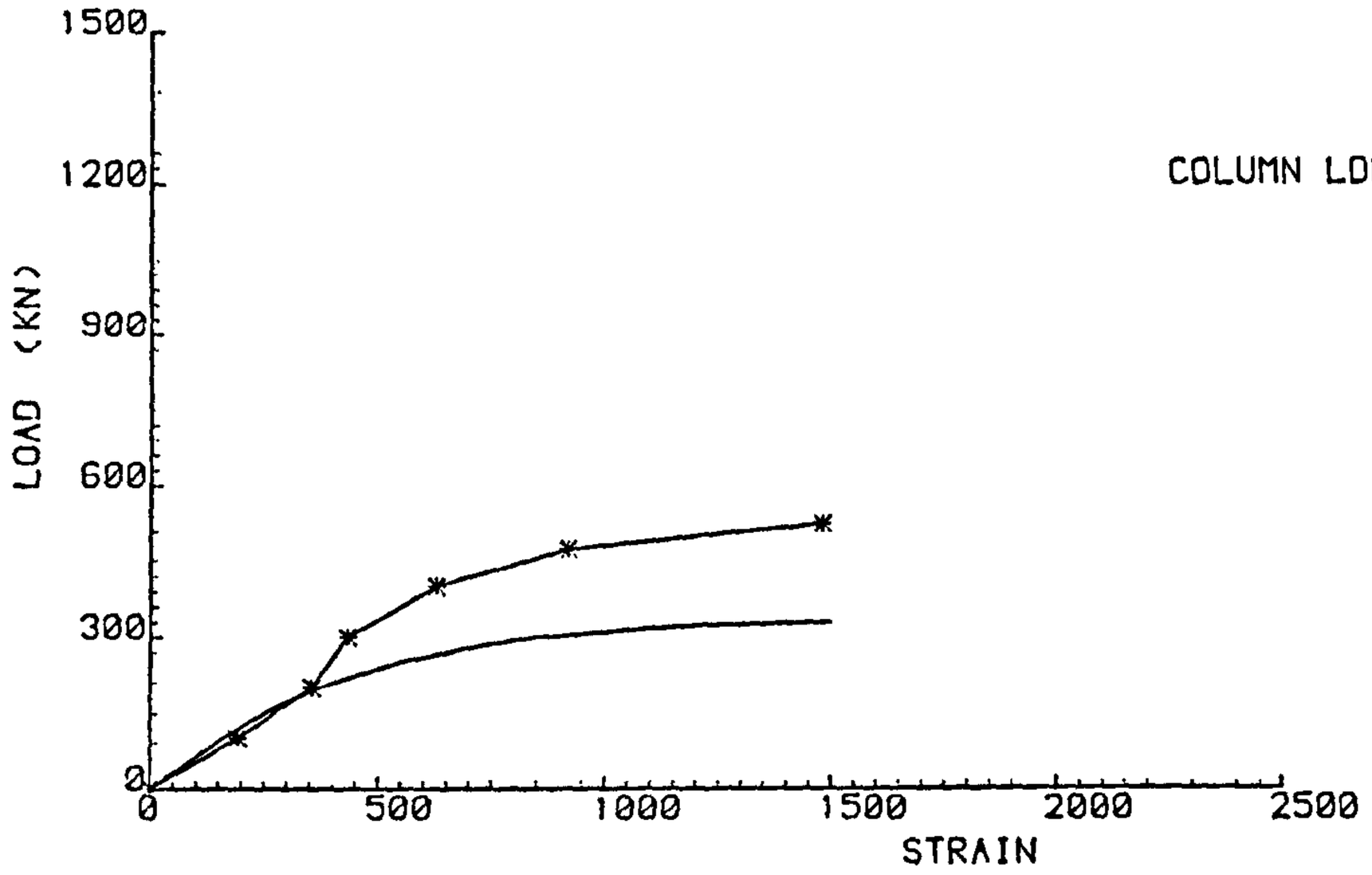

LOAD vs MAX. STRAIN

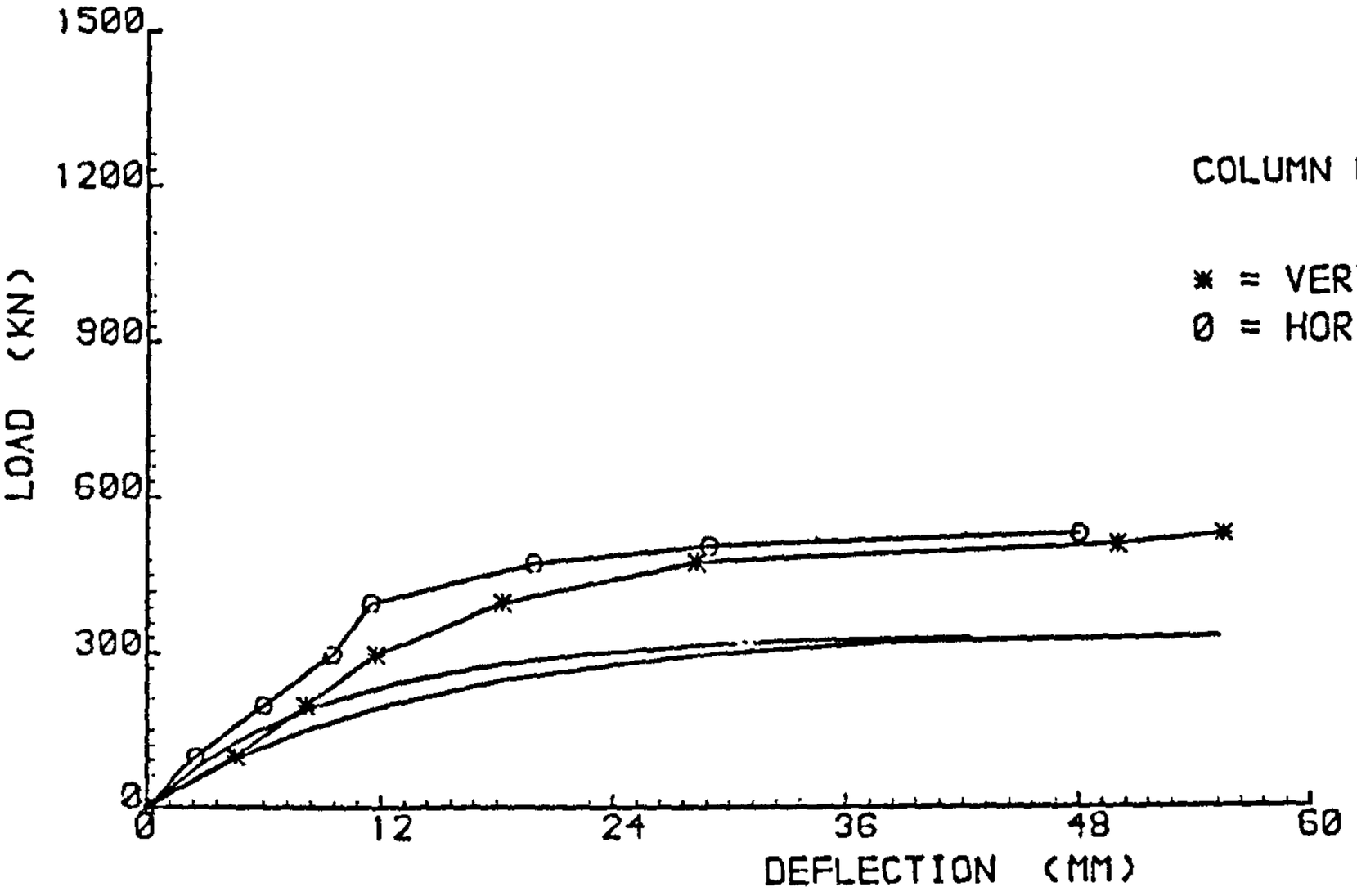

LOAD vs MAX. DEFLECTION

Fig. G.8 - Comparison between experimental and theoretical results for column LDBO-17

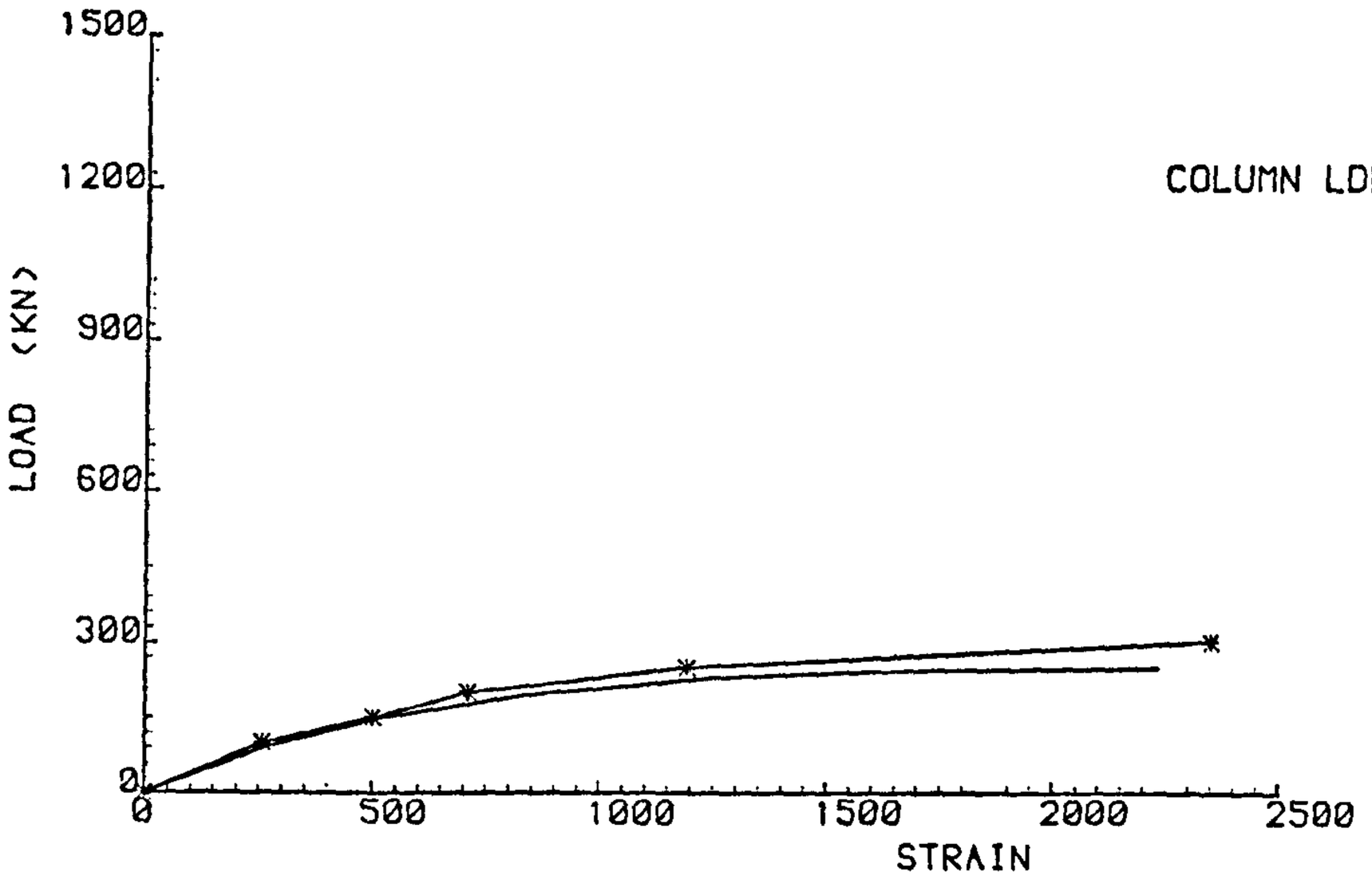

LOAD vs MAX. STRAIN

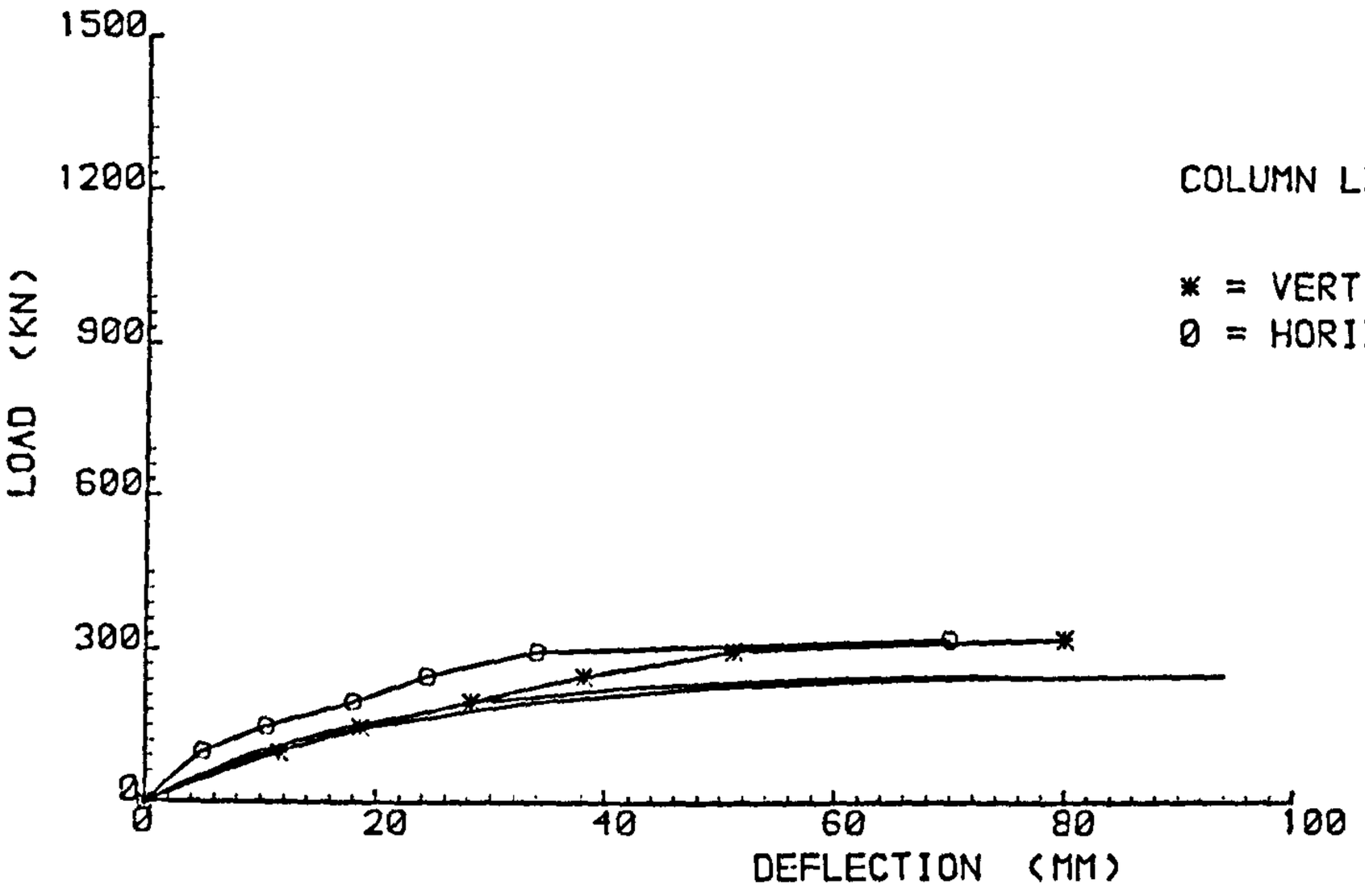

LOAD vs MAX. DEFLECTION

Fig. G.9 - Comparison between experimental and theoretical results For column LDBO-18

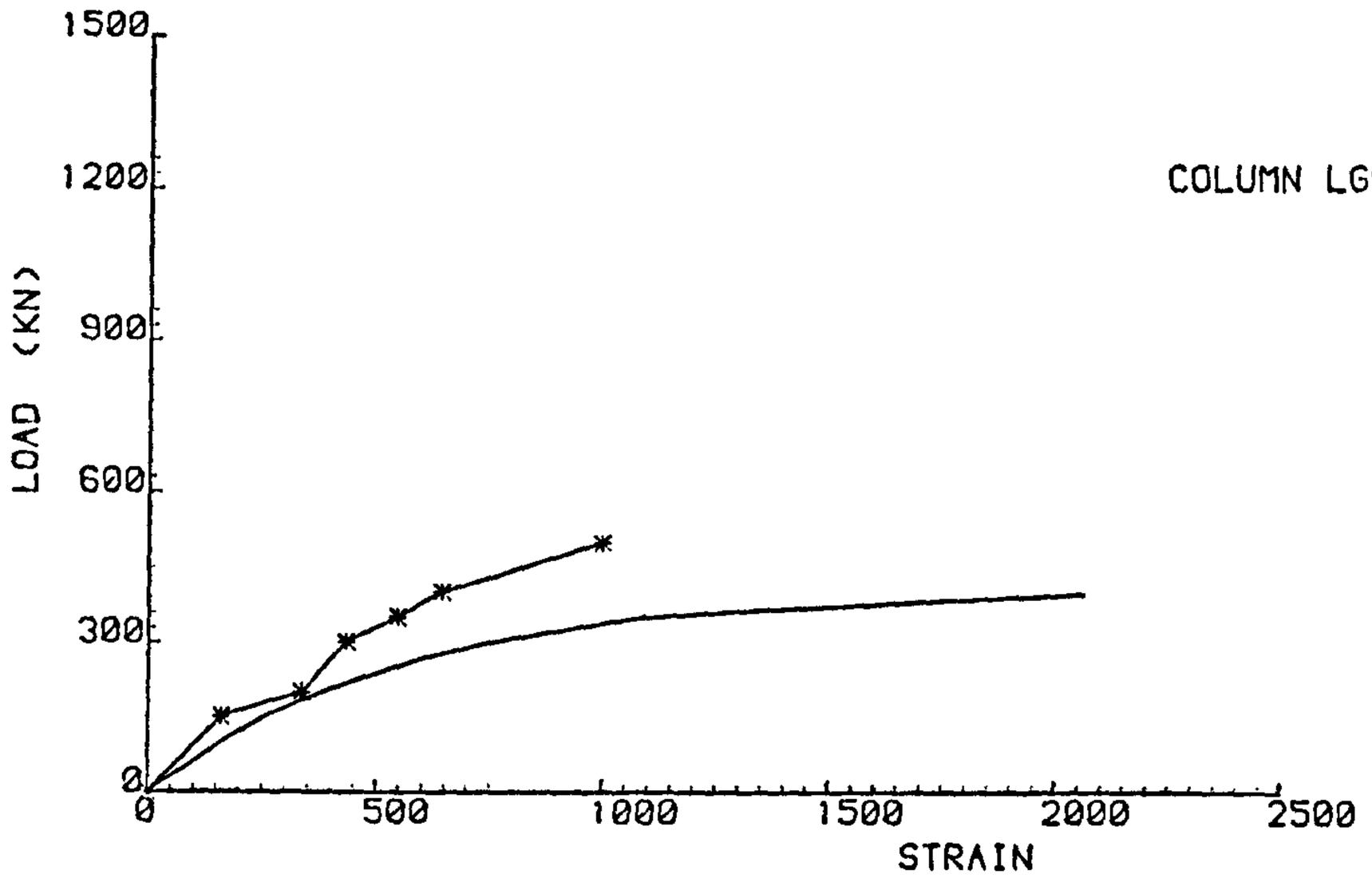

LOAD vs MAX. STRAIN

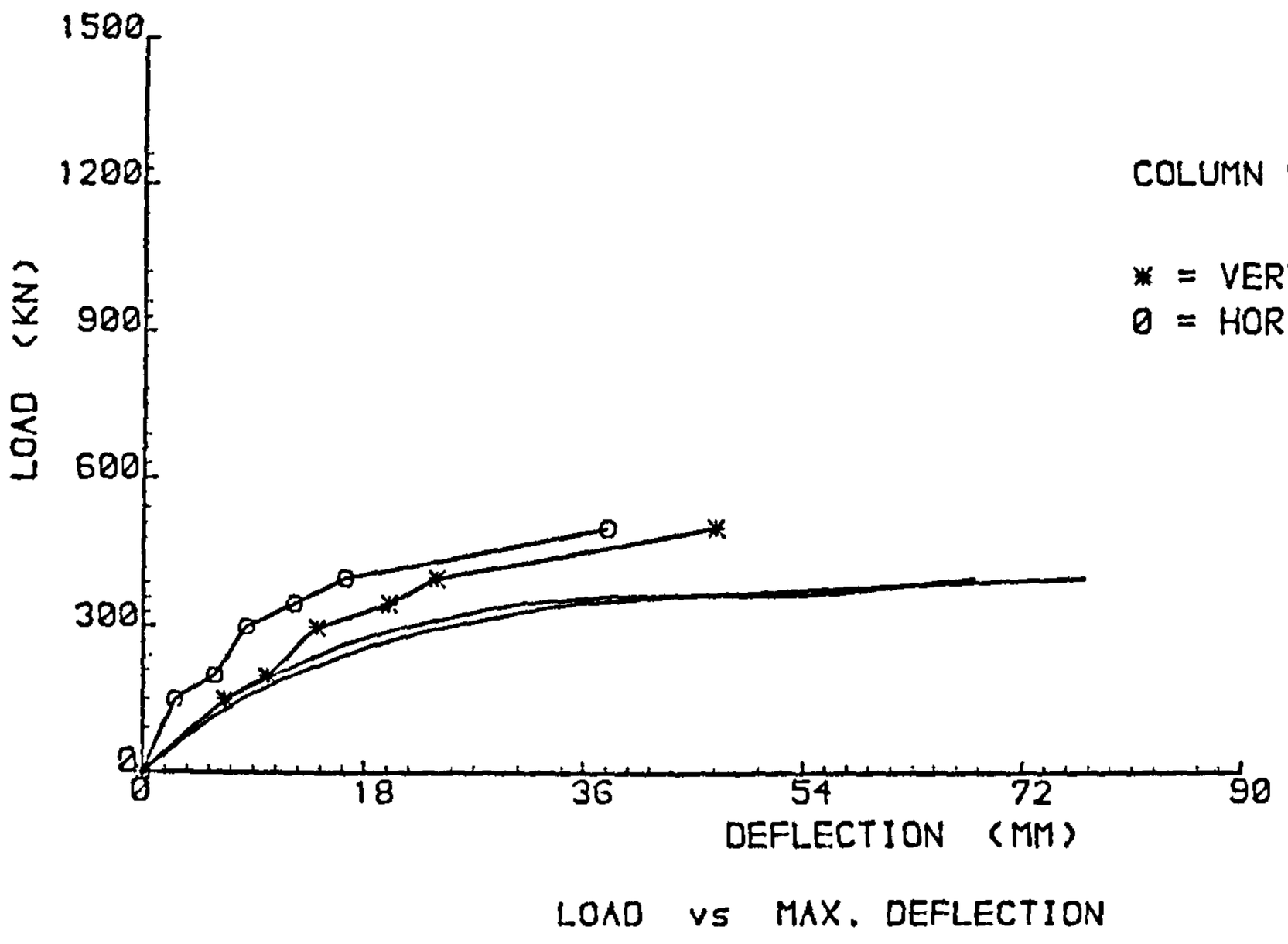

LOAD vs MAX. DEFLECTION

Fig. G.10 - Comparison between experimental and theoretical results for column LGBO-19

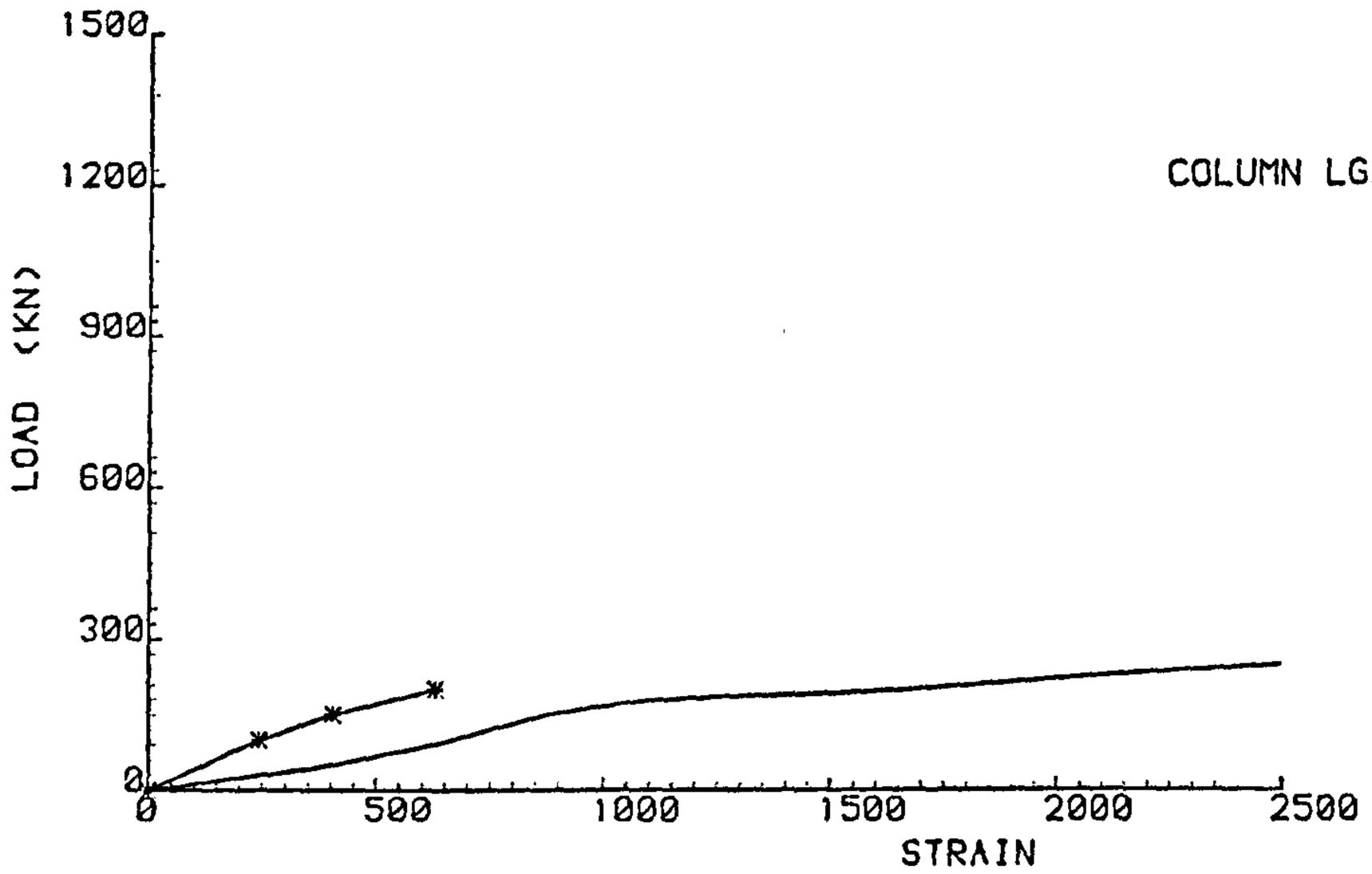

LOAD vs MAX. STRAIN

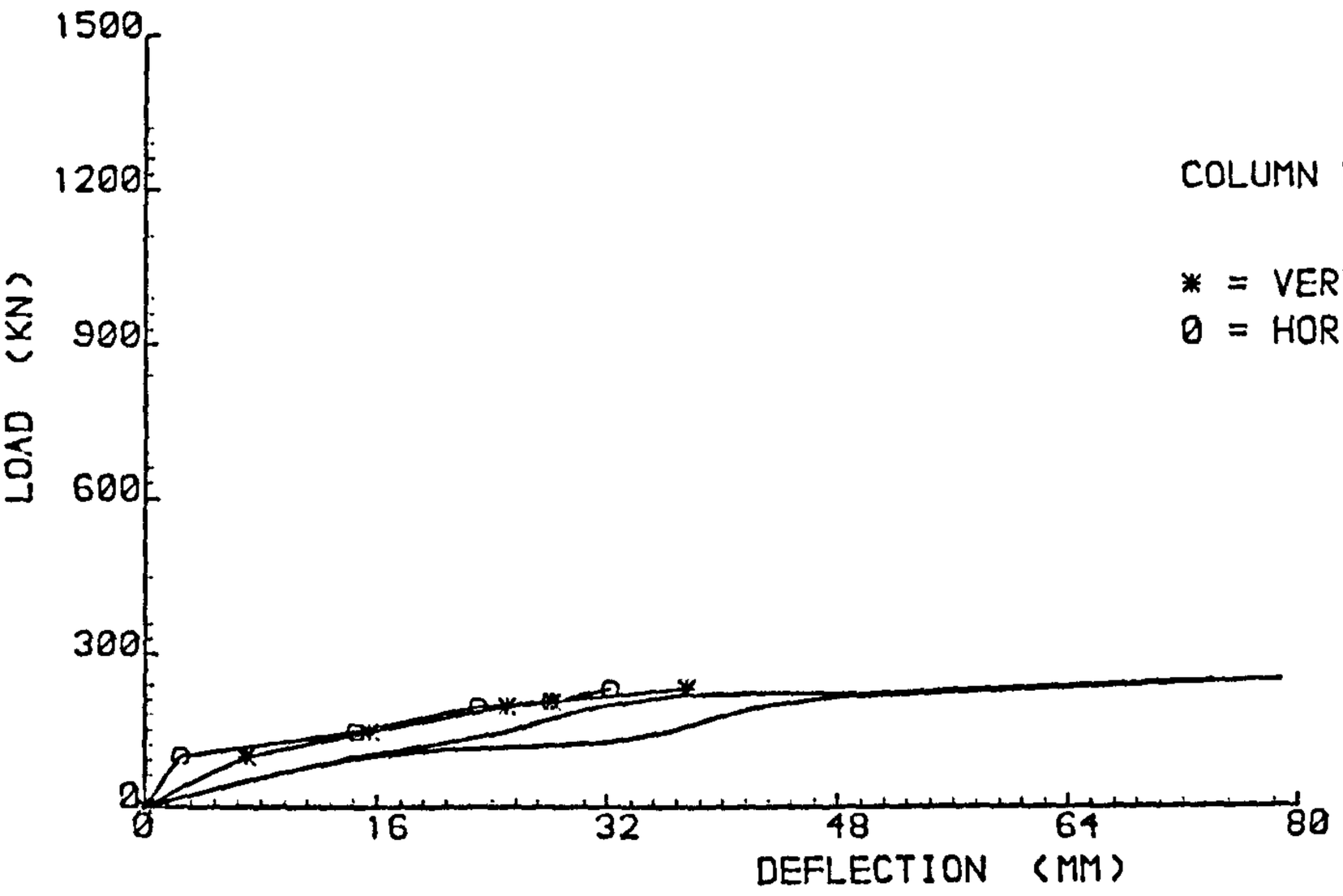

LOAD vs MAX. DEFLECTION

Fig. G.11 - Comparison between experimental and theoretical results for column LGBO-20

* observed strains

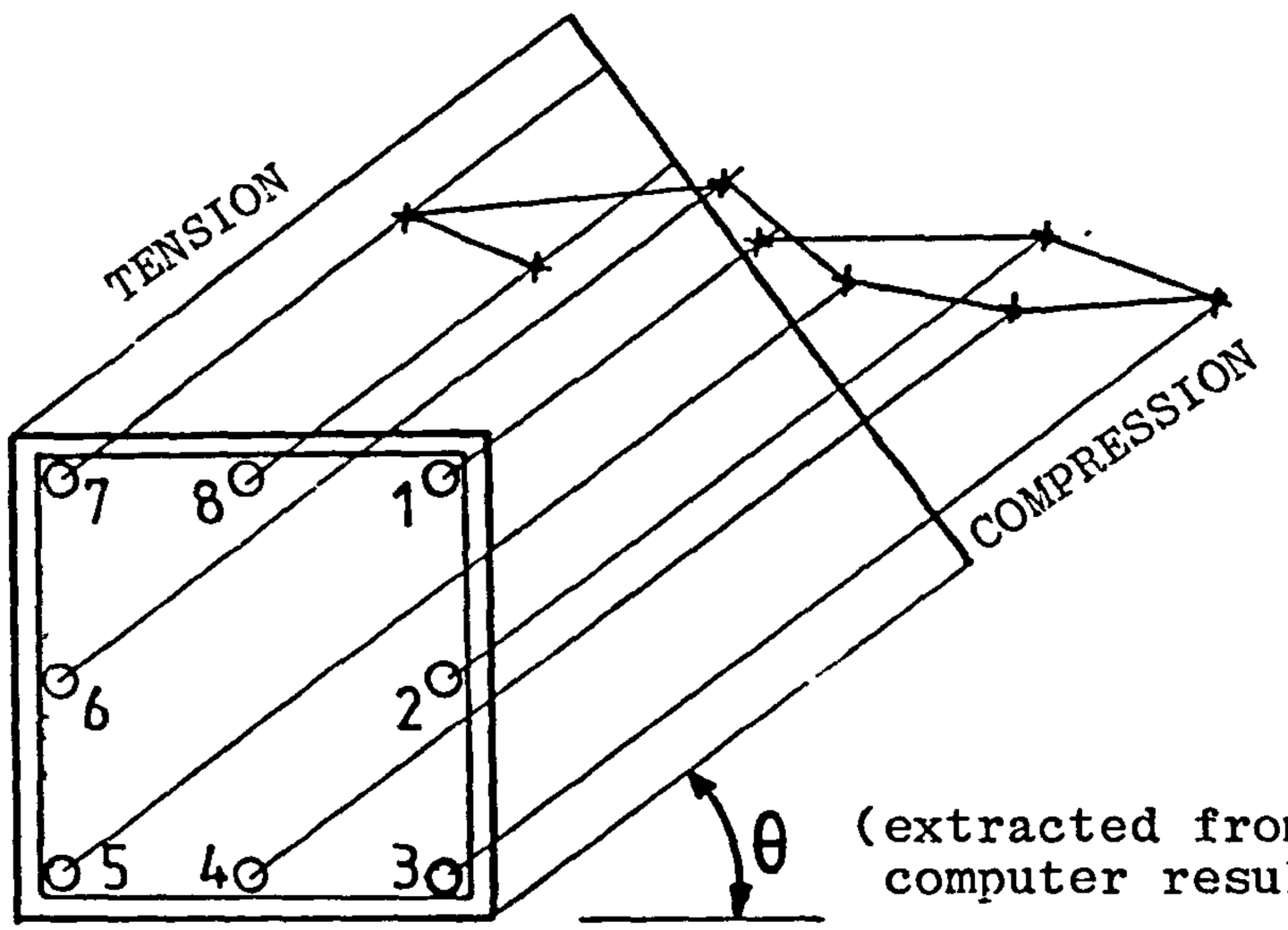

TAPERED COLUMNS

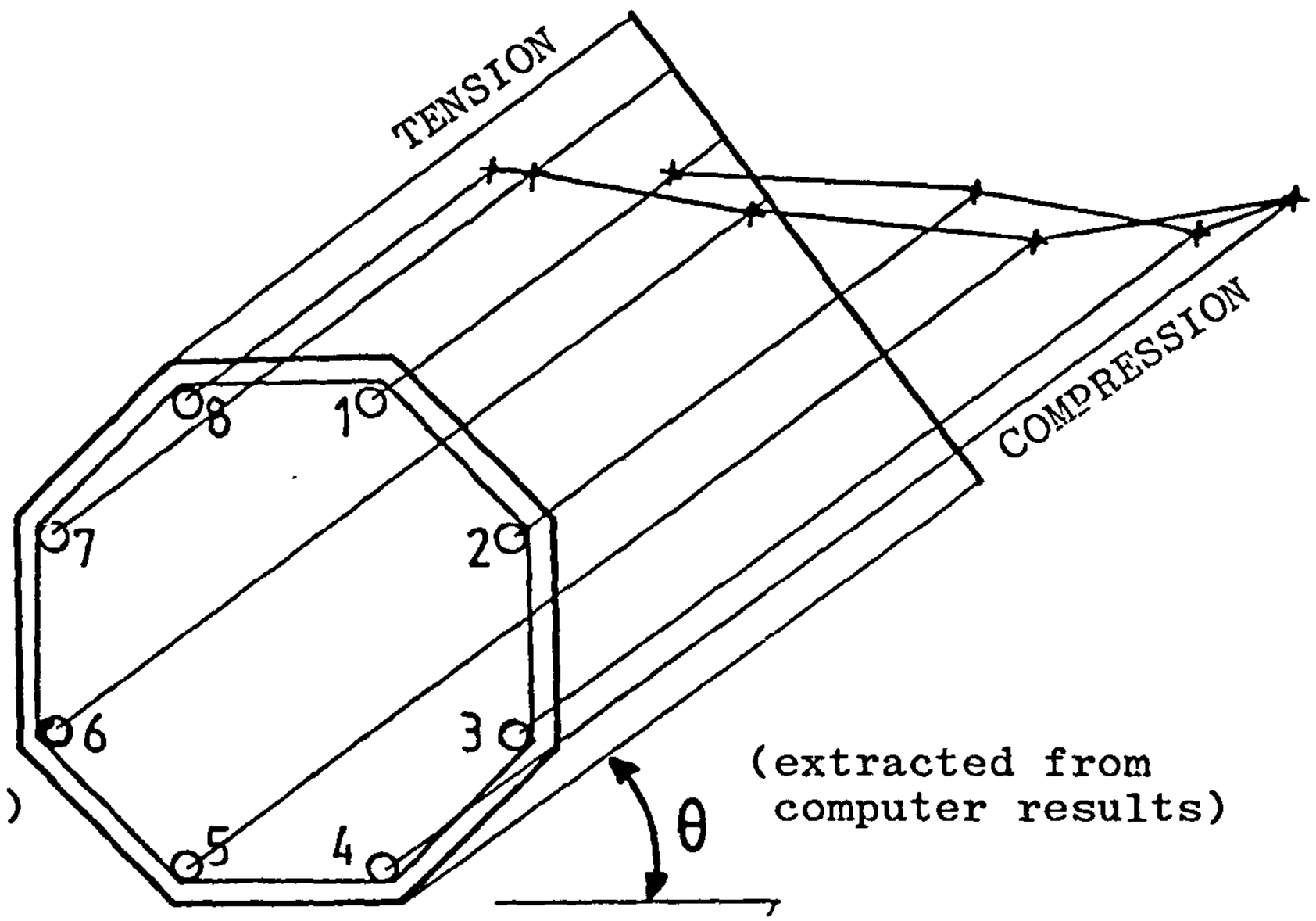

OCTAGONAL COLUMNS

Fig. 6.12. - PROCEDURE ADOPTED FOR PLOTTING STRAIN PROFILES FOR BIAXIAL BENDING

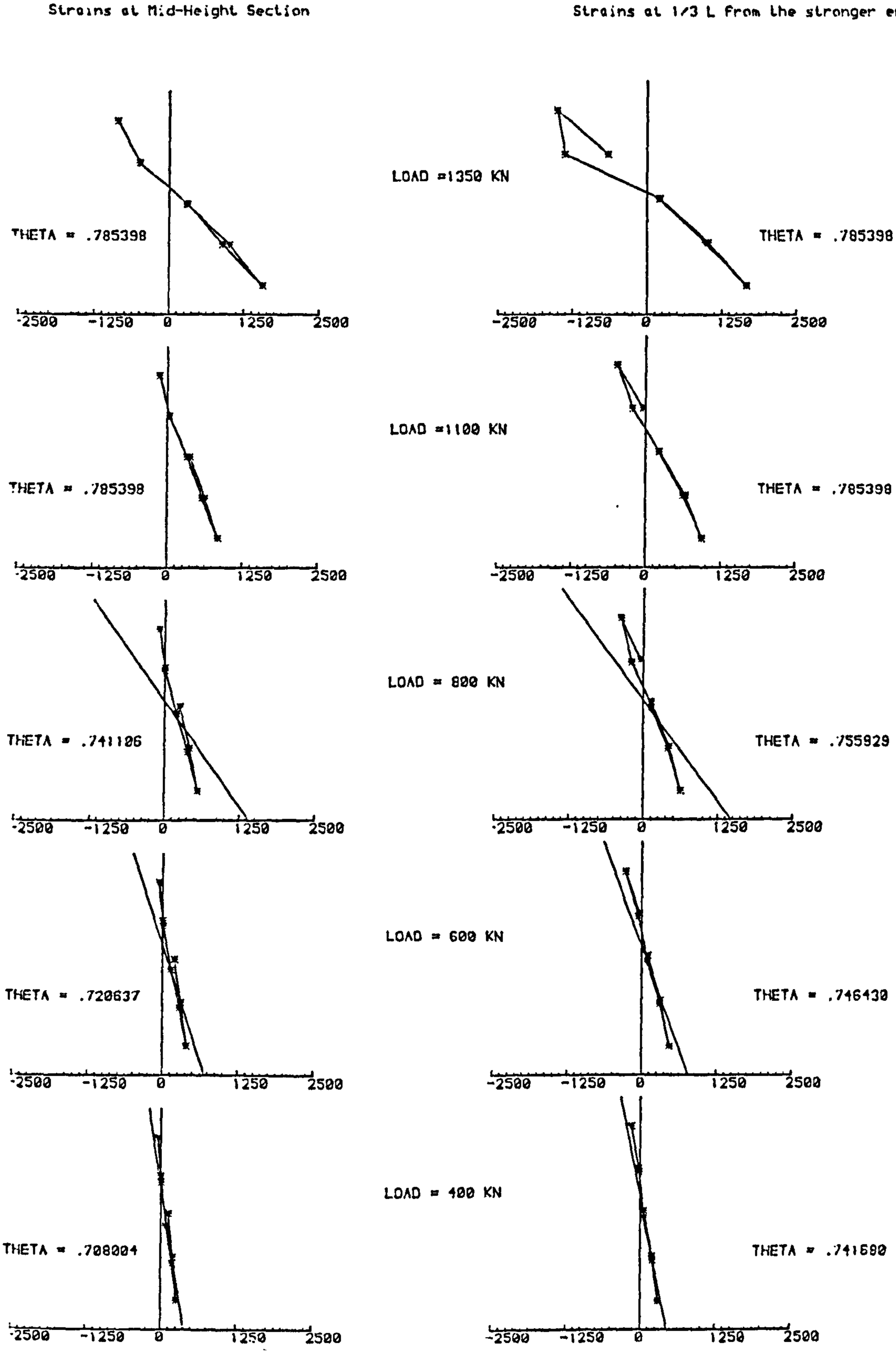

F.g. 6.13 - Strain profiles across the section for column LDU0-15

* strain values shown x10

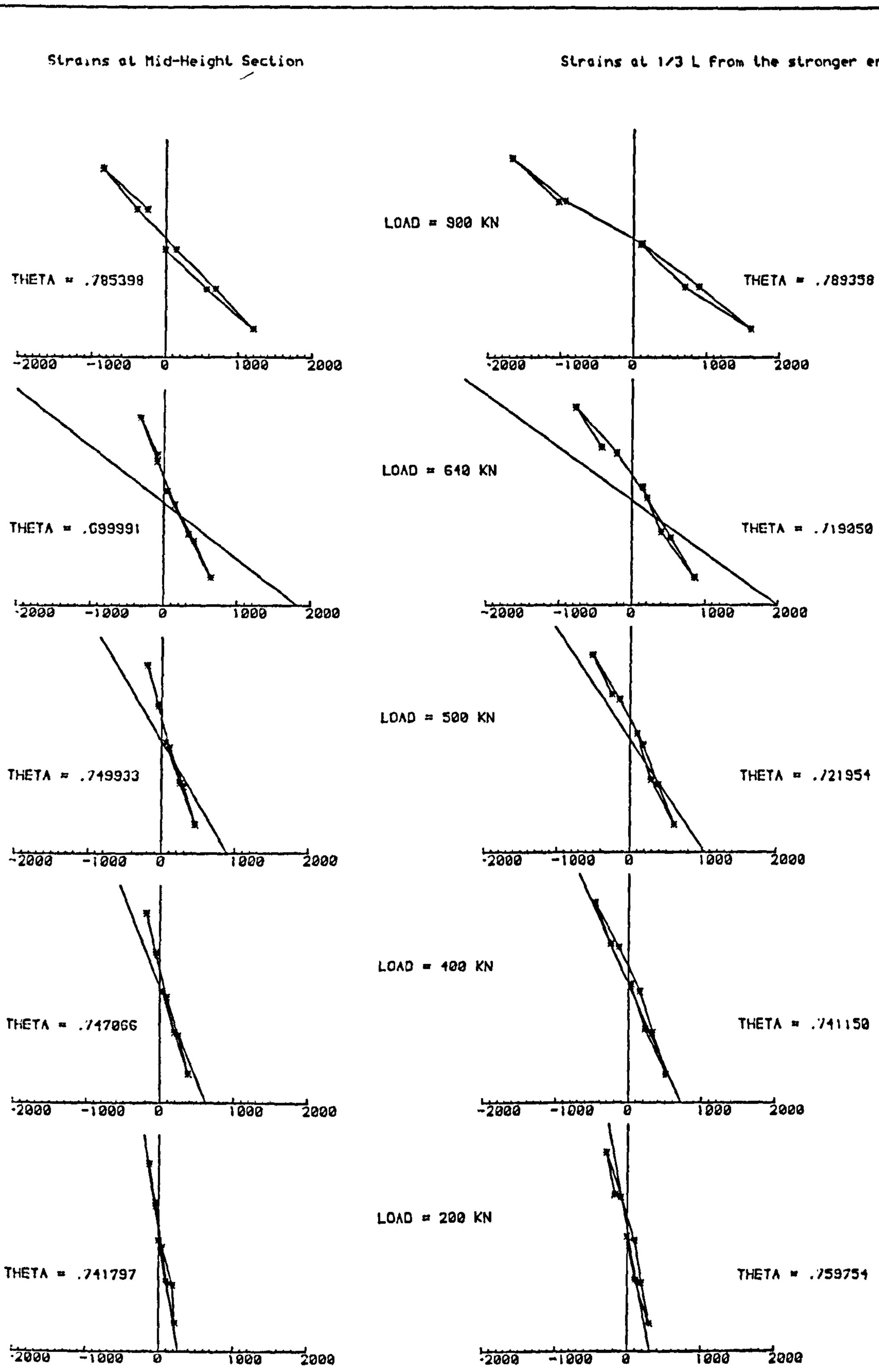

Fig. G.14 - Strain profiles across the section for column LDU0-16

* strain values shown x10

Strains at Mid-Height Section

Strains at 2/3 L From the stronger end

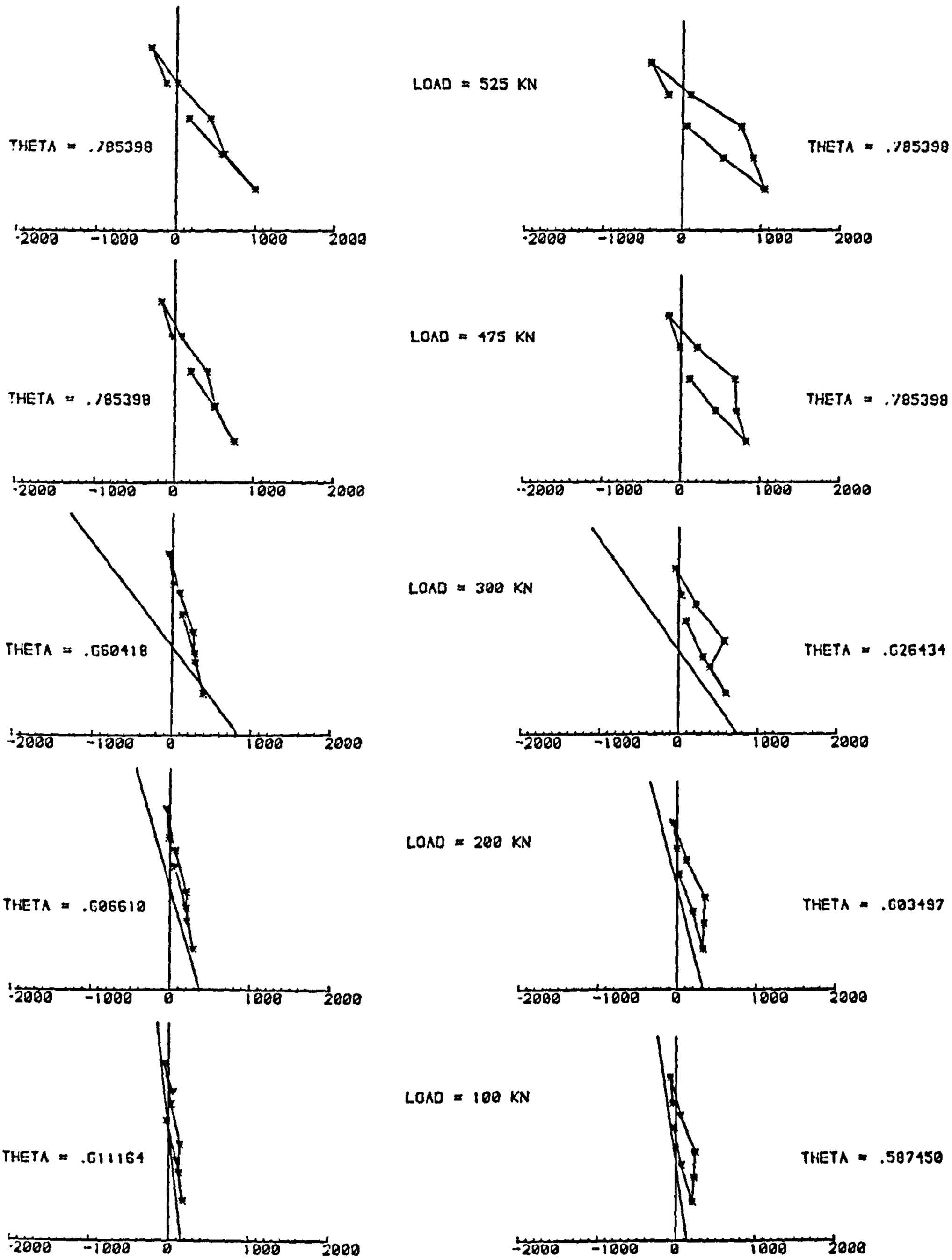

Fig. G.15 - Strain profiles across the section for column LDU0-17

* strain values shown x10

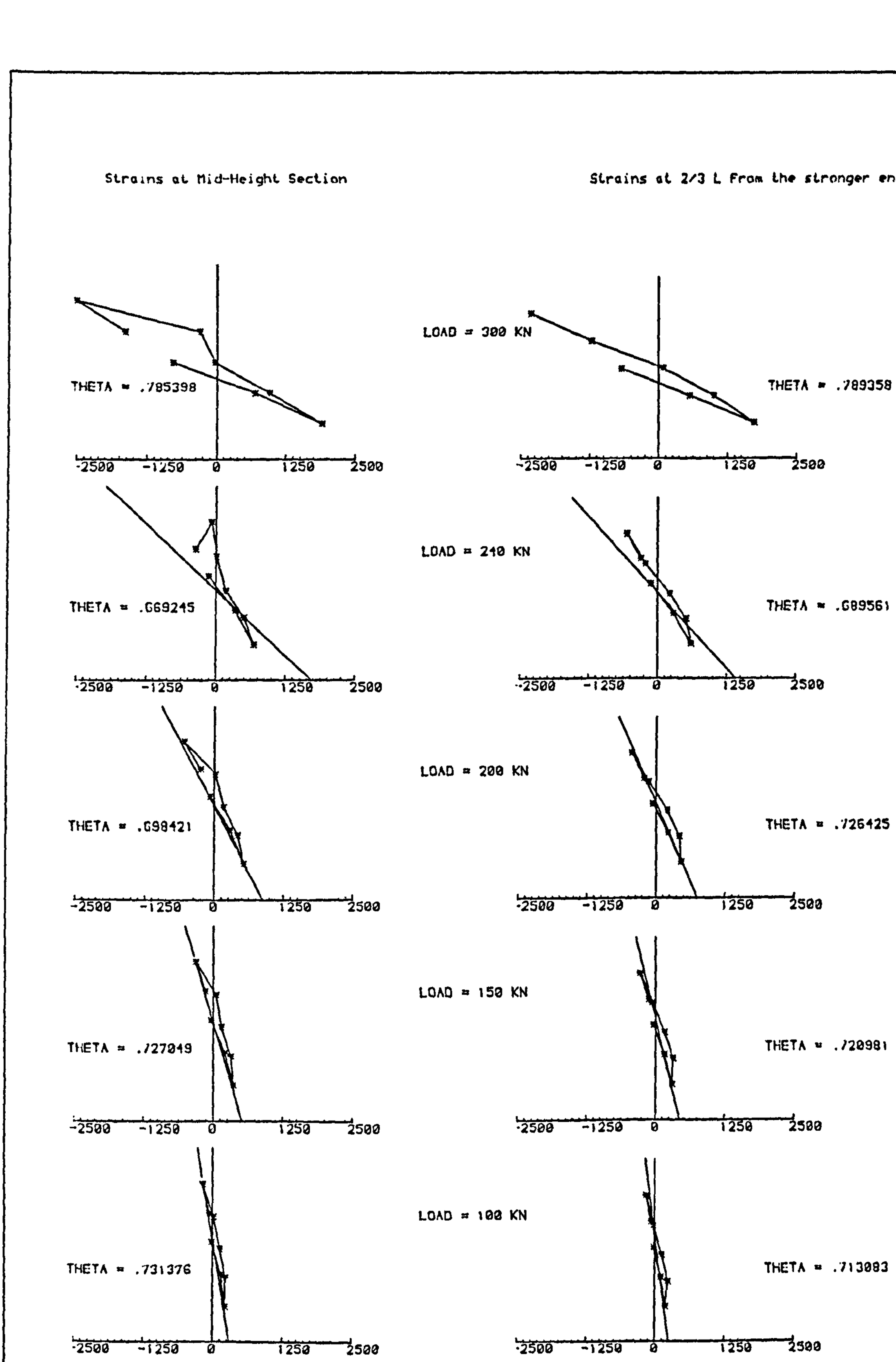

Fig. 6.16 - Strain profiles across the section for column LDUO-18

* strain values shown x10

Strains at Mid-Height Section

Strains at 1/3 L From the stronger end

Fig. C.17 - Strain profiles across the section for column LGU0-19

* strain values shown x10

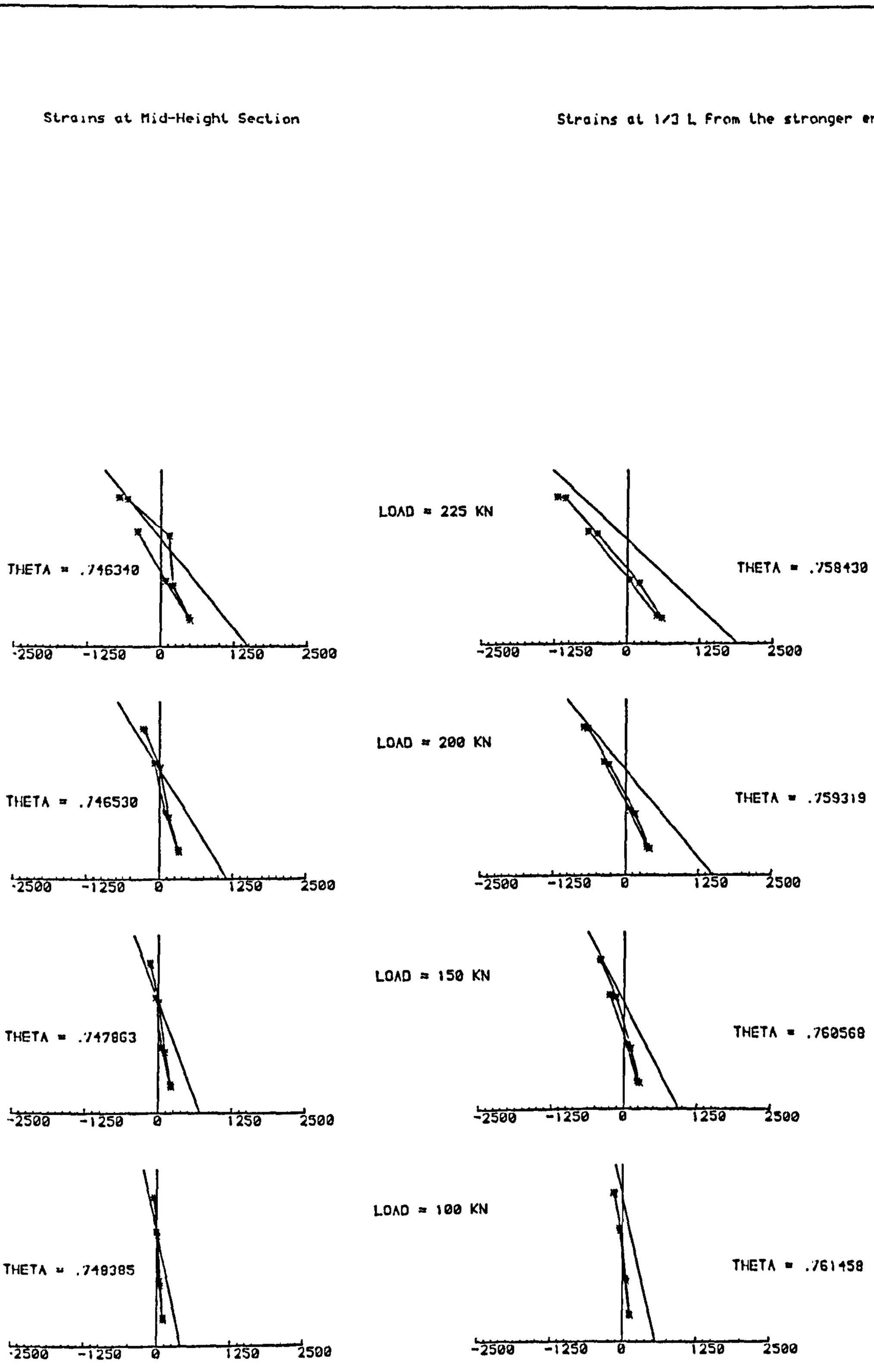

Fig. 6.18 - Strain profiles across the section for column LGUO-20

* strain values shown x10

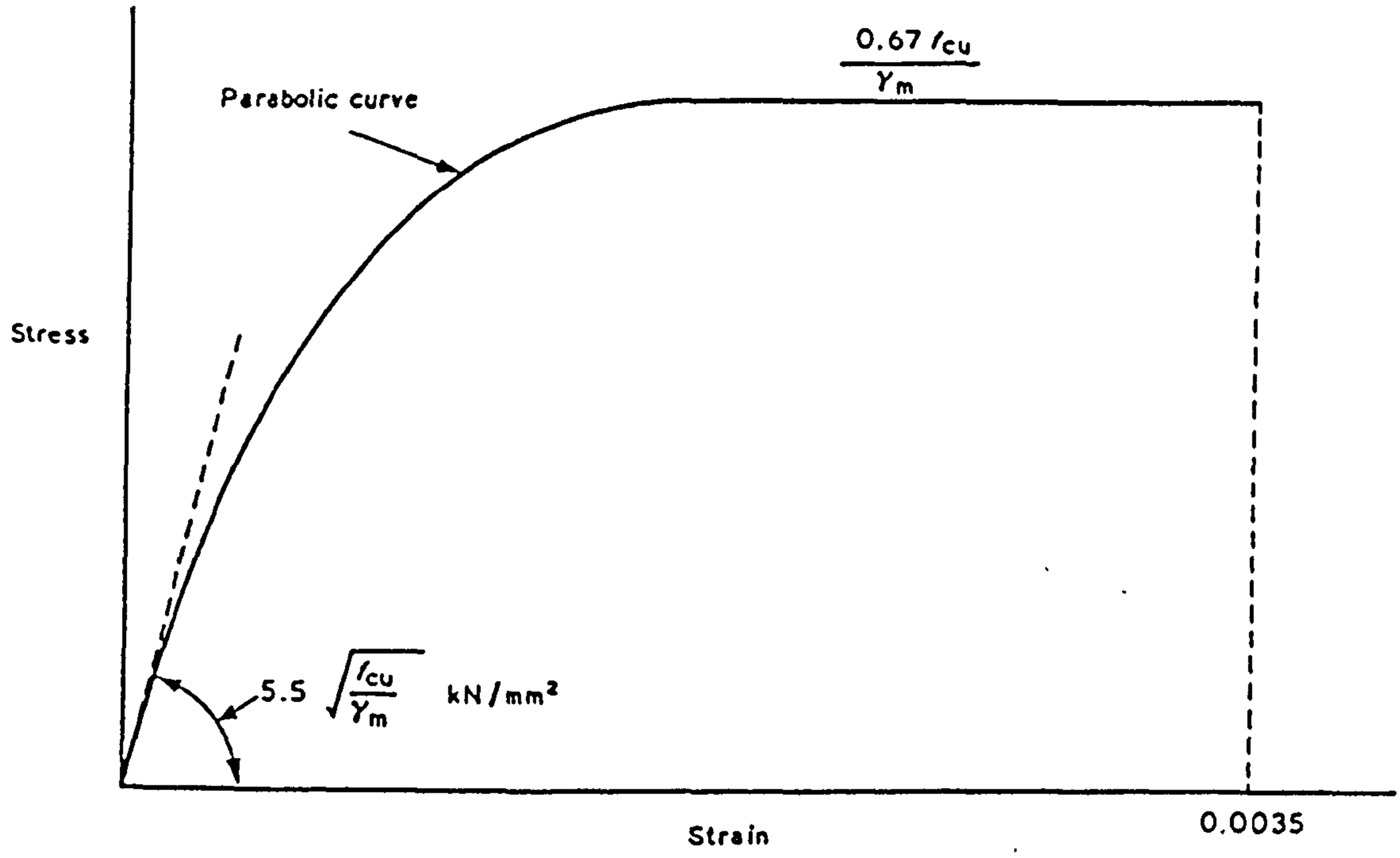

NOTE. f_{cu} in N/mm².

Fig. 7.1 - Design stress-strain curve for concrete

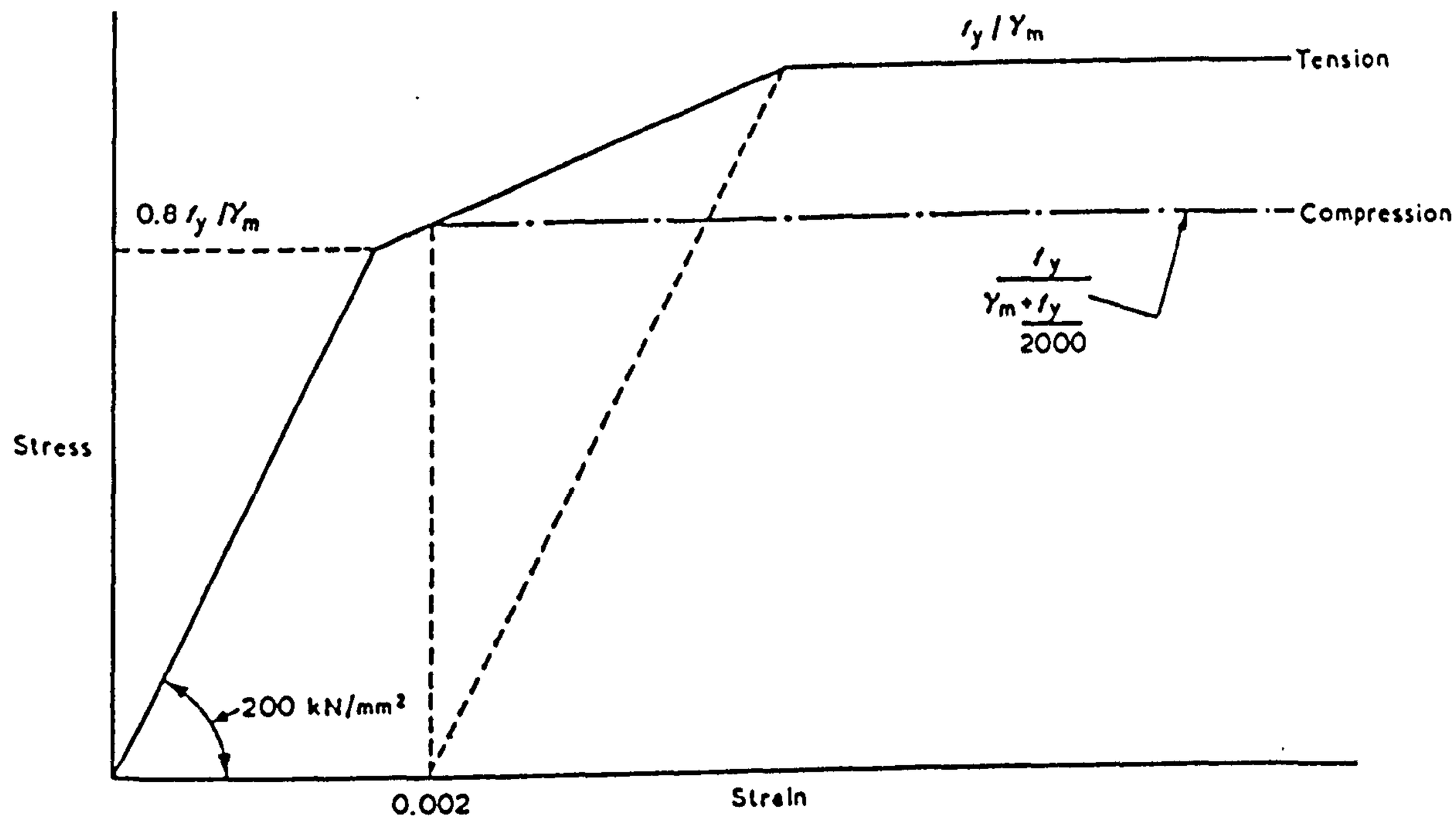

Note. f_y in N/mm².

Fig. 7.2 - Design stress strain curve for reinforcement

CROSS SECTION 100mm x 200mm

PERCENTAGE oF REINFORCEMENT = 1%

CURVE	LEVEL oF ECCENTRICITY
1	0
2	0.05h
3	0.10h
4	0.20h
5	0.40h

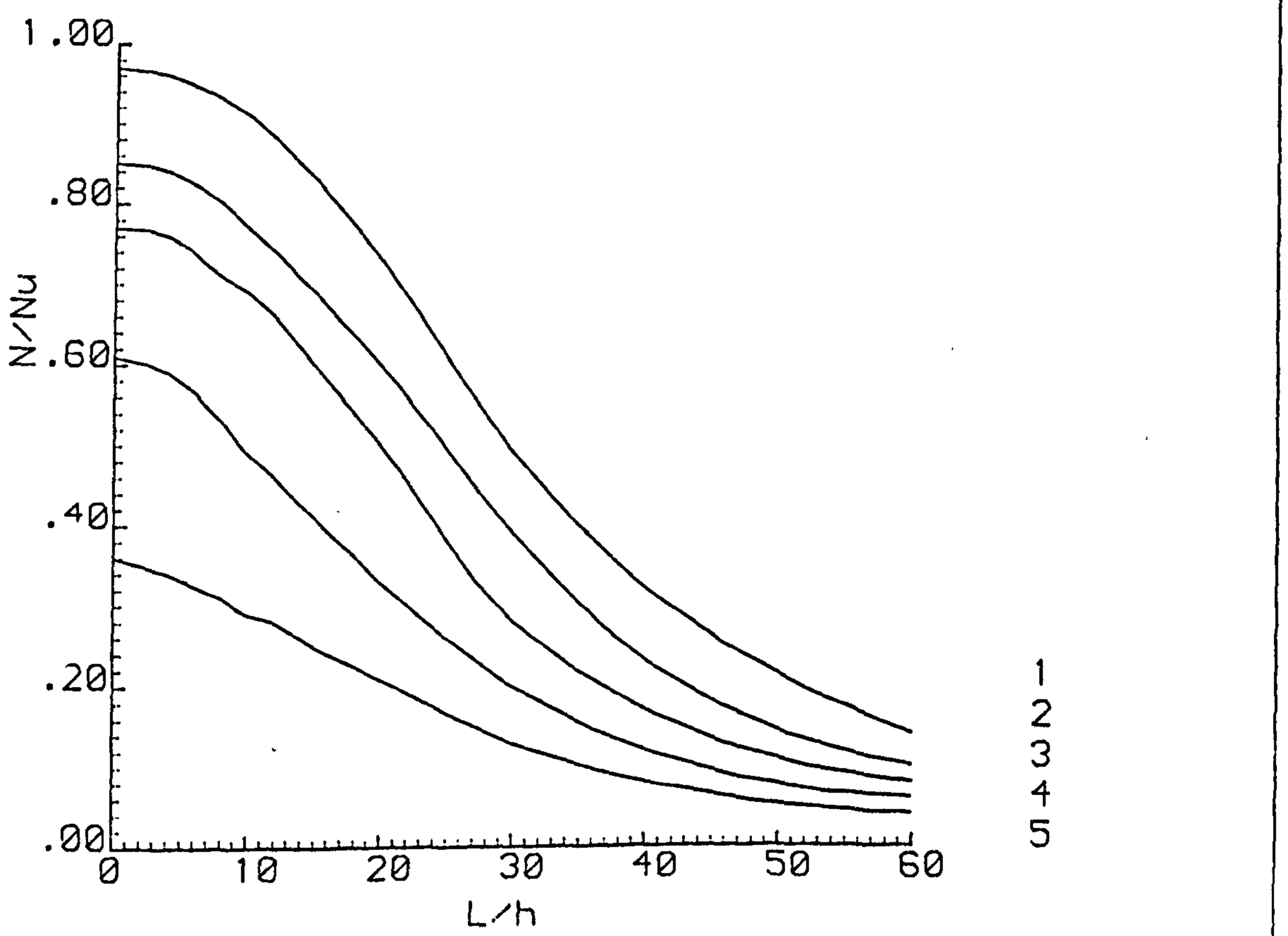

Fig. 7.3 - Variation oF nondimensional ultimate load with column slenderness For constant eccentricity

CROSS SECTION 200mm x 200mm

PERCENTAGE oF REINFORCEMENT = 1%

CURVE	LEVEL oF ECCENTRICITY
1	0
2	0.05h
3	0.10h
4	0.20h
5	0.40h

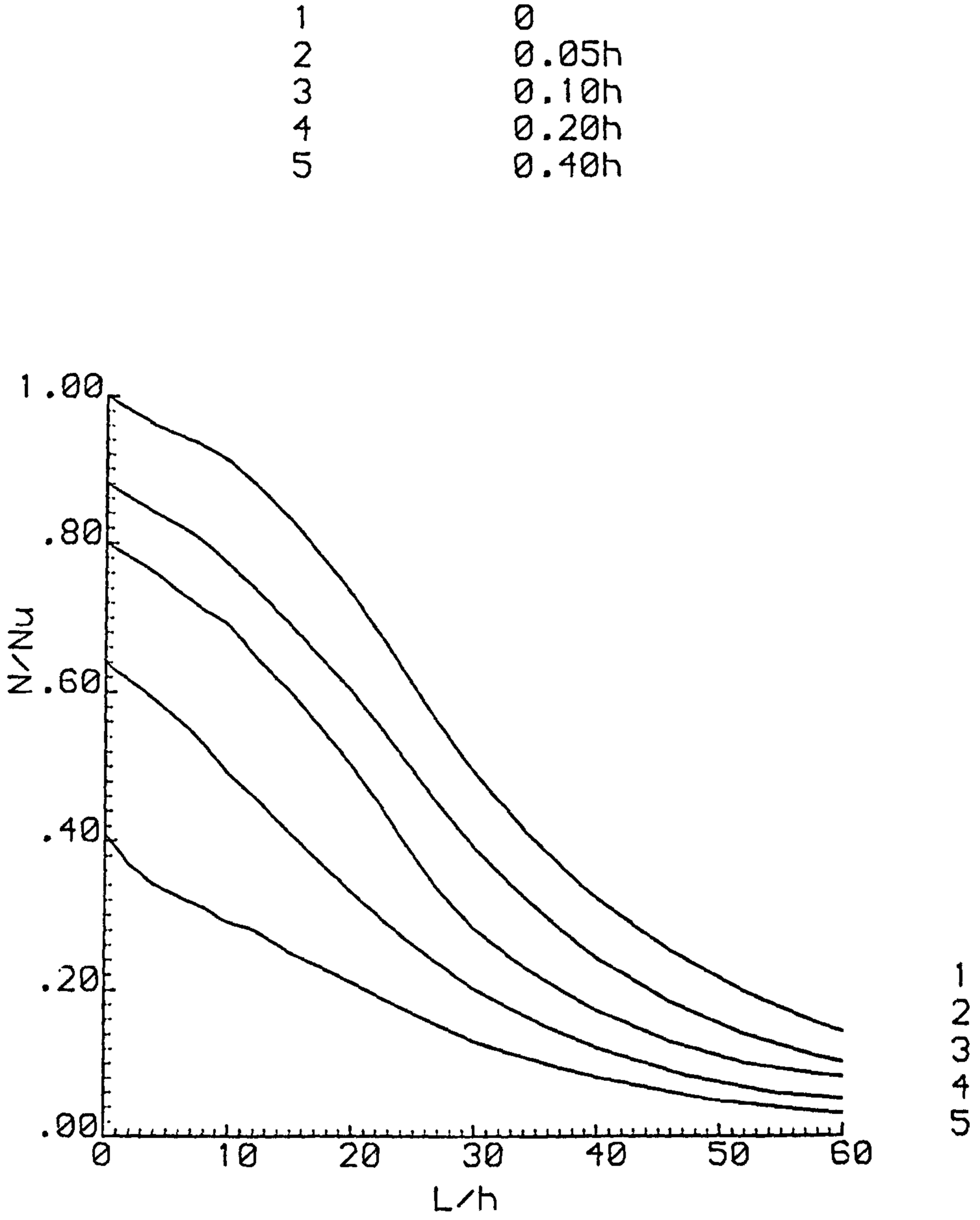

Fig. 7.4 - Variation of nondimensional ultimate load with column slenderness For constant eccentricity

CROSS SECTION 100mm x 300mm

PERCENTAGE oF REINFORCEMENT = 1%

CURVE	LEVEL oF ECCENTRICITY
1	0
2	0.05h
3	0.10h
4	0.20h
5	0.40h

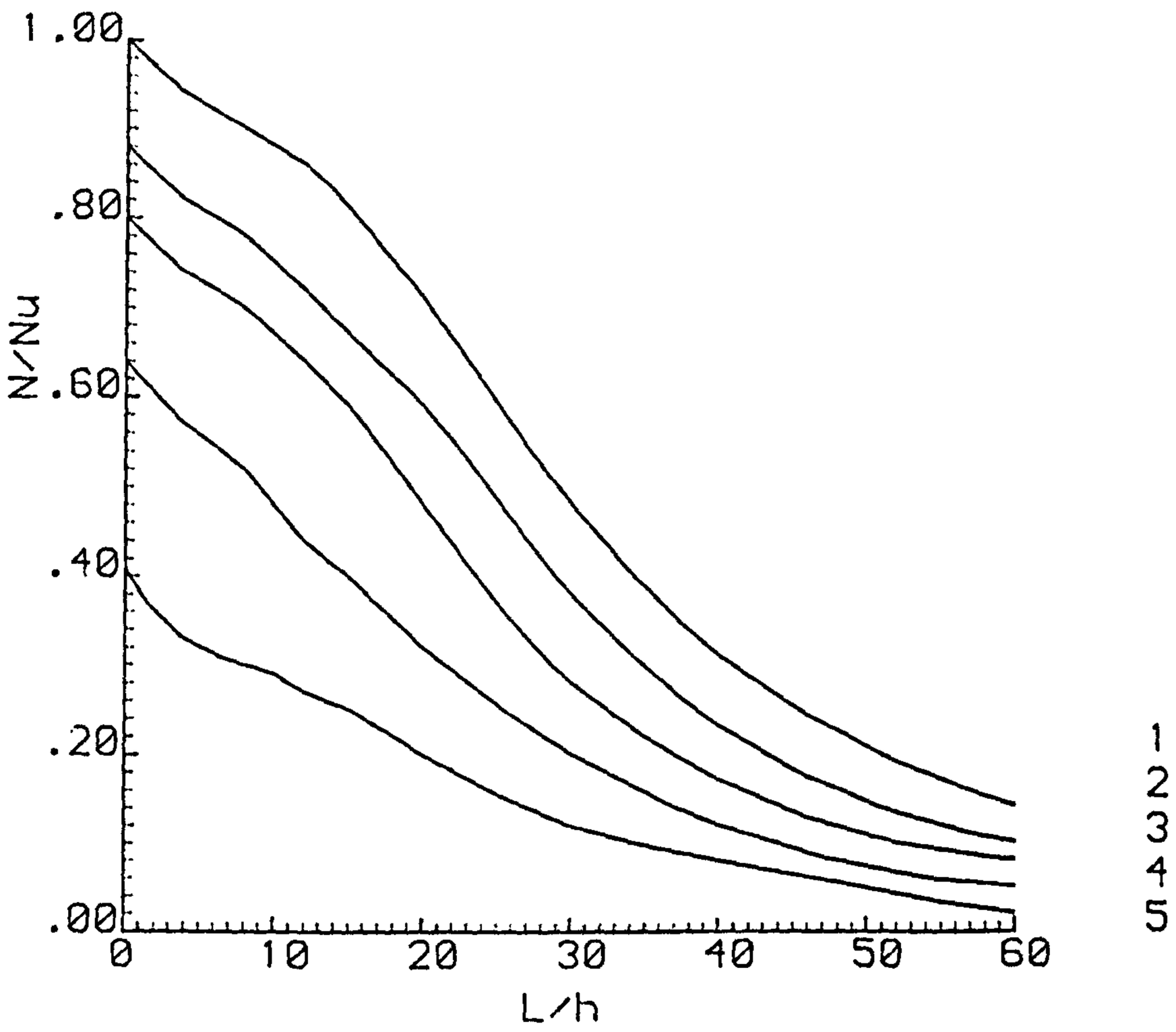

Fig. 7.5 - Variation of nondimensional ultimate load with column slenderness for constant eccentricity

CROSS SECTION 100mm x 200mm

PERCENTAGE oF REINFORCEMENT = 6%

CURVE	LEVEL oF ECCENTRICITY
1	0
2	0.05h
3	0.10h
4	0.20h
5	0.40h

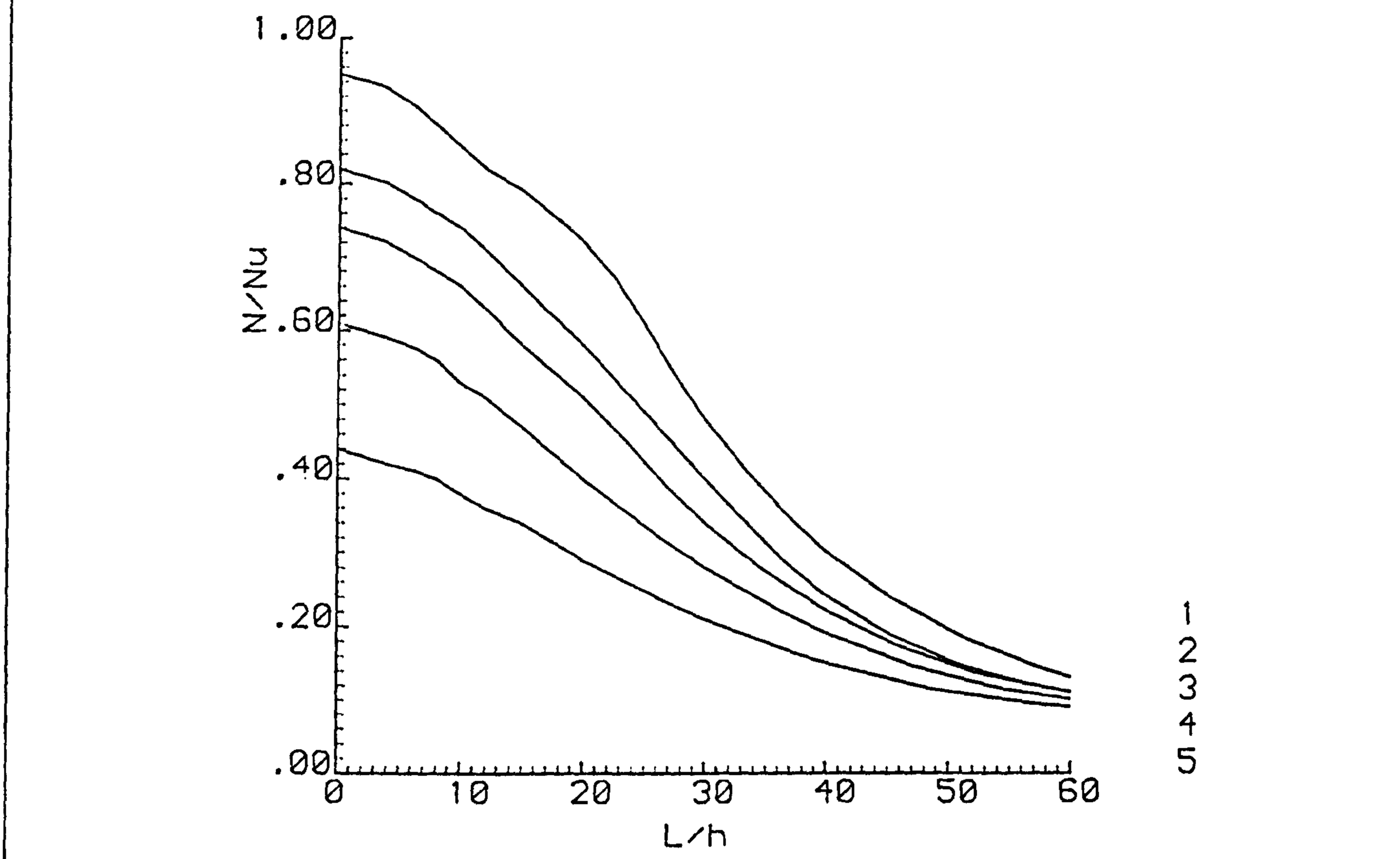

Fig. 7.6 - Variation of nondimensional ultimate load with column slenderness For constant eccentricity

CROSS SECTION 200mm x 200mm

PERCENTAGE oF REINFORCEMENT = 6%

CURVE	LEVEL oF ECCENTRICITY
1	0
2	0.05h
3	0.10h
4	0.20h
5	0.40h

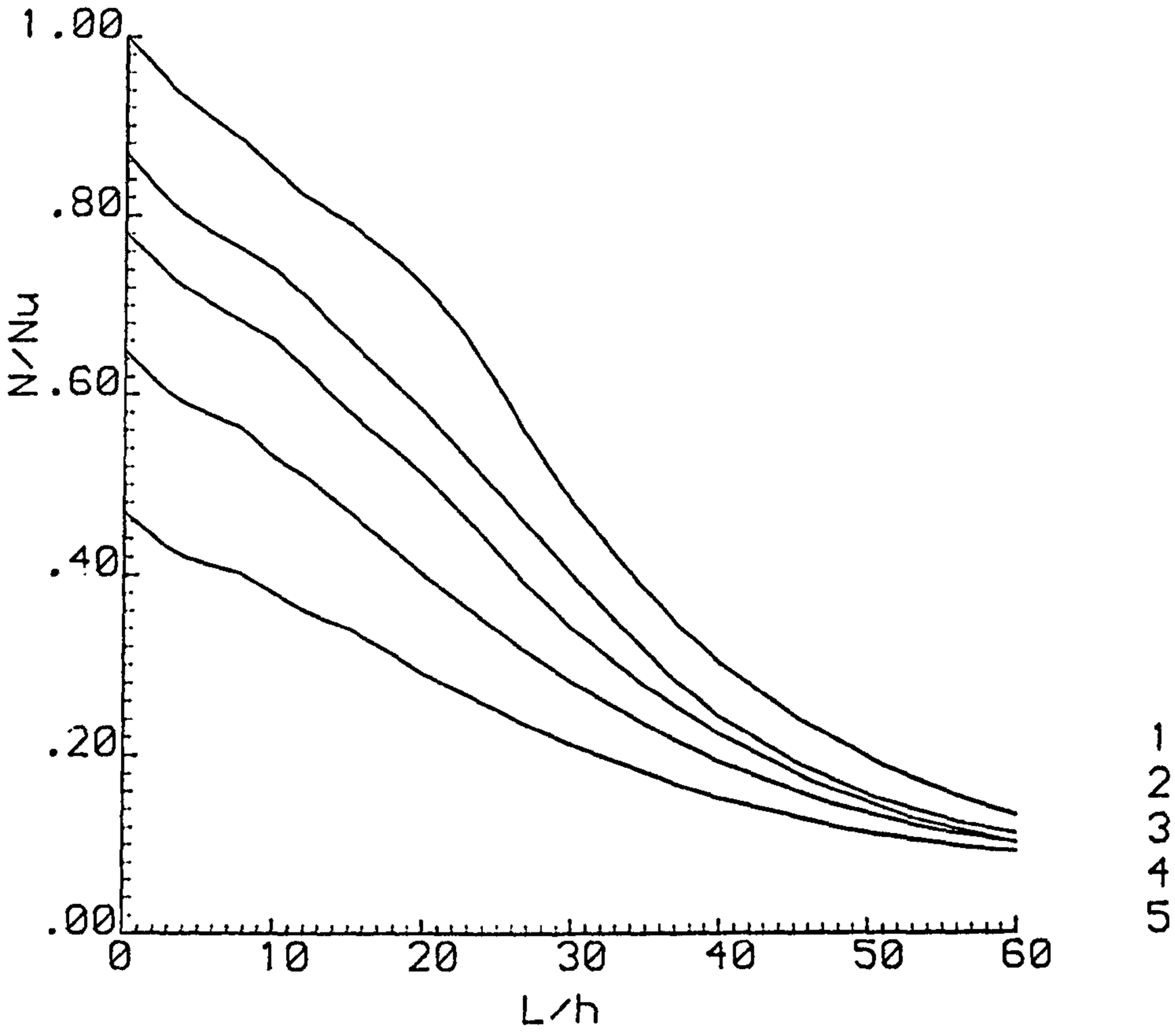

Fig. 7.7 - Variation of nondimensional ultimate load with column slenderness For constant eccentricity

CROSS SECTION 100mm x 300mm

PERCENTAGE oF REINFORCEMENT = 6%

CURVE	LEVEL oF ECCENTRICITY
1	0
2	0.05h
3	0.10h
4	0.20h
5	0.40h

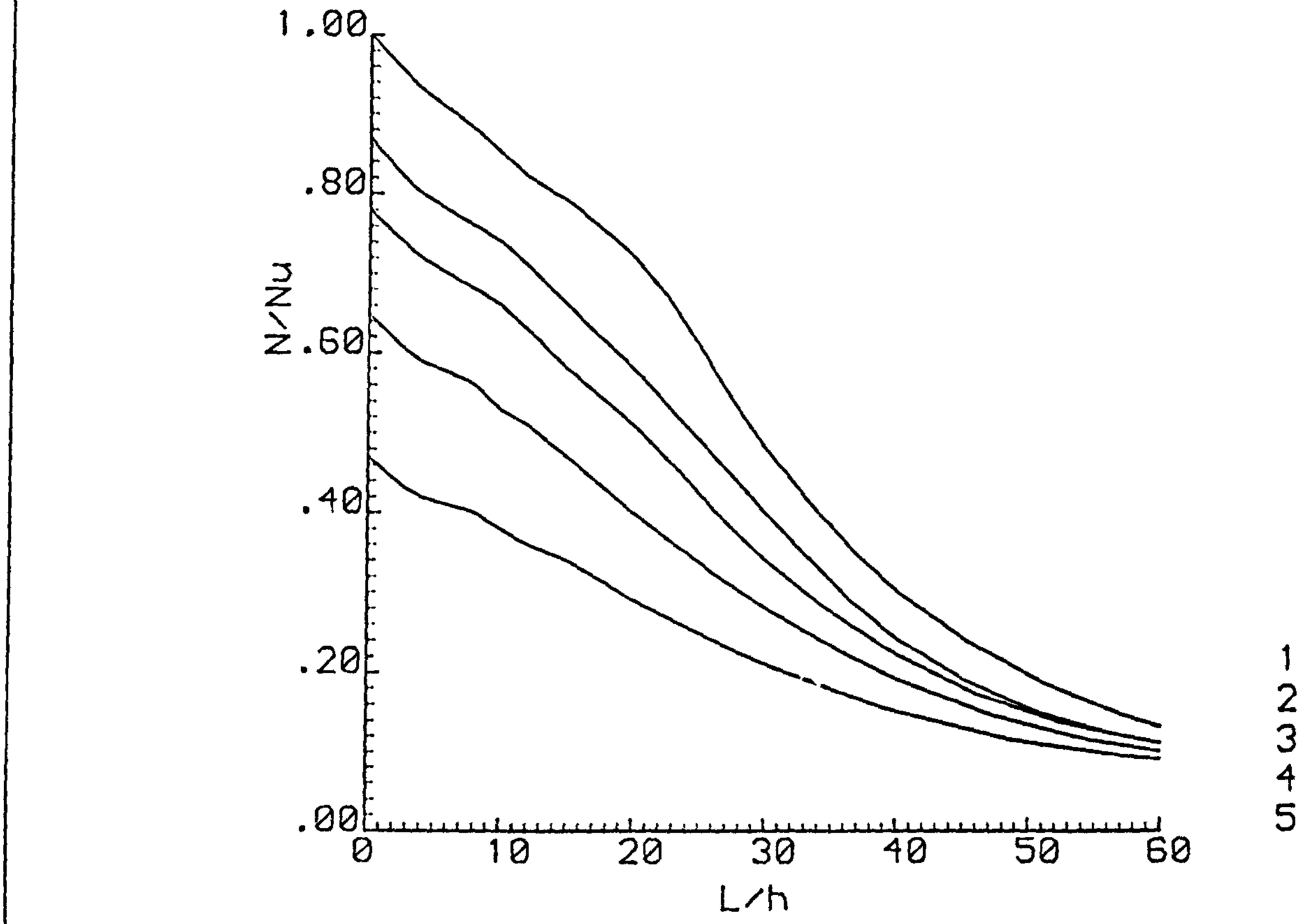

Fig. 7.8 - Variation of nondimensional ultimate load with column slenderness For constant eccentricity

ANGLE oF TAPER = 1:120

PERCENTAGE oF REINFORCEMENT = 2%

SYMBOL	MIDHEIGHT SECTION
*	400mm x 400mm
×	300mm x 300mm
+	250mm x 250mm

SET oF CURVES	LEVEL oF ECCENTRICITY
1	0.10h
2	0.20h
3	0.40h

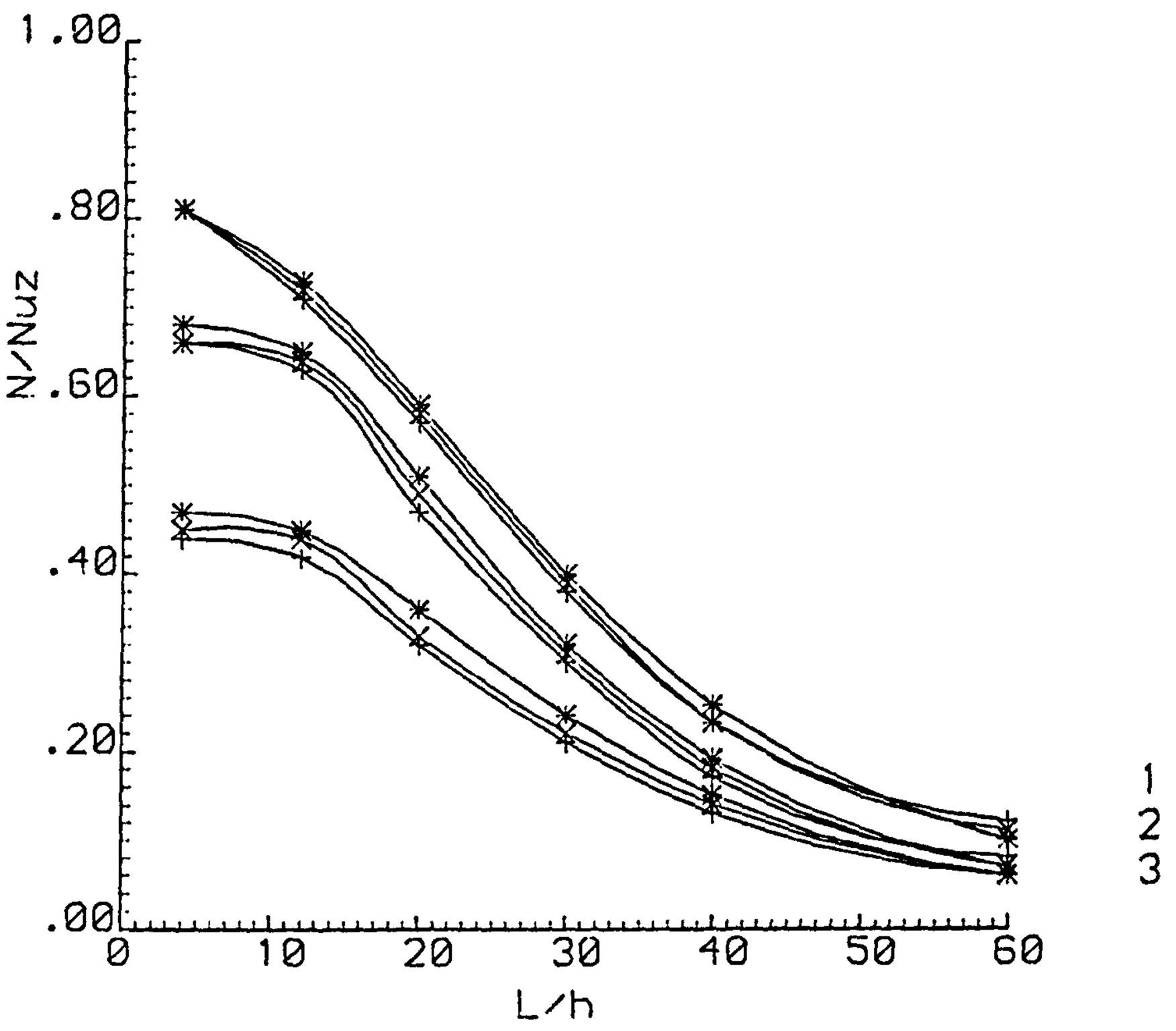

Fig. 7.9 - Variation of nondimensional ultimate load with column slenderness For constant eccentricity

ANGLE oF TAPER = 1:100

PERCENTAGE oF REINFORCEMENT = 2%

SYMBOL	MIDHEIGHT SECTION
*	400mm x 400mm
x	300mm x 300mm
+	250mm x 250mm

SET oF CURVES	LEVEL oF ECCENTRICITY Y
1	0.10h
2	0.20h
3	0.40h

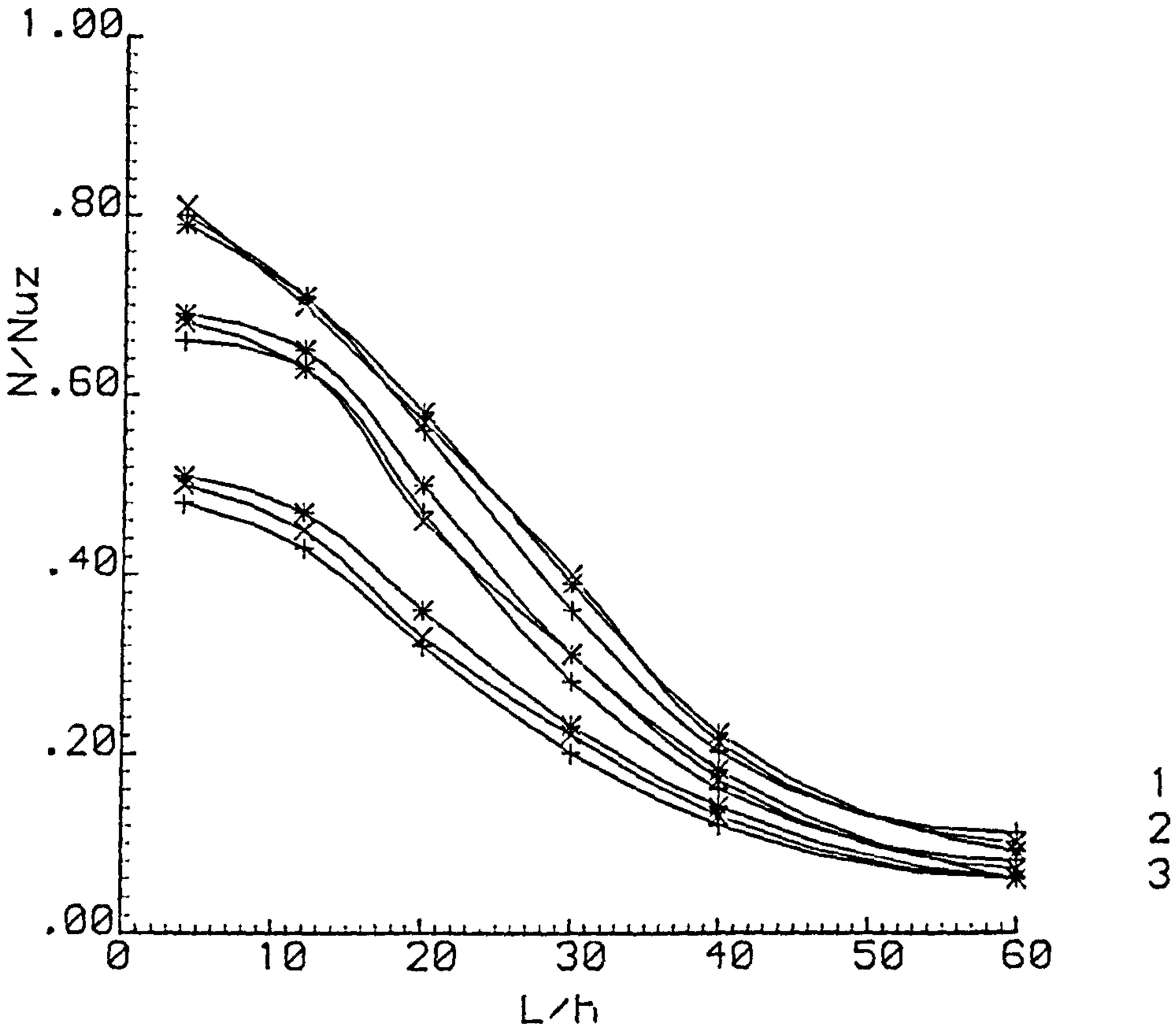

Fig. 7.10 - Variation of nondimensional ultimate load with column slenderness For constant eccentricity

ANGLE oF TAPER = 1:80

PERCENTAGE oF REINFORCEMENT = 2%

SYMBOL	MIDHEIGHT SECTION
*	400mm x 400mm
x	300mm x 300mm
+	250mm x 250mm

SET oF CURVES	LEVEL oF ECCENTRICITY
1	0.10h
2	0.20h
3	0.40h

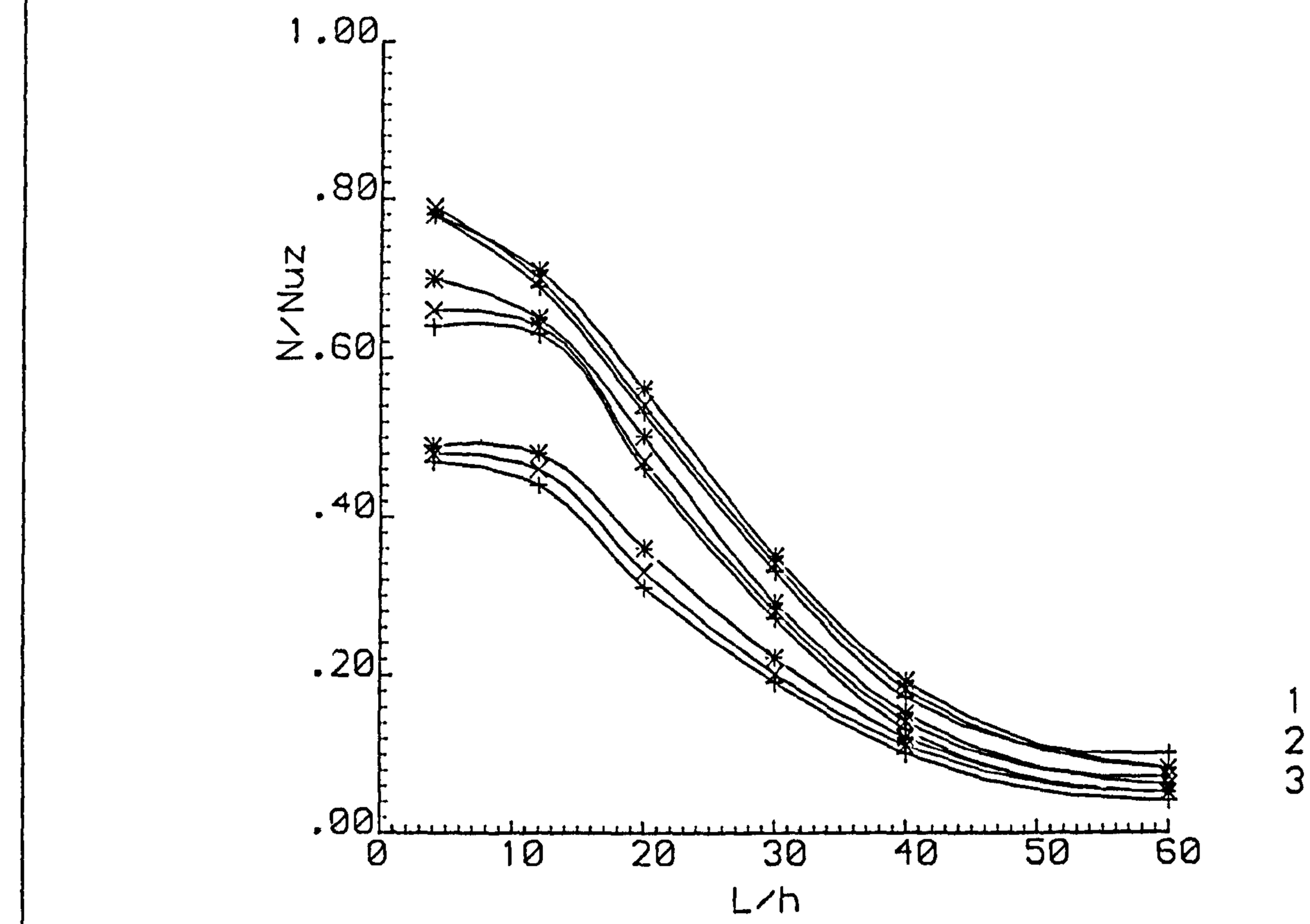

Fig. 7.11 - Variation of nondimensional ultimate load with column slenderness For constant eccentricity

FAMILY of CURVES for UNIFORM COLUMNS

PERCENTAGE of REINFORCEMENT = 1%

CURVE	LEVEL of ECCENTRICITY
1	0
2	0.05h
3	0.10h
4	0.20h
5	0.40h

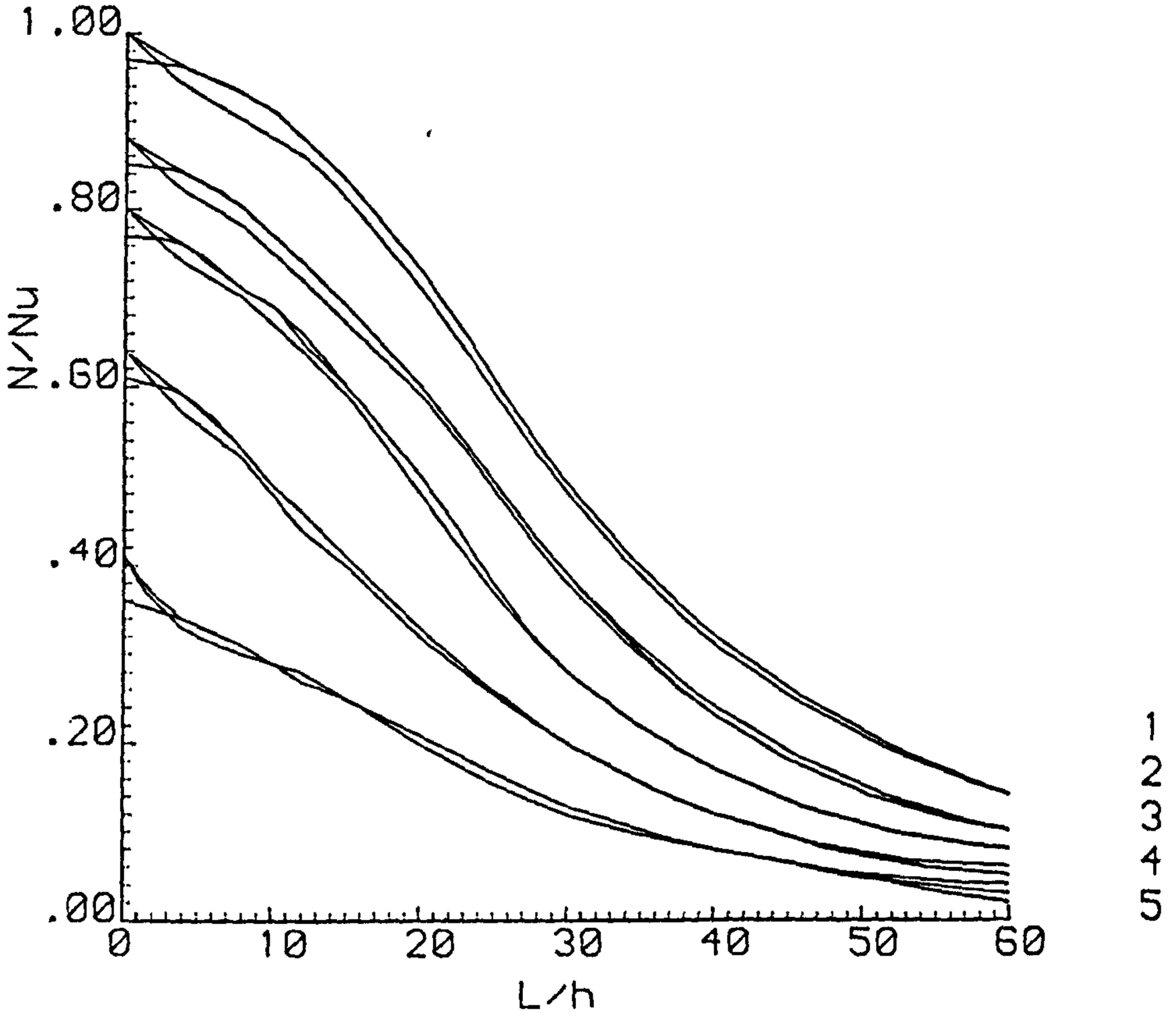

Fig. 7.12 - Family of curves for the variation of nondimensional ultimate load with column slenderness for constant eccentricity

FAMILY of CURVES for UNIFORM COLUMNS

PERCENTAGE of REINFORCEMENT = 6%

CURVE	LEVEL of ECCENTRICITY
1	0
2	0.05h
3	0.10h
4	0.20h
5	0.40h

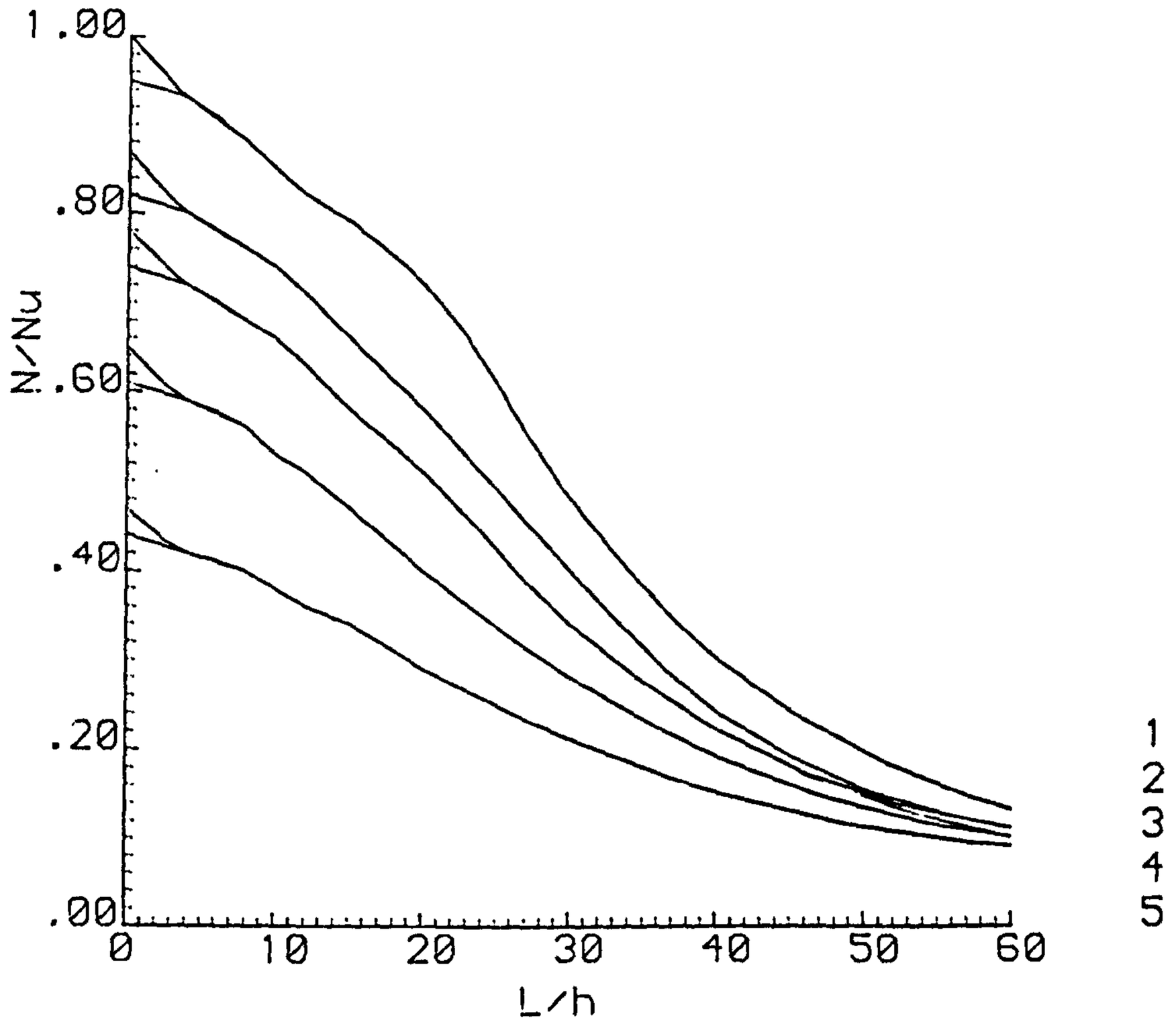

Fig. 7.13 - Family of curves for the variation of nondimensional ultimate load with column slenderness for constant eccentricity

ANGLE of TAPER = 1:120&1:100&1:80

PERCENTAGE of REINFORCEMENT = 2%

SYMBOL	MIDHEIGHT SECTION
*	400mm x 400mm
O	300mm x 300mm
+	250mm x 250mm

SET of CURVES	LEVEL of ECCENTRICITY
1	0.10h
2	0.20h
3	0.40h

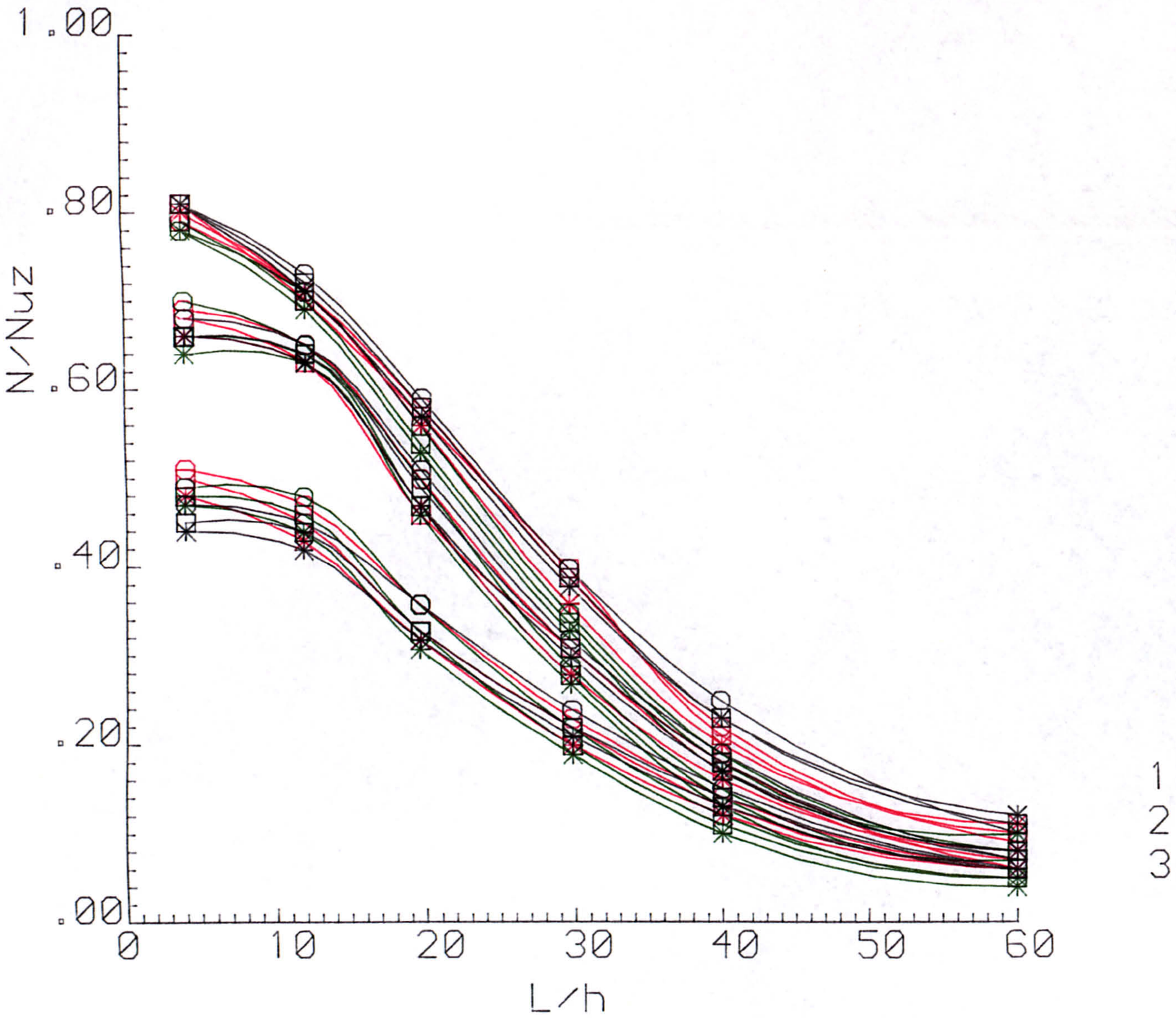

Fig. 7.14 - Family of curves for the variation of nondimensional ultimate load with column slenderness for constant eccentricity

SUPERIMPOSITION of UNIFORM COLUMNS

PERCENTAGE of REINFORCEMENT = 1%

SET of CURVES	N/Nuz
1	0.20
2	0.30
3	0.40
4	0.50
5	0.60
6	0.70

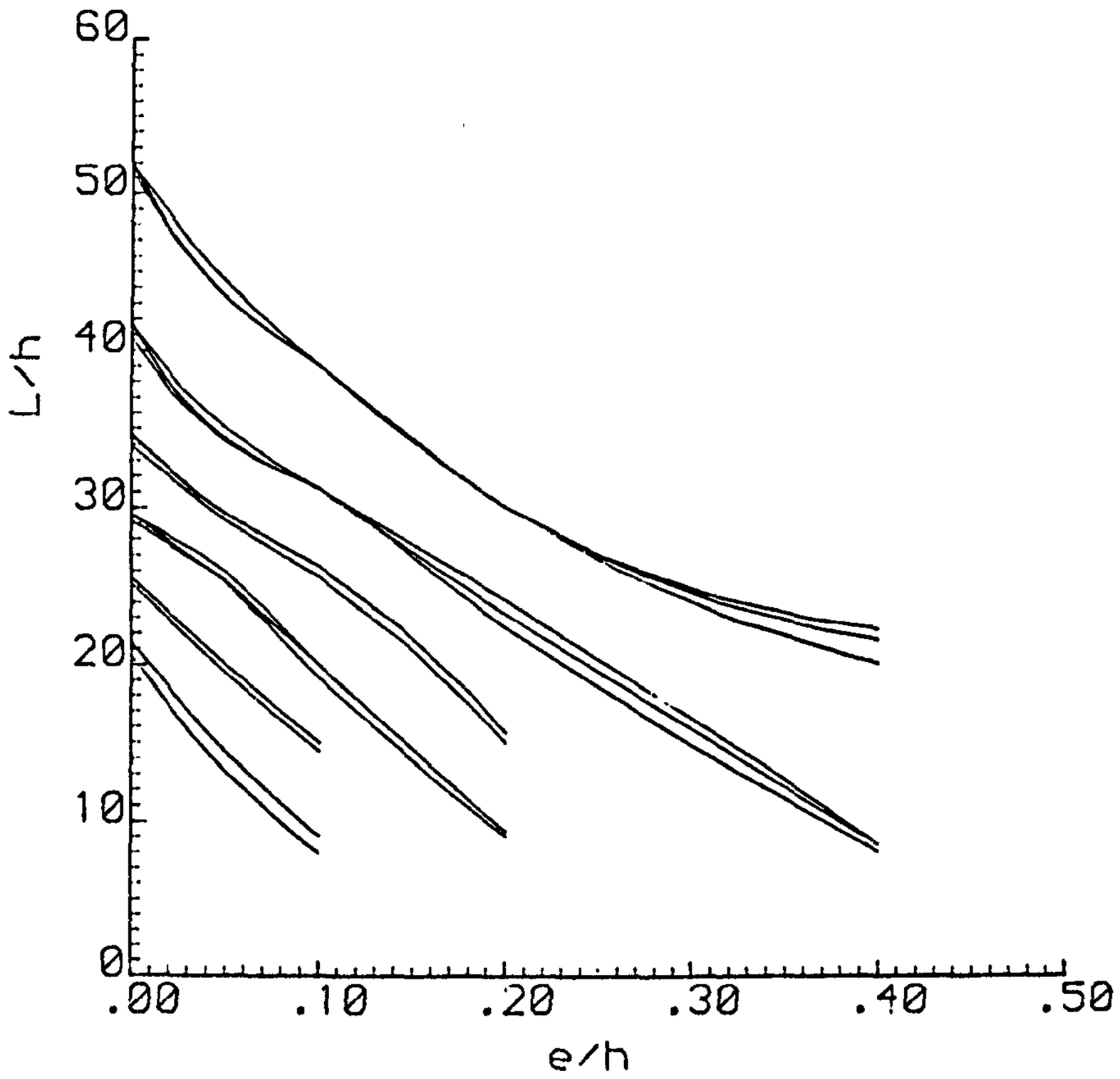

Fig. 7.15 - Variation of nondimensional eccentricity of loading with column slenderness for constant ultimate load

SUPERIMPOSITION oF UNIFORM COLUMNS

PERCENTAGE oF REINFORCEMENT = 6%

SET oF CURVES	N/Nuz
1	0.20
2	0.30
3	0.40
4	0.50
5	0.60
6	0.70

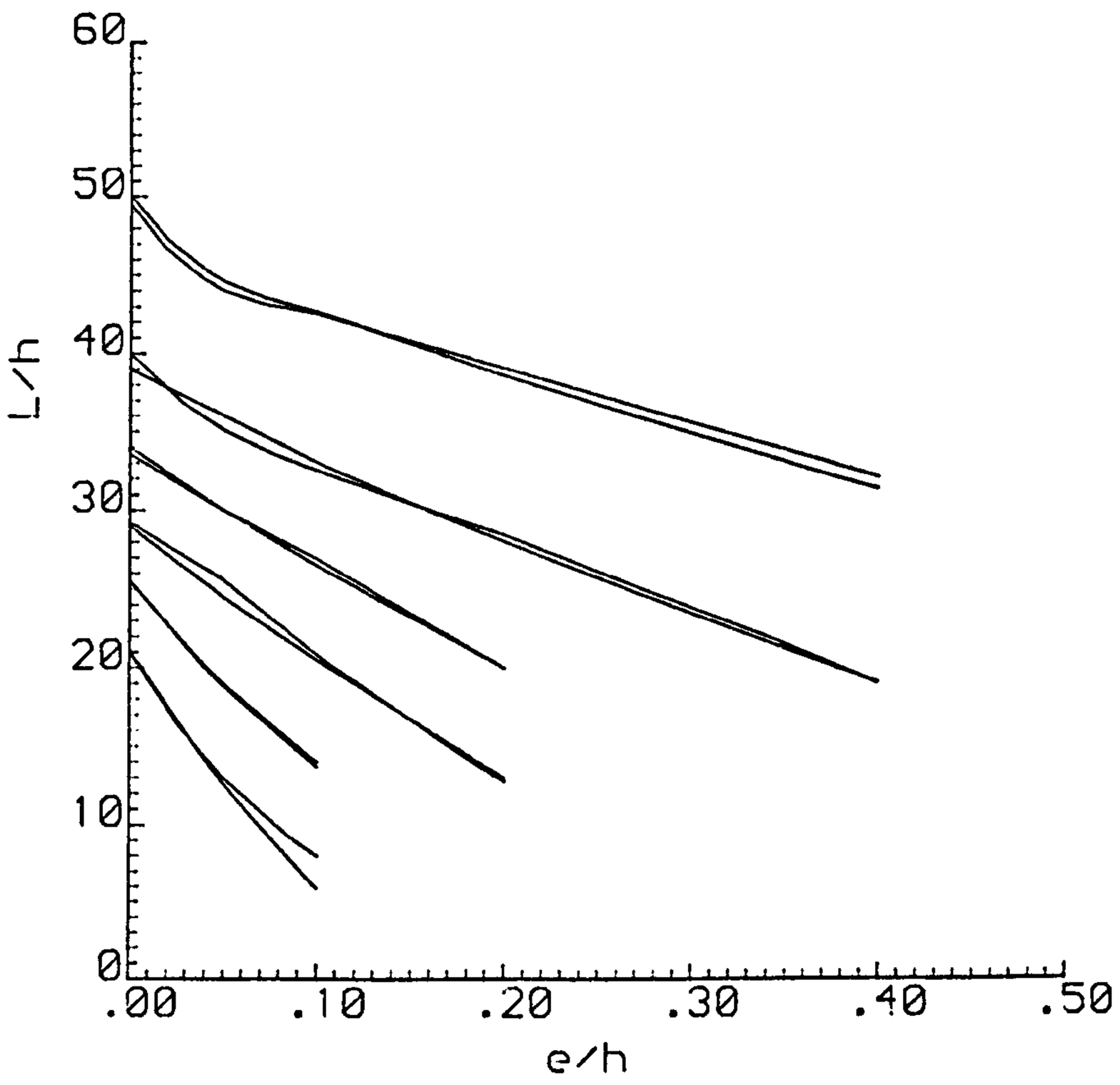

Fig. 7.16 - Variation of nondimensional eccentricity of loading with column slenderness For constant ultimate load

TAPERED COLUMNS

PERCENTAGE oF REINFORCEMENT = 2%

SET oF CURVES	N/Nuz
1	0.20
2	0.30
3	0.40
4	0.50
5	0.60

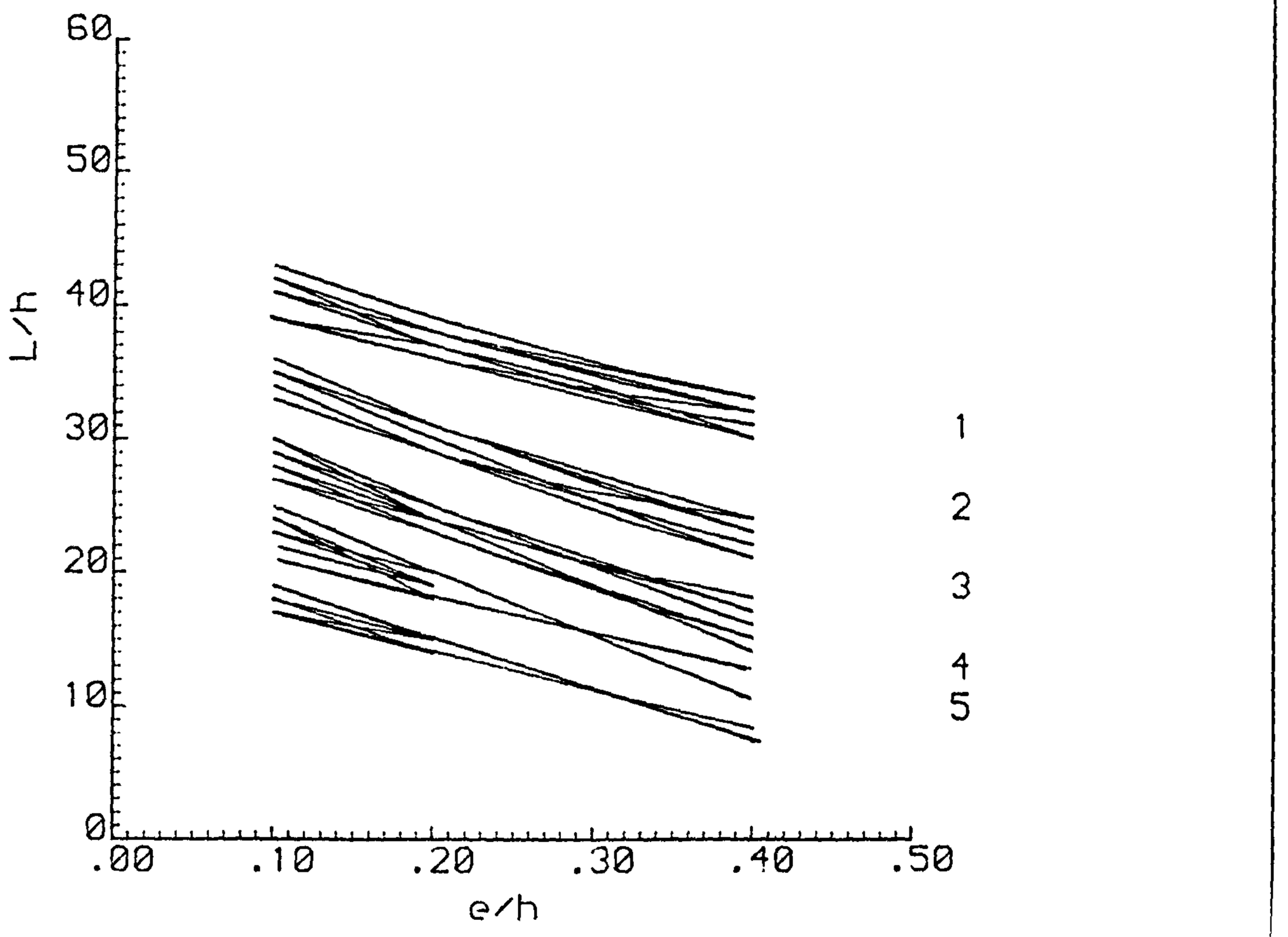

Fig. 7.17 - Variation of nondimensional eccentricity of loading with column slenderness For constant ultimate load

PERCENTAGE oF REINFORCEMENT = 1%

CURVES	N/Nuz
1	0.20
2	0.30
3	0.40
4	0.50
5	0.60
6	0.70

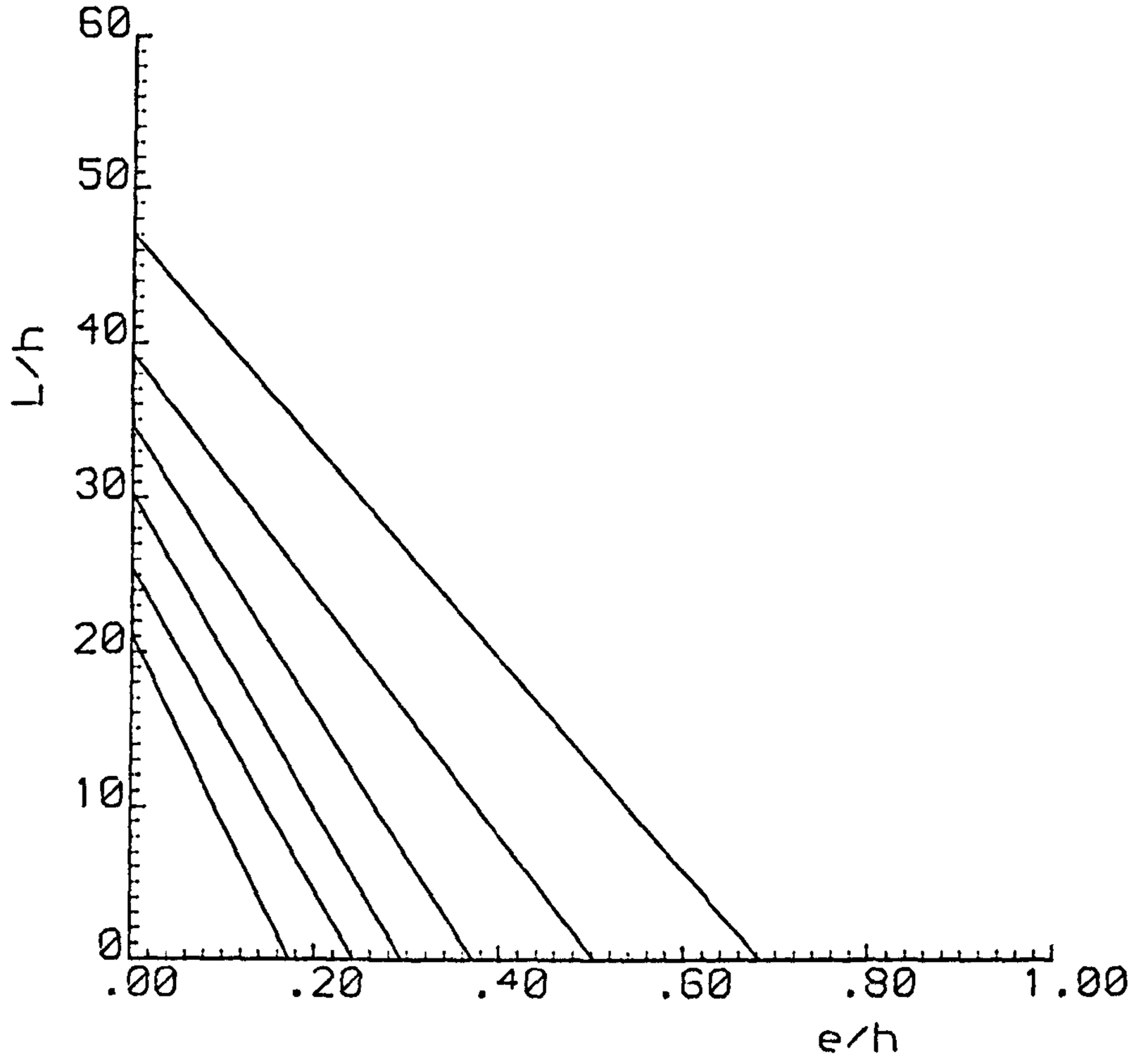

Fig. 7.18 - Lower bound curves for uniform columns

PERCENTAGE oF REINFORCEMENT = 6%

CURVES	N/Nuz
1	0.20
2	0.30
3	0.40
4	0.50
5	0.60
6	0.70

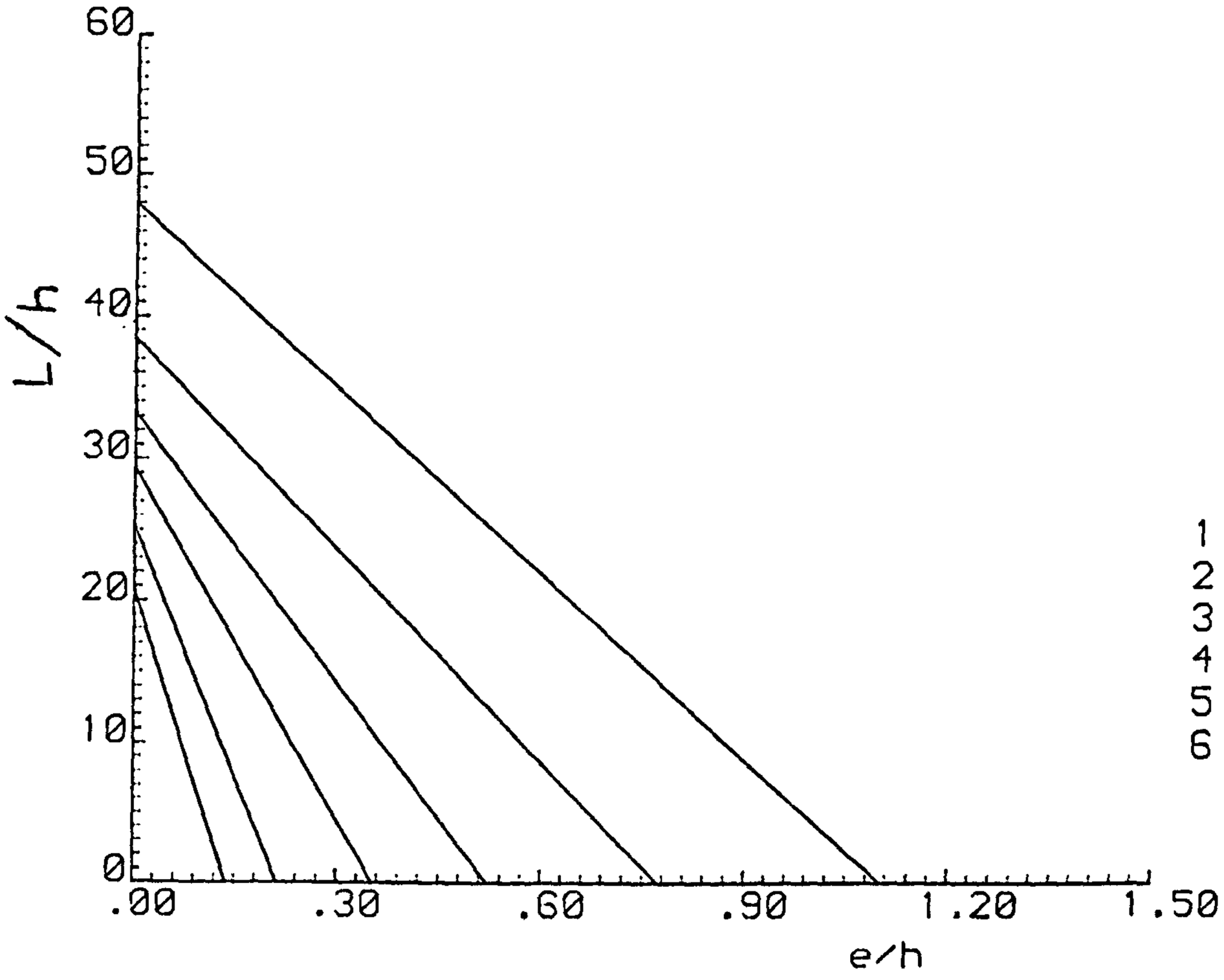

Fig. 7.19 - Lower bound curves for uniform columns

PERCENTAGE oF REINFORCEMENT = 2%

CURVES	N/Nuz
1	0.20
2	0.30
3	0.40
4	0.50
5	0.60

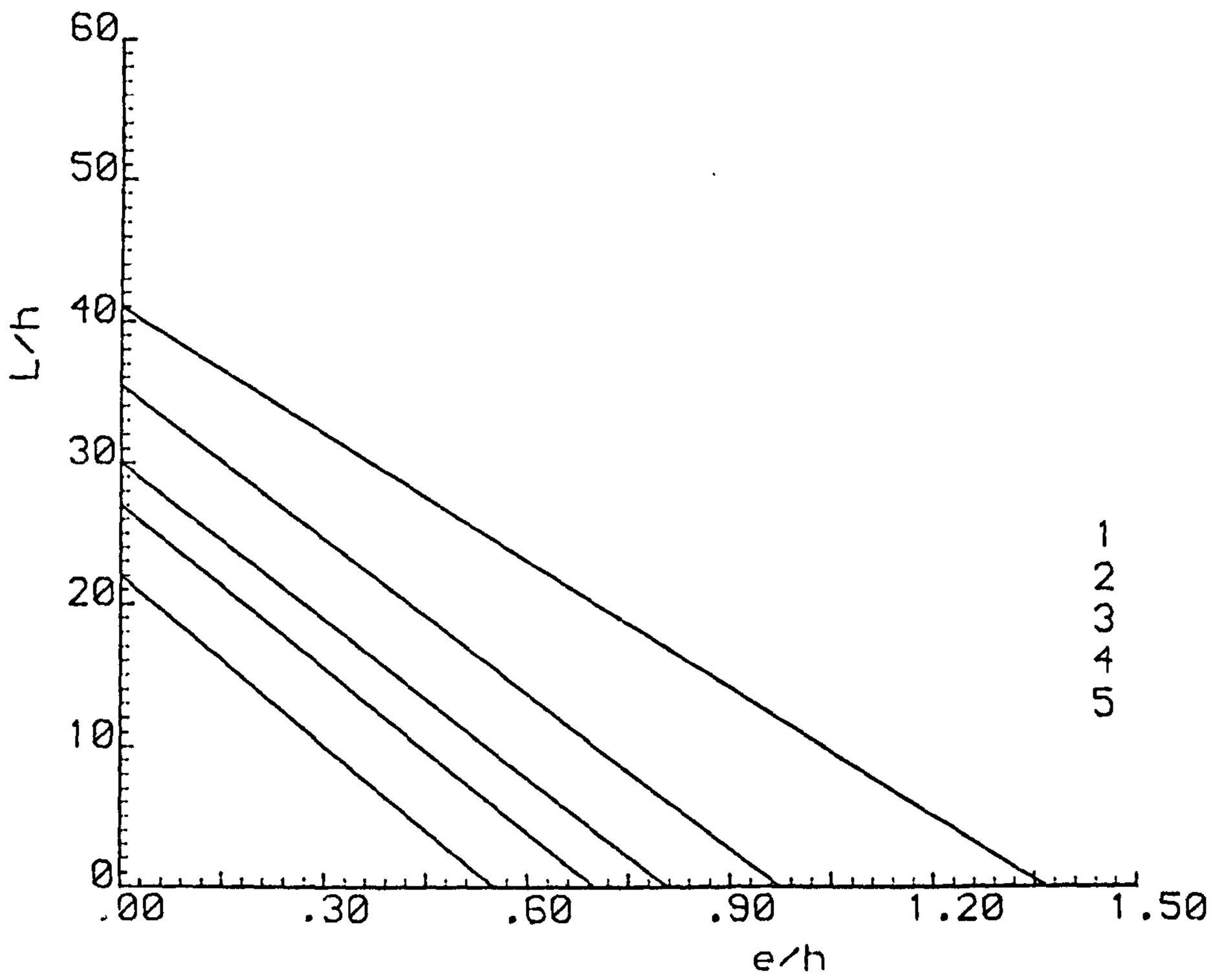

Fig. 7.20 - Lower bound curves for tapered columns

CROSS SECTION 100mm x 200mm

PERCENTAGE oF REINFORCEMENT = 1%

Fcu = 20 N/mm^2

CURVE	LEVEL oF ECCENTRICITY
1	0
2	0.05h
3	0.10h
4	0.20h
5	0.40h

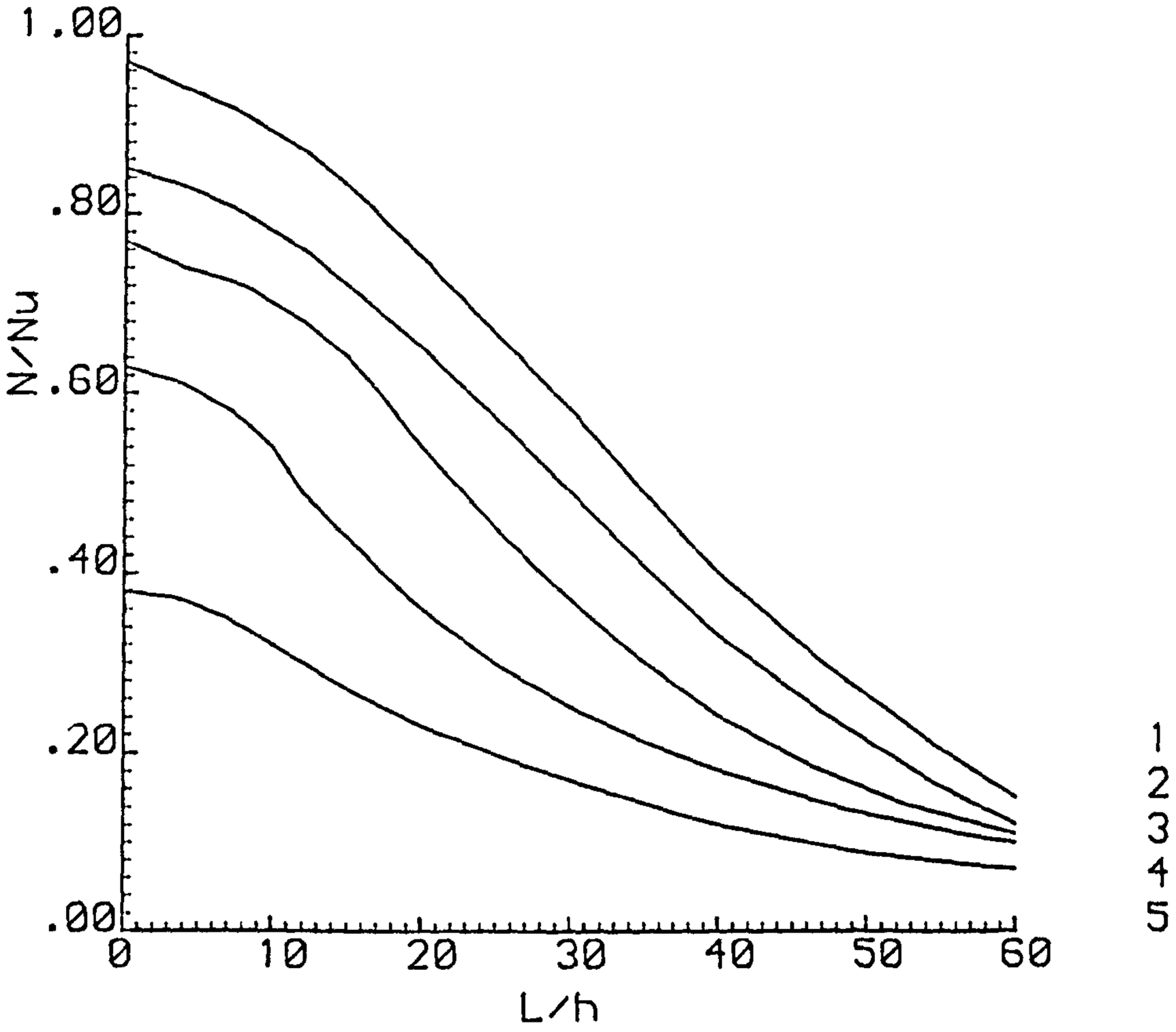

Fig. 7.21 - Variation of nondimensional ultimate load with column slenderness For constant eccentricity

CROSS SECTION 100mm × 200mm

PERCENTAGE oF REINFORCEMENT = 1%

Fcu = 50 N/mm^2

CURVE	LEVEL oF ECCENTRICITY
1	0
2	0.05h
3	0.10h
4	0.20h
5	0.40h

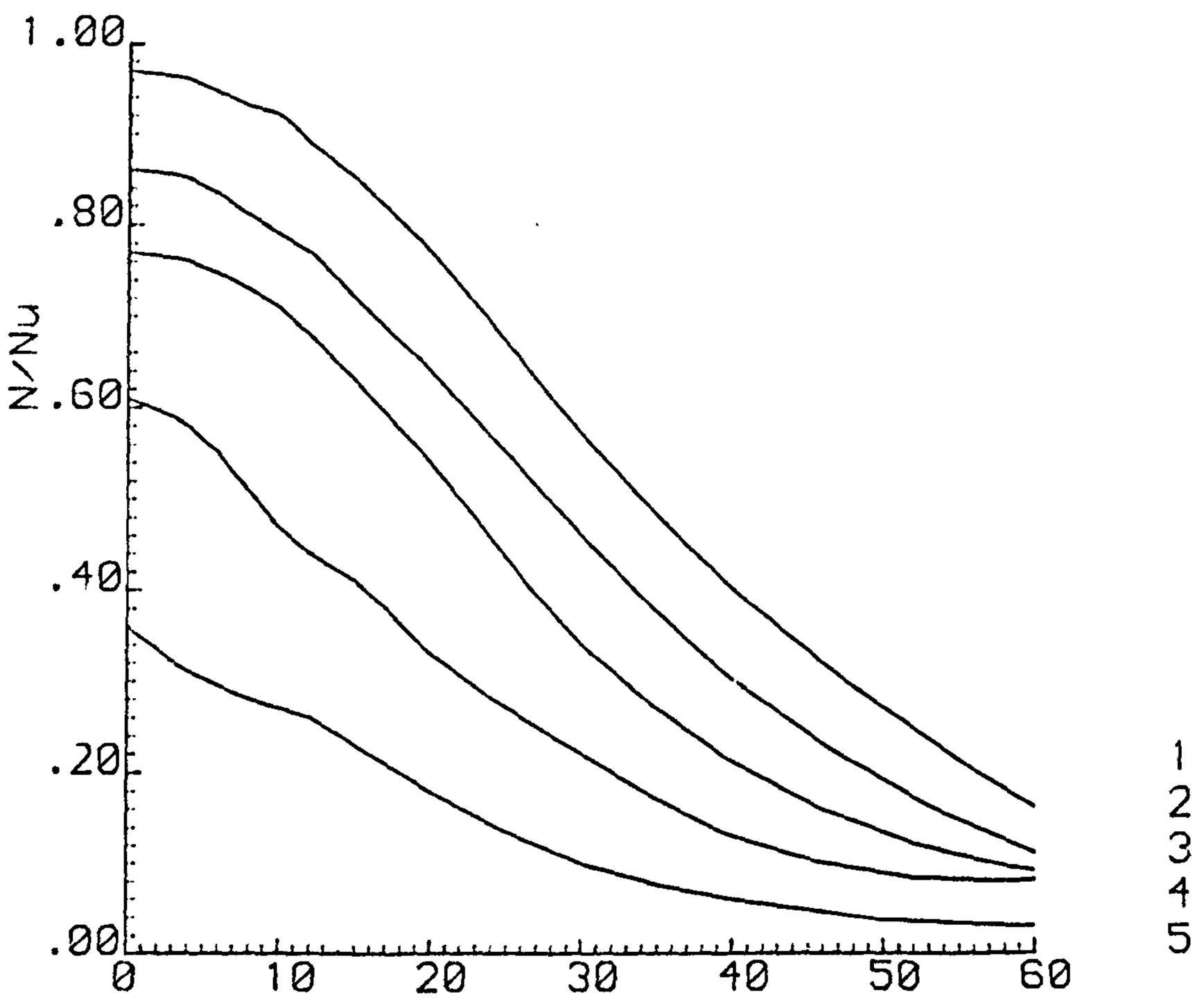

Fig. 7.22 - Variation oF nondimensional ultimate load with column slenderness For constant eccentricity

TABLE 2.1. - Details of tests reported by AAS - JAKOBSEN, A. and AAS - JAKOBSEN, K (1) and comparison between tests and calculated ultimate loads.

Test No.	b (mm)	h (mm)	dc (mm)	100ρ	$0{\cdot}67f_{cu}$ (N/mm^2)	f_y (N/mm^2)	L (mm)	e_{1x} (mm)	e_{1y} (mm)	e_{2x} (mm)	e_{2y} (mm)	$N_{u\ test}$ (kN)	$N_{u\ Calc}$ (kN)	$\frac{N_{u\ test}}{N_{u\ calc}}$
1.01	70	70	5.0	2.04	17.69	498.0	1535	169.5	0	169.5	0	9.8	7.5	1.31
1.02	"	"	"	"	17.69	498.0	"	86.0	"	86.0	"	19.6	17.1	1.15
1.03	"	"	"	"	17.69	471.0	"	42.0	"	42.0	"	39.2	29.0	1.35
1.04	"	"	"	"	17.69	471.0	"	22.5	"	22.5	"	59.0	42.2	1.40
1.05	"	"	"	"	24.46	530.0	"	182.0	"	182.0	"	9.8	8.4	1.17
1.06	"	"	"	"	24.46	530.0	"	96.5	"	96.5	"	19.6	15.9	1.23
1.07	"	"	"	"	24.46	530.0	"	54.5	"	54.5	"	40.0	27.8	1.44
1.08	"	"	"	"	24.46	530.0	"	36.5	"	36.5	"	56.0	37.7	1.49
1.09	"	"	"	"	18.49	431.0	"	161.0	"	161.0	"	9.8	7.9	1.24
1.10	"	"	"	"	"	412.0	"	75.0	"	75.0	"	19.6	16.7	1.17
1.11	"	"	"	"	"	412.0	"	38.5	"	38.5	"	39.2	29.7	1.32
1.12	"	"	"	"	"	500.0	"	91.0	"	91.0	"	19.6	16.0	1.23
1.13	"	"	"	3.20	"	461.0	"	224.0	"	224.0	"	9.8	8.3	1.18
1.14	"	"	"	1.63	"	461.0	"	224.0	"	224.0	"	10.3	8.4	1.23
1.15	"	"	"	0.92	"	461.0	"	114.0	"	114.0	"	20.3	15.4	1.32
1.16	"	"	"	3.20	"	461.0	"	64.5	"	64.5	"	37.0	28.8	1.28
2.01	"	"	"	2.33	15.75	206.0	3070	77.0	"	77.0	"	9.8	8.3	1.18
2.02	"	"	"	"	16.42	206.0	"	33.0	"	33.0	"	19.6	16.0	1.23
2.03	"	"	"	2.04	19.70	471.0	"	56.0	"	56.0	"	19.6	13.3	1.47
2.04	"	"	6.50	3.20	21.37	480.0	"	50.5	"	50.5	"	31.4	21.1	1.49

TABLE 2.2. - Details of tests reported by BRESLER, B (6)
and comparison between tests and calculated ultimate loads.

Test No:	b (mm)	h (mm)	dc (mm)	100ρ	$0{\cdot}67f_{cu}$ (N/mm^2)	f_y (N/mm^2)	L (mm)	e_{1x} (mm)	e_{1y} (mm)	e_{2x} (mm)	e_{2y} (mm)	$N_{u\ test}$ (kN)	$N_{u\ Calc}$ (kN)	$\frac{N_{u\ test}}{N_{u\ calc}}$
B.1	152	203	45	2.6	21.7	306.6	1220.0	152.0	0	152.0	0	106.8	98.6	1.08
B.2	"	"	"	"	22.9	"	"	76.0	0	76.0	0	266.9	212.5	1.26
B.3	"	"	"	"	21.7	"	"	0	101.5	0	101.5	311.4	248.9	1.25
B.4	"	"	"	"	27.0	"	"	0	203.0	0	203.0	142.3	124.6	1.14
B.5	"	"	"	"	18.8	"	"	76.0	101.5	76.0	101.5	142.3	136.2	1.04
B.6	"	"	"	"	21.7	"	"	152.0	203.0	152.0	203.0	75.6	69.5	1.09
B.7	"	"	"	"	20.7	"	"	152.0	101.5	152.0	101.5	93.4	82.7	1.13
B.8	"	"	"	"	21.3	"	"	76.0	203.0	76.0	203.0	106.8	106.4	1.00

TABLE 2.3. - Details of tests reported by CHANG, W.F. and FERGUSON, P.M. (13) and comparison between tests and calculated ultimate loads.

Test No.	b (mm)	h (mm)	dc (mm)	100ρ	$0{\cdot}67f_{cu}$ (N/mm^2)	f_y (N/mm^2)	L (mm)	e_{1x} (mm)	e_{1y} (mm)	e_{2x} (mm)	e_{2y} (mm)	$N_{u\ test}$ (kN)	$N_{u\ Calc}$ (kN)	$\frac{N_{u\ test}}{N_{u\ calc}}$
1	103	156	17	1.78	19.8	338.0	3200	7.5	0	7.5	0	168.1	147.4	1.14
2	"	"	"	"	29.7	"	"	40.2	"	40.2	"	68.9	34.2	2.01
3	"	"	"	"	24.6	"	"	6.2	"	6.2	"	189.5	177.0	1.07
4	"	"	"	"	25.6	"	"	39.1	"	39.1	"	72.5	42.7	1.70
5	"	"	"	"	27.8	"	"	21.6	"	21.6	"	122.8	109.9	1.12
6	"	"	"	"	28.5	400.0	"	6.2	"	6.2	"	197.5	186.3	1.06

TABLE 2.4. - Details of tests reported by CRANSTON, W.B. and STURROCK, R.D. (18) and comparison between tests and calculated ultimate loads.

Test No.	b (mm)	h (mm)	dc (mm)	100ρ	$0{\cdot}67f_{cu}$ (N/mm^2)	f_y (N/mm^2)	L (mm)	e_{1x} (mm)	e_{1y} (mm)	e_{2x} (mm)	e_{2y} (mm)	N_u test (kN)	N_u Calc (kN)	$\frac{N_u \text{ test}}{N_u \text{ calc}}$
3	100	400	19,32	1.27	32.8	290	5000	0	154.0	0	154.0	273.0	179.7	1.52
4	"	"	"	"	33.5	420	"	0	100.0	0	100.0	463.0	220.0	2.10
5	"	"	"	"	33.5	"	"	0	120.0	0	120.0	349.0	189.0	1.85
6	"	"	"	"	25.5	"	"	0	154.0	0	154.0	321.0	151.8	2.11
7	"	"	"	"	33.5	"	"	0	135.0	0	135.0	378.0	192.1	1.97
8	"	"	"	"	36.9	"	"	0	15.0	0	15.0	160.0	85.0	1.88
9	"	"	"	"	36.9	"	"	0	15.0	0	15.0	170.0	85.0	2.0
10	"	"	"	"	36.9	"	"	0	15.0	0	15.0	200.0	85.0	2.35

NOTE: Two values are given for d_c. These refer to the weak and strong axis respectively.

TABLE 2.5. - Details of tests reported by MACGREGGOR, J.G. and BARTER, S.L. (28) and comparison between tests and calculated ultimate loads.

Test No.	b (mm)	h (mm)	dc (mm)	100ρ	$0{\cdot}67f_{cu}$ (N/mm^2)	f_y (N/mm^2)	L (mm)	e_{1x} (mm)	e_{1y} (mm)	e_{2x} (mm)	e_{2y} (mm)	$N_{u\ test}$ (kN)	$N_{u\ Calc}$ (kN)	$\frac{N_{u\ test}}{N_{u\ calc}}$
A.1	63.50	112	20	4.0	28.6	308.2	1735	12.70	0	-12.70	0	168.8	153.3	1.10
A.2	"	"	"	"	27.8	306.1	"	12.70	"	-12.70	"	169.0	150.8	1.12
B.1	"	"	"	"	24.7	308.2	"	95.25	"	-95.25	"	33.1	30.4	1.09
B.2	"	"	"	"	27.7	"	"	95.25	"	-95.25	"	31.4	30.6	1.03
C.1	"	"	"	"	22.5	"	"	12.70	"	-12.70	"	169.1	185.3	0.91
C.2	"	"	"	"	25.4	"	"	12.70	"	-12.70	"	176.5	201.5	0.88
D.1	"	"	"	"	21.3	"	"	95.25	"	-95.25	"	41.5	50.0	0.83
D.2	"	"	"	"	26.7	"	"	95.25	"	-95.25	"	53.6	64.1	0.84

TABLE 2.6. - Details of tests reported by MARTIN, I and OLIVIERI, E (31) and comparison between tests and calculated ultimate loads.

Test No.	b (mm)	h (mm)	dc (mm)	100ρ	$0{\cdot}67f_{cu}$ (N/mm^2)	f_y (N/mm^2)	L (mm)	e_{1x} (mm)	e_{1y} (mm)	e_{2x} (mm)	e_{2y} (mm)	N_u test (kN)	N_u Calc (kN)	$\frac{N_u \text{ test}}{N_u \text{ calc}}$
402.1	90	127	25	2.50	25.5	275.8	3600	0	0	0	0	146.8	120.5	1.22
402.2	"	"	"	"	20.7	"	"	0	"	0	"	124.5	102.6	1.21
412.1	"	"	"	"	28.6	"	"	19.0	"	-9.5	"	117.9	85.7	1.38
412.1	"	"	"	"	21.3	"	"	19.0	"	-9.5	"	89.0	65.4	1.36
422.1	"	"	"	"	29.7	"	"	35.0	"	-17.5	"	93.4	71.8	1.30
422.2	"	"	"	"	21.9	"	"	35.0	"	-17.5	"	75.6	60.0	1.26
432.1	"	"	"	"	31.7	"	"	25.0	"	-12.5	"	95.6	82.8	1.15
432.2	"	"	"	"	22.5	"	"	25.0	"	-12.5	"	93.5	66.5	1.41

TABLE 2.7. - Details of tests reported by PANNEL, F.N. and ROBINSON, J.L. (37) and comparison between tests and calculated ultimate loads.

Test No.	b (mm)	h (mm)	dc (mm)	100ρ	$0{\cdot}67f_{cu}$ (N/mm^2)	f_y (N/mm^2)	L (mm)	e_{1x} (mm)	e_{1y} (mm)	e_{2x} (mm)	e_{2y} (mm)	$N_{u\ test}$ (kN)	$N_{u\ Calc}$ (kN)	$\frac{N_{u\ test}}{N_{u\ calc}}$
1A	63.5	95.3	12.7	3.25	16.6	352.0	2642	0	0	0	0	61.0	45.4	1.34
2A	"	"	"	"	15.9	365.0	2642	0	0	0	0	75.0	44.2	1.70
3A	"	"	"	"	14.8	365.0	1727	0	0	0	0	100.0	85.1	1.18
4A	"	"	"	"	18.4	365.0	965	0	0	0	0	174.0	144.5	1.20
5A	"	"	"	"	18.5	365.0	2032	0	0	0	0	99.0	77.3	1.28
6B	"	"	"	"	19.8	352.0	2642	0	90.0	0	90	15.0	12.0	1.25
7B	"	"	"	"	21.3	352.0	"	168.7	0	168.7	0	20.0	15.3	1.30
8B	"	"	"	"	13.9	352.0	"	0	10.7	0	10.7	55.0	42.3	1.31
9B	"	"	"	"	13.9	352.0	"	68.0	0	68.0	0	40.0	33.1	1.21
10C	"	"	"	"	15.0	352.0	"	76.2	108.0	76.2	108.0	20.0	8.7	2.30
11C	"	"	"	"	15.0	352.0	"	41.0	24.0	41.0	24.0	40.0	22.1	1.81
12C	"	"	"	"	15.6	285.0	"	8.8	18.3	8.8	18.3	40.0	26.1	1.53
13C	"	"	"	"	13.4	285.0	"	46.8	50.0	46.8	50.0	20.0	13.8	1.45
14C	"	"	"	"	14.0	285.0	"	106.2	42.7	106.2	42.7	20.0	12.2	1.64
15C	"	"	"	"	13.4	365.0	"	20.5	11.0	20.5	11.0	50.0	29.3	1.71
16C	"	"	"	"	13.4	365.0	2642.0	35.6	19.0	35.6	19.0	30.0	24.0	1.25
17C	"	"	"	"	24.5	352.0	2642.0	82.0	48.8	82.0	48.8	20.0	15.8	1.27

TABLE 2.8. - Details of tests reported by RAMA MURTHY, L.N. (40) and comparison between tests and calculated ultimate loads.

Test No.	b (mm)	h (mm)	dc (mm)	100ρ	$0{\cdot}67f_{cu}$ (N/mm^2)	f_y (N/mm^2)	L (mm)	e_{1x} (mm)	e_{1y} (mm)	e_{2x} (mm)	e_{2y} (mm)	N_u test (kN)	N_u Calc (kN)	$\frac{N_u \text{ test}}{N_u \text{ calc}}$
A-1	203	203	25	2.50	34.9	291.9	2032	98.3	26.3	98.3	26.3	564.9	401.6	1.41
A-2	"	"	"	"	38.3	"	"	132.8	35.6	132.8	35.6	395.9	285.9	1.38
A-3	"	"	"	"	37.0	"	"	133.4	35.7	133.4	35.7	378.1	280.1	1.35
A-4	"	"	"	"	32.1	"	"	152.4	40.8	152.4	40.8	283.6	224.9	1.26
A-5	"	"	"	"	28.6	"	"	177.8	47.6	177.8	47.6	235.7	179.5	1.31
A-6	"	"	"	"	27.0	"	"	202.8	52.4	202.8	52.4	171.9	151.2	1.14
A-7	"	"	"	"	29.9	"	"	254.1	50.8	254.1	50.8	146.8	120.2	1.22
A-8	"	"	"	"	21.3	"	"	87.7	31.9	87.7	31.9	475.9	338.6	1.41
A-9	"	"	"	"	31.0	"	"	152.4	55.5	152.4	55.5	280.2	210.3	1.33
A-10	"	"	"	"	37.1	"	"	100.0	57.6	100.0	57.6	462.6	340.6	1.36
A-11	"	"	"	"	38.5	"	"	153.2	78.0	153.2	78.0	264.7	234.1	1.13
A-12	"	"	"	"	33.3	"	"	189.0	109.1	189.0	109.1	170.1	146.8	1.16
A-13	"	"	"	"	14.0	"	"	152.4	101.6	152.4	101.6	164.6	140.8	1.17
A-14	"	"	"	"	19.9	"	"	203.2	101.6	203.2	101.6	160.1	122.8	1.30
A-15	"	"	"	"	15.9	"	"	89.8	89.8	89.8	89.8	266.9	214.8	1.24
B-1	"	"	"	3.88	21.7	322.6	"	88.1	23.6	88.1	23.6	629.0	459.8	1.37
B-2	"	"	"	"	19.2	"	"	52.7	21.8	52.7	21.8	771.7	601.0	1.28
B-3	"	"	"	"	24.9	"	"	93.5	54.0	93.5	54.0	533.8	406.9	1.31
B-4	"	"	"	"	23.8	"	"	116.7	67.4	116.7	67.4	395.9	325.0	1.22
B-5	"	"	"	"	14.6	"	"	41.7	41.7	41.7	41.7	598.3	504.1	1.19
B-6	"	"	"	"	20.5	"	"	71.1	71.1	71.1	71.1	500.4	389.8	1.28

TABLE 2.8. - Details of tests reported by RAMA MURTHY, L.N. (40) and comparison between tests and calculated ultimate loads.

Test No.	b (mm)	h (mm)	dc (mm)	100ρ	$0{\cdot}67f_{cu}$ (N/mm^2)	f_y (N/mm^2)	L (mm)	e_{1x} (mm)	e_{1y} (mm)	e_{2x} (mm)	e_{2y} (mm)	$N_{u\ test}$ (kN)	$N_{u\ Calc}$ (kN)	$\frac{N_{u\ test}}{N_{u\ calc}}$
B-7	"	"	"	"	21.9	"	"	76.9	76.9	76.9	76.9	516.0	376.7	1.37
B-8	"	"	"	"	25.4	"	"	111.0	111.0	111.0	111.0	370.0	286.2	1.29
C-1	152.4	152.4	"	2.50	23.2	275.8	1524	42.2	11.3	42.2	11.3	464.8	356.7	1.30
C-2	"	"	"	"	25.3	"	"	49.1	13.1	49.1	13.1	400.3	350.9	1.14
C-3	"	"	"	"	21.6	"	"	38.6	22.3	38.6	22.3	460.4	331.8	1.39
C-4	"	"	"	"	17.9	"	"	45.9	26.5	45.9	26.5	378.1	267.3	1.41
C-5	"	"	"	"	18.5	"	"	21.6	21.6	21.6	21.6	506.0	380.7	1.33
C-6	"	"	"	"	23.1	"	"	47.4	47.4	47.4	47.4	350.3	244.9	1.43
D-1	203	229	"	3.88	23.6	322.6	2032	44.6	29.7	44.6	29.7	785.1	688.3	1.14
D-2	"	"	"	"	18.9	"	"	93.0	62.1	93.0	62.1	400.3	321.2	1.25
D-3	"	"	"	"	18.2	"	"	123.6	82.4	123.6	82.4	311.4	231.1	1.35
D-4	"	"	"	"	18.7	"	"	38.8	38.8	38.8	38.8	680.5	587.1	1.16
D-5	"	"	"	"	23.0	"	"	89.0	89.0	89.0	89.0	378.1	293.9	1.29
D-6	"	"	"	"	17.8	"	"	45.7	79.2	45.7	79.2	400.3	383.9	1.04
E-1	"	305	"	"	17.5	"	"	120.6	120.6	120.6	120.6	464.8	410.9	1.13
E-2	"	"	"	"	15.9	"	"	162.6	81.3	162.6	81.3	311.5	300.1	1.04
E-3	"	"	"	"	20.6	"	"	92.1	92.1	92.1	92.1	435.9	388.7	1.12
E-4	"	"	"	"	18.5	"	"	38.1	66.0	38.1	66.0	542.7	540.3	1.00

TABLE 2.9. - Details of tests reported by SAENZ, L. and MARTIN, I. (42) and comparison between tests and calculated ultimate loads.

Test No.	b (mm)	h (mm)	dc (mm)	100ρ	$0{\cdot}67f_{cu}$ (N/mm^2)	f_y (N/mm^2)	L (mm)	e_{1x} (mm)	e_{1y} (mm)	e_{2x} (mm)	e_{2y} (mm)	$N_{u\ test}$ (kN)	$N_{u\ Calc}$ (kN)	$\frac{N_{u\ test}}{N_{u\ calc}}$
26D-3	90.4	127	15	1.10	19.36	263.4	2248	0	0	0	0	236.0	186.0	1.27
23D-2	"	"	"	2.48	16.42	247.5	2248	"	"	"	"	233.5	186.7	1.25
3E-2	"	"	"	1.10	26.33	263.5	2248	"	"	"	"	235.7	238.7	1.01
31D-3	"	"	"	2.48	29.15	247.5	2248	"	"	"	"	343.4	282.9	1.21
27D-3	"	"	"	1.10	20.57	263.4	2697	"	"	"	"	191.7	171.0	1.12
24D-2	"	"	"	2.48	17.42	247.5	2697	"	"	"	"	198.4	167.8	1.18
1E-1	"	"	"	1.10	28.48	263.4	2697	"	"	"	"	297.1	218.1	1.36
10E-2	"	"	"	2.48	26.73	247.5	2697	"	"	"	"	364.7	227.8	1.60
29D-2	"	"	"	1.10	18.43	263.4	3147	"	"	"	"	158.8	135.3	1.17
30D-1	"	"	"	2.48	17.62	247.5	3147	"	"	"	"	171.2	146.0	1.17
2E-2	"	"	"	1.10	30.95	263.4	3147	"	"	"	"	246.4	192.3	1.28
20D-2	"	"	"	1.10	24.05	247.5	3147	"	"	"	"	229.1	177.8	1.29
6E-3	"	"	"	1.10	16.08	263.4	3597	"	"	"	"	141.0	103.6	1.36
15E-2	"	"	"	2.48	16.82	247.5	3597	"	"	"	"	161.0	119.3	1.35
5E-1	"	"	"	1.10	32.29	263.4	3597	"	"	"	"	238.4	161.8	1.47
14E-3	"	"	"	2.48	24.52	247.5	3597	"	"	"	"	223.3	148.6	1.50
21F-3	"	"	"	2.48	15.28	247.5	3866	"	"	"	"	137.4	89.4	1.54
28F-1	"	"	"	2.48	25.26	247.5	3866	"	"	"	"	196.2	134.2	1.46

TABLE 2.10. - SUMMARY OF COMPARISON BETWEEN TEST RESULTS AND RESULTS FROM PROGRAM VARCOLS

Author	Reference	Number of Tests	$N_{u\ test}/N_{u\ calc}$ Mean	S. Dev.	Least
Aas-Jakobsen	[1]	20	1.294	0.113	1.15
Bresler	[6]	8	1.124	0.093	1.00
Chang	[13]	6	1.350	0.404	1.06
Cranston	[20]	10	1.973	0.241	1.52
MacGregor	[28]	8	0.975	0.125	0.83
Martin	[31]	8	1.286	0.092	1.15
Pannel	[37]	17	1.455	0.297	1.18
Ramamurthy	[40]	39	1.256	0.114	1.00
Saenz	[42]	18	1.311	0.158	1.01
		Overall	1.32	0.26	

TABLE 4.1. - RESULTS OF TESTS ON CUBE SPECIMENS

COLUMN LABEL	NO OF CUBES	SIZE OF CUBE (mm^3)	DATE CASTING	DATE TESTED	AGE (DAYS)	AVERAGE COMPRESSIVE STRENGTH (N/mm^2)	STANDARD DEVIATION (N/mm^2)
MCUO - Ø2	9	100x100x100	19.07.82	09.12.82	144	26.50	2.92
MDUO - Ø3	9	150x150x150	13.08.82	02.12.82	137	46.37	3.93
MTUO - Ø4	9	100x100x100	03.08.82	30.11.82	134	41.29	2.02
MDUO - Ø5	12	150x150x150	04.02.83	12.04.83	68	37.48	6.35
MTUO - Ø6	12	150x150x150	11.02.83	19.04.83	68	35.56	7.85
MGUO - Ø7	12	150x150x150	24.02.83	25.04.83	54	35.46	2.38
MGUO - Ø8	12	150x150x150	22.03.83	09.05.83	49	23.70	3.36

TABLE 4.2. - RESULTS OF TEST ON REINFORCEMENT BAR

No.	Specimen Diameter	Load at Elongation	Ultimate Load	0.2% Proof Stress	Ultimate Stress
	(mm)	(kN)	(kN)	(MPa)	(MPa)
1	15.72	91.6	104.0	475.0	536.51

TABLE 4.3.- Detail of Specimens and Comparison of Test Results with VARCOLS

RECTANGULAR CROSS SECTIONS

COLUMN LABEL	SERIES	STRONGER END b (mm)	STRONGER END h (mm)	WEAKER END b (mm)	WEAKER END h (mm)	DEPTH AT MID HEIGHT	LENGTH (mm)	$\frac{L}{h_t}$	ℓ_{1x} (mm)	ℓ_{1y} (mm)	ℓ_{2x} (mm)	ℓ_{2y} (mm)	fcu (N/mm²)	100ρ at MID LENGTH	fy (N/mm²)	N_u test (KN)	N_u calc (KN)	$\frac{N_u \text{ test}}{N_u \text{ calc}}$
MCUO - Ø2		400	400	400	400	400		15		110		55	26.5	1.00	446.0	2600.0	1980.0	1.31
MDUO - Ø3	A	300	300	200	200	250	6000	24	0	60	0	0	46.4	2.57	475.0	1565.0	1220.0	1.28
MTUO - Ø4			250		250					25			41.3	2.57	475.0	1597.0	1673.0	0.96
MDUO - Ø5	B	300	300	200	200	250	6000	24	0	90	0	0	37.5	2.57	475.0	1130.0	836.0	1.35
MTUO - Ø6			250		250								35.6	2.57	475.0	1195.0	810.0	1.48

OCTAGONAL CROSS SECTION

COLUMN LABEL	SERIES	D (mm)	LENGTH (mm)	L/D	ℓ_{1x}	ℓ_{1y} (mm)	ℓ_{2x}	ℓ_{2y}	fcu (N/mm²)	100ρ at MID LENGTH	fy (N/mm²)	N_u test (KN)	N_u calc (KN)	$\frac{N_u \text{ test}}{N_u \text{ calc}}$
MGUO - Ø7	B	250	6000	24	0	50	0	0	35.6	2.57	475.0	1130.0	795.0	1.42
MGUO - Ø8						100			23.7	2.57	475.0	741.0	441.9	1.68

TABLE 4.4. - LOCATION OF FAILED SECTION FROM THE ECCENTRICALLY LOADED END

Label	Experimental (mm)	Theoretical (mm)
MDUO-03	3750	3500
MTUO-04	3760	4000
MDUO-05	3700	3500
MTUO-06	3770	3000
MGUO-07	2200	2000
MGUO-08	1900	2000

TABLE 4.5.- COMPARISON OF TEST RESULTS WITH VARCOLS

Effect of Initial Imperfection

RECTANGULAR CROSS SECTIONS

Label	Series	N_{ut} (kN)	N_{uv1} (0.001L) (kN)	N_{uv2} (zero) (kN)	N_{ut}/N_{uv1}	N_{ut}/N_{uv2}
MCUO-02	A	2600	1980	2076	1.31	1.25
MDUO-03		1565	1220	1383	1.28	1.13
MTUO-04		1597	1673	1799	0.96	0.89
MDUO-05	B	1130	836	904	1.35	1.25
MTUO-06		1195	810	871	1.48	1.37

OCTAGONAL CROSS SECTIONS

MGUO-07	B	1130	795	886	1.42	1.28
MGUO-08		741	442	465	1.68	1.59

TABLE 4.6. - COMPARISON OF TEST RESULTS WITH BS5400:PART 4

RECTANGULAR CROSS SECTIONS

Label	Series	N_{ut} (kN)	N_{ucl} (kN)	N_{uc2} (kN)	N_{ut}/N_{ucl}	N_{ut}/N_{uc2}
MCUO-02	A	2600	1677	1520	1.55	1.71
MDUO-03		1565	1005	639	1.56	2.45
MTUO-04		1597	1088	719	1.57	2.22
MDUO-05	B	1130	783	562	1.44	2.01
MTUO-06		1195	763	562	1.57	2.13

OCTAGONAL CROSS SECTIONS

MGUO-07	B	1130	652	525	1.73	2.15
MGUO-08		741	450	324	1.65	2.29

TABLE 4.7 - RESULTS FROM TESTS ON STUB COLUMNS

STUB COLUMN REF NO	MAXIMUM RECORDED STRAIN (%)	AREA OF CONCRETE (mm^2)	STUB COLUMN STRENGTH (KN)	REINF CONTRIB (KN)	CONC CONTRIB (KN)	CONC STRENGTH f'c (N/mm^2)	CUBE STRENGTH fcu (N/mm^2)	CONCRETE REDUC-TION FACTOR	$1/_d$
8A	0.178	51777	1635	764	871	16.810	21.958	0.7656	3.9
8B	0.252	52026	1445	764	681	13.090	21.958	0.5961	3.0
7A	0.166	52442	2103	764	1339	25.530	34.226	0.7459	3.0
7B	0.183	52348	1834	764	1070	20.435	34.226	0.5971	2.9
4A	0.166	52993	2043	764	1279	24.136	40.038	0.6028	3.5
4B	0.246	56616	2143	764	1379	24.352	40.038	0.6082	3.1
3A	0.212	45990	2213	764	1449	31.496	43.933	0.7169	3.1
3B	0.372	50850	2213	764	1449	28.486	43.933	0.6484	3.1

TABLE 5.1. - RESULTS OF COMPRESSION TESTS ON CUBE SPECIMENS
(150mmx150mmx150mm cubes)

COLUMN LABEL	NUMBER OF CUBES	CASTING DATE	TEST DATE	AGE (Days)	AVERAGE STRENGTH N/mm^2	STANDARD DEVIATION N/mm^2
LDUO-09	13	02.06.83	04.10.83	123	32.52	2.24
LDUO-10	13	19.07.83	26.10.83	99	28.34	2.56
LDUO-11	13	28.09.83	15.11.83	48	33.18	2.18
LDUO-12	13	10.10.83	19.01.84	101	31.48	2.78
LGUO-13	13	25.11.83	30.01.84	66	37.03	3.74
LGUO-14	13	12.12.83	21.02.83	71	33.59	2.12

TABLE 5.2 - RESULTS OF TENSILE TEST ON REINFORCEMENT BARS

No.	Specimen Diameter	Load at Elongation	Ultimate Load	0.2% Proof Stress	Ultimate Stress
	(mm)	(kN)	(kN)	(MPa)	(MPa)
10 bars	15.72	91.6	104.0	475.0	536.51

TABLE 5.3 - Detail of Specimens and Comparison of Test Results with VARCOLS

RECTANGULAR CROSS SECTIONS

COLUMN LABEL	SERIES	STRONGER END b (mm)	STRONGER END h (mm)	WEAKER END b (mm)	WEAKER END h (mm)	DEPTH AT MID HEIGHT	LENGTH (mm)	$\frac{L}{h_t}$	ℓ_{1x} (mm)	ℓ_{1y} (mm)	ℓ_{2x} (mm)	ℓ_{2y} (mm)	fcu (N/mm²)	100ρ at MID LENGTH	fy (N/mm²)	N_u test (KN)	N_u calc (KN)	$\frac{N_u \text{ test}}{N_u \text{ calc}}$
LDUO-09	400	400	400	300	300	350	9000	26	0	100	0	0	32.52	1.31	475	2050	1150	1.78
LDUO-10										235			28.34			1000	608	1.65
LDUO-11		300	300	200	200	250		36		65			33.18	2.57		713	443	1.61
LDUO-12										175			31.48			375	272	1.38

OCTAGONAL CROSS SECTION

COLUMN LABEL	SERIES	D (mm)	LENGTH (mm)	L/D	ℓ_{1x}	ℓ_{1y} (mm)	ℓ_{2x}	ℓ_{2y}	fcu (N/mm²)	100ρ at MID LENGTH	fy (N/mm²)	N_u test (KN)	N_u calc (KN)	$\frac{N_u \text{ test}}{N_u \text{ calc}}$
LGUO-13	C	300	9000	30	0	90	0	0	33.59	1.79	475.0	815	650	1.25
LGUO-14						120			37.03		475.0	637.	538	1.18

Table 5.4. - CRACKING BEHAVIOUR

COLUMN LABEL	$0.20F_{cu}A_c$ (kN)	N_{uc2} (kN)	N_{test} (kN)	$N_{first\ cracks}$ (kN)	Surface width of cracks (mm)	Position of the cracks from the stronger end.
LDUO-09	797	807	2050	-	-	-
LDUO-10	694	474	1000	360	0.05	4500-6000
LDUO-11	415	379	713	250	0.03	2610-5000
LDUO-12	394	169	375	160	0.05	3000-6000
LGUO-13	500	427	815	320	0.04	3000-4000
LGUO-14	552	302	665	230	0.04	3000-4000

TABLE 5.5. – LOCATION OF FAILED SECTION FROM THE ECCENTRICALLY LOADED END

Label	Experimental (mm)	Theoretical (mm)
LDU0-09	4500	4000
LDU0-10	4000	4000
LDU0-11	5500	5000
LDU0-12	6000	5000
LGU0-13	3500	3750
LGU0-14	3500	3750

TABLE 5.6 -COMPARISON OF TEST RESULTS WITH BS5400:PART 4

RECTANGULAR CROSS SECTIONS

Label	Series	N_{ut} (kN)	N_{uc1} (kN)	N_{uc2} (kN)	N_{ut}/N_{uc1}	N_{ut}/N_{uc2}
LDUO-Ø9	C	2050	1021	807	2.01	2.54
LDUO-10		1000	612	474	1.63	2.11
LDUO-11		713	511	379	1.40	1.88
LDUO-12		375	228	169	1.64	2.22
	OCTAGONAL CROSS SECTIONS					
LGUO-13	C	815	470.0	427	1.73	1.91
LGUO-14		665	421.0	302	1.58	2.20

TABLE 6.1 - Result of test on cube specimens

COLUMN LABEL	NO. OF CUBES	CASTING DATE	TEST DATE	AGE (Days)	AVERAGE STRENGTH (N/mm^2)	STANDARD DEVIATION (N/mm^2)
LDBO-15	13	27-03-84	08-05-84	43	32.18	4.88
LDBO-16	13	10-04-84	06-06-84	55	33.09	4.07
LDBO-17	13	05-03-84	13-04-84	38	30.96	3.45
LDBO-18	13	16-03-84	19-04-84	30	32.94	2.17
LGBO-19	13	07-02-84	29-03-84	49	33.68	4.17
LGBO-20	13	20-02-84	04-04-84	44	30.71	3.93

TABLE 6.2 - RESULTS OF TENSILE TEST ON REINFORCEMENT BARS

No.	Specimen Diameter	Load at Elongation	Ultimate Load	0.2% Proof Stress	Ultimate Stress
	(mm)	(kN)	(kN)	(MPa)	(MPa)
10 bars	15.72	91.6	104.0	475.0	536.51

Table 6.3. - Detail of Specimens and Comparison of Test Results with VARCOLS

RECTANGULAR CROSS SECTIONS

COLUMN LABEL	SERIES	STRONGER END b (mm)	STRONGER END h (mm)	WEAKER END b (mm)	WEAKER END h (mm)	DEPTH AT MID HEIGHT	LENGTH (mm)	$\frac{L}{h_t}$	ℓ_{1x} (mm)	ℓ_{1y} (mm)	ℓ_{2x} (mm)	ℓ_{2y} (mm)	fcu (N/mm²)	100ρ at MID LENGTH	fy (N/mm²)	N_u test (KN)	N_u calc (KN)	$\frac{N_u \text{ test}}{N_u \text{ calc}}$
LDBO-15	D	400	400	300	300	350	9000	26	0	105	0	105	32.18	1.31	475	1380	843	1.64
LDBO-16	D	400	400	300	300	350	9000	26	0	150	0	150	33.09	1.31	475	1000	644	1.55
LDBO-17	D	300	300	200	200	250	9000	36	0	65	0	65	30.96	2.57	475	530	329	1.61
LDBO-18	D	300	300	200	200	250	9000	36	0	120	0	120	32.94	2.57	475	320	250	1.27

OCTAGONAL CROSS SECTION

COLUMN LABEL	SERIES	D (mm)	LENGTH (mm)	L/D	ℓ_{1x}	ℓ_{1y} (mm)	ℓ_{2x}	ℓ_{2y}	fcu (N/mm²)	100ρ at MID LENGTH	fy (N/mm²)	N_u test (KN)	N_u calc (KN)	$\frac{N_u \text{ test}}{N_u \text{ calc}}$
LGBO-19	D	300	9000	30	0	90	0	90	33.68	1.71	475.0	515	398	1.29
LGBO-20	D	300	9000	30	0	180	0	180	30.71	1.71	475.0	250	245	1.02

TABLE 6.4. - Cracking Behaviour

COLUMN LABEL	N_{test} (KN)	$N_{first\ cracks}$ (KN)	$\frac{N_{first}}{N_{test}}$ (%)	Surface width of cracks (mm)	Position of the cracks from the stronger end
LDBO-15	1375	604.35	44	0.03	2500-5000
LDBO-16	991	395	53	0.04	2000-5500
LDBO-17	525	210	58	0.03	3500-6000
LDBO-18	317	100	27	0.05	2000-6000
LGBO-19	515	200	40	0.04	2000-4000
LGBO-20	250	100	40	0.03	1000-3000

Table 6.5. - Location of failed section from the eccentrically loaded end.

COLUMN LABEL	EXPERIMENTAL (mm)	THEORETICAL (mm)
LDBO-15	4000	3000
LDBO-16	3250	3000
LDBO-17	3250	3750
LDBO-18	3500	3750
LGBO-19	3950	3000
LGBO-20	At the loaded end	3000

Table 7.1. - Detail of tests reported by CHANG and FERGUSON and comparison between tests and designed ultimate loads

TEST NO.	b (mm)	h (mm)	d/h	100	f_{cu} (N/mm^2)	f_y (N/mm^2)	e/h	L/h	N_{uz} (kN)	Nu_{TEST} (kN)	Nu_{CALC} (kN)	$\frac{Nu_{TEST}}{Nu_{CALC}}$
1	156	103	0.84	1.78	29.5	338	0.07	31	394	168	138	1.22
2	156	103	0.84	1.78	43.7	338	0.39	31	544	69	68	1.01
3	156	103	0.84	1.78	36.1	338	0.06	31	464	189	162	1.16
4	156	103	0.84	1.78	37.6	338	0.38	31	479	73	62	1.17
5	156	103	0.84	1.78	41.0	338	0.21	31	515	123	108	1.14
6	156	103	0.84	1.78	42.0	400	0.06	31	539	198	188	1.05

Table 7.2. - Detail of tests reported by ERNEST, HROMADIK and RIVELAND and comparison between tests and designed ultimate loads

TEST NO.	b (mm)	h (mm)	d/h	100	f_{cu} (N/mm^2)	f_y (N/mm^2)	e/h	L/h	N_{uz} (kN)	Nu_{TEST} (kN)	Nu_{CALC} (kN)	$\frac{Nu_{TEST}}{Nu_{CALC}}$
3	152	152	0.83	1.23	25.16	357	0	15	473	490	331	1.48
4	152	152	0.83	1.23	25.16	357	0	25	473	450	260	1.73
7	152	152	0.83	1.23	25.16	357	0.125	15	473	360	245	1.46
8	152	152	0.83	1.23	25.16	357	0.125	25	473	290	185	1.57
11	152	152	0.83	1.23	25.16	357	0.250	15	473	260	170	1.53
12	152	152	0.83	1.23	25.16	357	0.250	25	473	170	118	1.44
15	152	152	0.83	1.23	25.16	357	0.375	15	473	90	117	1.30
16	152	152	0.83	1.23	25.16	357	0.375	25	473	110	85	1.29

Table 7.3. - Detail of tests reported by GAEDE and comparison between tests and designed ultimate loads

TEST NO.	b (mm)	h (mm)	d/h	100	f_{cu} (N/mm^2)	f_y (N/mm^2)	e/h	L/h	N_{uz} (kN)	Nu_{TEST} (kN)	Nu_{CALC} (kN)	$\frac{Nu_{TEST}}{Nu_{CALC}}$
I1	154	100	0.87	1.0	24.7	335	0.20	29.4	297	75	71	1.06
I5	154	100	0.87	1.0	32.1	288	0.20	29.4	366	97	88	1.10
II4	154	100	0.87	1.0	30.1	273	0.50	29.4	345	35	31	1.13
II5	154	100	0.87	1.0	31.6	272	0.50	29.4	359	38	32	1.18
III1	154	100	0.87	1.0	32.9	326	0.50	35.4	379	33	23	1.45
III2	154	100	0.87	1.0	28.6	326	0.50	35.4	336	33	20	1.64
III3	154	100	0.87	1.0	28.4	327	0.50	35.4	334	34	20	1.64
III4	154	100	0.87	1.0	38.8	314	0.50	35.4	438	37	26	1.41

Table 7.4. - Detail of tests reported by KORDINA and comparison between tests and designed ultimate loads

TEST NO.	b (mm)	h (mm)	d/h	100	f_{cu} (N/mm^2)	f_y (N/mm^2)	e/h	L/h	N_{uz} (kN)	Nu_{TEST} (kN)	Nu_{CALC} (kN)	$\frac{Nu_{TEST}}{Nu_{CALC}}$
A1	154	100	0.87	1.01	35.4	294	0.20	29	404	117	99	1.18
A2	154	100	0.87	1.01	42.6	294	0.50	29	474	52	47	1.10
A3	154	100	0.87	1.01	32.6	294	0.10	29	373	118	91	1.29
A4	154	100	0.87	1.34	42.8	305	0.17	29	490	139	132	1.05

Table 7.5 Detail of tests reported by RAMBOLL and comparison between tests and designed ultimate loads

TEST NO.	b (mm)	h (mm)	d/h	100	f_{cu} (N/mm^2)	f_y (N/mm^2)	e/h	L/h	N_{uz} (kN)	Nu_{TEST} (kN)	Nu_{CALC} (kN)	$\frac{Nu_{TEST}}{Nu_{CALC}}$
1	182	144	0.79	0.97	35.6	294	0	9.1	686	860	494	1.74
2	181	141	0.79	1.0	31.8	294	0	9.1	603	640	434	1.47
3	182	143	0.81	0.98	33.0	294	0.08	9.1	636	690	394	1.75
4	181	141	0.82	1.00	28.4	294	0.08	9.1	513	590	318	1.85
5	181	143	0.77	0.98	34.7	294	0.17	9.1	661	510	357	1.43
6	181	143	0.79	0.98	31.4	294	0.17	9.1	604	530	326	1.63
7	180	145	0.79	0.97	29.6	294	0.33	9.1	578	340	202	1.68
8	181	144	0.79	0.97	31.6	294	0.33	9.1	613	305	215	1.42
9	181	142	0.79	0.99	29.2	294	0.67	9.1	563	118	85	1.40
10	181	144	0.80	0.97	30.6	294	0.67	9.1	596	06	89	1.19
11	181	141	0.80	1.00	32.2	294	0.83	9.1	611	78	55	1.42
12	181	141	0.80	1.00	26.9	294	0.83	9.1	522	78	47	1.66
13	181	142	0.79	0.99	35.6	294	0	13.2	672	580	437	1.33
14	181	142	0.83	0.99	32.0	294	0	13.2	612	690	398	1.73
15	181	147	0.78	0.95	30.9	294	0	13.2	610	650	397	1.64
16	181	146	0.78	0.95	30.9	294	0	13.2	610	650	397	1.64
17	180	142	0.79	0.99	31.4	294	0.08	13.2	597	580	352	1.65
18	181	144	0.80	0.97	29.5	294	0.08	13.2	576	530	340	1.56
19	180	142	0.79	0.99	30.2	294	0.17	13.2	577	470	289	1.63
20	182	143	0.79	0.98	30.4	294	0.17	13.2	590	510	295	1.73
21	183	145	0.80	0.96	28.8	294	0.33	13.2	573	305	175	1.75
22	182	144	0.79	0.97	29.1	294	0.33	13.2	572	305	175	1.75
23	181	144	0.78	0.97	29.3	294	0.67	13.2	572	94	69	1.37
24	181	144	0.79	0.97	27.4	294	0.67	13.2	540	94	65	1.45
25	182	144	0.79	0.97	35.2	294	0.83	13.2	677	69	54	1.27
26	181	141	0.80	1.00	33.4	294	0.83	13.2	631	67	50	1.33
27	182	141	0.77	0.99	36.6	294	0	13.2	689	580	448	1.30
28	183	146	0.79	0.95	35.7	294	0	13.2	700	490	455	1.08
29	182	144	0.79	0.97	36.9	294	0.17	13.2	708	335	345	0.97
30	182	143	0.76	0.98	33.9	294	0.33	13.2	651	195	195	1.00
31	183	144	0.79	0.96	36.4	294	0.67	13.2	703	73	84	0.87
32	183	142	0.79	0.98	36.8	294	0.83	13.2	701	57	56	1.02
33	183	143	0.81	0.97	34.4	294	0	30.1	663	495	328	1.51
34	182	145	0.80	0.96	36.9	294	0.08	29.6	713	410	250	1.64
35	183	144	0.70	1.71	33.2	294	0.17	29.9	692	235	173	1.36
36	182	145	0.80	0.96	34.0	294	0.33	29.6	661	118	109	1.08
37	183	143	0.79	0.97	33.6	294	0.67	30.1	649	56	39	1.44
38	182	145	0.79	0.96	40.5	294	0.83	29.6	776	44	23	1.89

Table 7.6. - Summary of comparison between test results and results from the proposed method of design

AUTHOR	Reference	No. of Tests	Nu_{test}/Nu_{calc}		
			Mean	S.Dev.	Least
CHANG & FERGUSON	13	8	1.12	0.08	1.01
ERNEST, HROMADIK, & RIVELAND	16	8	1.48	0.14	1.29
GAEDE	16	8	1.33	0.24	1.06
KORDINA	16	4	1.16	0.10	1.05
RAMBOLL	16	38	1.46	0.26	0.87
OVERALL		64	1.31	0.16	

Table 7.7 - Comparison between test results for tapered cross section columns subjected to uniaxial bending and designed ultimate loads

COLUMN LABEL	STRONGER END b (mm)	h (mm)	WEAKER END b (mm)	h (mm)	$h_{L/2}$ (mm)	L (mm)	L/i_t	e/h_t	N_{uz} (kN)	N_{TEST} (kN)	N_{CALC} (kN)	NTEST NCALC
MDUO-03	300	300	200	200	250	6000	24	0.125	2707	1565	1218	1.28
MTUO-04	300	250	200	250	250	6000	24	0.05	2493	1597	1296	1.23
MDUO-05	300	300	200	200	250	6000	24	0.18	2334	1130	887	1.27
MTUO-06	300	250	200	250	250	6000	24	0.18	2255	1195	857	1.39
LDUO-09	400	400	300	300	350	9000	26	0.15	3433	2050	1270	1.61
LDUO-10	400	400	300	300	350	9000	26	0.35	3090	1000	803	1.25
LDUO-11	300	300	200	200	250	9000	36	0.13	2153	713	474	1.50
LDUO-12	300	300	200	200	250	9000	36	0.35	2082	375	312	1.20

Mean = 1.34

Standard Deviation = 0.15